Refining and Characterizing Heat Release Rates from Electrical Enclosures During Fire

Volume 2:
Fire Modeling Guidance for Electrical Cabinets, Electric Motors, Indoor Dry Transformers, and the Main Control Board

U.S. Nuclear Regulatory Commission
Office of Nuclear Regulatory Research
Washington, D.C. 20555-0001

Electric Power Research Institute
3420 Hillview Avenue
Palo Alto, CA 94304-1338

U.S.NRC
United States Nuclear Regulatory Commission
Protecting People and the Environment

EPRI ELECTRIC POWER RESEARCH INSTITUTE

AVAILABILITY OF REFERENCE MATERIALS IN NRC PUBLICATIONS

NRC Reference Material

As of November 1999, you may electronically access NUREG-series publications and other NRC records at the NRC's Public Electronic Reading Room at http://www.nrc.gov/reading-rm.html. Publicly released records include, to name a few, NUREG-series publications; *Federal Register* notices; applicant, licensee, and vendor documents and correspondence; NRC correspondence and internal memoranda; bulletins and information notices; inspection and investigative reports; licensee event reports; and Commission papers and their attachments.

NRC publications in the NUREG series, NRC regulations, and Title 10, "Energy," in the *Code of Federal Regulations* may also be purchased from one of these two sources.

1. **The Superintendent of Documents**
   U.S. Government Publishing Office
   Washington, DC 20402-0001
   Internet: http://bookstore.gpo.gov
   Telephone: 1-866-512-1800
   Fax: (202) 512-2104

2. **The National Technical Information Service**
   5301 Shawnee Road
   Alexandria, VA 22161-0002
   http://www.ntis.gov
   1-800-553-6847 or, locally, (703) 605-6000

A single copy of each NRC draft report for comment is available free, to the extent of supply, upon written request as follows:

U.S. Nuclear Regulatory Commission
Office of Administration
Multimedia, Graphics and Storage & Distribution Branch
Washington, DC 20555-0001
E-mail: distribution.resource@nrc.gov
Facsimile: (301) 415-2289

Some publications in the NUREG series that are posted at the NRC's Web site address http://www.nrc.gov/reading-rm/doc-collections/nuregs are updated periodically and may differ from the last printed version. Although references to material found on a Web site bear the date the material was accessed, the material available on the date cited may subsequently be removed from the site.

Non-NRC Reference Material

Documents available from public and special technical libraries include all open literature items, such as books, journal articles, transactions, *Federal Register* notices, Federal and State legislation, and congressional reports. Such documents as theses, dissertations, foreign reports and translations, and non-NRC conference proceedings may be purchased from their sponsoring organization.

Copies of industry codes and standards used in a substantive manner in the NRC regulatory process are maintained at—

The NRC Technical Library
Two White Flint North
11545 Rockville Pike
Rockville, MD 20852-2738

These standards are available in the library for reference use by the public. Codes and standards are usually copyrighted and may be purchased from the originating organization or, if they are American National Standards, from—

American National Standards Institute
11 West 42nd Street
New York, NY 10036-8002
http://www.ansi.org
(212) 642-4900

Legally binding regulatory requirements are stated only in laws; NRC regulations; licenses, including technical specifications; or orders, not in NUREG-series publications. The views expressed in contractor-prepared publications in this series are not necessarily those of the NRC.

The NUREG series comprises (1) technical and administrative reports and books prepared by the staff (NUREG-XXXX) or agency contractors (NUREG/CR-XXXX), (2) proceedings of conferences (NUREG/CP-XXXX), (3) reports resulting from international agreements (NUREG/IA-XXXX), (4) brochures (NUREG/BR-XXXX), and (5) compilations of legal decisions and orders of the Commission and Atomic and Safety Licensing Boards and of Directors' decisions under Section 2.206 of NRC's regulations (NUREG-0750).

Refining and Characterizing Heat Release Rates from Electrical Enclosures During Fire

Volume 2:
Fire Modeling Guidance for Electrical Cabinets, Electric Motors, Indoor Dry Transformers, and the Main Control Board

Manuscript completed: December 2019
Date published: June 2020

U.S. Nuclear Regulatory Commission
Office of Nuclear Regulatory Research (RES)
Washington, D.C. 20555-0001

U.S. NRC-RES Project Manager
M. H. Salley

Electric Power Research Institute (EPRI)
3420 Hillview Avenue
Palo Alto, CA 94304-1338

EPRI Project Manager
A. Lindeman

DISCLAIMER OF WARRANTIES AND LIMITATION OF LIABILITIES

THE FOLLOWING ORGANIZATIONS PREPARED THIS REPORT:

Electric Power Research Institute

U.S. Nuclear Regulatory Commission, Office of Nuclear Regulatory Research

Jensen Hughes, Inc.

S. Nowlen (Consultant)

Engineering Planning and Management

Duke Energy

NOTE

ABSTRACT

NUREG-2178 Volume 1 refined the heat release rates (HRRs) associated with electrical cabinets and introduced an obstructed fire plume model for refining the vertical zone of influence (ZOI). As a result, Volume 1 has been implemented in a number of nuclear power plant fire probabilistic risk assessments to obtain a more realistic estimate of risk associated with electrical cabinet fires. Although the methodology in Volume 1 is focused on data analysis and the ZOI, it was realized that modeling refinements associated with other aspects of cabinet fires and other electrical ignition sources should be investigated. These targeted areas are further investigated in this report.

This report describes improved methods that will increase the realism in the modeling of selected ignition sources. The areas further investigated include the treatment of flame radiation and obstructed radiation, fire propagation between adjacent electrical cabinets, HRRs for electric motors and dry transformers, fire location factor, and the modeling of the main control board.

Keywords
Fire probabilistic risk assessment
Fire modeling
Fire Dynamics Simulator
Heat release rate
Obstructed fire plume
Zone of influence

TABLE OF CONTENTS

LIST OF FIGURES

LIST OF TABLES

EXECUTIVE SUMMARY

PRIMARY AUDIENCE: Fire probabilistic risk assessment (FPRA) engineers and fire protection engineers (FPEs) supporting the development and/or maintenance of FPRAs

SECONDARY AUDIENCE: Engineers, utility managers, and other stakeholders who review FPRAs, and who interface with FPRA methods

KEY RESEARCH QUESTION

How can nuclear power plant (NPP) fire operating experience, mathematical simulation, and experimental results be used to inform FPRA methodology and data?

RESEARCH OVERVIEW

This report is a product of a joint collaboration between the Electric Power Research Institute (EPRI) and the U.S. Nuclear Regulatory Commission Office of Nuclear Regulatory Research (NRC-RES) under a memorandum of understanding on fire research. Building upon the methodology and advancements of NUREG-2178 Volume 1 (and EPRI 3002005578) on heat release rates (HRRs) and obstructed plume, the working group continued to research other areas related to fire scenario modeling and HRRs.

The working group consisted of technical experts in experimental test programs, fire protection/fire modeling, FPRA, and fire events/operating experience representing both EPRI and the NRC. In general, the working group was responsible for the topics that were selected, research to resolve the technical issue, and method development. As necessary, additional experts were involved to perform calculations, interpret results, and present findings to the team. The working group met periodically to discuss the results and formalize the methods and data that are presented in this report.

Section 2, 3, and 6 are focused on the calculations used to develop the zone of influence (ZOI). The research focused on the empirical fire modeling equations and aimed to reduce the bias and uncertainty associated with the calculations. Both the radiation (see Sections 2 and 3) and fire location factor (see Section 6) developed a range of simulations in Fire Dynamics Simulator (FDS) and the outputs validated with relevant experimental test results to modify the empirical equations to reduce the error and bias in the calculations.

Section 4 leverages the operating experience in the United States to refine the screening guidance for postulated fire spread to adjacent electrical enclosures. The working group discussed common configurations and their potential for fire spread to an adjacent enclosure. Screening guidance is provided for a number of additional configurations, and more guidance has been developed for when fire spread should be postulated.

Section 5 seeks to determine revised HRRs and fire durations for electric motors and dry transformers.

A literature search did not yield experimental results that could inform the HRR and fire duration for these ignition sources. Even though a wide body of operating experience exists, it is difficult to determine these fire modeling parameters. In the absence of data, a Monte Carlo sampling approach is used that considers the size, content, and construction of motors and dry transformers.

Lastly, Section 7, the main control board (MCB), uses a combination of operating experience and fire modeling parameters to support the development of an event tree that more closely models the expected progressions of fire events in the MCB. Similar to Section 5, a Monte Carlo sampling process is used to determine the likelihood of end states for fire scenarios that grow beyond the component of origin.

KEY FINDINGS

- Sections 2 and 3 provide the technical basis and guidance for developing a horizontal ZOI caused by thermal radiation. Guidance is provided for unobstructed configurations (applicable to all ignition source ZOIs) and obstructed radiation (applicable to ignition sources where the radiation source may be shielded by a metal wall).

  Both the point source model and solid flame model are reviewed for their applicability to the ignition sources commonly found in NPPs. The solid flame model should generally be the preferred calculation method over the point source model because of the potential for large over and under predictions of the point source model. This is shown in Figure 2-9, where the point source model has two bands—one of larger overprediction and one of underprediction over the adjusted solid flame model.

  The solid flame model is adjusted in Section 2.2.3 to reduce the emissive power for small fires to limit the radiant fraction to the assumed radiant fraction. There are two methods to accomplish this: by correcting the emissive power so that the effective radiant fraction does not exceed the assumed radiant fraction (see Equation 2-5) or using the Shokri-Beyler correlation as is but modifying the target critical flux as if the correct emissive power were used (see Equation 2-6).

  Following this review of the empirical equations, Section 2.3 describes the approach and simulations for evaluating obstructed radiation. For obstructed radiation, prior to this research, the horizontal ZOI is computed as if it were an unobstructed fire. Similar to the obstructed plume approach, a series of simulations were performed using FDS to gather data and insights on the horizontal ZOI. Table 3-5 and Table 3-6 provide a summary of the results for medium (open and closed, respectively), and Table 3-7 and Table 3-8 for large electrical cabinets (open and closed, respectively). Table 3-9 (unvented faces) and Table 3-10 (vented faces) present results for electrical cabinets binned as Groups 1, 2, and 3 in NUREG-2178. Small cabinet radiation guidance is in Table 3-11. The results of the FDS studies can be used to more realistically define the horizontal ZOI.

- Section 4 provides screening guidance, technical basis for the assignment of a conditional probability of fire spread, and recommendations for characterizing the fire growth for fires scenarios resulting in propagation from one electrical cabinet to another.

Fire spread from one electrical enclosure to another does not need to be postulated for the following configurations (see Section 4.2.2 for the technical basis for each configuration):

- Double wall
- Open top/vertically oriented cables
- Very low fuel load
- Group 4c: small enclosure
- Low fuel/steel partition
- Low fuel exposing/very low exposed
- Group 1: switchgear and load centers
- Group 2: motor control center

For fire scenarios that do not meet one of the preceding configurations, fire spread should be postulated using a 0.02 split fraction for the multi-enclosure fire scenario. Fire spread should be limited to one adjacent electrical enclosure. See Section 4.4.2 for full details for the exposing and exposed electrical enclosure fire characteristics.

- Section 5 describes a mathematical approach to derive HRRs and fire duration for a variety of motor and indoor dry transformers based on size, content, construction, and material type.

  For electric motors counted in Bins 2, 9, 14, 21, 26, and 32, the recommended HRRs are summarized in the following table:

  HRR distribution parameters for motors

Motor Classification Group	Motor Size (horsepower)	α	β	75th Percentile (kW)	98th Percentile (kW)
A	>5–30	1.34	3.26	6	15
B	>30–100	1.17	8.69	14	37
C	>100	1.10	24.19	37	100

  Section 5.1.6.3 provides guidance on the fire base height for electric motors. The following growth, steady burning, and decay durations should be used for electrical motor fires (see Section 5.1.6.2):

  - Growth: 2 minutes, t-squared growth
  - Steady burning: 13 minutes
  - Decay: 2 minutes, linear decay

For dry transformers, the recommended HRRs are summarized in the following table:

HRR distribution parameters for dry transformers

Transformer Classification Group	Transformer Power (kVA)	α	β	75th Percentile (kW)	98th Percentile (kW)
A	>45–75	0.38	12.84	6	30
B	>75–750	0.41	28.57	15	70
C	>750	0.46	50.26	30	130

Section 5.2.6.3 provides guidance on the fire base height for dry transformers. The following growth, steady burning, and decay durations should be used for dry transformers (see Section 5.2.6.2):

- Growth: 0 minutes
- Steady burning: 10 minutes
- Decay: 10 minutes, linear decay

- Section 6 provides guidance and validation on the use of the new fire location factor. EPRI report 3002005303 previously studied the fire plume behavior near wall and corners. In 2017, the National Institute of Standards and Technology conducted a number of experiments involving fires near a corner or along a wall. The results of the experiments showed similar trends as in 3002005303. Consistent with the EPRI report, the fire location factors in the following table should be used for corner and wall configurations:

New fire location factor

Configuration	Location Factor 0–0.3 m (1 ft)	Location Factor 0.3 m–0.6 m (1–2 ft)	Location Factor >0.6 m (2 ft)
Corner	4	2	1
Wall	1	1	1

The model bias and uncertainty statistics for the plume temperature rise are calculated using the Heskestad fire plume correlation and shown in the following table. The results compare the different bias using both the traditional fire location factor and the modified fire location factor, as developed in EPRI report 3002005303.

Bias and uncertainty of modified and unmodified Heskestad Fire Plume Correlation for wall and corner configurations

Configuration, Location Factor Method	Bias	Model Uncertainty	Experimental Uncertainty [23]
Wall, traditional method (k_F = 2)	1.66	0.06	0.07
Wall, modified (k_F = 1)	1.10	0.13	0.07
Corner, traditional method (k_F = 4)	1.94	0.38	0.07
Corner, modified (k_F = 4,2,1)	1.27	0.15	0.07

- Section 7 provides a data review of fire events in the MCB and a new event tree for modeling the progressions of a MCB fire. This approach can be used as an alternative to Appendix L of NUREG/CR-6850.

  A revised at-power Bin 4 ignition frequency of 2.05E-03/year (see Table 7-3) is apportioned throughout the MCB as described in Section 7.3.2, and an updated control room non-suppression rate of 0.385 (see Table 7-6) is calculated.

  Section 7.2.1 provides guidance on how to develop a screening core damage frequency (CDF) for individual MCB panel sections. This screening CDF is used to determine which panels are candidates for more detailed treatment in Section 7.2.2. The more detailed treatment evaluates the following damage states: single subcomponent, small group of subcomponents, fire limited to a single panel, multipanel fires, and abandonment scenarios (including both loss of control and loss of habitability). Sections 7.4 through 7.7 detail the review of operating experience and analyze the fire model inputs that feed into the Monte Carlo sampling process.

  The event tree is summarized in Section 7.8 with Figure 7-11 depicting the event tree and Table 7-17 outlining the input parameters for the event tree model.

WHY THIS MATTERS

Although the base methodology for FPRA has been around for more than a decade, NUREG/CR-6850 (EPRI 1011989) in many cases does not provide the necessary methods or data to calculate a realistic representation of plant risk caused by fire. As a result, the FPRAs that have been developed contain oversimplifications and assumptions that lean in the conservative direction. Over the years, the industry and the NRC have worked to develop refined methods and data that are more realistic and representative of the operating experience with respect to fire. This report contains several approaches that can be used when developing or maintaining FPRAs. The refined methodologies presented in the report leverage the expertise from implementing and supplementing the existing methods with new operating experience, mathematical modeling and simulation, and experimental results to provide additional tools to more accurately characterize fire risk.

HOW TO APPLY RESULTS

The methodologies presented in this report were developed acknowledging the different states of development of FPRAs. The approaches described in this report can be used by analysts developing or maintaining FPRAs. The research and technical basis are typically presented up front, and the guidance for the user is described at the end of the section. A summary of the methodologies is found in Section 8.

LEARNING AND ENGAGEMENT OPPORTUNITIES

Users of this report may be interested in FPRA training, sponsored jointly between EPRI and the U.S. NRC-RES. The two modules that may be of interest are Module III: Fire Analysis and Module V: Advanced Fire Modeling. The Fire Analysis course is geared toward probabilistic risk assessment practitioners responsible for treating those aspects related to fire growth and damage assessment. This discusses the basics of plant partitioning, fire frequency analysis, and the development and analysis of fire scenarios from fire ignition to target impact and fire suppression. The Advanced Fire Modeling course covers fundamentals of fire science and guidance on the use of fire models to predict fire generated conditions that may impact NPP safety functions.

EPRI CONTACT: Ashley Lindeman, Senior Technical Leader, 704.595.2538, alindeman@epri.com

NRC CONTACT: David Stroup, Senior Fire Protection Engineer, 301.415.1649, david.stroup@nrc.gov

PROGRAMS: Nuclear Power, P41; and Risk and Safety Management, P41.07.01

IMPLEMENTATION CATEGORY: Plant Optimization

CITATIONS

This report was prepared by the following:

U.S. Nuclear Regulatory Commission
Washington, D.C. 20555-0001
Principal Investigators:
N. Melly
B. Metzger
D. Stroup

Under contract to NRC:

Consultant
42 Sacred Way
Glorieta, NM 87535
Principal Investigator:
S. Nowlen

Electric Power Research Institute
3420 Hillview Avenue
Palo Alto, CA 94304
Principal Investigator:
A. Lindeman

Under contract to EPRI:

Jensen Hughes, Inc.
3610 Commerce Dr. Suite 817
Baltimore, MD 21227
Principal Investigators:
J. Floyd
F. Joglar
J. DeJoseph
O. Gonzalez
V. Ontiveros
J. Williamson

Engineering Planning and Management
5520 Dillard Drive, Suite 250
Cary, NC 27518
Principal Investigator:
D. Miskiewicz

Duke Energy
526 S Church St.
Charlotte, NC 28202
T. Groch

This report describes research sponsored jointly by the U.S. Nuclear Regulatory Commission's (NRC) Office of Nuclear Regulatory Research (RES) and the Electric Power Research Institute (EPRI).

The report is a corporate document that should be cited in the literature in the following manner: *Refining and Characterizing Heat Release Rates from Electrical Enclosures During Fire, Volume 2: Fire Modeling Guidance for Electrical Cabinets, Electric Motors, Indoor Dry Transformers, and the Main Control Board*, U.S. Nuclear Regulatory Commission, Office of Nuclear Regulatory Research (RES), Rockville, MD, and Electric Power Research Institute (EPRI), Palo Alto, CA: 2019. NUREG-2178, V2, and EPRI 3002016052. (While the NRC and EPRI reports have different publication dates, they are essentially the same report.)

ACKNOWLEDGMENTS

A draft of this report was Noticed in the Federal Register for public comment on June 28, 2019, (84 FR 31125). The authors thank those members of the public and organizations who provided comments during the public comment period, specifically Victoria Anderson, Nuclear Energy Institute; Georgi Georgiev, Jacobsen Analytics, Ltd; Dennis Henneke; and the Center for Nuclear Waste Regulatory Analysis (CNWRA); all of whom provided insightful comments on the draft of the report. The authors' resolution of comments on the draft report is available in the Agencywide Documents Access and Management System (ADAMS) under accession number ML19347B923. The comments received from CNWRA and their responses to the authors' resolution of those comments are available in ADAMS under accession numbers ML19345F202 and ML19345F221, respectively.

ACRONYMS

AST	adiabatic surface temperature
AWG	American wire gauge
BWR	boiling water reactor
CCDP	conditional core damage probability
CDF	core damage frequency
CFAST	Consolidated Fire Growth and Smoke Transport Model
CFD	computational fluid dynamics
CLERP	conditional large early release probability
EHC	electro-hydraulic control
EPRI	Electric Power Research Institute
FAQ	frequently asked question
FDS	Fire Dynamics Simulator
FDT^s	Fire Dynamics Tools
FFT	fast Fourier transform
FEDB	fire events database
FPIE	full-power initiating events
FPRA	fire probabilistic risk assessment
FR	flame-retarded
HEAF	high-energy arcing fault
HGL	hot gas layer
HP	horsepower
HR	high resolution
HRR	heat release rate
HRRPUA	heat release rate per unit area
HVAC	heating, ventilation, and air conditioning
I&C	instrumentation and controls
kW	kilowatt

LPSD	low power shut down
LR	low resolution
MCB	main control board
MCC	motor control center
MCR	main control room
MSO	multiple spurious operation
MOV	motor-operated valve
MR	medium resolution
NEMA	National Electrical Manufacturers Association
NFPA	National Fire Protection Association
NIST	National Institute of Standards and Technology
NPP	nuclear power plant
NRC	Nuclear Regulatory Commission
NSP	non-suppression probability
PAI	polyamide-imide
PEI	polyesterimide
PRA	probabilistic risk assessment
PUR	polyurethane
PWR	pressurized water reactor
QTP	qualified thermoplastic
RES	NRC's Office of Nuclear Regulatory Research
SF	severity factor
SFPE	Society of Fire Protection Engineers
SIS	Synthetic Insulated Switchboard Wire or XLPE-Insulated Conductor
SNL	Sandia National Laboratories
THIEF	Thermally Induced Electrical Failure
TP	thermoplastic
TS	thermoset
US	United States
VBA	Visual Basic for Applications
WTC	World Trade Center
ZOI	zone of influence

1
INTRODUCTION

1.1 Background

In 2005, the Electric Power Research Institute (EPRI) and the Nuclear Regulatory Commission's (NRC's) Office of Nuclear Regulatory Research (RES) issued a joint technical report titled *EPRI/NRC-RES Fire PRA Methodology for Nuclear Power Facilities* (EPRI 1011989, NUREG/CR-6850) [1].[1] This report documented methods, tools, and data for conducting a fire probabilistic risk assessment (FPRA) for a commercial nuclear power plant (NPP) application. Following this publication, many utilities developed FPRAs using the guidance in NUREG/CR-6850 to support risk-informed applications, including the transition to National Fire Protection Association (NFPA) 805 among others. The results obtained from the FPRA models have suggested specific elements in the fire scenario analysis where improved methods and/or guidance can reduce conservatism and increase realism in the risk estimates. Consequently, over the past 15 years, FPRA research covering the areas of fire ignition frequencies (for example, NUREG-2169 [EPRI 3002002936]), fire modeling (for example, NUREG-2178 Vol. 1 [EPRI 3002005578] and NUREG/CR-7197), human reliability analysis (NUREG-1921 [EPRI 1023001]), and spurious operations (for example, NUREG/CR-7150 Vol. 2 [EPRI 3002001989]) have been published and made available to the industry.

The first volume of NUREG-2178 [2] was published in April 2016. This document included methods focused on refining the modeling of fires in electrical cabinets, including new heat release rate (HRR) probability distributions and an obstructed fire plume model. Upon publication, the working group discussed developing additional methods to further refine the modeling of selected ignition sources within the FPRA. As in the case of Volume 1 of NUREG-2178, this volume describes improved methods for achieving realism by reducing some of the conservatisms present in current methods. As such, the guidance and methods described in this report do not replace or invalidate existing methods or guidance, but rather, provide more realistic methods and data than previously published.

This second volume of NUREG-2178 includes the following methods that can be used for refining the modeling of selected ignition sources:

- **Flame radiation and obstructed radiation**. This report describes and reviews existing methods for calculating flame radiation. From that discussion, the report offers a modified approach for computing flame radiation. The report then develops a detailed method for determining the thermal radiation impact from fires inside electrical cabinets. As such, this approach extends the research documented in NUREG-2178 Volume 1 associated with modeling plume temperatures generated by fires inside electrical cabinets (that is, the obstructed plume temperature model) by developing guidance on predicting thermal radiation that is obstructed by vented or unvented cabinet walls.

[1] NUREG/CR-6850 (EPRI 1011989) is hereafter referred to as *NUREG/CR-6850*.

- **Fire propagation between adjacent electrical cabinets**. The report describes a detailed approach for modeling fire propagation between vertical sections in a bank of electrical cabinets. This method expands upon the guidance provided in Appendix S of NUREG/CR-6850.
- **HRRs for electric motors and dry transformers**. Appendix G of NUREG/CR-6850 recommended HRR values for electric motors and dry transformers based on the values assessed for electrical cabinet fires. However, electric motors and dry transformers are different in terms of ignition sources, modes of ignition, and combustible configuration in comparison to electrical cabinets. Consequently, this report recommends revised HRRs for electric motors (including those motors associated with pumps) and dry transformers based on the size (horsepower or kVA, respectively) of the equipment.
- **Fire location factor**. Existing guidance suggests that fires adjacent to walls or in corners may generate elevated plume temperatures when compared with fires away from these surfaces (sometimes referred to as the *wall/corner plume correction factors*). This report presents new guidance for estimating the plume temperatures for ignition source fires located along walls or in corners. The guidance is applicable to both fixed and transient ignition sources.
- **Main control board**. Appendix L of NUREG/CR-6850 described a simplified model for determining the severity factor (SF) and non-suppression probability (NSP) for fire scenarios associated with the main control board (MCB) based on a predefined zone of influence (ZOI) (that is, a defined set of damage target components). Although easy to apply, this model limits the ability to integrate the MCB scenarios with other elements associated with the risk quantification of fire scenarios inside the main control room (MCR). This report describes a comprehensive event-tree based approach for characterizing the fire scenario progression following ignition of a component in the MCB.

1.2 Technical Approach

Similar to Volume 1 of NUREG-2178, the research documented in this report was developed by a working group that included members of both the regulator and the nuclear power industry. The working group members are listed, along with their affiliations, are as follows:

- Joelle DeJoseph, Jensen Hughes
- Tim Groch, Duke Energy
- Francisco Joglar, Jensen Hughes
- Ashley Lindeman, EPRI
- Nicholas Melly, NRC-RES
- Brian Metzger, NRC-NRR
- David Miskiewicz, Engineering Planning and Management (EPM)
- Steven Nowlen, Consultant[2]
- David Stroup, NRC-RES

[2] Steven Nowlen (retired) was a distinguished member of the technical staff at Sandia National Laboratories from 1983 to 2014 and is now a private consultant.

In general, the working group debated and discussed the topics, proposed a technical path forward, and oversaw the technical work. The following subject matter experts assisted in the data analysis, numerical simulation studies, and the development and review of this report:

- Dr. Jason Floyd (Jensen Hughes): flame radiation, obstructed radiation, motor/transformer HRRs, and MCB modeling
- Dr. Justin Williamson (Jensen Hughes): MCB modeling, motor/transformer HRRs, fire location factors, fire propagation between adjacent electrical cabinets
- Dr. Orelvis Gonzalez (Jensen Hughes): MCB modeling and motor/transformer HRRs, fire propagation between adjacent electrical cabinets
- Dr. Victor Ontiveros (Jensen Hughes): MCB modeling, motor/transformer HRRs, fire location factor, and fire propagation between adjacent electrical cabinets

1.3 Terminology

The research documented in this report deals with the analysis of fires that originate in electrical or electronic equipment housed within a support structure, generally metal, that is either enclosed or made up of open rack-type panels or supports. In this report, these housings are interchangeably referred to as *electrical enclosures* and *electrical cabinets*.

The terms *electrical enclosures* and *electrical cabinets*, as used in this report, are inclusive of cabinets, panels, and relay racks because those terms are used in NUREG/CR-6850 and other related FPRA documents and standards.

In NUREG/CR-6850 the term *enclosure* is used in two other contexts—the regulatory issue of cables and components that share a common enclosure (for example, cables routed in the same cable tray), and the modeling of enclosure fires (that is, fires that occur within a room as opposed to fires that occur in an open unconfined space). The discussion presented in Section 4 of this report relates to fires spreading between adjacent electrical enclosures and uses the term *enclosure fire* to represent an electrical enclosure. The reader is cautioned to consider the context of the discussion, specifically, with respect to the use of the term *enclosure*.

1.4 Report Organization

Each section in this report is focused on a specific technical approach or methodology. The report is organized as follows:

Section 2 examines the underlying assumptions impacting the solid flame and point source models routinely used for calculating flame radiation. An adjustment to the solid flame model calculation is presented, including validation of the proposed change. For scenarios where the fire is shielded by a metal cabinet wall, a series of simulations were performed to understand the effect of this shielding. The results of these simulations are presented in Tables 2-3 through 2-6.

Section 3 provides guidance for implementing the results and insights from the Fire Dynamics Simulator (FDS) calculations of obstructed radiation. The results can be implemented in one of three ways: 1) screening targets based on adjusted radiation zone of influence, 2) reducing the severity factor for targets, and 3) use in detailed fire modeling.

Section 4 provides additional guidance beyond that in NUREG/CR-6850, Appendix S for screening fire spread to adjacent cabinets. For scenario configurations evaluating cabinet-to-cabinet propagation that are not screened, a conditional probability of a multicabinet fire is calculated along with guidance related to the secondary fire timing and intensity.

Section 5 investigates electrical fire characteristics specific to motors and dry transformers using a Monte Carlo sampling technique that randomizes the parameters that may affect the fire's intensity and duration. Some of the model input parameters are based on insights from a review of the number and range of equipment sizes expected to be considered in the FPRA for these ignition sources.

Section 6 covers revised guidance on fire location factors, which need to be considered for fires located near a wall or in a corner location, and to determine when the correction factors apply. The guidance includes model validation against a set of experiments performed at the National Institute of Standards and Technology (NIST) in August 2017.

Section 7 provides a new and comprehensive model for the evaluation of a fire scenario progression for fires initiated within the MCB.

Section 8 provides the summary and conclusions of the research documented in this report.

Section 9 lists the references used in the development of this report.

Appendix A covers the development of a damage integral method to model time to failure for cables exposed to elevated temperatures or heat fluxes based on the empirical results documented in NUREG/CR-6850 Appendix H.

Appendix B compares the results from the obstructed radiation research against the adjusted solid flame model (Section 3 compares the obstructed radiation results against the unadjusted solid flame model).

Appendix C provides the template for the FDS input files supporting the development of obstructed radiation described in Sections 2 and 3.

Appendix D presents five example applications of the cabinet-to-cabinet fire spread guidance covered in Section 4.

2
BASIS OF RADIATION ZOI: MOTIVATION, METHODOLOGY, AND SUMMARY OF INSIGHTS FROM FDS RUNS

2.1 Motivation

The motivation for the research is to increase realism in determining the horizontal zone of influence (ZOI), typically based on radiation emitted, for a fire either out in the open or inside of an electrical cabinet. These two categories are respectively referred to as *unobstructed* and *obstructed* fires. For fire probabilistic risk assessment (FPRA) applications, there are three basic approaches to computing the horizontal ZOI: a point source model [3], a solid flame model [3], or the use of a field model such as the Fire Dynamics Simulator (FDS) [4, 5].

As implemented in NUREG-1805 Fire Dynamics Tools (FDT^s) [3], the first two approaches have underlying assumptions that have not been critically examined in the context of nuclear power plant (NPP) ignition sources and specifically the application to electrical cabinets. These assumptions and their impact on the use of those approaches is examined in Section 2.2. It should be remembered that the correlations in NUREG-1805 are based on general fire protection engineering applications. One of the goals of this report is to customize these simple correlations to specific NPP applications.

In addition, there is no explicit guidance on how to evaluate the radiation (horizontal) ZOI for an electrical cabinet fire (that is, obstructed fire configuration). In the absence of guidance, a typical approach is to evaluate an electrical cabinet fire as if it were a fire in the open—that is, an unobstructed fire. This method, however, can be overly conservative because it does not account for the radiation shielding provided by the wall of the electrical cabinet. This is examined in detail in Section 2.3.

2.2 Unobstructed Radiation

The FDT^s correlations [3] for flame radiation are largely based upon Beyler's chapter on large outdoor hydrocarbon fires in the Society of Fire Protection Engineers (SFPE) Handbook [6]. This chapter is focused on assessing hazards from tank farms, petrochemical processing facilities, and similar locations where large quantities of hydrocarbons are stored and/or processed. Large fires in this case means fires that could be tens of meters in diameter, and the hazards of concern include damage to structures (at incident heat flux exposures over 20 kW/m^2), radiative ignition of exposed combustibles (at incident heat flux exposures over 10 kW/m^2), and skin burns (at heat flux exposures above 1 kW/m^2). The next two sections investigate the FDT^s correlations as they are currently used in FPRA applications. The fires postulated in a FPRA are typically an order of magnitude smaller in physical size.

2.2.1 Point Source Model

The point source model is depicted in Figure 2-1. A fire characterized by a diameter, *D*, a radiative fraction, χ_r, a heat release rate, $\dot{Q}$, and a flame length, L_F, exposes a target at some distance, *L*, from the fire. For the point source model, the radiative heat flux at the target, $\dot{q}_r^{"}$, is computed by uniformly distributing radiative output of the fire, $\chi_r\dot{Q}$, over a sphere whose radius is the distance of the target to the center of the sphere, $D/2 + L$. There are two primary assumptions to the point source model, as follows:

- The radiative emissions from the fire are isotropic (that is, emission has the same magnitude when measured in different directions). For an unobstructed fire, this is a reasonable assumption. Photons carrying radiative heat away from the fire will be emitted in random directions with no bias toward any single direction.
- The fire can be considered a point with zero surface area when computing the radiation view factor. This requires that the target be located at a sufficiently large distance from the fire. The FDT^s radiation models are largely based upon the work of Shokri and Beyler [6], who indicate that this assumption is satisfied if the target distance is 2.5 times the characteristic size of the fire, the larger of the flame length or the diameter. In radiation protection, where the point source approximation is often used, a typical rule of thumb is 3 times the largest dimension of the source [7].

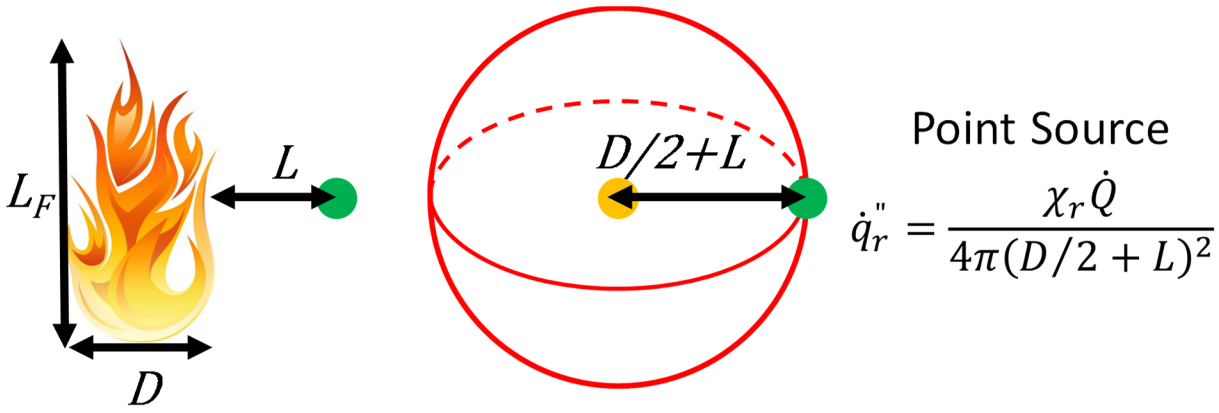

Figure 2-1
Illustration of point source model

In FPRA applications, the primary concern is the fire's ability to damage targets located away from the fire. Those targets are generally electrical cables but may also be other targets such as sensitive electronics. Appendix H of NUREG/CR-6850 [1] defines screening fluxes for these items as 3 kW/m^2 for sensitive electronics, 6 kW/m^2 for thermoplastic (TP) cable, and 11 kW/m^2 for thermoset (TS) cables. Using the point source model, the target distances for these heat fluxes can be computed for a range of typical ignition sources. Table 2-1 shows the fire size (diameter and flame length computed using the FDT^S, Heskestad's flame length correlation). and total distances, D/2+L, required to meet previously covered heat fluxes for a range of ignition sources. A 30% radiative fraction is assumed for all fires—this is the default value in the FDT^S spreadsheet for radiant heat flux, and typical FPRA practice is to use this default. Except for large oil spills, the ratio of target distance for threshold damage to the fire source dimension is one or less for all target types. It is not until the 379 l (100 gal) spill at the threshold distance for sensitive electronics that ratios close to 2.5 are seen. Although NUREG-1824 [8] indicates that the point source model is conservatively biased, it should be recognized that in general,

NPP ignition sources that are capable of damaging a target do not meet the assumptions to justify the use of the point source model. The impact of this will be assessed in Section 2.2.4, where it will be shown that although the point source model is generally conservative, there are cases where its use can be more nonconservative than other simple calculation methods.

Table 2-1
Evaluation of point source model applicability for various ignition sources

Source	98th Percentile Fire Size (kW [Ref.])	Source Dimension (m) [ft]		Distance for Heat Flux (m) [ft]			Distance Ratio		
				Target Flux (kW/m2)			Target Flux (kW/m^2)		
		D	LF	3	6	11	3	6	11
Small cabinet (0.004 m^3 [1 ft^3] cube)	45 [2]	0.34 [1.1]	0.73 [2.4]	0.60 [2.0]	0.42 [1.4]	0.31 [1.0]	0.82	0.58	0.43
Medium cabinet (0.05 m^3 [12 ft^3], 0.6 m x 0.6 m x 0.9 m [2 ft x 2 ft x 3 ft])	325 [2]	0.69 [2.3]	1.67 [5.5]	1.6 [5.3]	1.1 [3.7]	0.84 [2.8]	0.96	0.68	0.50
Large cabinet (0.2 m^3 [54 ft^3], 0.9 m x 0.9 m x 0.6 m [3 ft x 3 ft x 6 ft])	1000 [2]	1.03 [3.4]	2.67 [8.8]	2.8 [9.3]	2.0 [6.5]	1.5 [4.8]	1.1	0.75	0.55
Small motor (0.1 m^2 [1 ft^2] base)	69 [1]	0.34 [1.1]	0.92 [3.0]	0.74 [2.4]	0.52 [1.7]	0.39 [1.3]	0.80	0.56	0.42
Transient (Three 41.64-l [11-gal] bags)	317 [1]	0.50 [1.6]	1.8 [6.0]	1.6 [5.2]	1.1 [3.7]	0.83 [2.7]	0.86	0.61	0.45
Lube oil spill (3.8 l [1 gal])	6700 [9]	2.6 [8.5]	5.3 [17]	7.3 [24]	5.2 [17]	3.8 [13]	1.4	1.0	0.7
Lube oil spill (38 l [10 gal])	67000 [9]	8.3 [27]	12 [38]	23 [76]	16 [54]	12 [40]	2.0	1.4	1.0
Lube oil spill (380 l [100 gal])	160000 [9]	13 [43]	15 [49]	36 [120]	25 [82]	19 [62]	2.3	1.7	1.2

2.2.2 Solid Flame Model

The solid flame model is illustrated in Figure 2-2. A fire characterized by a diameter (m), D, and a flame length (m), L_F, exposes a target at some distance (m), L, from the edge of the fire and some distance (m), H, above the base of the fire. The solid flame model assumes that the fire can be represented as a right, circular cylinder with dimensions of the flame height and the diameter. The cylinder is assumed to uniformly emit radiation from its surface. The radiative

heat flux at the target (kW/m^2), $\dot{q}_r^{''}$, is computed by multiplying the emissive power of the cylinder, *E* in kW/m^2, by the view factor, *F*, of the cylinder from the target. The view factor computation depends on the fire size, target distance, target orientation, and any wind effects (usually not considered) on the fire.

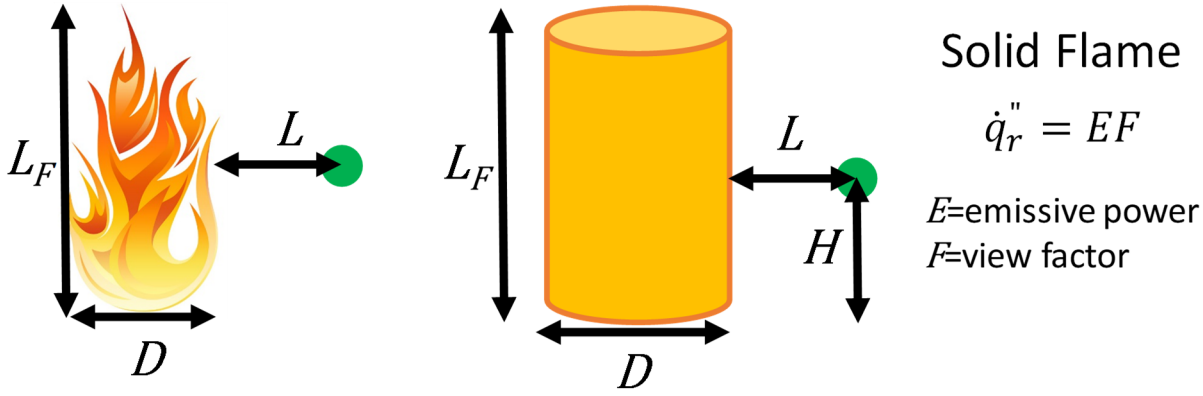

Figure 2-2
Illustration of solid flame model

Consider the implications of this model by drawing a surface, *S*, completely around the fire, as shown on the left side of Figure 2-3. Using the solid flame model, one can compute the radiant flux normal to this surface at every point around the cylinder. If the flux is integrated over the entire surface, the result is the total radiant heat output of the fire (kW), $\dot{q}_r$. Normalizing this by the total heat release rate (HRR) of the fire (kW), $\dot{q}$, will yield the radiant fraction, χ_r. This is shown in Equation 2-1. Because the emissive power is assumed to be constant over the cylinder, it can be pulled outside the integral, leaving the integration of the view factor over the surface of the cylinder.

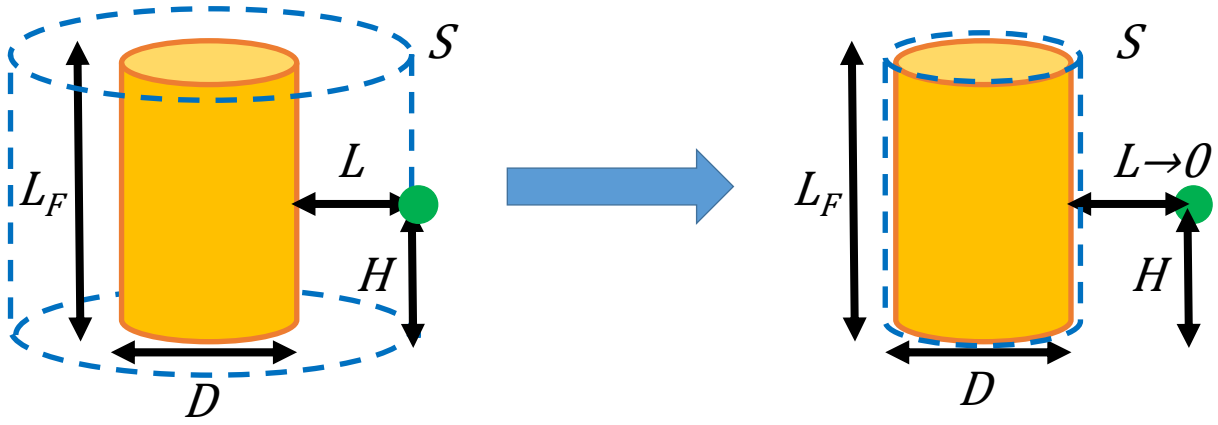

Figure 2-3
Computing the radiant heat release using the solid flame model

$$\chi_r = \frac{\iint \dot{q}_r'' dS}{\dot{Q}} = \frac{\iint EF(L,H) dS}{\dot{Q}} = \frac{E \iint F(L,H) dS}{\dot{Q}} = \frac{\dot{q}_r}{\dot{Q}} \quad \textbf{(2-1)}$$

If the integration is performed at the limit of $L \rightarrow 0$, the view factor, F, will be 1 everywhere except for the top and bottom edge of the cylinder. However, the edges mathematically have zero area in the surface integral; therefore, they can be ignored. The area of bottom of the cylinder can be ignored because measurements of the radiative fraction of fires typically omit the radiant feedback to the fuel surface. Furthermore, if the conservative assumption is made that all of the radiant heat is through the sides of the cylinder—that is, the top is ignored—the result of the integration is shown in Equation 2-2.

$$\chi_r = \frac{E \int F(L,H) dS}{\dot{Q}} = \frac{E \int dS}{\dot{Q}} = \frac{E \pi D \mathrm{L_f}}{\dot{Q}} \quad \textbf{(2-2)}$$

The total radiant flux is the surface area of the cylinder side times the emissive power. The FDT^s compute the emissive power using a correlation from Shokri and Beyler [10]. This correlation, shown in Equation 2-3, was developed using test data from large pool fires.

$$E = 58 \times 10^{-0.00823D} \quad \textbf{(2-3)}$$

where D is the diameter of the pool in meters.

Using Equations 2-2 and 2-3, the effective radiative fraction as a function of fire size can be plotted. Figure 2-4 shows the effective radiative fraction as a function of the fire size. The fire diameter is computed assuming fire Froude numbers of 0.2, a weak diffusion flame fire source, and 2.5, a strong diffusion flame fire source. These values should bound typical FPRA ignition sources. The plot contains two shaded regions. The green shaded region represents the range of HRRs for typical ignition sources other than large oil fires. The orange region represents very large fires, as might occur with large oil spill fires or catastrophic turbine generator fires. Within the green region, for almost all fires, the FDT^s solid flame model results in radiant fractions larger than the typical assumption used in FPRA of $\chi_r = 0.3$. For small fires, the solid flame radiant fraction can exceed one. This is a result of applying the Shokri-Beyler emissive power correlation outside the range of test data used to develop it. For the very large fires, the effective radiant fractions are all lower than 0.3, which is as expected from test data for very large fires. This is a result of soot in cooler regions at the edge of fire shielding the target from the hot core of the fire and plume. The very large effective radiant fractions for small fires means that ZOIs predicted using the FDT^s solid flame model for typical NPP ignition sources lack realism as the use of the Shokri and Beyler correlation results in artificially high radiative heat fluxes.

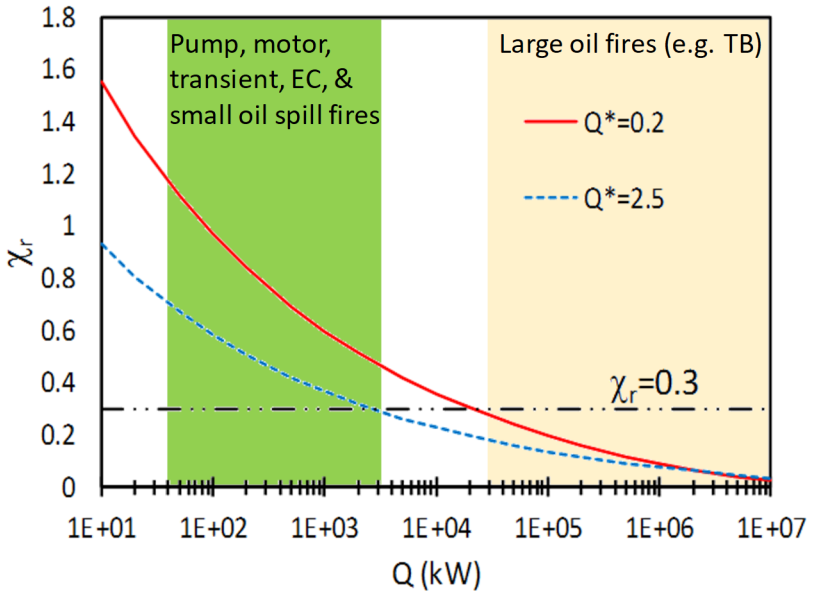

Figure 2-4
Radiant fraction of a fire computed using the solid flame model and two fire Froude numbers

2.2.3 Adjusted Solid Flame Model

2.2.3.1 Proposed Solid Flame Model Change

The results in Figure 2-4 suggest that the emissive power should be reduced for small fires to limit the radiant fraction to the assumed radiant fraction. That is, the product of the emissive power times the area of the cylinder representing the fire in the solid flame model should not exceed the assumed radiant HRR. Based upon the radiant flux equation shown in Figure 2-2, there are two methods to accomplish this.

The first approach is to correct the emissive power so that the effective radiant fraction does not exceed the assumed radiant fraction. Equation 2-2 can be solved for the emissive power.

$$E = \frac{\chi_r \dot{Q}}{\pi D L_f} \qquad \textbf{(2-4)}$$

where E is the emissive power (kW /m^2), χ_r is radiant fraction, $\dot{Q}$ is the total HRR of the fire (kW), D is the diameter (m), and L_F is the flame length (m).

Using Equation 2-4, a modified emissive power correlation can be derived by taking the minimum of Equation 2-3 and Equation 2-4. This is shown in Equation 2-5. This approach could be used in fire modeling tools where the user can either specify their own emissive power or change the method through which the emissive power is computed.

$$E = \mathbf{Min}\left(\mathbf{58} \times \mathbf{10}^{-\mathbf{0.00823}D}, \frac{\chi_r \dot{Q}}{\pi D L_f}\right) \qquad \textbf{(2-5)}$$

As an example, consider a 200 kW fire with a 0.5-m (1.6-ft) diameter and with an assumed 30% radiant fraction. Using the Shokri-Beyler correlation in Equation 2-3, the emissive power is 57 kW/m^2. Using the FDT^s flame height correlation, this fire has a flame height of 1.4 m (4.6 ft).

This gives a cylinder area of 2.2 m^2 (24 ft^2). The radiant HRR of the fire is 60 kW. Based on cylinder area, the emissive power is 60 kW/2.2 m^2 = 27 kW/m^2. This is a factor of 2 lower.

Some modeling tools, such as the current FDT^s worksheet for the solid flame model, do not allow the user to modify the computation of the emissive power. An alternate approach is to use the Shokri-Beyler correlation as is, but the target critical flux is modified to evaluate the ZOI as if the correct emissive power were being used. In effect, one can compensate for having too high of an emissive power by evaluating the ZOI using a higher critical heat flux. This modified target heat flux is determined by multiplying the desired heat flux by the ratio of the Shokri-Beyler correlation to Equation 2-4. This is shown in Equation 2-6. For very large fires with self-shielding, the correction factor is limited to 1 to prevent reduction of the actual critical heat flux.

$$\dot{q}''_{r,critical\ effective} = \dot{q}''_{r,critical} \mathrm{Max}\left(1, \frac{58\times10^{-0.00823D}\pi D L_f}{\chi_r \dot{Q}}\right) \quad \textbf{(2-6)}$$

As an example, the second method is used to determine the ZOI for a thermoplastic target (critical flux of 6 kW/m^2) for the fire that was used in the prior example. From the prior example, the Shokri-Beyler emissive power was 57 kW/m^2 and the emissive power based on the radiant fraction was 27 kW/m^2. The ratio of the two is 2.1. Therefore, rather than using the first method for adjusting the emissive power, the second method could be used, and one would establish the ZOI for the effective critical flux of 2.1 x 6 kW/m^2 = 13 kW/m^2.

The change to the expression for the emissive power does not change the application space of the solid flame model. Existing limits on application, such as the validation range from NUREG-1824 Supplement 1 [8], still apply.

2.2.3.2 Validation of Proposed Change

This approach is validated using the datasets contained in NUREG-1824 Supplement 1 [8]. Three test series were used to validate the approaches in the FDT^s: Fleury [11], National Institute of Standards and Technology (NIST)-NRC [12], and the World Trade Center (WTC) [13].

The Fleury tests [11] used a small gas burner with fire sizes from 100 kW to 300 kW. The rectangular burner was 30 cm (11.8 in.) on one side with the other side having an aspect ratio of 1:1, 2:1, or 3:1. In these tests, a vertical rake of heat flux gauges was positioned at various distances from two adjacent sides of the burner. The heat flux gauges were pointed directly toward the fire. This configuration represents the concept of how a ZOI is determined, the target within the flame height and pointed directly at the fire. Additionally, these fires are representative of the size of many typical ignition sources. This data set is well-suited for validation of the FDT^s as applied in FPRA.

The NIST-NRC tests [12] used a downward pointing spray nozzle in large compartment with varied mechanical and natural ventilation. The effective fire diameter was approximately 1 m (3.3 ft) with fire sizes from 400 kW to 2300 kW. These fire sizes are representative of large electrical cabinets or small quantities of flammable liquid (for example, lube oil). The heat flux gauges in these tests were not generally pointed directly at the fire and were also exposed to hot layer effects. These gauges were placed to measure the exposure to the tops and bottoms of cable trays. This configuration, of gauges not pointed directly toward the fire and exposed to hot layer effects, is not ideal for comparison to the FDT^s.

The WTC tests [13] used two downward pointing spray nozzles in a compartment containing structural steel. The effective fire diameter was approximately 1.6 m (5.2 ft) with fire sizes from 2000 kW to 3200 kW. These fires are representative of small quantities, on the order of 3.8 l (1 gal), of flammable liquid. The heat flux gauges in these tests were positioned to measure the

exposure to the various faces of structural steel members. As with the NIST-NRC tests, the gauges were not pointed toward the fire and included hot layer effects. This test configuration is also not ideal for comparison to the FDT^s.

Results for the Fleury tests are shown in Figure 2-5. The left figure is all of the data from all of the tests. Because the solid flame model assumes a cylindrical fire, that assumption does not hold as well for larger aspect ratios (the fire begins to look less like a cylinder and more like a line). The plot on the right shows only the 1:1 aspect ratio (square burner) tests. For all tests, the left plot shows that the adjusted results have a lower error (σ from 0.35 to 0.28) and a greatly reduced (yet still conservative) bias (δ from 2.3 to 1.1). For just the 1:1 aspect ratio tests, the reductions are σ from 0.62 to 0.19 and δ from 2.1 to 1.1. Because the NIST and WTC test series contain many measurement devices that are not oriented in a manner commensurate with the solid flame model, the all Fleury test results of σ = 0.28 and δ = 1.1 are recommended for the adjusted solid flame model.

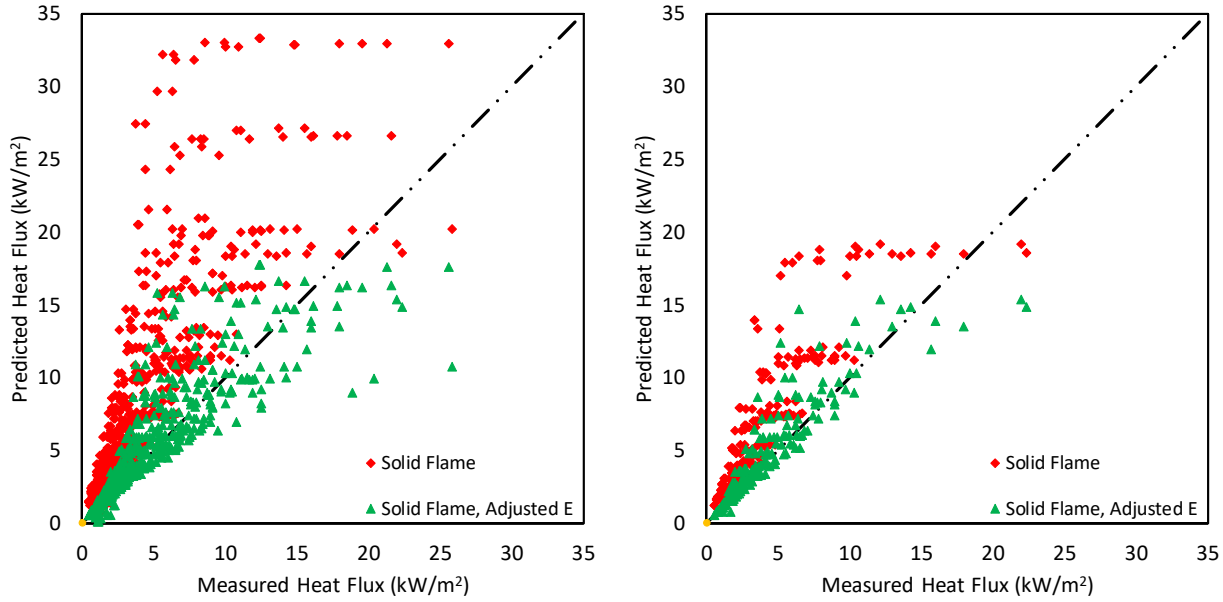

Figure 2-5
Measured versus predicted radiative heat flux for the Fleury Tests [11] using the solid flame model with (green) and without (red) correcting the emissive power (left, all data; right, only 1:1 aspect ratio data)

Results for the NIST-NRC tests are shown in Figure 2-6. During these tests, the radiometers remained fixed. For a few tests, the burner was relocated. The outlier points in the upper left of the left plot are from a test where the fire location resulted in the radiometer being almost directly above the fire. This is a target location where the solid flame model view factor formula is not applicable. The plot on the right is a rescaled plot that removes the outlier data point. Because the fire sizes used in these tests are larger, the results in Figure 2-6 should reflect an expectation that the modified approach will be a minor correction. This is seen in the results. The overall error goes from σ = 0.60 to σ = 0.58, and the bias goes from δ = 2.8 to δ = 2.4. As previously noted, the heat flux gauges in these tests were located on cable trays and were generally not oriented to point directly at the fire resulting in smaller view factors than assumed in the solid flame model. As a result, the solid flame model is biased to significantly over predicting the flux.

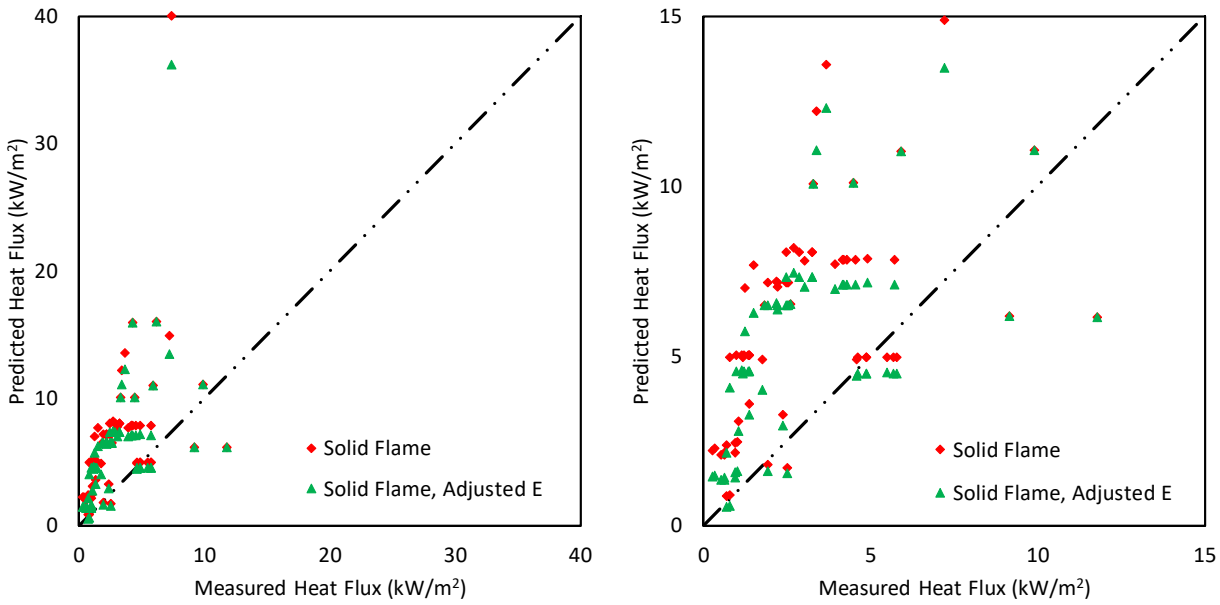

Figure 2-6
Measured versus predicted radiative heat flux for the NIST/NRC tests [12] using the solid flame model with (green) and without (red) correcting the emissive power (left, all data; right, outlier point removed)

Results for the WTC tests are shown in Figure 2-7. As previously noted, the radiometers in these tests were intended to measure exposure to structural elements and were not generally positioned in a manner that measured the direct radiative flux. As with the NIST-NRC results, the FDT^s, which compute peak flux, overpredict by varying degrees for the non-ideally located radiometers. The larger fire sizes better comport with the Shorki-Beyler correlation than the smaller Fleury fires do, and, as a result, little adjustment is occurring for much of the data. A slight reduction in bias (δ = 2.6 to δ = 2.5) but not error (σ = 1.2 in both cases) is seen.

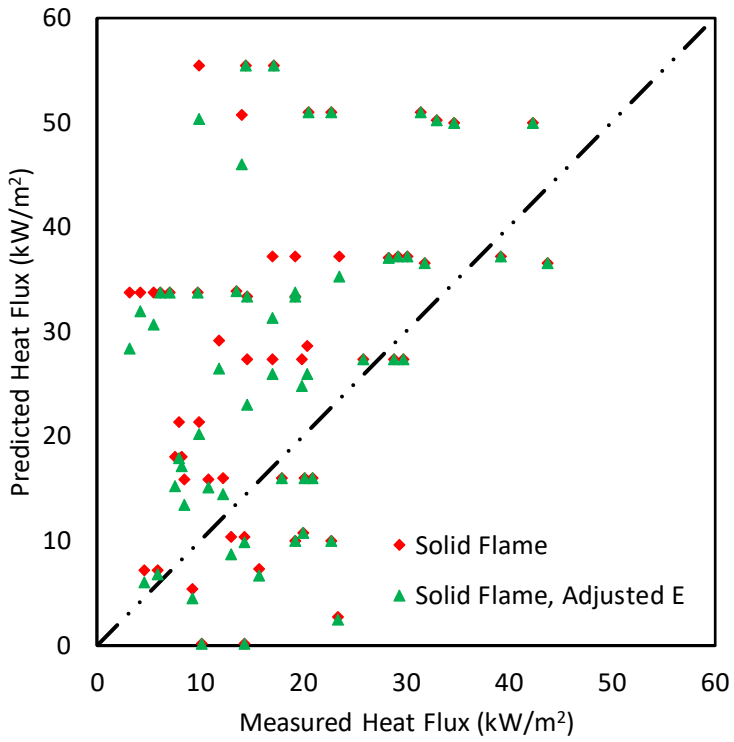

Figure 2-7
Measured versus predicted radiative heat flux for the WTC tests [13] using the solid flame model with (green) and without (red) correcting the emissive power

Results for the three test series are combined in Figure 2-8. Overall, the new solid flame model slightly reduces error from σ = 0.51 to σ = 0.50 and significantly reduces bias from δ = 2.4 to δ=1.3.

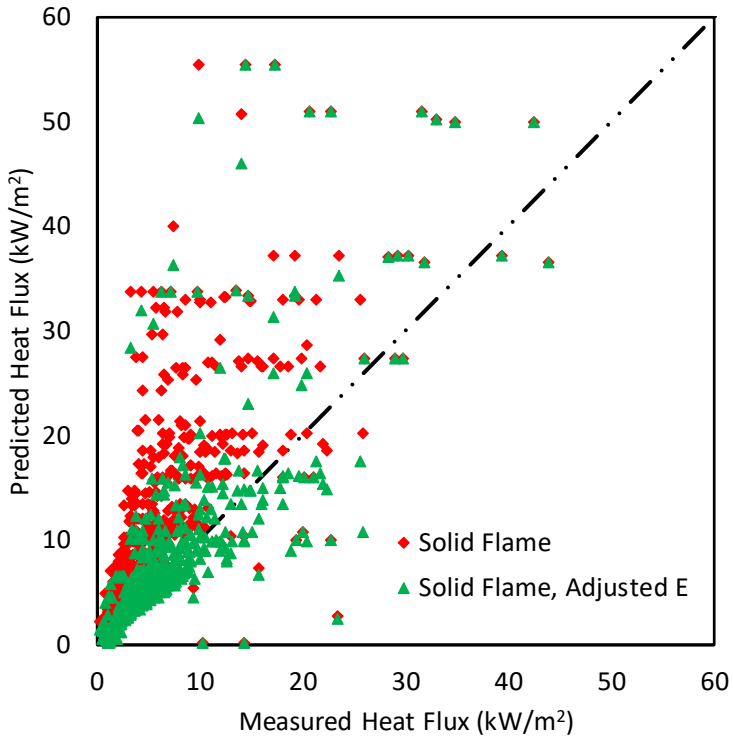

Figure 2-8
Measured versus predicted radiative heat flux for all test series using the solid flame model with (green) and without (red) correcting the emissive power

2.2.4 Revisiting the Point Source Method

As mentioned in Section 2.2.1, the applicability of the point source model is evaluated in the context of the proposed adjusted solid flame model. The Fleury test data are shown in Figure 2-9 along with predictions of both the point source model and the adjusted solid flame model. Both models have similar error and bias with both having $\sigma = 0.28$ and $\delta = 1.1$. However, examining the scatter plot shows that the point source model has two bands where there is a larger overprediction than the adjusted solid flame model and a larger underprediction than the adjusted solid flame model. These bands essentially cancel each other in terms of the bias. The larger errors in these bands are compensated for by lower errors for other test points, resulting in a similar error to the adjusted solid flame model. Overall, in cases where underprediction is occurring, the maximum amount of underprediction can be higher with the point source model than with the solid flame model. This effect is primarily occurring near the base of the flame and at distances of approximately one flame length from the burner (the maximum distance in the Fleury tests).

The conclusion of this is that the adjusted solid flame model should generally be considered a preferred method over the point source method.

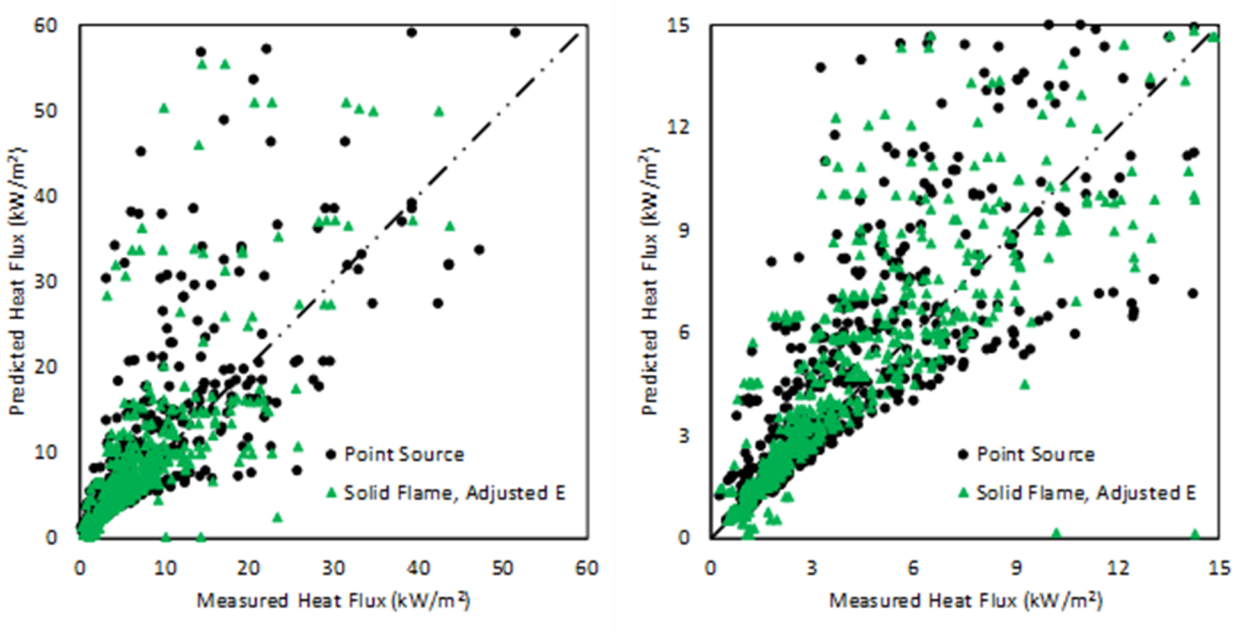

Figure 2-9
Measured versus predicted radiative heat flux for all test series using the point source model (black) and the adjusted solid flame model (green) (left, all data; right, zoomed data)

2.3 Obstructed Radiation

2.3.1 Overview of Current Approach

In the absence of guidance for treating obstructed fires, the horizontal ZOI is computed as if it were an unobstructed fire. This approach does not account for any potential shielding provided by the walls such as those of an electrical cabinet.

To demonstrate the potential conservatism, consider a fire in large, open, electrical cabinet that is 1.8 m^3 (0.91 m x 0.91 m x 2.13 m) with thermoplastic cables. The 98th percentile based on guidance from NUREG-2178 [2] is a 1,000 kW fire. This fire would have an effective diameter of 1.03 m and a FDT^s predicted flame height of 2.7 m (8.9 ft) (the flame would slightly extend outside the door). Using the adjusted solid flame model, emissive power is corrected from 57 to 35 kW/m^2. This results in horizontal ZOIs of 1.65 m (5.4 ft) and 0.93 m (3.1 ft) from the edge of the fire respectively for the TP (6 kW/m^2) and TS threshold damage fluxes (11 kW/m^2).

A target outside the cabinet, however, is not directly exposed to the flame radiation from the fire. Instead, the target sees the metal wall of the cabinet, which is heated by the fire. An estimate of the ZOI for this configuration can be determined by assuming the cabinet wall is heated by a combination of radiation from a blackbody with the same emissive power as the solid flame model plus convection from flame contact to the cabinet wall. This is depicted in Figure 2-10. The cabinet wall temperature can be determined by a steady-state heat transfer computation. The wall temperature can then be used along with a view factor computation for a flat plate to a target to determine the ZOI.

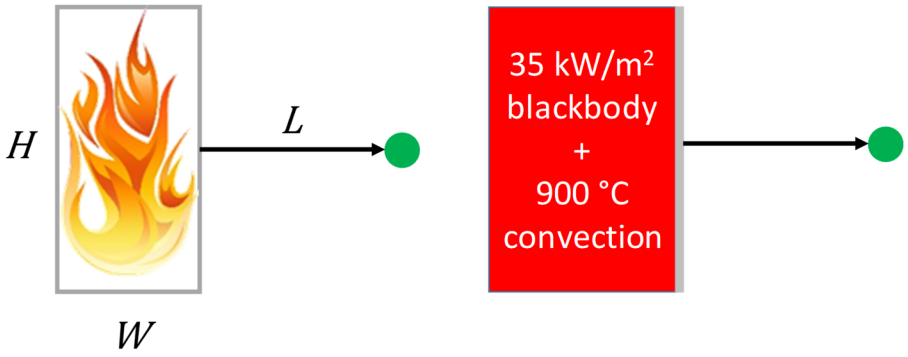

Figure 2-10
Analogous one-dimensional heat transfer problem for a target exposed to an electrical cabinet fire

The steady-state temperature can be evaluated by solving Equation 2-7 for T_w, the cabinet wall temperature.

$$\varepsilon_{in}\left(E-\sigma T_w^4\right)+h_{in}\left(T_g-T_w\right)=\varepsilon_{out}\sigma\left(T_w^4-T_{amb}^4\right)+h_{out}\left(T_w-T_{amb}\right) \qquad (2\text{-}7)$$

where ε_{in} and ε_{out} are the inner and outer cabinet wall emissivities (assume 0.95 for painted surfaces), σ is the Stefan-Boltzman constant (5.67x10^{-8} W/(m^2·K^4)), E is the emissive power of 35 kW/m^2, T_g is the flame temperature 1173 K (900°C) [14], T_{amb} is the ambient temperature 298 K (25°C), h_{in} is the inner convection heat transfer coefficient (35 W/(m^2·K)) [15]), and h_{out} is the outer convection heat transfer coefficient (for natural convection from a vertical flat plate $h_{out}=1.31\Delta T^{1/3}$ W/(m^2·K) [16]). This results in a wall temperature of 798 K (51°C [961°F]). The maximum radiative flux from a uniform temperature flat plate to a target is given by Equation 2-8 [17]:

$$A=\frac{H}{2L};\ B=\frac{W}{2L}$$
$$\dot{q}_r'''=\frac{2\varepsilon\sigma T_w^4}{\pi}\left(\frac{A}{\sqrt{1+A^2}}\tan^{-1}\left[\frac{B}{\sqrt{1+A^2}}\right]+\frac{B}{\sqrt{1+B^2}}\tan^{-1}\left[\frac{A}{\sqrt{1+B^2}}\right]\right) \qquad (2\text{-}8)$$

where *H* and *W* are the plate dimensions—that is, the cabinet wall—and *L* is the distance from the plate (wall) to the target. For TP and TS targets, this respectively gives ZOIs of 1.16 m (3.8 ft) and 0.66 m (2.2 ft) from the edge of the cabinet. Both distances are approximately 70% of the values obtained using the adjusted solid flame model.

2.3.2 NIST Cabinet Fire Test Series

In October 2017, NIST conducted a weeklong test series involving fires in electrical cabinets [18]. The primary goal of the test series was to collect data for validation of the obstructed plume approach in NUREG-2178 [2]. The test series used two electrical cabinet mockups with vents in the top surface of the cabinet, vents along the top of the cabinet walls, and a removable door. Primary data collection was focused on measuring the plume temperature of hot gases exiting the cabinet; however, in support of this EPRI/NRC analysis, NIST also placed eight plate thermometers around the cabinets being tested [19]. Additional test instrumentation included thermocouple trees in the compartment, a thermocouple tree inside the cabinet, and a single cabinet wall temperature thermocouple. The two cabinet mockups are shown in Figure 2-11. As seen by the cabinet dimensions, the two cabinets correspond with the medium and large cabinet types from NUREG-2178.

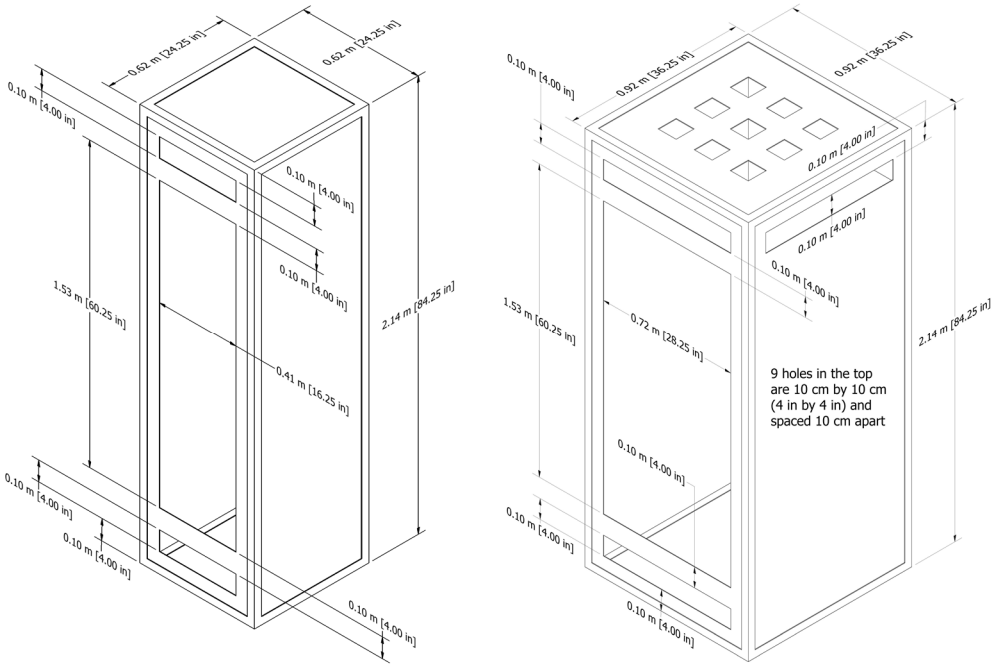

Figure 2-11
Schematic diagrams of NIST cabinet mockups (left, medium; right, large)

The plate thermometers were placed 0.61 m (2 ft) from the sides of cabinets at distances of 0.76 m (2.5 ft) and 1.37 m (4.5 ft) above the floor. Plate numbers 5 and 6 were located facing the removable cabinet door (for example, they saw inside the cabinet in the tests with the door open).

Ten cabinet tests were performed. Six tests were run with the large cabinet (two with the door open), and four tests were run with the medium cabinet (two with the door open). Top vents and side vents were varied test to test. The fire source was a natural gas burner in the bottom of the cabinet. For each test, the fire size was increased in steps every 15 minutes until it reached the maximum TP fire size for the cabinet size and door status based on NUREG-2178—that is, 325 and 1000 kW for medium and large cabinets, respectively.

Plate thermometers measure a quantity called the adiabatic surface temperature (AST) [19]. The estimated error of this measurement is 5% [20]. The AST is a method of expressing the unbiased exposure to a surface, and it is a convenient means to transfer exposure data from computational fluid dynamics (CFD) codes to thermal analysis codes. It represents the equivalent blackbody temperature that would be required to result in the equivalent convective and radiative exposure to the surface. The plate thermometer can be converted to an equivalent incident cold wall radiative flux, $\dot{q}_r''$, using Equation 2-9.

$$\dot{q}_r'' = \sigma T_{AST}^4 + \frac{(h+K)(T_{AST}-T_G)+\rho c\delta \, dT_{AST}/dt}{\varepsilon} - \sigma T_\infty^4 \qquad \textbf{(2-9)}$$

where ε is the plate emissivity (0.85 [20]), σ is the Stefan-Boltzman constant, T_{AST} is the measured plate thermometer temperature, T_G is the measured gas temperature at the plate thermometer, T_∞ is ambient temperature, h is the convective heat transfer coefficient (10 W/(m^2·K) [20]), K is a correction factor (4 W/(m^2·K) [18]), ρ is the plate density (8,470 kg/m^3 [20]), c is the plate specific heat (502 J/(kg·K) [20]), and δ is the plate thickness (0.79 mm) [20].

The plate thermometer equivalent radiative flux computed using Equation 2-9 is compared with FDT^s predictions in Figure 2-12 and Figure 2-13. Figure 2-12 shows a comparison against the

unadjusted FDT^s, and Figure 2-13 shows a comparison against the adjusted FDT^s. The figures show that except for plate thermometers facing an open door, almost all plate thermometers show lower measured values than predicted using either solid flame model. The unadjusted solid flame model shows much larger over predictions of heat flux than the adjusted solid flame model. The error and bias for the unadjusted FDT^s are 0.82 and 4.7. The error and bias for the adjusted FDT^s are 0.62 and 2.2.

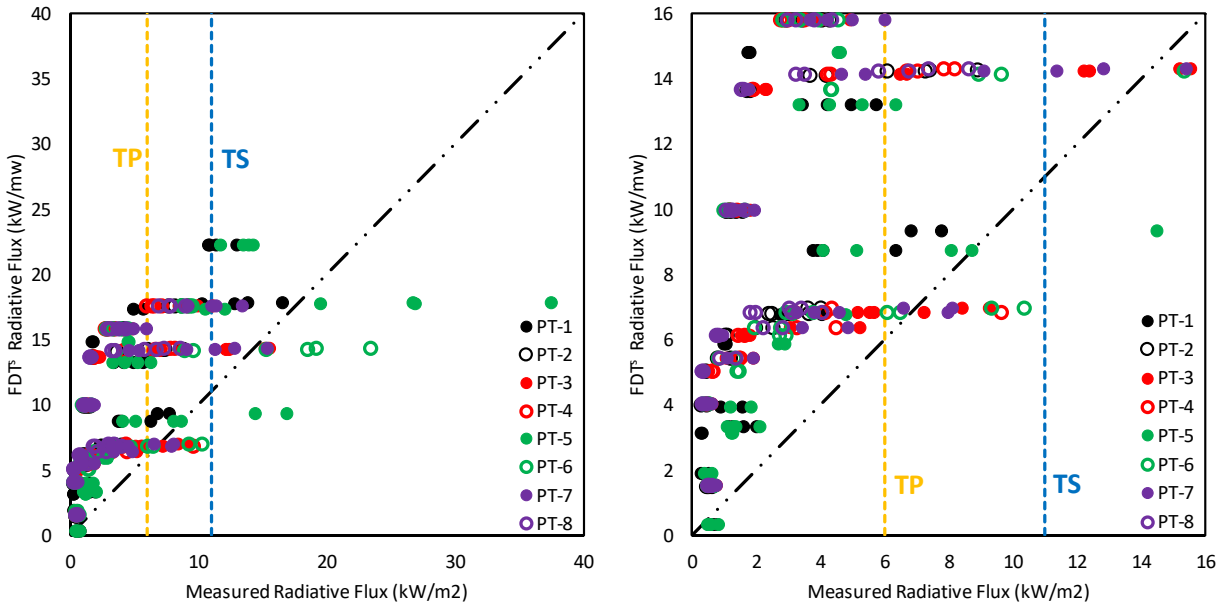

Figure 2-12
NIST cabinet test data versus unadjusted FDT^s (PT-5 and PT-6 are on the side with the open door for open door tests. For reference, the dotted lines show the TS and TP damage thresholds [left, all data; right, zooms to non-open door data].)

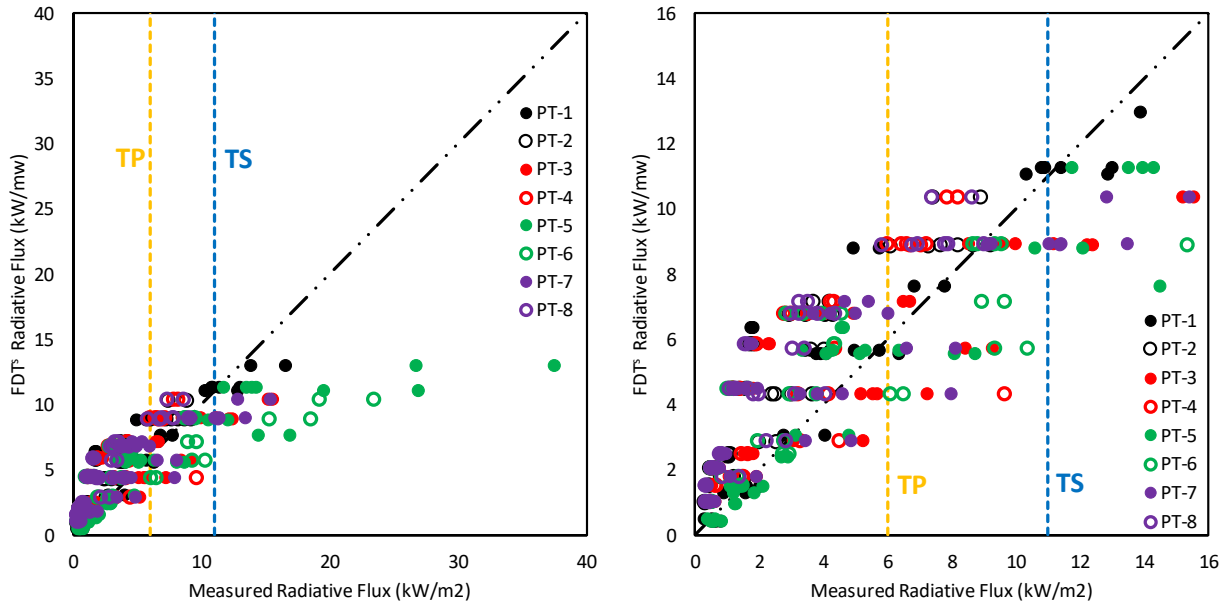

Figure 2-13
NIST cabinet test data versus adjusted FDT^s (PT-5 and PT-6 are on the side with the open door for open door tests. For reference, the dotted lines show the TS and TP damage thresholds [left, all data; right, zooms to non-open door data].)

All of the cabinet tests have been added to the FDS validation suite [21]. The input files from the validation suite were modified to increase the grid resolution around the cabinets and plate thermometers to similar resolutions as used in the modeling documented in Section 2.3.3. Results of these simulations are shown in Figure 2-14. The FDS predicted that plate thermometer temperatures have a model error of 0.12 and a model bias of 0.99. Conversion of the AST to heat flux is shown in Figure 2-15. The fourth power dependence of the heat flux on temperature results in an increase in the model error and bias to 0.22 and 1.14, respectively.

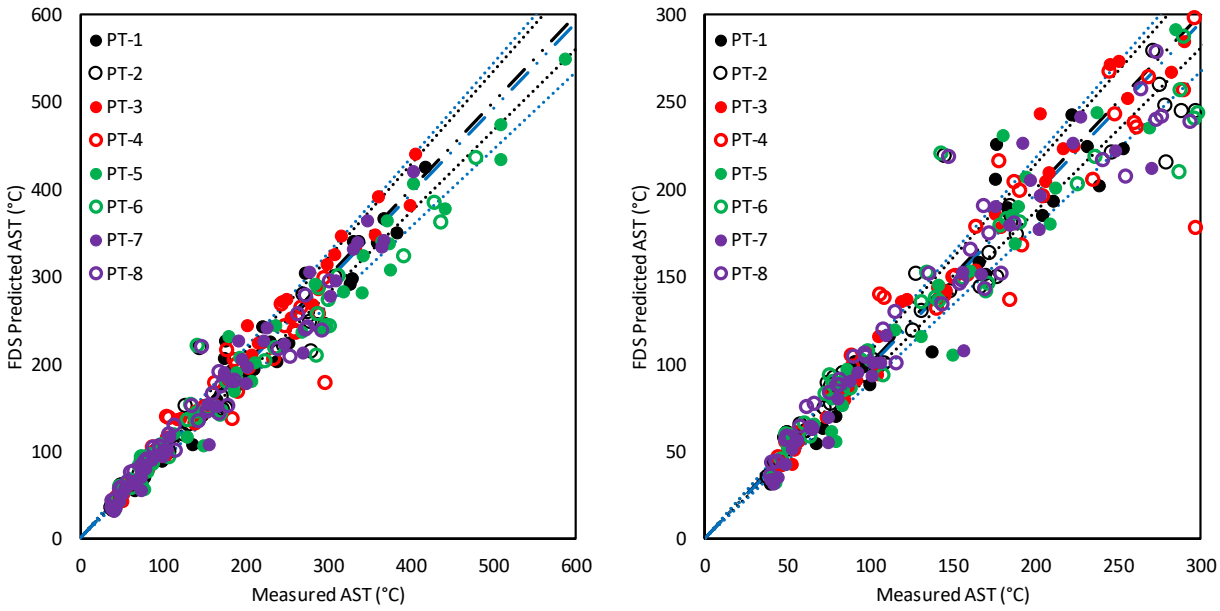

Figure 2-14
NIST cabinet measured AST versus FDS predicted AST (PT-5 and PT-6 are on the side with the open door for open door tests. Black lines indicate data mean [dash-dot] and error (dotted). Blue lines indicate adjusted mean [dash-dot] and error [dotted] based on model error and bias [left, all data; right, zoomed].)

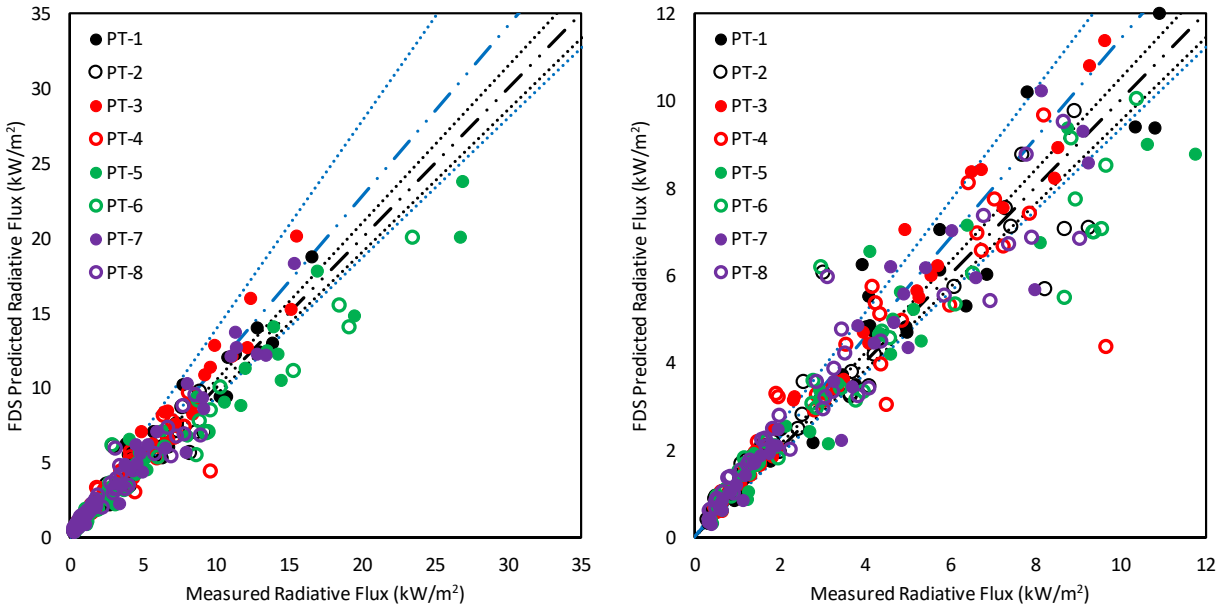

Figure 2-15
NIST cabinet measured radiative heat flux versus FDS predicted radiative heat flux (PT-5 and PT-6 are on the side with the open door for open door tests. Black lines indicate data mean [dash-dot] and error [dotted]. Blue lines indicate adjusted mean [dash-dot] and error [dotted] based on model error and bias [left, all data; right, zoomed].)

2.3.3 CFD Modeling

The simple hand calculation in Section 2.3.1 and the results of the NIST cabinet tests in Section 2.3.2 show that the use of the FDT^s for predicting ZOIs of electrical cabinets can result in artificially high values and, therefore, unrealistic (conservative) target damage estimates. ZOIs in many cases are being greatly overpredicted by the FDT^s. Investigating this for a larger range of cabinet shapes and sizes, fire sizes, and other parameters requires the application of fire modeling. Of the two classes of fire models available, zone models and CFD, only CFD can account for nonuniform heating of cabinet walls and the radiative flux contribution of plumes from cabinet vents or open cabinet faces. To develop guidance on applying FDT^s calculations to obstructed fires, detailed modeling of electrical cabinet fires was performed using FDS v6.5.3 [4, 5]. Two sets of simulations were executed. The first set modeled steady-state fires and examined the impact of fire size, location, and shape; cabinet size; cabinet ventilation; and cabinet aspect ratio on the threshold ZOI distances. The second set used a fixed cabinet configuration based on the results of the first set and modeled time-dependent fires of varying size. Results of the second set were used to develop FPRA guidance for determining the ZOI for obstructed fires.

The following definitions apply to this study and the remainder of Sections 2 and 3:

- **Small/medium/large cabinet**. These refer to the Group 4 cabinet sizes in NUREG-2178 [2]. A large cabinet is a cabinet whose volume is greater than 1.42 m^3 (50 ft^3), a medium cabinet has a volume between 0.34 m^3 (12 ft^3) and 1.42 m^3 (50 ft^3), and a small cabinet has a volume under 0.34 m^3 (12 ft^3).
- **Open/closed cabinet**. These refer to the definition of open and closed in NUREG-2178 [2]. An open cabinet is one where one or more sides are substantially (50% or more) open (for example, missing). This includes no panel being present, large areas of wire mesh, or plastic covers that would be expected to melt in a fire. A closed cabinet is any cabinet that is not open.
- **Vented/unvented face**. A vented cabinet face is a face where there are openings to support substantial air flow in or out of the cabinet. These would include louvers for passive or mechanical ventilation, areas of wire mesh, large areas with no panel present, or a face with an access panel/door that is not robustly secured (according to the definition in Section 6.5.6 Task 6 Bin 15 of NUREG/CR-6850 [1]). An *unvented fac*e is a face with no significant openings to support substantial air flow in or out of the cabinet. A solid face with small openings or feedthroughs for cables would be considered unvented.

ZOI evaluations in this study were performed for TP and TS cable types based upon the cable failure data in Appendix H of NUREG/CR-6850 [1]. The radiation ZOI is based upon radiative heat flux rather than gas temperature such as the vertical (plume) ZOI. Based on the test results in NUREG/CR-7102 [22] and guidance in FAQ 08-0053 Revision 1, TP damage criteria can be assumed for Kerite-FR cable, and TS damage criteria can be assumed for Kerite FR-II, FR-III, and HT cable.

2.3.3.1 Modeling Approach

FDS was used to model medium and large cabinets. Grid sizes for the baseline cabinets were 5.1 cm (2 in.) for the medium cabinet and 7.3 cm (2.9 in.) for the large cabinet. These grid sizes put 12 cells across the width of the cabinets and represent a D*/dx value of 4 for a 60th percentile TP fire in a closed cabinet. Cabinets were defined with single grid cell thick walls with a heat transfer thickness of 1.5 mm (16 gauge) and used the properties for steel from

NUREG-1934 [23]. The cabinet floor was assumed to be 10 cm (4 in.) of concrete (that is, the modeling assumed cabinets on the floor) also using properties from NUREG-1934. Assuming a cabinet on the floor is a conservative assumption because an elevated cabinet with air below it would have more heat losses from its base and, therefore, a lower internal temperature. The overall domain extents were determined using the 98th percentile TP fire in a closed cabinet from NUREG-2178 [2]. The extents were set to a domain width of 150% of the horizontal ZOI for TP cable as computed by the unadjusted solid flame FDT^s (no emissive power adjustment) and a domain height of the cabinet height plus 150% of the flame height as computed by the FDT^s.

Closed and open cabinet configurations were modeled. The open cabinet scenarios had one face of the cabinet removed. The closed cabinet scenarios defined a pressure zone for the interior of the cabinet and used the localized leakage model to represent louvers venting one face of the cabinet. In FDS, the pressure zone concept allows the user to denote a region in the model with its own background pressure. FDS solves for the pressure perturbation and obtains total pressure by adding the local background pressure to that perturbation. By defining a pressure zone in the cabinet, any bulk pressure rise in the cabinet due to the fire will be captured by FDS. The localized leakage model allows the user to define two wall regions and a leakage area between them. FDS then links the two regions using an equivalent heating, ventilation, and air conditioning (HVAC) duct with flow losses and duct area equivalent to the leakage path. With this approach, the louvered opening will be solid from the viewpoint of the radiation model, and the temperature of the louvers will be computed as a steel surface; however, the flow solver will see the louvers as a flow path through the HVAC submodel. Louvers were defined for each grid cell row within the louvered area of the cabinet. This is depicted in Figure 2-16 for a large cabinet. The alternating green and blue stripes represent the individual leakage paths defined in FDS. Each stripe would have its own velocity solution coming from the HVAC model based upon the local pressure gradient across the cabinet face (including the effects of background pressure). Two louver configurations were modeled: a full-face louver and a top-bottom louver with the top and bottom quarter of a face defined as louvers. The latter case is depicted in Figure 2-16.

Note that in discussion of results, the face with the door or louvers is referred to as the *north face*, and its opposite face is referred to as the *south face*.

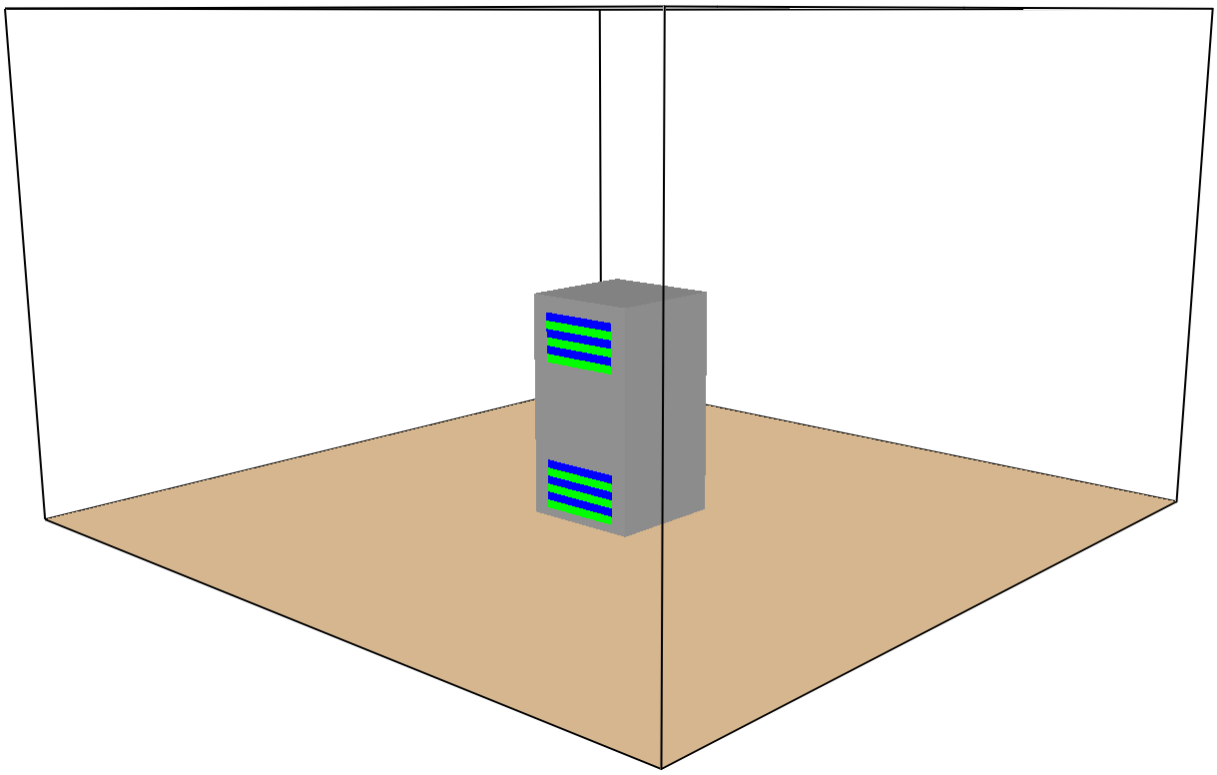

Figure 2-16
Rendering of the large cabinet geometry showing louver locations (blue and green)

The FDS models were run assuming ethylene with a 12% soot yield. This maintains a 2:1 ratio of hydrogen to carbon that is a characteristic of many polymers while also using a species with predefined and self-consistent thermophysical properties.

Heat flux to targets was measured using three two-dimensional (2-D) arrays of point measurement devices (see Figure 2-17). Arrays were located centered on the vented face, the opposite unvented face, and a side face. Each point in the array consisted of three co-located devices measuring radiative heat flux. In FDS, radiative heat flux devices integrate the gas phase radiative flux over a hemisphere centered on the normal vector to the device. Because one does not know *a priori* the specific angle that is required to obtain the maximum flux, the three devices measure flux with the normal pointed parallel to the floor and toward the cabinet, in the positive-z direction, and in the negative-z direction. The maximum potential flux can then be estimated using Equation 2-10 where $\dot{q}_r''$ is the heat flux measured by a device and the remainder of the subscript indicates the direction in which the device is pointing [6]:

$$\dot{\boldsymbol{q}}''_{\boldsymbol{r,max}} = \mathrm{Max}\left(\sqrt{\dot{\boldsymbol{q}}''_{\boldsymbol{r,cabinet}}{}^{\boldsymbol{2}} + \dot{\boldsymbol{q}}''_{\boldsymbol{r,ceiling}}{}^{\boldsymbol{2}}}, \sqrt{\dot{\boldsymbol{q}}''_{\boldsymbol{r,cabinet}}{}^{\boldsymbol{2}} + \dot{\boldsymbol{q}}''_{\boldsymbol{r,floor}}{}^{\boldsymbol{2}}}\right) \qquad \textbf{(2-10)}$$

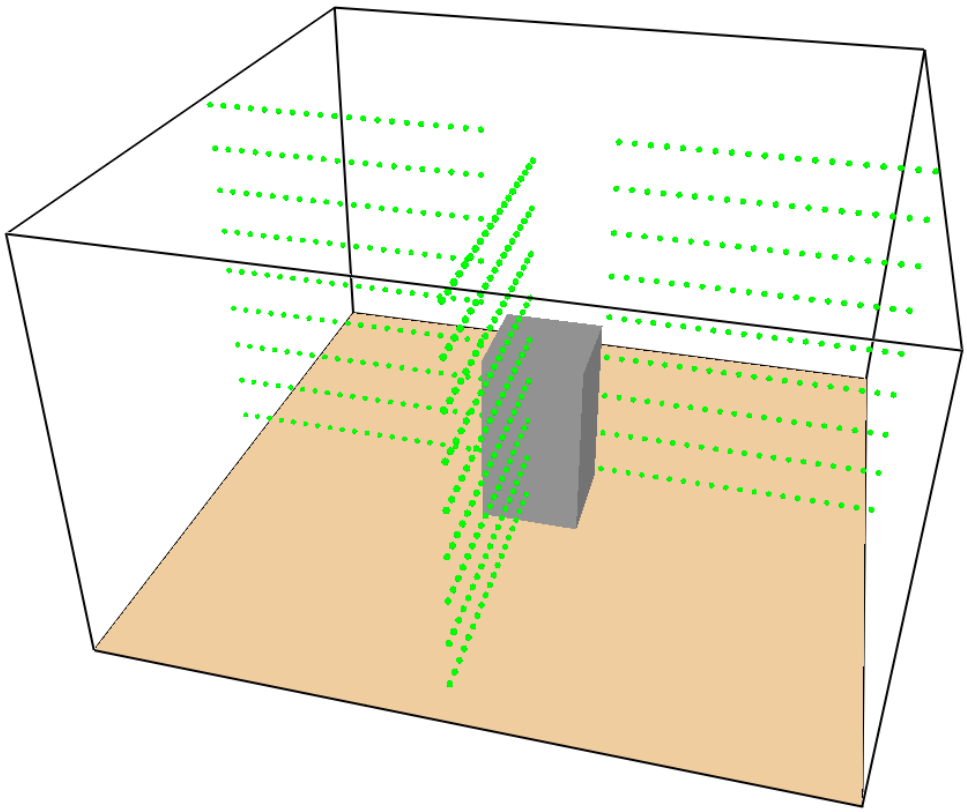

Figure 2-17
Rendering of the large cabinet geometry showing radiative heat flux device locations (green dots); louvered face (north) is the nonvisible instrumented face

2.3.3.2 Steady-State Fire Results

A set of 60 simulations were performed using steady-state fires in medium and large electrical cabinets. A listing of simulations is provided in Table 2-2. Simulations are named as aaa-bbb-ccc-ddd-eees follows:

- aaa = cabinet size
  - Medium cabinets: m12 (0.3 m^3 (12 ft^3), 0.9 m (3 ft) tall), m31 (0.9 m^3 (31 ft^3), 1.5 m (5 ft) tall), and m50 (1.4 m^3 (50 ft^3) 1.8 m (6 ft) tall)
  - Large cabinets: l50 (1.4 m^3 (50 ft^3), 1.8 m (6 ft) tall), l75 (2.1 m^3 (75 ft^3), 2.1 m (7 ft) tall), l100 (2.8 m^3 (100 ft^3), 2.1 m (7 ft) tall)
- bbb = fire size as percentile of open or closed HRR and medium or large cabinet size
- ccc = ventilation: op (open cabinet, one face), ful (closed cabinet, one full face 50% open louver), and tbl (closed cabinet, with 50% open louvers at the top and bottom quarter of a face)
- ddd = fire shape/location: cyl-cen (cylindrical source at the cabinet center), cyl-wal (cylindrical source centered on the back wall), cyl-cor (cylindrical source in the SE corner), floor (square burner on the floor), and mid (square burner at the mid-height)
- eee = floor aspect ratio: sq (square) and re (rectangular with 3:1 aspect ratio with ventilation on long side)

Table 2-2
List of FDS simulations of steady-state cabinet fires

FDS Steady-State Cabinet Fire Simulation Attributes		
m12-75th-op-cyl-cen-sq	m12-75th-tbl-cyl-cen-sq	l50-80th-ful-cyl-cen-sq
m12-80th-op-cyl-cen-sq	m12-98th-tbl-cyl-cen-sq	l50-85th-ful-cyl-cen-sq
m12-85th-op-cyl-cen-sq	m12-75th-tbl-cyl-cen-re	l50-90th-ful-cyl-cen-sq
m12-90th-op-cyl-cen-sq	m12-98th-tbl-cyl-cen-re	l50-98th-ful-cyl-cen-sq
m12-98th-op-cyl-cen-sq	m31-75th-ful-cyl-cen-sq	l50-85th-ful-mid-sq
m12-85th-op-mid-sq	m31-98th-ful-cyl-cen-sq	l50-85th-ful-floor-sq
m12-85th-op-floor-sq	m50-75th-ful-cyl-cen-sq	l50-85th-ful-cyl-cor-sq
m12-85th-op-cyl-cor-sq	m50-98th-ful-cyl-cen-sq	l50-85th-ful-cyl-wal-sq
m12-85th-op-cyl-wal-sq	m50-75th-tbl-cyl-cen-sq	l50-75th-ful-cyl-cen-re
m12-75th-ful-cyl-cen-sq	m50-98th-tbl-cyl-cen-sq	l50-98th-ful-cyl-cen-re
m12-80th-ful-cyl-cen-sq	l50-75th-op-cyl-cen-sq	l50-75th-tbl-cyl-cen-sq
m12-85th-ful-cyl-cen-sq	l50-80th-op-cyl-cen-sq	l50-98th-tbl-cyl-cen-sq
m12-90th-ful-cyl-cen-sq	l50-85th-op-cyl-cen-sq	l50-75th-tbl-cyl-cen-re
m12-98th-ful-cyl-cen-sq	l50-90th-op-cyl-cen-sq	l50-98th-tbl-cyl-cen-re
m12-85th-ful-floor-sq	l50-98th-op-cyl-sq	l75-75th-ful-cyl-cen-sq
m12-85th-ful-mid-sq	l50-85th-op-mid-sq	l75-98th-ful-cyl-cen-sq
m12-85th-ful-cyl-cor-sq	l50-85th-op-floor-sq	l100-75th-ful-cyl-cen-sq
m12-85th-ful-cyl-wal-sq	l50-85th-op-cyl-cor-sq	l100-75th-tbl-cyl-cen-sq
m12-75th-ful-cyl-cen-re	l50-85th-op-cyl-wal-sq	l100-98th-ful-cyl-cen-sq
m12-98th-ful-cyl-cen-re	l50-75th-ful-cyl-cen-sq	l100-98th-tbl-cyl-cen-sq

Results of all simulations are shown in Figure 2-18. The figures plot the FDS prediction of ZOI to the 6 kW/m^2 and 11 kW/m^2 threshold fluxes for TP and TS cables against the prediction made by the unadjusted FDT^s solid flame model. The ZOI is defined as the distance from the edge of the cabinet. If no external ZOI was predicted by FDS, a ZOI of 0 m (0 ft) was used. North indicates the louvered face of cabinet. The results show that many simulations result in no ZOI outside the cabinet for the south and west faces. Without the proposed adjustment to the FDT^s, almost all FDS-predicted ZOIs are less than the FDT^s-predicted ZOIs. ZOIs on the north face are in large part driven by the fire plume leaving the cabinet.

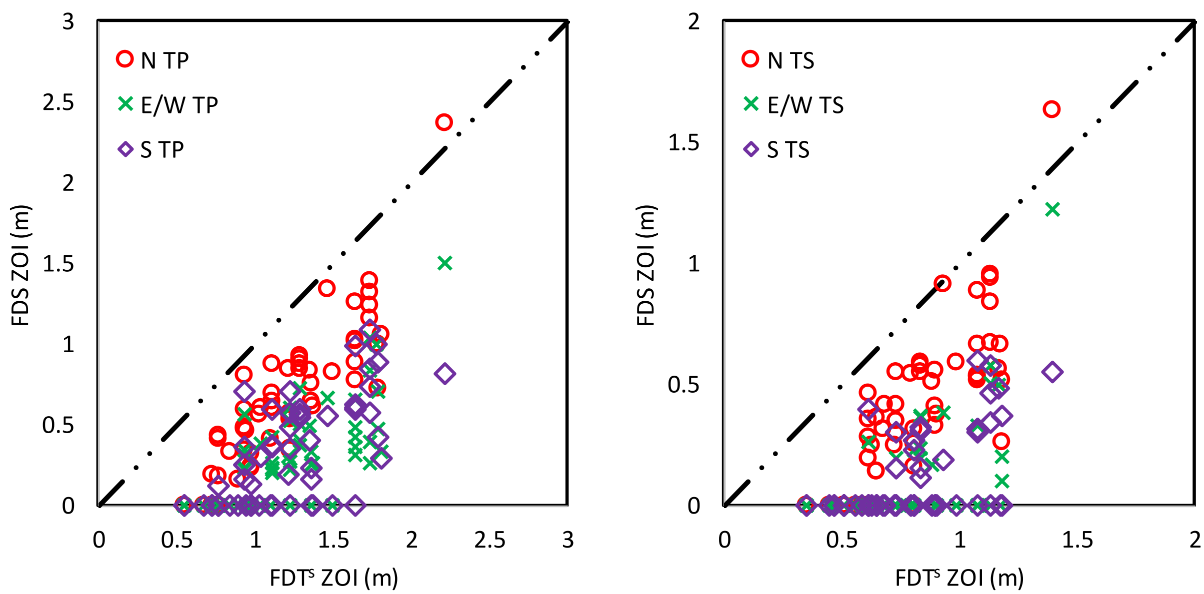

Figure 2-18
FDS predicted cabinet ZOI versus unadjusted FDT^s predicted open fire ZOI for all simulations (left, TP results; right, TS results)

Results after adjusting the FDT^s emissive power are shown in Figure 2-19. The north (louvered) face with ventilation has a ZOI that is less than the adjusted FDT^s ZOI for 30% of the TP ZOIs and 32% of the TS ZOIs. For both cable types, the FDS ZOIs for the north (louvered) face are greater than 110% of the adjusted FDT^s ZOIs for 48% of the results for that face. This is primarily due to the fire plume exiting the vented face of the cabinet. For the south and east/west faces, the FDS-predicted ZOIs are less than the adjusted FDT^s ZOIs for 85–92% of the results; 3–8% of the FDS ZOIs for the east/west faces are greater than 110% of the adjusted FDT^s ZOIs for those faces.

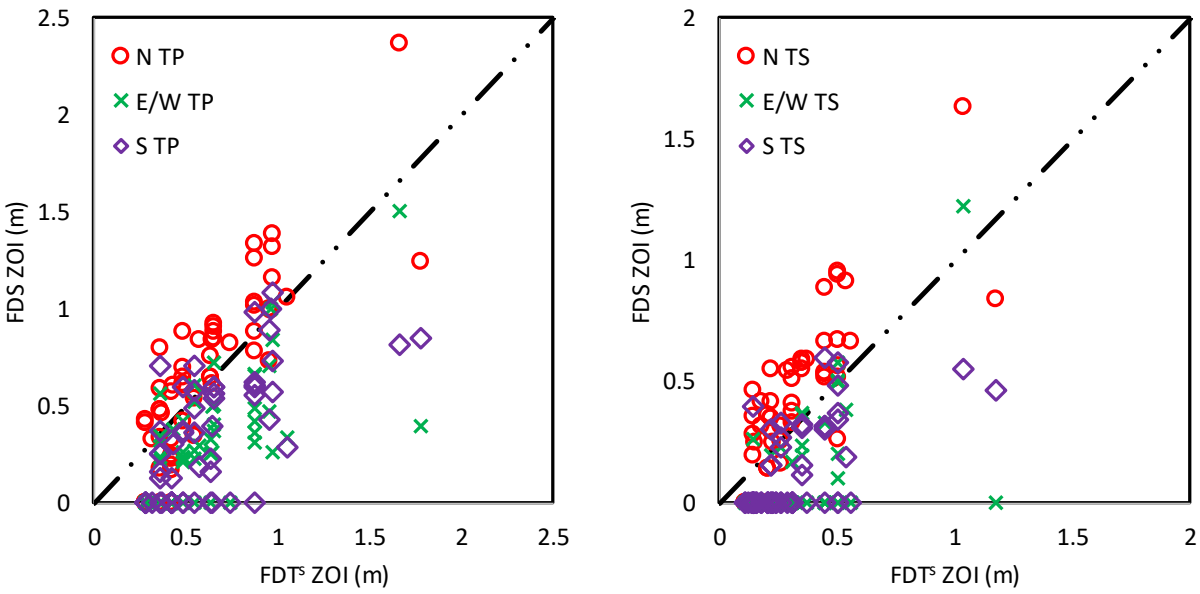

Figure 2-19
FDS predicted cabinet ZOI versus adjusted FDT^s predicted open fire ZOI for all simulations (left, TP results; right, TS results)

The data in Figure 2-18 are divided into the closed (top/bottom and full-face louvers) cabinet simulations in Figure 2-20 and open (fully open door) simulations in Figure 2-21. The results show similar behavior for both configurations. The vented side of the cabinet shows ZOIs that are with one exception, less than or equal to the FDT^s predicted values, and unvented faces generally show lower values. This results from a combination of hot gases leaving the vents and, for larger fires, hotter wall temperatures on the vented face where oxygen is being made available for combustion. These two effects are shown in Figure 2-22.

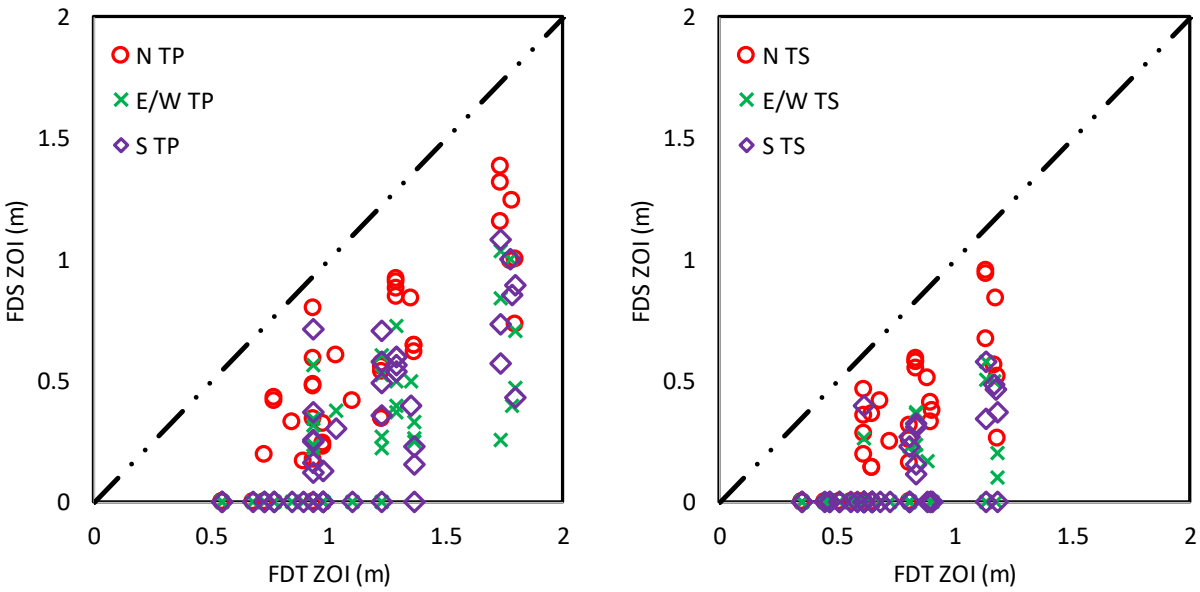

Figure 2-20
FDS predicted cabinet ZOI versus unadjusted FDT^s predicted open fire ZOI for all closed cabinet simulations (left, TP results; right, TS results)

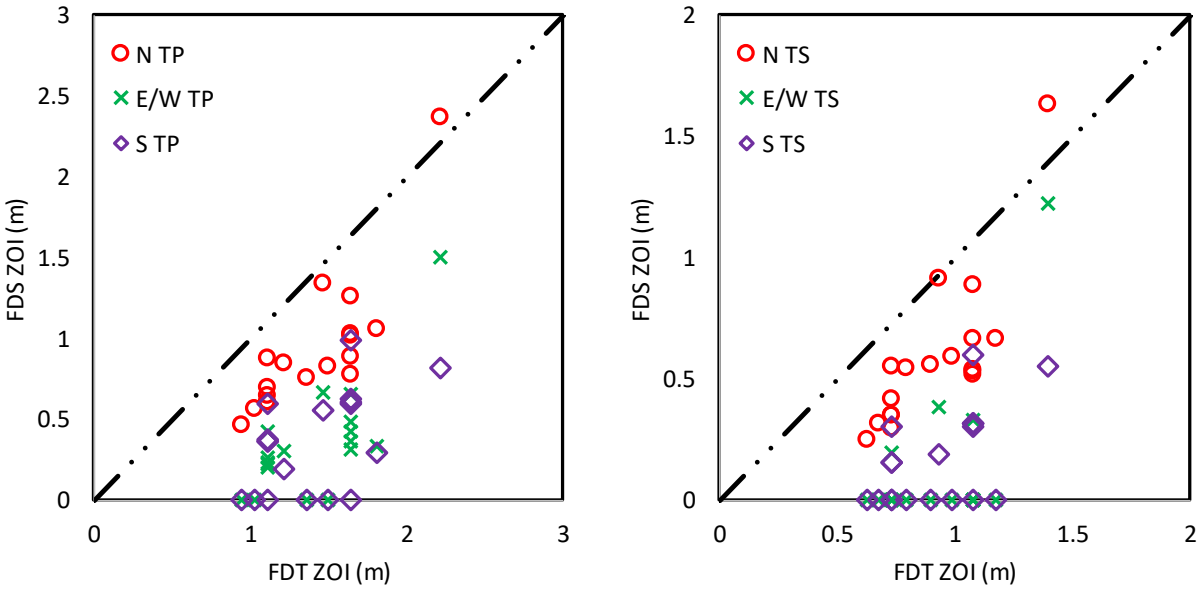

Figure 2-21
FDS predicted cabinet ZOI versus unadjusted FDT^s predicted open fire ZOI for open cabinet simulations (left, TP results; right, TS results)

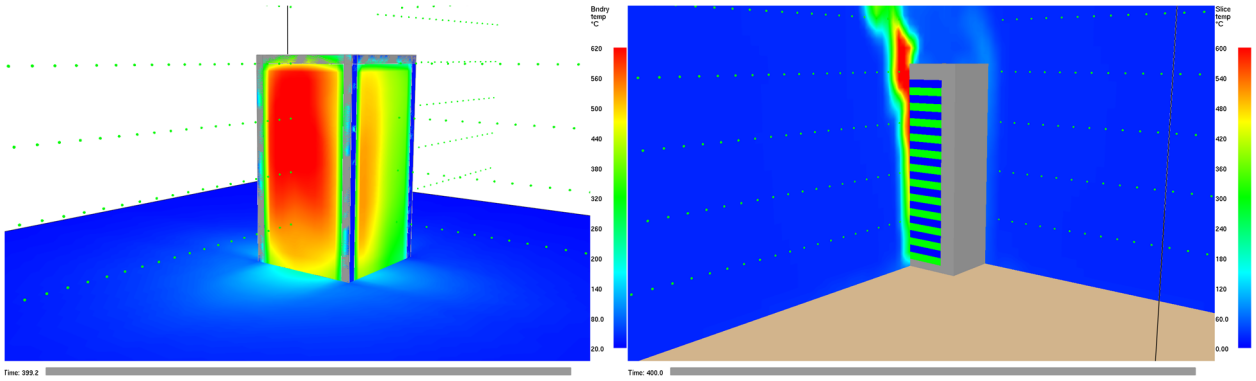

Figure 2-22
FDS predicted wall temperature (left) and gas temperature (right) for a large cabinet with a full-face vent and a 98th percentile fire

The effect of fire location on the ZOI computed can be examined by comparing the predicted ZOIs versus the unadjusted FDT^s ZOIs for the various fire locations modeled. In a typical FPRA application, a cabinet fire is modeled as a burner at or slightly below the top of the cabinet. For doing CFD modeling to determine realistic heat fluxes from the cabinet, the fire should be modeled to reflect a more real-world distribution of the fuel. Using the recommended cable tray burning rates from NUREG/CR-7010 [24] (for example, 250 kW/m^2 for TP cables), and compute the burner area required to give the 98th percentile electrical cabinet fire, the equivalent tray area ranges from 0.8 to 2.1 m^2 (8.6 to 22.6 ft^2) for medium cabinets and 1.6 to 4.7 m^2 (17.2 to 50.6 ft^2) for larger cabinets. This represents the area of cables inside the cabinet that would have to be burning to give that heat release rate. These areas are larger than the base area of typical cabinets and indicate that to obtain the higher HRRs, where a hazard is seen outside the cabinet, the fuel must be distributed over the height of the cabinet versus being represented as a single burner. Additionally, for ease of maintainability of the cabinet contents, the expectation is that cables and combustible components will generally be located away from the cabinet face to provide access to the cabinet interior when the door is opened. Therefore, although the burner on the floor and burner at the cabinet mid height were simulated, these do not represent a likely fuel distribution within the cabinet. Figure 2-23 shows the ZOIs predicted for the various faces of a cabinet for the five fire locations considered. These results reflect 85th percentile fires for large and medium cabinets. Overall, the cylindrical fire source located in the back corner of a cabinet gives larger ZOIs than the cylindrical sources in the center or against the back wall. The burner sources give larger ZOIs in general; however, as noted previously they do not represent a realistic fuel distribution for obtaining higher HRRs. Based upon this, the cylindrical source in the corner was selected for the time-dependent modeling documented in Section 2.3.3.4.

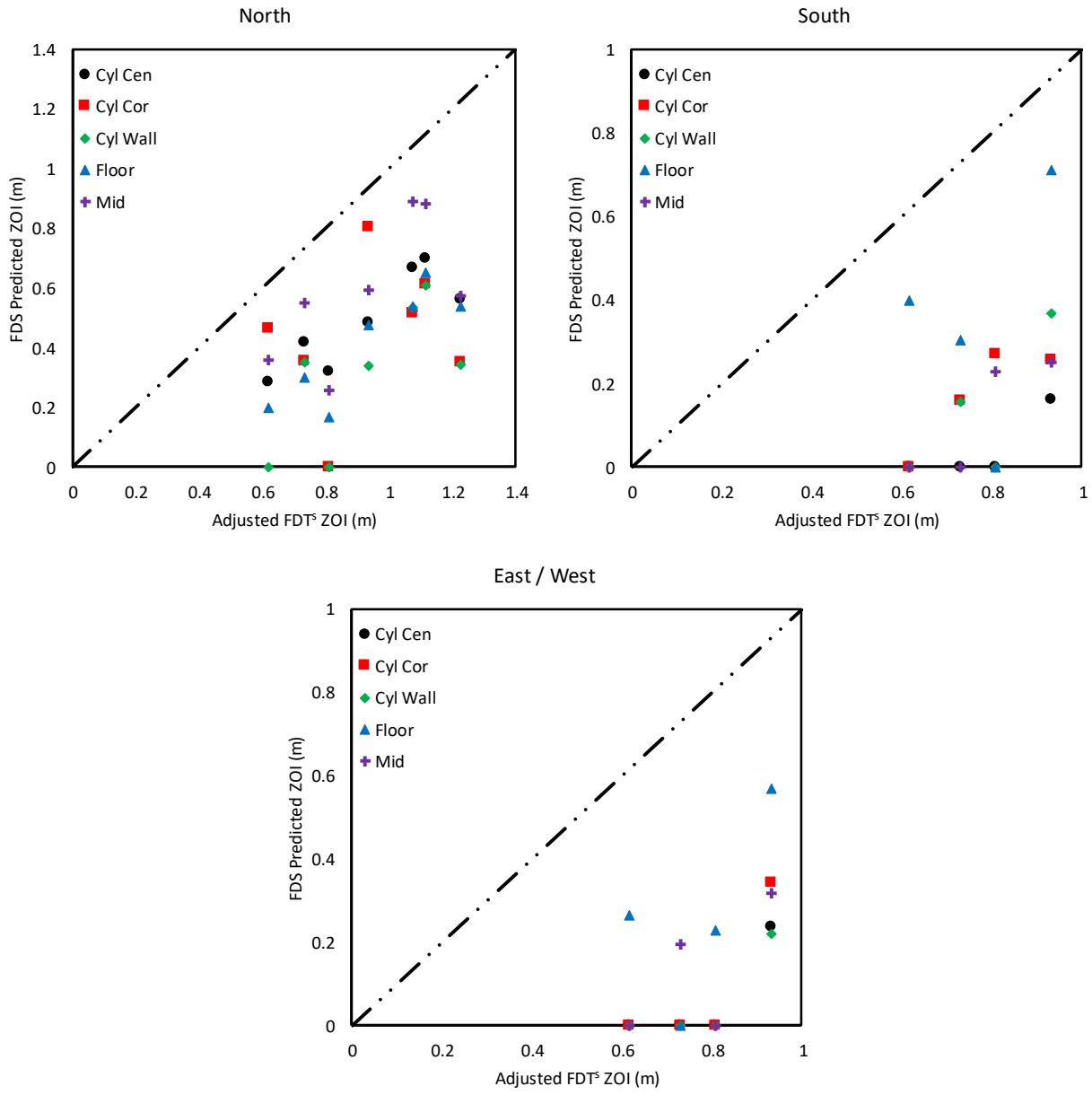

Figure 2-23
FDS predicted ZOI versus unadjusted FDTˢ predicted ZOI as a function of fire shape and location (top left, north face; top right, south face; bottom, east/west face)

The impact of cabinet shape is shown in Figure 2-24. In general, the ZOI for a square cabinet cross section exceeds that of a rectangular cabinet cross section. Therefore, square cabinet cross-sections were used for the simulations in Section 2.3.3.4.

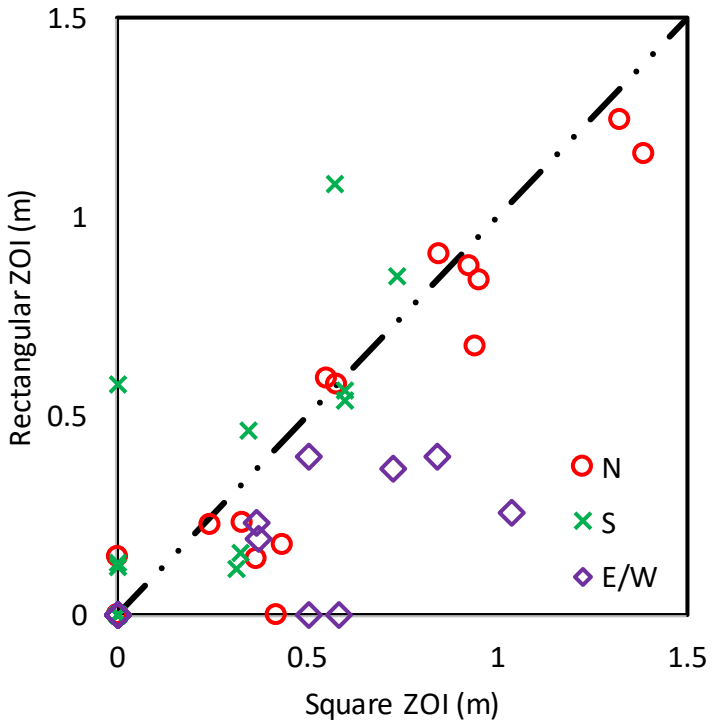

Figure 2-24
FDS predicted ZOI for square versus rectangular (3:1 aspect ratio) cabinets

The impact of cabinet size is shown in Figure 2-25. These data represent both large and medium cabinets. The letters in the legend refer to different sizes of medium and large electrical cabinets. The volume of a small (S) medium cabinet is 0.3 m^3 (12 ft^3) and for a large (L) medium cabinet is 1.4 m^3 (50 ft^3). The volume of a small (S) large cabinet is 1.4 m^3 (50 ft^3) and for a large (L) large cabinet is 2.8 m^3 (100 ft^3). The medium (M) size is the midpoint of each range or 0.9 m^3 (31 ft^3) and 2.1 m^3 (75 ft^3), respectively, for a medium and large cabinet. Unsurprisingly, the smaller the cabinet volume, the higher the cabinet wall temperature and the larger the ZOI. Simulations in Section 2.3.3.3 all used the lower bound size for medium and large cabinets.

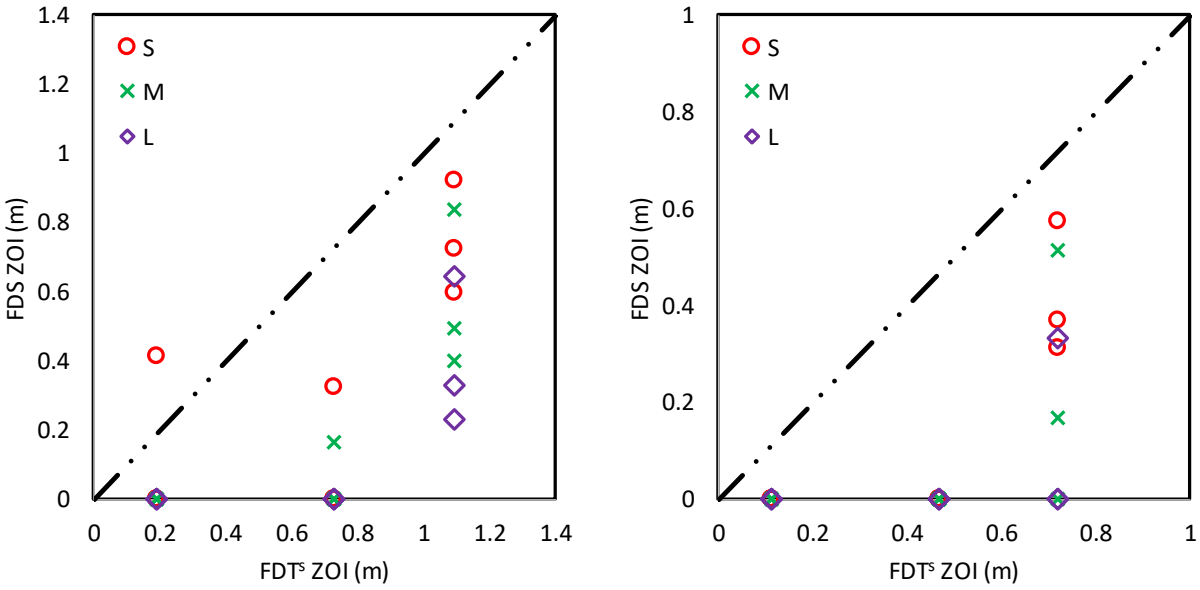

Figure 2-25
FDS predicted ZOI versus unadjusted FDT^s ZOI for different cabinet sizes (TP, left; TS, right)

2.3.3.3 Grid Sensitivity Study

A grid sensitivity study was performed using a 0.3 m^3 (12 ft^3) medium cabinet with a 75th percentile, steady-state fire in the central cylinder configuration. The baseline grid size (medium resolution [MR]) was decreased by 50% (low resolution [LR]) and increased by 50% (high resolution [HR]). Run times were approximately 0.15, 2.4, and 27 central processing unit days for the three grid resolutions. There is a significant increase in the predicted flux from the low to the medium resolution and lesser increase (20–30%) from the medium to the high resolution. Results of modeling the NIST tests, which use the medium grid resolution, show a 10% positive bias. This indicates that the use of the medium resolution would result in a positive bias and high resolution a larger positive bias. Additionally, it is noted that the heat soak method covered in Appendix A also shows a positive bias. Of the nine tests shown in Figure A-6, five show a faster time to damage, one shows a slower time to damage, and three show an equivalent time to damage. Note that bias in time to damage does not directly correlate with bias in heat flux due to nonlinear response as a function of heat flux. Compensation will occur based on the heat soak method covered in Appendix A. Given that the NIST validation exercise shows a positive bias for the medium grid, that additional bias will result from the heat soak method, and the computational resource requirements for the various grid resolutions, the medium grid was selected for use in simulations. Figure 2-26 shows the grid study results of predicted heat flux as a function of distance from the cabinet for each cabinet face at three vertical locations: near the top of the cabinet, near the bottom of the cabinet, and at the mid-height of the cabinet.

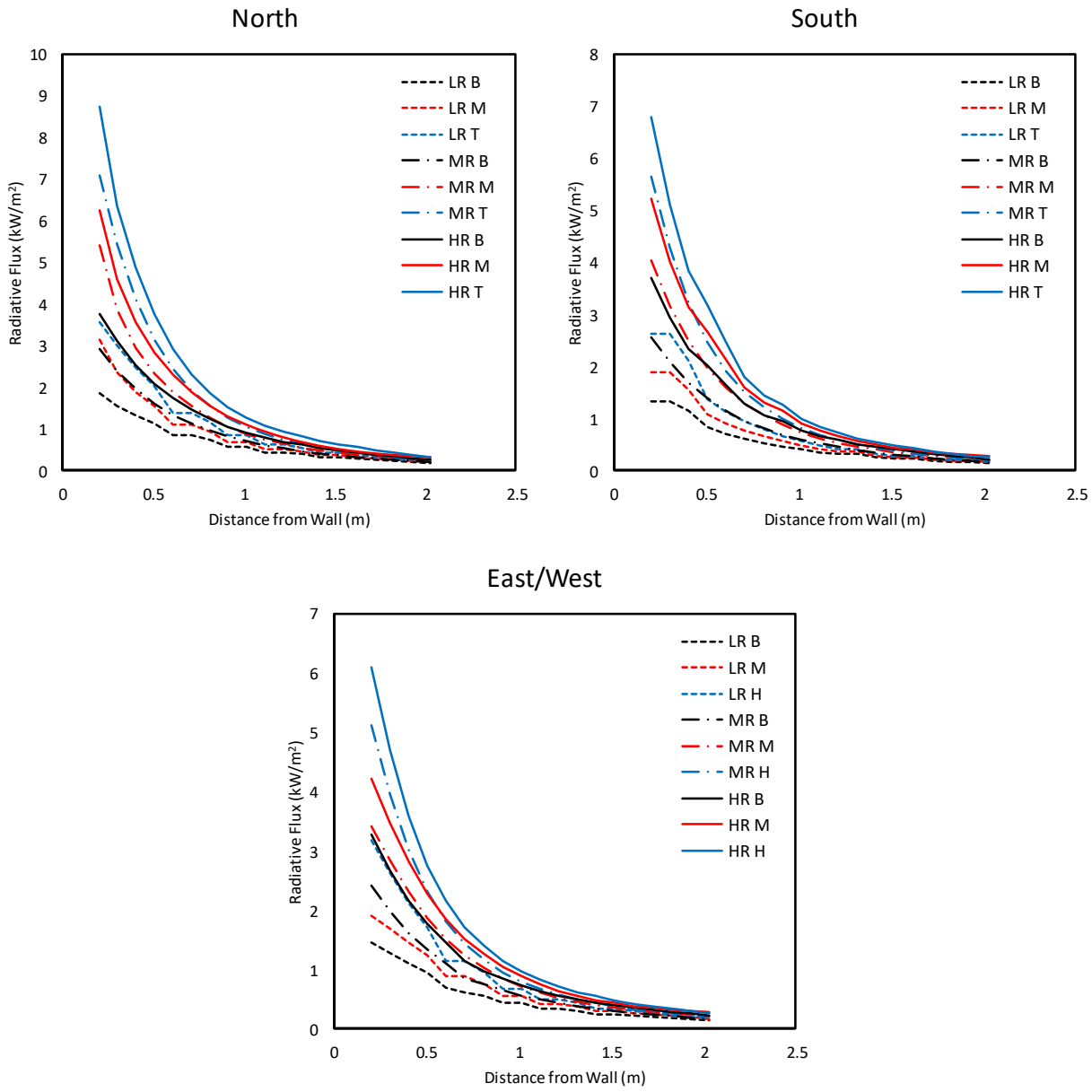

Figure 2-26
Predicted heat fluxes as a function of distance at cabinet bottom (B), mid-height (M), and top (T) for the low (LR), medium (MR), and high resolution (HR) simulations

2.3.3.4 Time-Dependent Fire Results

Actual electrical cabinet fires are not steady-state fires as modeled in the prior section but rather consist of a growth period, a sustained burning period, and a decay phase. The values for these periods for electrical cabinets from NUREG/CR-6850 [1] are 12 minutes, 8 minutes, and 19 minutes, respectively. Figure 2-27 shows the normalized HRR for a cabinet fire along with the normalized increase in wall temperature. These values were obtained from a Consolidated Fire Growth and Smoke Transport (CFAST) [25, 26] calculation. At the threshold exposure values used in the prior section, it takes 19 minutes to damage a cable according to the tables in Appendix H of NUREG/CR-6850. This time is indicated as a shaded region on the

plot. As seen, the peak wall temperature is seen near the end of the sustained burning period. This would be the point in time where the maximum heat flux would be seen outside the cabinet. However, the average wall temperature over the most damaging 19-minute period is less than this peak value. Therefore, for a time-dependent cabinet fire to damage a cable, the cabinet must reach a peak heat flux at the target that exceeds the damage thresholds in NUREG/CR-6850 [1].

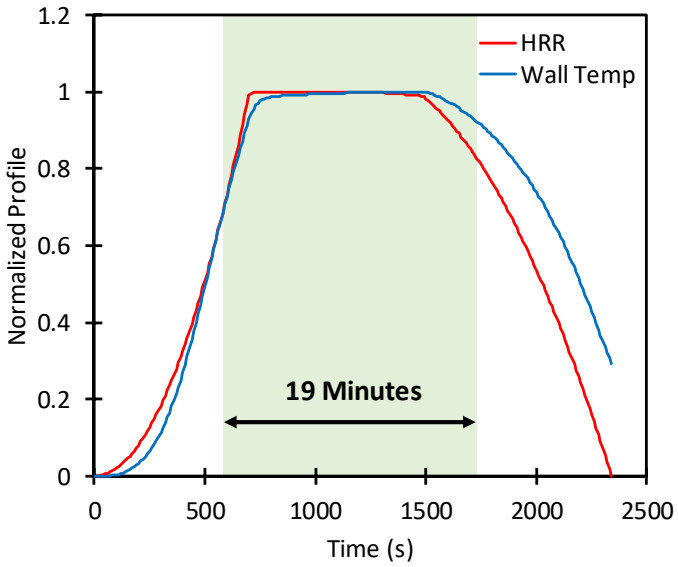

Figure 2-27
Normalized HRR and wall temperature change for an electrical cabinet fire

To assess cable damage under time-dependent fire conditions, a series of FDS runs were made using time-dependent fires. The simulations used the 0.3 m^3 (12 ft^3) medium and 1.4 m^3 (50 ft^3) large cabinet geometries described in Section 2.3.3.2. Fire size was varied from the 50th to the 98th percentile fire size for open and closed cabinets using the TP gamma distribution from NUREG-2178 [2]. Based on the scoping results shown in Figure 2-23 and the fact that a large cabinet fire would require a distributed fuel source, the cylindrical fire in a corner location source was used in all simulations. The heat flux at each measurement location was evaluated using two methods. The first was the threshold method of locating the furthest location on each face where either 6 kW/m^2 or 11 kW/m^2 was seen. This approach is bounding because it is primarily a function of the peak HRR, and the combined 12-minute growth and 8-minute sustained burning period is sufficient to reach steady-state cabinet wall temperatures. The second was a damage integral method; this method is covered in Appendix A. This method accounts for time-varying heat fluxes to a generic cable target by using the data in Appendix H of NUREG/CR-6850 [1] to define heat flux dependent damage rates that are then integrated in time until damage occurs.

As covered previously, the vented face of a cabinet sees a larger ZOI due to effects related to the plume venting from the cabinet. The fire plume leaving the vent can also damage a cable if it is immersed in the plume. The threshold temperatures required for this in Appendix H of NUREG/CR-6850 [1] are 205°C (400°F) for TP cable and 330°C (625°F) for TS cable. In NUREG-2178 [2], this effect was examined as part of the obstructed plume correction to Heskestad's plume temperature correlation. In NUREG-2178, it was concluded that even though an obstructed plume leaving a vented cabinet results in damaging temperatures horizontally beyond the confines of the cabinet, the horizontal distance away where the plume

became vertical was always less than the radiation ZOI computed using the unadjusted FDT^s. The scoping results presented earlier show that the radiation ZOI for a cabinet can be significantly less than the ZOI predicted by the unadjusted FDT^s. This requires that the NUREG-2178 conclusion that the radiation ZOI is bounding be reevaluated. This was done by using Smokeview to view a 2-D slice file of temperature through the center of the vent. The slice was colored to highlight contours of 205°C (400°F) and 330°C (625°F). By viewing the slice over time, the furthest distance at which either temperature is seen was determined. This distance was then compared with the radiation ZOI. This approach was only done for the threshold ZOI and is illustrated in Figure 2-28.

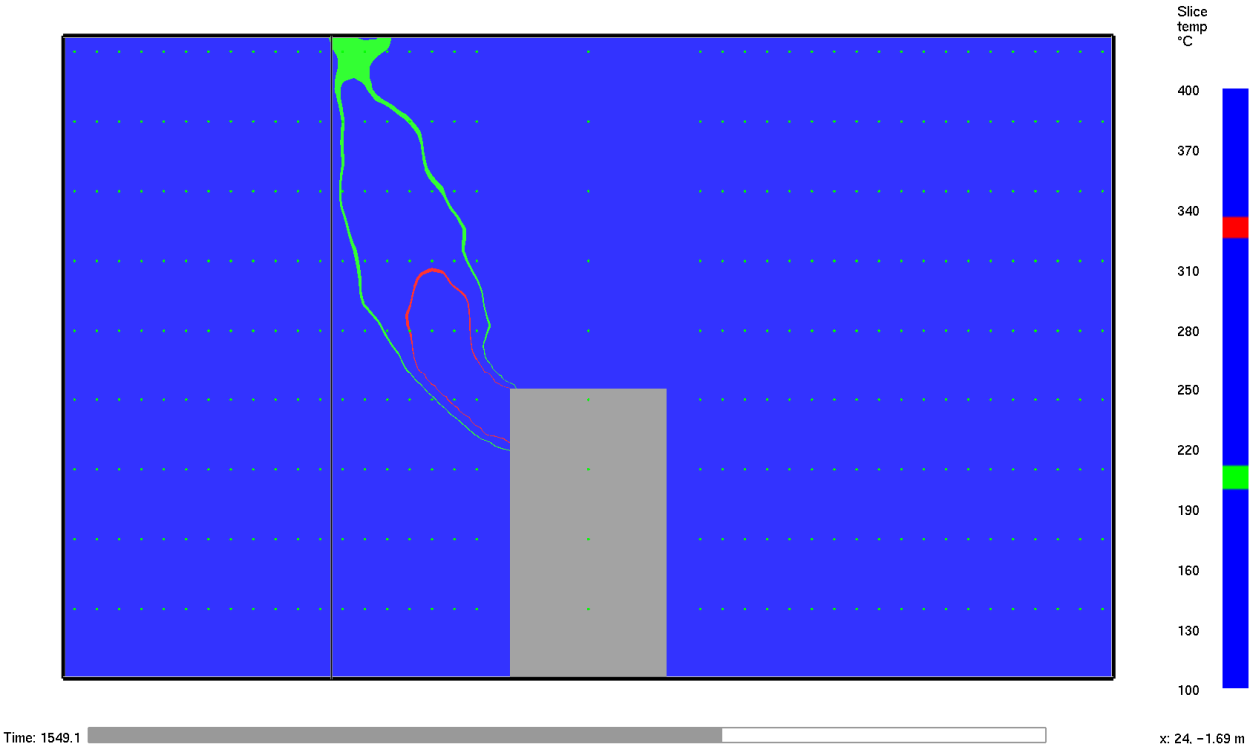

Figure 2-28
Determining plume ZOI for large, open, 98th percentile TP fire (green contour, TP threshold; red contour, TS threshold)

Results of evaluating the plume ZOI are shown in Figure 2-29. This figure shows the radiation versus plume ZOI for all cabinet scenarios where at least one of either the plume or the radiation ZOI extends beyond the walls of the cabinet. For the larger fire sizes over all cabinet configurations, the radiation ZOI is larger than the plume ZOI. At smaller fire sizes, however, the plume ZOI can extend further than the radiation ZOI.

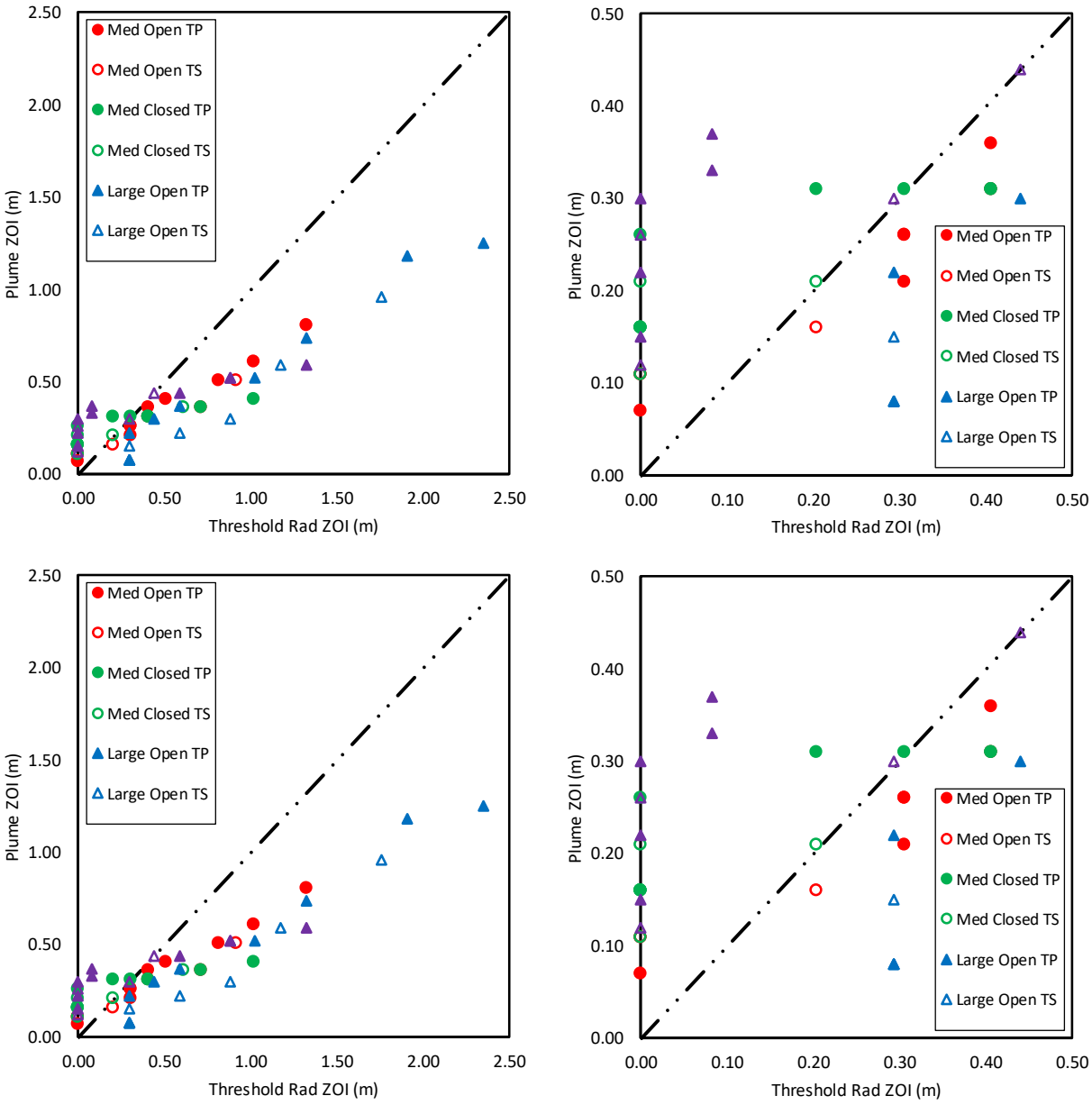

Figure 2-29
Plume ZOI vs radiation ZOI for all cabinet scenarios with a ZOI (top, threshold radiation ZOI; bottom, damage integral radiation ZOI)

Tables 2-3 through Table 2-6 show the FDT^s predicted ZOI (unadjusted and adjusted) and FDS predicted ZOI for open and closed medium and large electrical cabinets. The first three columns in each table provide the percentile fire size based on cable type (TP or TS) and fuel load (**default**, **low**, or **very low**). These are based upon the HRR gamma distributions in NUREG-2178 [2]. The next two columns contain the unadjusted and adjusted FDT^s ZOIs. The remaining columns show the FDS-predicted ZOIs as a function of cabinet face and cable type (TP or TS). In each cell for the FDS ZOIs, there are two distances. The top number is the ZOI for the threshold damage fluxes—either 6 kW/m^2 (TP) or 11 kW/m^2 (TS). The bottom number is the ZOI computed using the damage integral approach. Green text with N/A indicates fire sizes

where no damaging flux exists outside of the electrical cabinet. Cases where the FDS ZOI is significantly greater than the unadjusted FDT^s ZOI have red text. This was defined as an FDS ZOI that was 10% larger and at least 2 cm larger than the FDT^s ZOI. Cases where the ZOI is defined by the plume have purple text.

Table 2-3
FDT^s and FDS predicted radiation (horizontal) ZOI (m) for open, medium (0.3 m^3 [12 ft^3] to 1.4 m^3 [50 ft^3]), electrical cabinets[1]

Fire **Size (kW)**	**Percentile HRR for Fuel Load**			FDT^s ZOI **(m) [ft]**				FDS ZOI[2] **(m) [ft]**					
	Default TP **TS**	Low TP **TS**	Very Low TP **TS**	**Unadj.**		**Adj.**		North (Vented/ **Open)**		South **(Unvented)**		East/West **(Unvented)**	
				TP	**TS**	**TP**	**TS**	**TP**	**TS**	**TP**	**TS**	**TP**	**TS**
28	50 70	77 83	92 92	0.53 [1.7]	0.35 [1.1]	0.20 [0.7]	0.09 [0.3]	N/A N/A	N/A N/A	N/A N/A	N/A N/A	N/A N/A	N/A N/A
43	60 76	84 88	98 98	0.71 [2.3]	0.47 [1.5]	0.26 [0.9]	0.10 [0.3]	*0.07* *[0.2]* *0.07* *[0.2]*	N/A N/A	N/A N/A	N/A N/A	N/A N/A	N/A N/A
65	70 82	90 92	>98 >98	0.87 [2.9]	0.58 [1.9]	0.33 [1.1]	0.13 [0.4]	0.30 [1.0] *0.21* *[0.7]*	*0.11* *[0.4]* *0.11* *[0.4]*	N/A N/A	N/A N/A	N/A N/A	N/A N/A
80	75 85	93 94	>98 >98	0.95 [3.1]	0.63 [2.1]	0.37 [1.2]	0.15 [0.5]	0.30 [1.0] 0.30 [1.0]	*0.11* *[0.4]* *0.11* *[0.4]*	N/A N/A	N/A N/A	N/A N/A	N/A N/A
99	80 87	95 96	>98 >98	1.03 [3.4]	0.68 [2.2]	0.42 [1.4]	0.18 [0.6]	0.41 [1.4] 0.41 [1.4]	0.20 [0.7] 0.20 [0.7]	0.20 [0.7] N/A	N/A N/A	N/A N/A	N/A N/A
125	85 90	97 97	>98 >98	1.12 [3.7]	0.73 [2.4]	0.49 [1.6]	0.22 [0.7]	0.51 [1.7] 0.51 [1.7]	0.30 [1.0] 0.30 [1.0]	0.30 [1.0] 0.30 [1.0]	N/A N/A	0.20 [0.7] N/A	N/A N/A
163	90 93	98 98	>98 >98	1.21 [4.0]	0.79 [2.6]	0.58 [1.9]	0.29 [1.0]	0.81 [2.7] 0.71 [2.3]	0.41 [1.3] 0.41 [1.3]	0.41 [1.3] 0.41 [1.3]	0.20 [0.7] 0.20 [0.7]	0.41 [1.3] 0.30 [1.0]	N/A N/A

Table 2-3
FDT^s and FDS predicted radiation (horizontal) ZOI (m) for open, medium (0.3 m^3 [12 ft^3] to 1.4 m^3 [50 ft^3]), Electrical Cabinets[1] (continued)

Fire Size (kW)	Percentile HRR for Fuel Load			FDT^s ZOI (m) [ft]				FDS ZOI[2] (m) [ft]					
	Default TP TS	Low TP TS	Very Low TP TS	Unadj.		Adj.		North (Vented/ Open)		South (Unvented)		East/West (Unvented)	
				TP	TS	TP	TS	TP	TS	TP	TS	TP	TS
231	95	>98	>98	1.34 [4.4]	0.86 [2.8]	0.71 [2.3]	0.40 [1.3]	1.02 [3.4]	0.71 [2.3]	0.51 [1.7]	0.30 [1.0]	0.51 [1.7]	0.30 [1.0]
	96	>98	>98					0.91 [3.0]	0.71 [2.3]	0.51 [1.7]	0.30 [1.0]	0.51 [1.7]	0.30 [1.0]
325	98	>98	>98	1.47 [4.8]	0.93 [3.1]	0.88 [2.9]	0.54 [1.8]	1.32 [4.3]	0.91 [3.0]	0.61 [2.0]	0.41 [1.3]	0.81 [2.7]	0.41 [1.3]
	98	>98	>98					1.22 [4.0]	0.91 [3.0]	0.61 [2.0]	0.41 [1.3]	0.71 [2.3]	0.41 [1.3]

1 Italic, purple indicates that ZOI is due to obstructed plume; Red, underline indicates FDS ZOI >1.1 unadjusted FDT^s ZOI; N/A indicates no ZOI outside of the cabinet.
2 Threshold ZOI presented in top portion, damage integral ZOI in bottom portion.

Table 2-4
FDT^s and FDS predicted radiation (horizontal) ZOI (m) for closed, medium (0.3 m^3 [12 ft^3] to 1.4 m^3 [50 ft^3]), electrical cabinets[1]

Fire Size (kW)	Percentile HRR for Fuel Load			FDT^s ZOI (m) [ft]				FDS ZOI[2] (m) [ft]					
	Default TP TS	Low TP TS	Very Low TP TS	Unadj.		Adj.		North (Vented)		South (Unvented)		East/West (Unvented)	
				TP	TS	TP	TS	TP	TS	TP	TS	TP	TS
17	50 69	65 77	79 79	0.29 [1.0]	0.19 [0.6]	0.15 [0.5]	0.09 [0.3]	N/A N/A	N/A N/A	N/A N/A	N/A N/A	N/A N/A	N/A N/A
27	60 76	77 84	91 91	0.52 [1.7]	0.34 [1.1]	0.20 [0.7]	0.09 [0.3]	*0.16* *[0.5]* *0.16* *[0.5]*	N/A N/A	N/A N/A	N/A N/A	N/A N/A	N/A N/A
40	70 82	85 90	97 97	0.68 [2.2]	0.45 [1.5]	0.25 [0.8]	0.10 [0.3]	*0.16* *[0.5]* *0.16* *[0.5]*	*0.11* *[0.4]* *0.11* *[0.4]*	N/A N/A	N/A N/A	N/A N/A	N/A N/A
50	75 85	90 92	>98 >98	0.77 [2.5]	0.51 [1.7]	0.28 [0.9]	0.11 [0.4]	*0.26* *[0.9]* *0.26* *[0.9]*	*0.16* *[0.5]* *0.16* *[0.5]*	N/A N/A	N/A N/A	N/A N/A	N/A N/A
61	80 87	93 94	>98 >98	0.85 [2.8]	0.56 [1.8]	0.31 [1.0]	0.12 [0.4]	*0.31* *[1.0]* *0.31* *[1.0]*	*0.16* *[0.5]* *0.16* *[0.5]*	0.20 [0.7] N/A	N/A N/A	N/A N/A	N/A N/A
77	85 90	96 96	>98 >98	0.93 [3.1]	0.62 [2.0]	0.36 [1.2]	0.14 [0.5]	*0.31* *[1.0]* *0.31* *[1.0]*	*0.21* *[0.7]* *0.21* *[0.7]*	0.41 [1.3] 0.30 [1.0]	N/A N/A	0.30 [1.0] 0.20 [0.7]	N/A N/A
101	90 93	98 98	>98 >98	1.04 [3.4]	0.68 [2.2]	0.43 [1.4]	0.18 [0.6]	0.41 [1.3] 0.41 [1.3]	*0.21* *[0.7]* *0.21* *[0.7]*	0.41 [1.3] 0.41 [1.3]	0.20 [0.7] 0.20 [0.7]	0.41 [1.3] 0.30 [1.0]	0.20 [0.7] 0.20 [0.7]
143	95 96	>98 >98	>98 >98	1.17 [3.8]	0.76 [2.5]	0.53 [1.7]	0.25 [0.8]	0.71 [2.3] 0.51 [1.7]	0.41 [1.3] 0.41 [1.3]	0.61 [2.0] 0.51 [1.7]	0.41 [1.3] 0.41 [1.3]	0.61 [2.0] 0.51 [1.7]	0.41 [1.3] 0.41 [1.3]

Table 2-4
FDT^s and FDS predicted radiation (horizontal) ZOI (m) for closed, medium (0.3 m^3 [12 ft^3] to 1.4 m^3 [50 ft^3]), electrical cabinets[1] (continued)

Fire Size (kW)	Percentile HRR for Fuel Load			FDT^s ZOI (m) [ft]				FDS ZOI[2] (m) [ft]					
	Default TP TS	Low TP TS	Very Low TP TS	Unadj.		Adj.		North (Vented)		South (Unvented)		East/West (Unvented)	
				TP	TS	TP	TS	TP	TS	TP	TS	TP	TS
200	98	>98	>98	1.29 [4.2]	0.83 [2.7]	0.65 [2.1]	0.35 [1.1]	1.02 [3.3]	0.61 [2.0]	0.80 [2.6]	0.41 [1.3]	0.81 [2.7]	0.51 [1.7]
	98	>98	>98					0.81 [2.7]	0.61 [2.0]	0.71 [2.3]	0.41 [1.3]	0.71 [2.3]	0.51 [1.7]

[1] Italic, purple indicates that ZOI is due to obstructed plume; Red, underline indicates FDS ZOI >1.1 unadjusted FDT^s ZOI; N/A indicates no ZOI outside of the cabinet.
[2] Threshold ZOI presented in top portion, damage integral ZOI in bottom portion.

Table 2-5
FDT^s and FDS predicted radiation (horizontal) ZOI (m) for open, large (>1.4 m^3 [50 ft^3]), electrical cabinets[1]

Fire Size (kW)	%ile HRR for Fuel Load			FDT^s ZOI (m) [ft]				FDS ZOI[2] (m) [ft]					
	Default TP TS	Low TP TS	Very Low TP TS	Unadj.		Adj.		North (Vented/ Open)		South (Unvented)		East/West (Unvented)	
				TP	TS	TP	TS	TP	TS	TP	TS	TP	TS
54	50 65	63 76	94 95	0.60 [2.0]	0.39 [1.3]	0.30 [1.0]	0.16 [0.5]	N/A N/A	N/A N/A	N/A N/A	N/A N/A	N/A N/A	N/A N/A
94	60 74	74 84	>98 >98	0.94 [3.1]	0.62 [2.0]	0.41 [1.3]	0.20 [0.7]	0.29 [1.0] N/A	N/A N/A	N/A N/A	N/A N/A	N/A N/A	N/A N/A
156	70 82	84 91	>98 >98	1.23 [4.0]	0.81 [2.7]	0.55 [1.8]	0.26 [0.9]	0.29 [1.0] 0.29 [1.0]	0.29 [1.0] *0.08* *[0.3]*	N/A N/A	N/A N/A	N/A N/A	N/A N/A
200	75 85	88 94	>98 >98	1.36 [4.5]	0.90 [3.0]	0.64 [2.1]	0.31 [1.0]	0.44 [1.4] 0.44 [1.4]	0.29 [1.0] 0.29 [1.0]	0.29 [1.0] 0.29 [1.0]	N/A N/A	N/A N/A	N/A N/A
258	80 89	92 96	>98 >98	1.50 [4.9]	0.99 [3.2]	0.74 [2.4]	0.37 [1.2]	0.59 [1.9] 0.55 [1.8]	0.29 [1.0] 0.29 [1.0]	0.29 [1.0] 0.29 [1.0]	N/A N/A	0.29 [1.0] N/A	N/A N/A
338	85 92	95 98	>98 >98	1.65 [5.4]	1.08 [3.5]	0.88 [2.9]	0.45 [1.5]	1.03 [3.4] 0.88 [2.9]	0.59 [1.9] 0.59 [1.9]	0.59 [1.9] 0.59 [1.9]	0.44 [1.4] 0.29 [1.0]	0.29 [1.0] 0.29 [1.0]	N/A N/A
460	90 95	97 >98	>98 >98	1.81 [5.9]	1.17 [3.8]	1.05 [3.4]	0.56 [1.8]	1.32 [4.3] 1.17 [3.8]	0.88 [2.9] 0.88 [2.9]	0.88 [2.9] 0.73 [2.4]	0.44 [1.4] 0.44 [1.4]	0.59 [1.9] 0.59 [1.9]	0.29 [1.0] 0.29 [1.0]
684	95 98	>98 >98	>98 >98	2.02 [6.6]	1.29 [4.2]	1.33 [4.4]	0.78 [2.6]	1.91 [6.3] 1.61 [5.3]	1.17 [3.8] 1.17 [3.8]	1.17 [3.8] 0.88 [2.9]	0.59 [1.9] 0.58 [1.9]	1.03 [3.4] 0.88 [2.9]	0.59 [1.9] 0.59 [1.9]

Table 2-5 FDT^s and FDS predicted radiation (horizontal) ZOI (m) for open, large (>1.4 m^3 [50 ft^3]), electrical cabinets[1] (continued)

Fire Size (kW)	%ile HRR for Fuel Load			FDT^s ZOI (m) [ft]				FDS ZOI[2] (m) [ft]					
	Default TP TS	Low TP TS	Very Low TP TS	Unadj.		Adj.		North (Vented/ Open)		South (Unvented)		East/West (Unvented)	
				TP	TS	TP	TS	TP	TS	TP	TS	TP	TS
1000	98	>98	>98	2.22	1.40	1.66	1.03	2.35	1.76	1.32	0.88	1.47	0.88
				[7.3]	[4.6]	[5.4]	[3.4]	[7.7]	[5.8]	[4.3]	[2.9]	[4.8]	[2.9]
	>98	>98	>98					2.20	1.76	1.17	0.88	1.17	0.88
								[7.2]	[5.8]	[3.8]	[2.9]	[3.8]	[2.9]

1 Italic, purple indicates that ZOI is due to obstructed plume; Red, underline indicates FDS ZOI >1.1 unadjusted FDT^s ZOI; N/A indicates no ZOI outside of the cabinet.

2 Threshold ZOI presented in top portion, damage integral ZOI in bottom portion.

Table 2-6
FDT^s and FDS predicted radiation (horizontal) ZOI (m) for closed, large (>1.4 m^3 [50 ft^3]), electrical cabinets[1]

Fire Size (kW)	Percentile HRR			FDT^s ZOI (m) [ft]				FDS ZOI[2] (m) [ft]					
	Default TP TS	Low TP TS	Very Low TP TS	Unadj.		Adj.		North (Vented)		South (Unvented)		East/West (Unvented)	
				TP	TS	TP	TS	TP	TS	TP	TS	TP	TS
35	50 70	66 80	85 90	0.25 [0.8]	0.15 [0.5]	0.23 [0.8]	0.14 [0.5]	N/A N/A	N/A N/A	N/A N/A	N/A N/A	N/A N/A	N/A N/A
54	60 76	77 86	94 95	0.60 [2.0]	0.39 [1.3]	0.30 [1.0]	0.16 [0.5]	*0.15 [0.5]* *0.15 [0.5]*	N/A N/A	N/A N/A	N/A N/A	N/A N/A	N/A N/A
81	70 82	86 91	98 98	0.85 [2.8]	0.56 [1.8]	0.38 [1.2]	0.19 [0.6]	*0.22 [0.7]* *0.22 [0.7]*	N/A N/A	N/A N/A	N/A N/A	N/A N/A	N/A N/A
100	75 85	90 93	>98 >98	0.98 [3.2]	0.65 [2.1]	0.42 [1.4]	0.20 [0.7]	*0.30 [1.0]* *0.30 [1.0]*	N/A N/A	N/A N/A	N/A N/A	N/A N/A	N/A N/A
124	80 87	93 95	>98 >98	1.10 [3.6]	0.73 [2.4]	0.48 [1.6]	0.23 [0.8]	*0.32 [1.0]* *0.32 [1.0]*	*0.12 [0.4]* *0.12 [0.4]*	0.08 [0.3] N/A	N/A N/A	N/A N/A	N/A N/A
155	85 90	96 97	>98 >98	1.22 [4.0]	0.81 [2.7]	0.55 [1.8]	0.26 [0.9]	*0.37 [1.2]* *0.37 [1.2]*	*0.26 [0.9]* *0.26 [0.9]*	0.08 [0.3] 0.08 [0.3]	N/A N/A	N/A N/A	N/A N/A
202	90 93	98 98	>98 >98	1.37 [4.5]	0.90 [3.0]	0.64 [2.1]	0.31 [1.0]	0.59 [1.9] *0.44 [1.4]*	*0.30 [1.0]* *0.30 [1.0]*	0.59 [1.9] 0.44 [1.4]	0.29 [1.0] 0.29 [1.0]	0.29 [1.0] 0.44 [1.4]	N/A N/A
285	95 96	>98 >98	>98 >98	1.55 [5.1]	1.02 [3.3]	0.79 [2.6]	0.40 [1.3]	0.88 [2.9] 0.59 [1.9]	0.44 [1.4] 0.44 [1.4]	0.88 [2.9] 0.73 [2.4]	0.44 [1.4] 0.44 [1.4]	0.59 [1.9] 0.59 [1.9]	0.29 [1.0] 0.29 [1.0]
400	98 98	>98 >98	>98 >98	1.74 [5.7]	1.13 [3.7]	0.97 [3.2]	0.51 [1.7]	1.32 [4.3] 1.17 [3.8]	0.88 [2.9] 0.88 [2.9]	1.17 [3.8] 1.03 [3.4]	0.59 [1.9] 0.59 [1.9]	0.88 [2.9] 0.73 [2.4]	0.59 [1.9] 0.59 [1.9]

1 Italic, purple indicates that ZOI is due to obstructed plume; Red, underline indicates FDS ZOI >1.1 unadjusted FDT^s ZOI; N/A indicates no ZOI outside of the cabinet.

2 Threshold ZOI presented in top portion, damage integral ZOI in bottom portion.

The following observations are made for Tables 2-3 through 2-6:

- Fire sizes over the 50th percentile for **default**, TP fuel loads are required before a damaging flux is seen outside of a vented face of the cabinet.
- Fire sizes over the 70th percentile for **default**, TP fuel loads are required before a damaging flux is seen outside of an unvented face of the cabinet.
- Unvented faces see smaller ZOIs than the vented face.
- Vented face ZOIs are similar to the unadjusted FDT^s values for larger fires and exceed the adjusted FDT^s values for larger fires. This results from the heat flux contribution of the plume leaving the vented face.
- For **very low** fuel loads, there is no external horizontal ZOI for the unvented face.

3
GUIDANCE FOR INCORPORATING RADIATION INTO FPRA

Three methods of applying the results of the obstructed radiation study to fire probabilistic risk assessment (FPRA) are presented in the following sections. These methods are applicable to cabinets with closed tops. For cabinets where there are significant openings on the cabinet top (5% according to the NUREG-2178 Vol. 1 obstructed plume definition), previous methods of using the Fire Dynamics Tools (FDT^s) or Fire Dynamics Simulator (FDS) should be used. The new methods covered in this section are as follows:

1. **Method for screening targets based on an adjusted radiation zone of influence (ZOI)**. This applies to cabinet Groups 1–3, 4a, and 4b and is covered in Section 3.1 (Group 4a and 4b) and Section 3.4 (Groups 1–3).
2. **Method for reducing the severity factor for targets**. This applies to all cabinet groups and is covered in Section 3.1 (Groups 4a and 4b), Section 3.4 (Groups 1–3), and Section 3.5 (Group 4c).
3. **Method for detailed fire modeling**. This applies to cabinet Groups 1–3, 4a, and 4b and is covered in Section 3.3 (Group 4a and 4b) and Section 3.4 (Groups 1-3).
4. **Method for use in FDS**. This applies to all cabinet groups and is covered in Section 3.6.

3.1 Obstructed Radiation Zone of Influence

The obstructed radiation (horizontal) ZOI referred to in this section is measured from the face of the cabinet and extends from the cabinet base upward until the top of the plume or obstructed plume (vertical) ZOI. This is shown as the box around the cabinet in Figure 3-1.

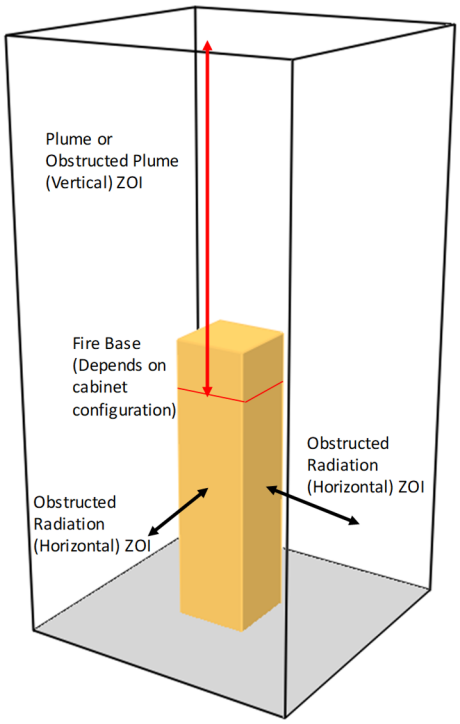

Figure 3-1
Depiction of the ZOIs for an electrical cabinet

3.1.1 Discussion

Results of the obstructed radiation simulations show that the radiation (horizontal) ZOI is generally reduced for unvented cabinet faces and sometimes reduced for vented faces. This is depicted in Figure 3-2 where the blue square is a cabinet whose left face is vented and the orange and purple dots represent cable targets. The red box indicates the radiation ZOI computed using the unadjusted solid flame model. The green box indicates the radiation ZOI based upon the FDS simulations covered in Section 2. With the unadjusted FDT^s solid flame approach, both cables lie within the radiation (horizontal) ZOI. To account for the reduced ZOI obtained from the FDS simulations, the unadjusted FDT^s ZOI, distance A measured from the cabinet wall, is adjusted by a factor, Obs_fac, and becomes the distance B measured from the cabinet wall. In the example shown in Figure 3-2, one of the cables screens with the reduced ZOI. Note that the Obs_fac will vary depending on cabinet size, fuel load, ventilation, and cable type.

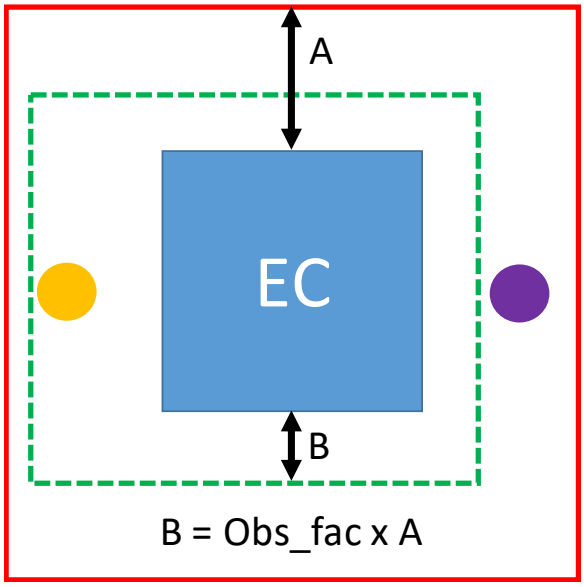

Figure 3-2
Depiction of unobstructed (red) and obstructed (green) radiation (horizontal) ZOI for a cabinet with default fuel loading (This example depicts the left cabinet face as vented and the remaining faces as unvented.)

The Obs_fac values are tabulated as a function of cabinet size, ventilation, cable type, and fuel loading in Table 3-1 and Table 3-2. Table 3-1 contains the Obs_fac for unvented cabinet faces, and Table 3-2 contains the Obs_fac for vented faces. A value of SCRN (screen) indicates that there is no radiation (horizontal) ZOI outside the cabinet. To use the tables, compute the radiation (horizontal) ZOI for the 98th percentile for the cabinet type being considered using the unadjusted FDT^s. Then. multiply that ZOI by the Obs_fac from the tables. Examples are given after Table 3-2. In the tables the threshold approach ZOI factor is the Obs_fac if the threshold damage method was used to process the FDS results, and the damage integral approach ZOI factor is the Obs_fac is the heat soak method in Appendix A is used to process the FDS results.

Note that in one case—large, open, TP cabinet with **default** fuel load—the Obs_fac is greater than one. This indicates that for this specific scenario the cabinet ZOI is larger than that for the unadjusted FDT^s. If obstructed radiation values are being applied, this result should be preserved and not revert back to the original FDT^s value.

Appendix B provides an equivalent set of tables for use if the adjusted FDT^s are used for the baseline ZOI.

It is noted that the 98th percentile Obs_fac is bounding for lower percentiles. Therefore one can get a conservative estimate on the ZOI for percentiles other than the 98th percentile values in Table 3-1 and Table 3-2, by computing the ZOI using the unadjusted solid flame model and applying the 98th percentile ZOI. Conversely, one could also use the values shown in Table 2-6.

In Table 3-1 and Table 3-2 and other tables in this section and Appendix B, the following definitions apply:

- **Small, medium, large**. These refer to the electrical cabinet sizes as defined in Table 4-2 of NUREG-2178 Vol. 1 [2] where a small cabinet is less than or equal to 0.34 m^3 (12 ft^3) and larger cabinet is 1.42 m^3 (50 ft^3).

- **Open/closed**. These refer to the definition in Section 3.1.5 of NUREG-2178 Vol. 1 [2] where an open cabinet is a cabinet with one more sides that are substantially open. Note that plastic panels that will melt during a fire should be considered as an opening.
- **Vented/unvented**. A vented face is a cabinet face that contains an opening that could be due to a plastic panel, a louvered opening, a missing panel, and so on. A cabinet face with a non-robustly secured door (according to the definition in Section 6.5.6 Task 6 Bin 15 of NUREG/CR-6850 [1]) would be considered a vented face. An unvented face is any face that is not vented. Note that an unvented face can contain small openings for cable feedthroughs.

Table 3-1
Obstructed radiation (horizontal) ZOI factor (Obs_fac) for unvented[1] cabinet faces, based on unadjusted solid flame FDT^s

Cabinet Size	Cabinet Ventilation[3]	Cable Type	Threshold Approach ZOI Factor[2] (Very Low/Low/Default)	Damage Integral Approach ZOI Factor (Very Low/Low/Default)
Large (>1.4 m^3 [50 ft^3])	Open	TP	SCRN/0.58/0.66	SCRN/0.44/0.53
		TS	SCRN/0.41/0.45	SCRN/0.27/0.45
	Closed	TP	SCRN/0.43/0.68	SCRN/0.32/0.59
		TS	SCRN/0.32/0.52	SCRN/0.32/0.52
Medium (0.3 m^3 [12 ft^3] to 1.4 m^3 [50 ft^3])	Open	TP	SCRN/0.33/0.55	SCRN/0.33/0.48
		TS	SCRN/0.26/0.44	SCRN/0.26/0.44
	Closed	TP	SCRN/0.39/0.63	SCRN/0.39/0.55
		TS	SCRN/0.30/0.61	SCRN/0.30/0.61

1 Unvented indicates a face that does not support significant ventilation (for example, a louver, meshed opening, missing panel, or the face with a door for a non-robustly secured cabinet).

2 SCRN (screen) indicates no ZOI outside of cabinet.

3 *Open/closed* refers to open/closed definitions in NUREG-2178.

Table 3-2
Obstructed radiation (horizontal) ZOI factor (Obs_fac) for vented[1] cabinet faces, based on unadjusted solid flame FDT^s

Cabinet Size	Cabinet Ventilation[3]	Cable Type	Threshold Approach ZOI Factor[2] (Very Low/Low/Default)	Damage Integral Approach ZOI Factor (Very Low/Low/Default)
Large (>1.4 m^3 (50 ft^3))	Open	TP	0.31/0.94/1.06	SCRN/0.80/0.99
		TS	SCRN/0.55/0.91	SCRN/0.55/0.91
	Closed	TP	0.26/0.43/0.76	0.26/0.21/0.68
		TS	SCRN/0.32/0.78	SCRN/0.32/0.78
Medium (0.3 m^3 (12 ft^3) to 1.4 m^3 (50 ft^3))	Open	TP	0.10/0.67/0.90	0.10/0.59/0.83
		TS	SCRN/0.51/0.98	SCRN/0.51/0.98
	Closed	TP	0.34/0.39/0.79	0.34/0.39/0.63
		TS	0.31/0.30/0.73	0.31/0.30/0.73

1 Vented indicates a face that supports significant ventilation (for example, a louver, meshed opening, missing panel, or the face with the door for a non-robustly secured cabinet).

2 SCRN (screen) indicates no ZOI outside of cabinet.

3 *Open/closed* refers to open/closed definitions in NUREG-2178.

3.1.2 Example

As an example, consider a medium, closed, electrical cabinet with a **very low** fuel load of thermoplastic (TP) cable. According to the distributions in Table 4-2 of NUREG-2178 Vol 1. [2], this would have a heat release rate (HRR) of 45 kW at the 98th percentile. Using the 0.61 m (2 ft) x 0.61 m (2 ft) base from the medium cabinets modeled with FDS for Table 2-4 as the fire area, the unadjusted FDTs for this would give a radiation (horizontal) ZOI of 0.73 m (2.4 ft). The Obs_fac for an unvented face for this cabinet from Table 3-3 is SCRN. This means that there is no ZOI outside the cabinet for the unvented face.

As a second example, consider a large, open, thermoset (TS) cable electrical cabinet with a **default** fuel load. According to the distributions in Table 4-2 of NUREG-2178 Vol 1. [2], this would have a HRR of 700 kW at the 98th percentile. Using the 0.88 m (2.9 ft) x 0.88 m (2.9 ft) base from the medium cabinets modeled with FDS for Table 2-5 as the fire area, the unadjusted FDTs for this would give a ZOI of 1.30 m (4.3 ft). From Table 3-2, The Obs_fac for an unvented face for this cabinet is 0.91. This means the actual ZOI would be 1.30×0.91 = 1.18 m (3.8 ft).

3.2 Maximum Severity Factor

3.2.1 Discussion

In a probabilistic risk assessment (PRA) application, when a target is determined to lie within the 98th percentile ZOI for an ignition source, credit can be taken by using the FDT^s to determine exactly what size fire is required to damage that target. By using the HRR gamma distributions from NUREG-2178 Vol. 1, the minimum fire size needed to damage the target can be converted

to a percentile and used to define a severity factor (SF). The SF is the fraction of fires for an ignition source that could damage a specific target. For a fire in an electrical cabinet, determining the SF is no longer a simple analytical process using a correlation. One approach, covered in the next section, would be to use a detailed tabulation of the radiation (horizontal) ZOI as a function of cabinet size, fire size, cable type, fuel loading, and cabinet ventilation to determine the SF. A second approach would be to simply take credit for the fraction of fires that have no external ZOI. For each combination of cabinet size, cable type, and cabinet ventilation, there is a fire size below which no ZOI exists outside the cabinet. These fire sizes can be converted into maximum SFs. For any target within the ZOI for a cabinet, the actual SF cannot be larger than the maximum factor. It could be less; however, as noted previously, this would involve target-specific table lookups, which could be time consuming for large numbers of targets.

This is depicted in Figure 3-3. A cable, orange, exactly at the ZOI, defined using the 98th percentile fire, has a SF of 0.02. A cable, purple, right at the cabinet face has a SF based on the largest fire size needed to have a radiation (horizontal) ZOI outside of the cabinet. This is, the maximum possible SF because one cannot get any closer to cabinet. Any other target, for example, red, therefore has a SF that is between the two but is always bounded by the maximum SF.

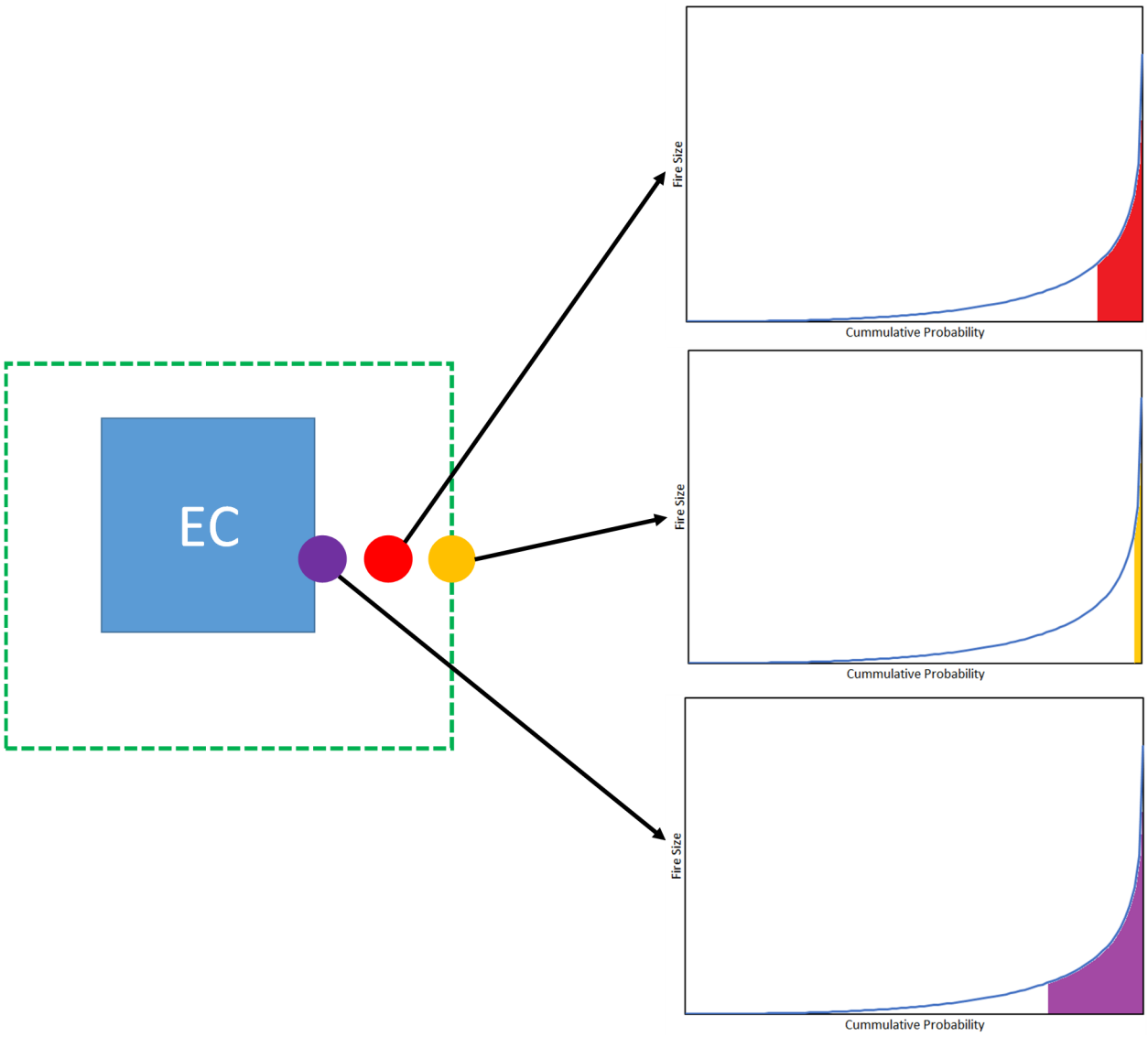

Figure 3-3
Depiction of the maximum severity factor (The yellow cable is at the 98th percentile ZOI with a severity factor of 0.02. The purple cable is at the cabinet face and has the maximum severity factor. The red cable has a severity factor between the two, but bounded by the maximum.)

Tables 3-3 and 3-4 show the maximum severity factor as a function of cabinet size, ventilation, cable type, and fuel loading. These values are derived from the FDS determined ZOIs. Table 3-3 shows results for unvented cabinet faces, and Table 3-4 shows results for vented cabinet faces.

Table 3-3
Obstructed radiation maximum severity factor for unvented[1] cabinet faces

Cabinet Size	Cabinet Ventilation[2]	Cable Type	Threshold Approach (Very Low/Low/Default)	Damage Integral Approach (Very Low/Low/Default)
Large (>1.4 m^3 [50 ft^3])	Open	TP	SCRN[3]/0.16/0.30	SCRN/0.16/0.30
		TS	SCRN/0.04/0.11	SCRN/0.04/0.11
	Closed	TP	SCRN/0.10/0.25	SCRN/0.07/0.20
		TS	SCRN/0.03/0.10	SCRN/0.03/0.10
Medium (0.3 m^3 [12 ft^3]to 1.4 m^3 [50 ft^3])	Open	TP	SCRN/0.08/0.25	SCRN/0.05/0.20
		TS	SCRN/0.03/0.10	SCRN/0.03/0.10
	Closed	TP	SCRN/0.10/0.25	SCRN/0.07/0.20
		TS	SCRN/0.04/0.10	SCRN/0.04/0.10

1 Unvented indicates a face that does not support significant ventilation (for example, a louver, meshed opening, missing panel, or the face with the door for a non-robustly secured cabinet).

2 *Open/Closed* refers to open/closed definitions in NUREG-2178.

3 SCRN indicates scenario screens at 98th percentile.

Table 3-4
Obstructed radiation maximum severity factor for vented[1] cabinet faces

Cabinet Size	Cabinet Ventilation[2]	Cable Type	Threshold Approach (Very Low/Low/Default)	Damage Integral Approach (Very Low/Low/Default)
Large (>1.4 m^3 [50 ft^3])	Open	TP	0.06/0.37/0.50	SCRN/0.26/0.40
		TS	SCRN/0.16/0.26	SCRN/0.16/0.26
	Closed	TP	0.15/0.34/0.50	0.15/0.34/0.50
		TS	SCRN/0.07/0.15	SCRN/0.07/0.15
Medium (0.3 m^3 [12 ft^3] to 1.4 m^3 [50 ft^3])	Open	TP	0.08/0.23/0.50	0.08/0.23/0.50
		TS	0.02/0.12/0.24	0.02/0.12/0.24
	Closed	TP	0.21/0.35/0.51	0.21/0.35/0.51
		TS	0.09/0.16/0.24	0.09/0.16/0.24

1 Vented indicates a face that supports significant ventilation (for example, a louver, meshed opening, missing panel, or the face with the door for a non-robustly secured cabinet).

2 *Open/Closed* refers to open/closed definitions in NUREG-2178.

3.2.2 Example

Consider a TP electrical cable that is located 0.25 m (0.8 ft) from the unvented face of large, closed, TP cabinet with a **default** fuel load. From Table 2-6 the ZOI for this cabinet for a 98th percentile is 1.03 m (2.4 ft) using the threshold approach or 1.17 (2.9 ft) using the damage integral approach. This cable would not screen at the 98th percentile fire. For this cabinet Table 3-3, indicates a maximum SF of 0.25 for the threshold approach and 0.20 for the damage integral approach.

Note that the actual SF for the cable is likely less than the maximum SFs in Table 3-3 and Table 3-4. Using the data in Table 2-6, the 85th percentile threshold ZOI is 0.08 m (3 in.) and the 90th percentile threshold ZOI is 0.59 m (1.9 ft). Interpolation would give a ZOI of 0.25 m at the 87th percentile for an actual severity factor of 0.13.

3.3 Detailed Fire Modeling

3.3.1 Overview

The final method for applying the results of the obstructed radiation study is intended for detailed fire modeling. Tables 3-5 through 3-8 provide the ZOI measured from the cabinet face as a function of the cabinet type, cable type, fuel loading, and fire size. These values are computed using the damage integral approach. A value of N/A means that there is no ZOI outside the cabinet for that fire size. Given a specific target, the target distance can be looked up in the table to determine the fire size percentile that applies to the target. This could be done by interpolation or more conservatively by picking the lower percentile if a target distance falls between two rows in the table. Note that these tables include the effects of the obstructed plume shown in Tables 2-3 through 2-6.

Table 3-5
Radiation (horizontal) ZOI measured from the cabinet face for a medium (0.3 m^3 [12 ft^3]) to 1.4 m^3 [50 ft^3]), open cabinet using the damage integral approach

Cable Type	Fire Size (kW)	Fire Size Percentile for Fuel Loading (%)			Vented[1] Face ZOI (m) [ft]	Unvented[2] Face ZOI (m) [ft]
		Default Fuel	Low Fuel	Very Low Fuel		
TP	28	50	77	92	N/A	N/A
	43	60	84	98	0.07 [0.23]	N/A
	65	70	90	>98	0.21 [0.69]	N/A
	80	75	93	>98	0.30 [0.98]	N/A
	99	80	95	>98	0.41 [1.35]	N/A
	125	85	97	>98	0.51 [1.67]	0.30 [1.0]
	163	90	98	>98	0.71 [2.33]	0.41 [1.3]
	231	95	>98	>98	0.91 [2.99]	0.51 [1.7]
	325	98	>98	>98	1.22 [4.0]	0.71 [2.3]
TS	43	76	88	98	N/A	N/A
	65	82	92	>98	0.11 [0.36]	N/A
	80	85	94	>98	0.11 [0.36]	N/A
	99	87	96	>98	0.20 [0.66]	N/A
	125	90	97	>98	0.30 [0.98]	N/A

Table 3-5
Radiation (horizontal) ZOI measured from the cabinet face for a medium (0.3 m^3 [12 ft^3]) to 1.4 m^3 [50 ft^3]), open cabinet using the damage integral approach (continued)

Cable Type	Fire Size (kW)	Fire Size Percentile for Fuel Loading (%)			Vented[1] Face ZOI (m) [ft]	Unvented[2] Face ZOI (m) [ft]
		Default Fuel	Low Fuel	Very Low Fuel		
TS	163	93	98	>98	0.41 [1.35]	0.20 [0.66]
	231	96	>98	>98	0.71 [2.33]	0.30 [0.98]
	325	98	>98	>98	0.91 [2.99]	0.41 [1.35]

1 Vented indicates a face that supports significant ventilation (for example, a louver, meshed opening, missing panel, or the face with the door for a non-robustly secured cabinet).

2 Unvented indicates a face that does not support significant ventilation (for example, a louver, meshed opening, missing panel, or the face with a door for a non-robustly secured cabinet).

Table 3-6
Radiation (horizontal) ZOI measured from the cabinet face for a medium (0.3 m^3 [12 ft^3]) to 1.4 m^3 [50 ft^3]), closed cabinet using the damage integral approach

Cable Type	Fire Size (kW)	Fire Size Percentile for Fuel Loading (%)			Vented[1] Face ZOI (m) [ft]	Unvented[2] Face ZOI (m) [ft]
		Default Fuel	Low Fuel	Very Low Fuel		
TP	17	50	65	79	N/A	N/A
	27	60	77	91	0.16 [0.52]	N/A
	40	70	85	97	0.16 [0.52]	N/A
	50	75	90	>98	0.26 [0.85]	N/A
	61	80	93	>98	0.31 [1.02]	N/A
	77	85	96	>98	0.31 [1.02]	0.30 [0.98]
	101	90	98	>98	0.41 [1.35]	0.41 [1.35]
	143	95	>98	>98	0.51 [1.67]	0.51 [1.67]
	200	98	>98	>98	0.81 [2.66]	0.71 [2.33]
TS	27	76	84	91	N/A	N/A
	40	82	90	97	0.11 [0.36]	N/A
	50	85	92	>98	0.16 [0.52]	N/A
	61	87	94	>98	0.16 [0.52]	N/A
	77	90	96	>98	0.21 [0.69]	N/A

Table 3-6
Radiation (horizontal) ZOI measured from the cabinet face for a medium (0.3 m^3 [12 ft^3]) to 1.4 m^3 [50 ft^3]), closed cabinet using the damage integral approach (continued)

Cable Type	Fire Size (kW)	Fire Size Percentile for Fuel Loading (%)			Vented[1] Face ZOI (m) [ft]	Unvented[2] Face ZOI (m) [ft]
		Default Fuel	Low Fuel	Very Low Fuel		
TS	101	93	98	>98	0.21 [0.69]	0.20 [0.66]
	143	96	>98	>98	0.41 [1.35]	0.41 [1.35]
	200	98	>98	>98	0.61 [2.0]	0.51 [1.67]

1 Vented indicates a face that supports significant ventilation (for example, a louver, meshed opening, missing panel, or the face with the door for a non-robustly secured cabinet).

2 Unvented indicates a face that does not support significant ventilation (for example, a louver, meshed opening, missing panel, or the face with a door for a non-robustly secured cabinet).

Table 3-7
Radiation (horizontal) ZOI measured from the cabinet face for a large (>1.4 m^3 [50 ft^3]), open cabinet using the damage integral approach

Cable Type	Fire Size (kW)	Fire Size Percentile for Fuel Loading (%)			Vented[1] Face ZOI (m) [ft]	Unvented[2] Face ZOI (m) [ft]
		Default Fuel	Low Fuel	Very Low Fuel		
TP	94	60	74	>98	N/A	N/A
	156	70	84	>98	0.29 [0.95]	N/A
	200	75	88	>98	0.44 [1.44]	0.29 [0.95]
	258	80	92	>98	0.55 [1.8]	0.29 [0.95]
	338	85	95	>98	0.88 [2.89]	0.59 [1.94]
	460	90	97	>98	1.17 [3.84]	0.73 [2.4]
	684	95	>98	>98	1.61 [5.28]	0.88 [2.89]
	1000	98	>98	>98	2.20 [7.22]	1.17 [3.84]
TS	94	74	84	>98	N/A	N/A
	156	82	91	>98	0.08 [0.26]	N/A
	200	85	94	>98	0.29 [0.95]	N/A
	258	89	96	>98	0.29 [0.95]	N/A
	338	92	98	>98	0.59 [1.94]	0.29 [0.95]

Table 3-7
Radiation (horizontal) ZOI measured from the cabinet face for a large (>1.4 m^3 [50 ft^3]), open cabinet using the damage integral approach (continued)

Cable Type	Fire Size (kW)	Fire Size Percentile for Fuel Loading (%)			Vented[1] Face ZOI (m) [ft]	Unvented[2] Face ZOI (m) [ft]
		Default Fuel	Low Fuel	Very Low Fuel		
TS	460	95	>98	>98	0.88 [2.89]	0.44 [1.44]
	684	98	>98	>98	1.17 [3.84]	0.59 [1.94]
	1000	>98	>98	>98	1.76 [5.77]	0.88 [2.89]

1 Vented indicates a face that supports significant ventilation (for example, a louver, meshed opening, missing panel, or the face with the door for a non-robustly secured cabinet).

2 Unvented indicates a face that does not support significant ventilation (for example, a louver, meshed opening, missing panel, or the face with a door for a non-robustly secured cabinet).

Table 3-8
Radiation (horizontal) ZOI measured from the cabinet face for a large (>1.4 m^3 [50 ft^3]), closed, cabinet using the damage integral approach

Cable Type	Fire Size (kW)	Fire Size Percentile for Fuel Loading (%)			Vented[1] Face ZOI (m) [ft]	Unvented[2] Face ZOI (m) [ft]
		Default Fuel	Low Fuel	Very Low Fuel		
TP	35	50	66	85	N/A	N/A
	54	60	77	94	0.15 [0.49]	N/A
	81	70	86	98	0.22 [0.72]	N/A
	100	75	90	>98	0.30 [0.98]	N/A
	124	80	93	>98	0.32 [1.05]	N/A
	155	85	96	>98	0.37 [1.21]	0.08 [0.26]
	202	90	98	>98	0.44 [1.44]	0.44 [1.44]
	285	95	>98	>98	0.59 [1.94]	0.73 [2.4]
	400	98	>98	>98	1.17 [3.84]	1.03 [3.38]
TS	100	85	93	>98	N/A	N/A
	124	87	95	>98	0.12 [0.39]	N/A
	155	90	97	>98	0.26 [0.85]	N/A
	202	93	98	>98	0.30 [0.98]	0.29 [0.95]
	285	96	>98	>98	0.44 [1.44]	0.44 [1.44]
	400	98	>98	>98	0.88 [2.89]	0.59 [1.94]

[1] Vented indicates a face that supports significant ventilation (for example, a louver, meshed opening, missing panel, or the face with the door for a non-robustly secured cabinet).

[2] Unvented indicates a face that does not support significant ventilation (for example, a louver, meshed opening, missing panel, or the face with a door for a non-robustly secured cabinet).

3.3.2 Example

The target of interest is a TP target 0.4 m (1.3 ft) from the vented face of a large, closed cabinet. This target lies within the 98th percentile ZOI from Table 2-6. Table 3-4 could be used to obtain the maximum severity factor of 0.5. Using Table 3-8, it is seen that this target sits between the 85th and the 90th percentile. The 85th percentile could be selected or the table could be interpolated to obtain the 87th percentile. Respectively, those two lookup methods would have severity factors of 0.15 and 0.13 versus the maximum severity factor of 0.5 from Table 3-4.

3.4 Application to Groups 1, 2, and 3

The ZOI from other cabinets (Group 1, switchgear and load centers; Group 2, motor control centers (MCCs) and battery chargers; and Group 3, power inverters) can be estimated using the medium and large cabinet results. This can be done by selecting the modeled cabinet configuration that bounds the desired cabinet. The ZOI Obs_fac and the maximum severity factor is summarized in Table 3-9 and Table 3-10 for the assumption that the cabinets are closed and have a **default** fuel load. The Obs_fac are interpolated using the applicable 98th percentile fire size and the data in Table 2-4 and Table2-6. Note that other fire sizes can be determined by interpolating the fire size using Table 2-4 and Table 2-6.

Table 3-9
Unvented[1] face obstruction factor and maximum severity factor for Groups 1, 2, and 3

Cabinet Type	Size	98th Fire Size (kW)	Obs_fac[2]		Limiting Severity Factor[2]	
			TP	TS	TP	TS
Switchgear and load centers	Medium (0.3 m^3 [12 ft^3] to 1.4 m^3 [50 ft^3])	170	0.57 0.49	0.53 0.53	0.32 0.25	0.10 0.10
	Large (>1.4 m^3 [50 ft^3])	170	0.19 0.15	0.11 0.11	0.11 0.06	0.03 0.03
MCCs and battery chargers	Medium (0.3 m^3 [12 ft^3] to 1.4 m^3 [50 ft^3])	130	0.49 0.42	0.47 0.47	0.26 0.18	0.07 0.07
	Large (>1.4 m^3 [50 ft^3])	130	0.01 0.01	SCRN SCRN	0.06 0.03	SCRN SCRN
Power inverters	Medium (0.3 m^3 [12 ft^3] to 1.4 m^3 [50 ft^3])	200	0.63 0.55	0.61 0.61	0.26 0.21	0.11 0.11
	Large (>1.4 m^3 [50 ft^3])	200	0.42 0.31	0.31 0.31	0.11 0.07	0.04 0.04

1 Unvented indicates a face that does not support significant ventilation (for example, a louver, meshed opening, missing panel, or the face with a door for a non-robustly secured cabinet).

2 Threshold ZOI presented in top portion, damage integral ZOI in bottom portion.

Table 3-10
Vented[1] face obstruction factor and limiting severity factor for Groups 1, 2, and 3

Cabinet Type	Size	98th Fire Size (kW)	Obs_fac[2]		Limiting Severity Factor[2]	
			TP	TS	TP	TS
Switchgear and load centers	Medium (0.3 m^3 (12 ft^3) to 1.4 m^3 (50 ft^3))	170	0.70 0.53	0.58 0.58	0.68 0.68	0.27 0.27
	Large (>1.4 m^3 (50 ft^3))	170	0.35 0.36	0.33 0.33	0.45 0.45	0.07 0.07
MCCs and battery chargers	Medium (0.3 m^3 (12 ft^3) to 1.4 m^3 (50 ft^3))	130	0.55 0.42	0.47 0.47	0.67 0.67	0.24 0.24
	Large (>1.4 m^3 (50 ft^3))	130	0.29 0.29	0.20 0.20	0.40 0.40	0.04 0.04
Power inverters	Medium (0.3 m^3 (12 ft^3) to 1.4 m^3 (50 ft^3))	200	0.79 0.63	0.73 0.72	0.52 0.52	0.25 0.25
	Large (>1.4 m^3 (50 ft^3))	200	0.43 0.32	0.33 0.33	0.35 0.35	0.08 0.08

1 Vented indicates a face that supports significant ventilation (for example, a louver, meshed opening, missing panel, or the face with the door for a non-robustly secured cabinet).

2 Threshold ZOI presented in top portion, damage integral ZOI in bottom portion.

For example, the cabinet exposing a target is a 0.61 m x 0.61 m x 1.8 m (2 ft x 2 ft x 6 ft) battery charger. This has a volume of 0.68 m^3 (24 ft^3) which is bounded by the medium cabinet modeled in the study. If the target was a TP cable on an unvented face and the threshold approach was being used, Table 3-9 indicates that the FDT^s ZOI could be reduced using the Obs_fac of 0.49 for the threshold approach. If the target did not screen at this reduced distance, the limiting severity factor of 0.26 could be applied.

3.5 Group 4c: Small Cabinets

NUREG-2178 Vol. 1 [2] defines the medium and large cabinets with a lower bound for the size. This allowed for fire modeling to use the lower bound and determine the radiation (horizontal) ZOI. Using the lower bound, Figure 2-25 maximizes the cabinet wall temperature. Without a defined lower bound an analogous process is not possible for small cabinets. However, the

adjusted FDT^s can be used to generate a maximum radiation (horizontal) ZOI. As covered in NUREG-2178, small cabinets are expected to be closed and generally have limited fuel available in them. The 98th percentile fire size for a small cabinet is 45 kW. An example in NUREG-2178 shows that a typical consumer grade 10-cup coffee maker would have a peak HRR of approximately 40 kW. The radiation (horizontal) ZOI for a small cabinet using the adjusted FDT^s is shown in Table 3-11. This table assumes the cabinet has a 0.1 m^2 (1 ft^2) footprint (the range from 0.02 m^2 (0.25 ft^2) to 0.2 m^2 (2.25 ft^2) results in only 1–2 cm (0.4–0.8 in.) shifts in the ZOI). Results from the medium and large cabinets indicate that after a ZOI of 7–8 cm (2.8–3.1 in.) is reached, that the next 10th percentile is the threshold size for a ZOI outside the cabinet. It is assumed that this behavior continues for the small cabinet.

Table 3-11
Radiation (horizontal) ZOI for small cabinets (<12 ft^3) computed using the adjusted FDT^s

Fire Size Percentile	Fire Size (kW)	ZOI (m) [ft]	
		TP	TS
40	5	SCRN[1]	SCRN
50	7	0.07 [0.23]	SCRN
60	9	0.09 [0.3]	SCRN
70	12	0.11 [0.36]	SCRN
75	15	0.13 0.43]	SCRN
80	17	0.14 [0.46]	SCRN
85	21	0.17 [0.56]	SCRN
90	25	0.19 [0.62]	0.07 [0.23]
95	34	0.23 [0.75]	0.10 [0.3]
98	45	0.28 [0.92]	0.13 [0.43]

[1] SCRN indicates the scenario screens with no ZOI outside the cabinet.

3.6 FDS Modeling Guidance

Instead of applying the generic guidance in Sections 3.1 through 3.5, one could model a specific cabinet's size and vent opening configuration using FDS. This section provides guidance on using FDS for modeling fires in electrical cabinets. The following list notes some considerations for modeling cabinet fires:

- Avoid the use of thin obstructions—see the FDS User's Guide [5]— when using the default fast Fourier transform (FFT) pressure solver. This pressure solver has small normal velocity errors at solid surfaces. This can result in poor vent flow predictions, especially for cabinets where the area of vents is a small fraction of the cabinet surface area.
- Even with solid obstructions, for a closed cabinet decrease the VELOCITY_TOLERANCE and increase the MAX_PRESSURE_ITERATIONS. This study respectively used 0.001 and 50.
- Increase the default NUMBER_RADIATION_ANGLES to reduce streaming effects. This study used 200 angles.
- Twelve or more grid cells across the width of cabinet are required to reasonably resolve the radiation field.
- The fire location within the cabinet will have an impact on the radiative field. To the extent possible, characterizing a realistic distribution of the heat release within the cabinet will result in more realism for the external radiative flux.
- The FDS device output of INTEGRATED INTENSITY is not a flux output. This output measures radiation over all angles and will overestimate the flux to a target. It is better to use a device that measures RADIATIVE HEAT FLUX GAS. If the target is a plane, set the device ORIENTATION to represent the true surface normal of the target. Otherwise, if the target is something with a curved surface such as a cable, use three devices. Set the first device ORIENTATION to point the device directly at the electrical cabinet. Set the second and third devices to be rotated 90° up and down along the cabinet axis. The maximum orientation independent target flux can then be found by performing a vector norm for each pair of up and direct and down and direct and taking the maximum value:
  (Max$\left[\sqrt{up^2 + direct^2}, \sqrt{down^2 + direct^2}\right]$)
- Modeling of cabinet ventilation will depend on the type of vent.
  - Louvered vents should use the localized leakage model. Create at least one leakage path for each row of grid cells over the height of the louvered vent. It may be necessary to reduce the default value of HVAC_PRES_RELAX to avoid instabilities; this study used 0.3.
  - Fully open vents that are not resolvable on the grid (vents are less than a few grid cells across) should be modeled using the localized leakage model. Examples of these might be an unsealed cable penetration in the wall or top of a cabinet.
  - Vents covered in wire or expanded metal mesh can be modeled using the screen drag model. Examples are provided in the FDS User's Guide [5] for simple wire screens and the FDS Validation Guide (FM Datacenter Tests) [21] for expanded metal mesh.
  - If all of the vents in a cabinet are defined using the localized leakage model, define a pressure ZONE for the cabinet.

- If the cabinet is in a larger overall space where the required cabinet resolution is impractical for the entire space, use multiple meshes with a finer mesh around the cabinet that extends at least one cabinet width away in all directions.
- The size of the flame volume and the amount of combustion realized inside the cabinet versus outside of the cabinet is critical to correctly predicting the cabinet wall temperatures. This requires a fuel chemistry definition that is consistent with both the heat of combustion of the fuel and the energy released per unit mass of oxygen (EPUMO2). Most ordinary combustibles have and EPUMO2 near 13,100 kJ/kg O_2 [27]. Fuels with heats of combustion below 40,000 kJ/kg should be defined with sufficient O or N in the fuel molecule to obtain an EPUMO2 near 13,100 kJ/kg O_2. As an example, if the chemical formula of the fuel was specified as CH_4 (methane), the heat of combustion was defined as 20,000 kJ/kg, and no soot or CO yield was specified, one CH_4 of fuel would require two moles of O_2 to burn and make one mole of CO_2 and two moles of H_2O. The EPUMO2 could be computed as 20,000 kJ/kg CH4 x 0.016 kg CH_4 ÷ 0.064 kg O_2 = 5,000 kJ/kg O_2. This is too low of a value. However, if the fuel were CH_4O (methanol), 1.5 moles of O_2 would be required and the fuel molecular weight would be higher. The EPUMO2 would be 20,000 kJ/kg CH4 x 0.032 kg CH_4 ÷ 0.048 kg O_2 = 13,300 kJ/kg O_2.

4
FIRE SPREAD BETWEEN ADJACENT ELECTRICAL ENCLOSURES

4.1 Overview and Terminology

4.1.1 Background

Fire probabilistic risk assessments (FPRAs) include scenarios where a fire initiated in one electrical enclosure is assumed to propagate to an adjacent enclosure. This is referred to as *cabinet-to-cabinet fire spread* in NUREG/CR-6850 (EPRI 1011989) [1]. The NUREG/CR-6850 method derives largely from the individual plant examination of external events fire vulnerability assessment methods documented in the *Fire PRA Implementation Guide* [28] and has not been updated since publication of NUREG/CR-6850 in 2005. According to that guidance, a fire is assumed to spread from the electrical enclosure of fire origin (the exposing enclosure) to an adjacent enclosure (the exposed enclosure) after 10–15 minutes unless the partition(s) between the two enclosures meet one of two exclusionary configurations: cabinets are separated by a double wall with an air gap, or either the exposed or exposing cabinet has an open top, and there is an internal wall possibly with some openings, and there is no diagonal cable run between the exposing and exposed cabinet.

The guidance makes no distinctions based on factors that would be expected to influence this behavior. Such factors would include the physical characteristics of both the exposing and exposed electrical enclosures, and the fire properties (for example, peak heat release rate [HRR]) assigned to the exposing enclosure. There is also no limit stated as to how many electrical enclosures might ultimately become involved; therefore, the extent of fire spread is, under some interpretations, limited only based on the non-suppression probability (NSP) as a function of time.

This section presents a refined methodology for the analysis of multi-cabinet fire scenarios. The methods presented here explicitly consider scenario likelihood and characteristics, including guidance for characterizing the fire intensity (that is, HRR) associated with a multi-enclosure fire, and provides guidance for avoiding double-counting[1] of risk contributions when evaluating single- and multi-enclosure scenarios.

[1] The method described in this section uses a split fraction approach to eliminate the double-counting concerns for evaluating the potential of a fire spreading to an adjacent electrical enclosure.

4.1.2 Terminology

To simplify the wording of the guidance described in this section, two new terms are defined as follows:

- *Exposing enclosure*. The electrical enclosure where the fire is assumed to originate (referred to as the “exposing cabinet” in NUREG/CR-6850).
- *Exposed enclosure*. An electrical enclosure that is adjacent to the exposing enclosure and to which fire spread may be considered (referred to as the *exposed cabinet* in NUREG/CR-6850).

It should also be noted that the term *enclosure* is often used to reference a room or compartment in the fire protection/fire modeling literature. Special care must be taken to clearly identify which definition of enclosure is being used when documenting any analysis.

4.1.3 Enclosure-to-Enclosure Fire Spread Methodology

The enclosure-to-enclosure methodology is presented in three parts, each of which is covered in the sections which follow:

- Screening guidance to identify configurations where enclosure-to-enclosure fire spread does not need to be postulated (see Section 4.2)
- A method for assigning a conditional probability of enclosure-to-enclosure fire spread to cases where enclosure-to-enclosure spread is postulated (see Section 4.3)
- Recommendations for characterizing the fire growth profile (HRR versus time) for the multi-enclosure fire scenario (see Section 4.4)

Examples can be found in Appendix D.

4.1.4 Assumptions and Limitations

The following assumptions and limitations are applicable to the enclosure-to-enclosure fire spread methodology:

- The method applicable to electrical cabinets (Bin 15) and the main control board (Bin 4) ignition sources in the FPRA. This does not include junction boxes (Bin 18), which are already covered in frequently asked question (FAQ) 13-0005 [29].
- The methodology and analysis apply only to the determination and analysis of fires *spreading* from one electrical enclosure to another immediately adjacent electrical enclosure for the purposes of establishing a HRR profile. Time to ignition should be considered in the damage estimates. There are no changes to the rules governing the functional *damage* to equipment due to fire affecting cables and components.
- Propagation to an adjacent enclosure should be assumed if there is not enough information available to determine whether fire spread should be postulated—that is, if there is not enough information to satisfy any of the screening guidance, assume that propagation between electrical enclosures is possible. In many cases application of the guidance may require one or more adjoining enclosures to be opened to confirm configurations (for example, fuel loading or orientation of cables).
- This methodology is limited to fire spread between adjacent cabinets due to thermal fires and does not apply to high-energy arcing fault (HEAF) scenarios.

4.2 Screening Guidance for Enclosure-to-Enclosure Fire Spread Potential

4.2.1 Background

The initial step for the assessment of fire spread from one electrical enclosure to an adjacent enclosure considers the physical characteristics of both the exposing and exposed enclosures through a set of go/no-go criteria. The guidance builds in part on the revised electrical enclosure fire characterization approach documented in NUREG-2178, Vol. 1 [2]. The guidance incorporates the fuel loading configurations as defined in NUREG-2178 and, in particular, the **low** and **very low** fuel loading conditions. The guidance also considers the nature of the barriers that separate the exposing and exposed enclosures.

The following points clarify the general intent:

- Any given enclosure might play the role of either exposed or exposing enclosure depending on the fire scenario. However, if the exposing/exposed role is reversed, the net risk result can change. For example, the screening criteria consider the fuel loading conditions in both the exposing and exposed enclosures; therefore, if the fuel loading is different in two adjacent enclosures, fire spread may be plausible in one direction but not plausible in the opposite direction (that is, if the role of exposing/exposed is reversed).
- Electrical enclosures as covered here are considered in the same context as the counting of electrical cabinet fire sources in the Task 6 fire frequency analysis. That is, an *electrical enclosure*, as covered in this report is equivalent to a *distinct vertical section*, according to the fire frequency ignition source counting guidance.
- The screening guidance makes extensive reference to the **low** and **very low** fuel loading conditions and to enclosure size classification (that is, small, medium, and large). These references are defined according to the NUREG-2178 Vol. 1 [2] guidance on the classification of electrical enclosure fire characteristics.

The following guidelines for determining the likelihood of ignition of adjacent enclosures are presented and described in the subsequent sections:

- Double wall
- Open top/vertically oriented cables
- Very low fuel load
- Group 4c: Small enclosure
- Low fuel/steel partition
- Low fuel exposing/very low exposed
- Group 1: Switchgear and load centers
- Group 2: Motor control center (MCC)

4.2.2 Basis for Screening Guidance

This section describes the screening guidelines and provides the technical basis for each screening rule.

4.2.2.1 Double Wall

Do not postulate fire spread to an adjacent electrical enclosure if both the exposing and exposed enclosures have solid steel panels on their adjacent sides.

Basis: This criterion promulgates one of two no-spread criteria specified in NUREG/CR-6850 Appendix S [1]: the double wall with air gap case. This configuration is characteristic of stand-alone electrical enclosures that are set side by side to form a bank of enclosures. Enclosures may be open or closed, vented or un-vented according to the guidance provided in NUREG-2178 [2]. Both enclosures must have solid steel partitions on the neighboring faces. The basis for this criterion is wall temperature measurements made during the original Nuclear Regulatory Commission-Office of Nuclear Regulatory Research (NRC-RES)/Sandia National Laboratories (SNL) electrical enclosure fire tests [30]. Measurements showed that, for this configuration, wall temperatures for the exposed enclosure remained well below either the ignition or damage thresholds for cables and control components. Therefore, the original test reports stated that fire spread to an adjacent enclosure under these conditions was not likely.

Note that NUREG/CR-6850 remained silent, intentionally, regarding the size of the air gap, and this has been the point of some misunderstanding. Given two adjacent electrical enclosures, each with its own steel side panel, the authors of NUREG/CR-6850 intended that the presence of an air gap would be implied and need not be demonstrated. It was also intended that incidental contact between the two panels would not negate the effect. The wording changes as expressed here are intended to clarify the original intent: it is the presence of two steel panels (that is, the double wall configuration) that is key, and there is no expectation that the analyst demonstrate that an air gap actually exists between those two steel panels.

4.2.2.2 Open Top/Vertically Oriented Cables

Do not postulate fire spread to an adjacent electrical enclosure if the following three conditions occur:

- The exposing or exposed enclosure (or both) has (have) an open top.
- There is an internal wall between the vertical sections, possibly with some unsealed openings.
- There are no cables running in an upward direction (that is, either vertically or diagonally) leading from the exposing enclosure into the exposed enclosure through the partition wall between sections.

Note: All three conditions must be met for the exclusion to apply.

An electrical enclosure with an open top configuration allows the heat generated by the fire to be transferred outside of the enclosure reducing the likelihood of propagation. For the purposes of modeling fire propagation between electrical enclosures, this methodology uses the definition of an *open enclosure* defined in Section 3.2.1 of NUREG-2178 [2]. Therefore, consistent with the definition in Section 3.2.1 of NUREG-2178, an open top configuration consists of the top surface being substantially or effectively missing—that is, if half or more of the top surface is open or effectively missing.

Vents positioned on (or in) the vertical side panels of an electrical enclosure, even if adjacent to the top surface, do not meet the top venting criteria.

Assessing the openings in a wall panel between sections will require judgment. In general, openings representing up to 5% of the total surface area of the neighboring face would be acceptable.

Basis: This criterion promulgates the second of two no spread criteria specified in NUREG/CR-6850 Appendix S [1]. The basis for this criterion is a combination of wall temperature measurements and fire behavior observations made during the original NRC-RES/SNL electrical enclosure fire tests and as stated in NUREG/CR-4527 [30]. Based on qualitative observations of fires within electrical enclosures, configurations with no top will experience internal air temperatures and enclosure wall temperatures much lower than those seen when an enclosure has a top panel. Wall temperatures for the exposed enclosure in this case remained well below either the ignition or damage thresholds for cables (NUREG/CR-6850, Appendix S [1]).

Also, propagation of fire among cables within open-top enclosures is expected to be dominated by vertical flame spread with little or no horizontal flame spread (which was only observed in the most intense fires [30]). As seen in the available experimental evidence, enclosures with a substantially closed top panel had a tendency to contain hot gasses within the enclosure, which enhanced re-radiation to enclosure internals and, in turn, led to more aggressive fire spread behaviors including horizontal spread along cable bundles [30]. As a result, for open-top enclosures fire spread along horizontal cable runs within the cabinet is considered unlikely.

Therefore, fire spread to the adjacent enclosure would require both a horizontal and vertical element to fire spread through *diagonally* oriented cables (that is, running in an upward orientation across the partition wall and into the exposed enclosure). The experimental evidence shows that fire may propagate up vertically oriented cables [30]. Therefore, *diagonally* oriented cables are used here to account for the chance that vertically oriented cables may not be exactly vertical. Lacking this configuration, fire spread to the adjacent enclosure should not be postulated.

4.2.2.3 Very Low Fuel Load

Do not postulate fire spread to any adjacent electrical enclosure if the exposing enclosure has a **very low** *fuel load*.

Basis: Based on the fire characterization guidance in NUREG-2178 Vol. 1, Section 4 [2], a **very low** fuel load in the exposing enclosure implies little potential for the development of a large, aggressively growing fire. Even at the 98th percentile condition, the largest peak HRR of 75kW for large enclosures is estimated. Fire spread from an exposing to exposed enclosure requires flames spreading horizontally and, as observed in both the NRC-RES/SNL [30] and the NUREG/CR-7197 fire tests [31], horizontal flame spread was only seen given very intense internal fire conditions (for example, high internal heat fluxes and temperatures). The radiation zone of influence (ZOI) results in Section 2 show no external ZOI for **very low** fuel load enclosures. Bulk ignition of cable trays will not occur given the lack of an external ZOI. A **very low** fuel load implies a **very low** fire intensity so that, while vertical flame spread may occur, horizontal flame spread would not be expected.

Note that this is not intended to preclude fire spread or damage to exposed components or cables outside the electrical enclosure. The guidance presented in this chapter is only applicable to the spread of fire between electrical enclosures and only precludes the spread of fire horizontally to an adjacent electrical enclosure.

4.2.2.4 Group 4c: Small Enclosure

Do not postulate fire spread to an adjacent electrical enclosure if the exposing enclosure has been categorized as a *small electrical enclosure*.

Basis: Given the fire characterization guidance in NUREG-2178 [2], a Group 4c: small electrical enclosure has an inherently **low** fire potential. Even at the 98th percentile, a small electrical enclosure is assumed to reach a peak of just 45kW. As noted previously, enclosure-to-enclosure fire spread requires a high-intensity fire in the exposing enclosure. Given the NUREG-2178 probability distributions for HRRs, small electrical enclosures are simply not capable of creating such conditions.

Note that this is not intended to preclude fire spread or damage to exposed components or cables outside the small electrical enclosure. The guidance presented in this section is only applicable to the spread of fire between electrical enclosures and only precludes the spread of fire horizontally to an adjacent electrical enclosure.

4.2.2.5 Low Fuel/Steel Partition

Do not postulate fire spread to an adjacent electrical enclosure if there is a full steel panel partition between the exposing and exposed enclosures, possibly with some unsealed/open penetrations (up to 5% of the total area of the panel partition) in combination with any one of the following conditions:

- A **low** fuel load in the exposing enclosure
- A **low** fuel load in the exposed enclosure provided that the combustible fuels in the exposed enclosure do not come into contact with the separating steel partition
- A **very low** fuel load in the exposed enclosure provided that the combustible fuels in the exposed enclosure do not come into contact with the separating steel partition

Basis: As recognized by NUREG/CR-6850 [1] and based on the original NRC-RES/SNL enclosure fire tests [30], a single solid steel partition wall is a substantial barrier to fire spread between enclosure sections. The original test report concluded that fire spread would not be expected unless there were fuel materials (for example, cables or components) in the exposed enclosure that were mounted in contact with the partition wall. That is, the tests showed that the wall temperatures for single wall partitions were in some cases high enough to cause failure and ignition of cables or components in physical contact with the partition wall; however, the wall temperatures were too low to generate radiant energy conditions sufficient to damage other cables or components (that is, those that are not in direct contact with the partition panel).

As stated here, this recommendation is designed as an extension of the Open Top/Vertically Oriented Cables guidance (see Section 4.2.2.2), which reiterates one of the two original NUREG/CR-6850 exclusions. The extension introduced here recognizes that fuel loading conditions for the enclosures under analysis would clearly impact the potential for fire spread between enclosures. The Low Fuel/Steel Partition guidance is based on the combined effect of two conditions: a substantive steel barrier present between the exposing and exposed enclosures and the **low** and **very low** fuel loading configurations in the exposing and/or exposed enclosures and the fire intensity potential those conditions imply. This combination of factors inherently limits fire intensity so that enclosure-to-enclosure fire spread is not credible and does not need to be postulated.

4.2.2.6 Low Fuel Exposing/Very Low Exposed

Do not postulate fire spread to an adjacent electrical enclosure if the exposing enclosure has a **low** fuel load and the exposed enclosure has a **very low** fuel load regardless of the nature of the separation/partitions—no separation or vented or open partitions—between enclosures.

Basis: With a **low** fuel load, the fire potential of the exposing enclosure is inherently limited. Further, the **low** load ranking means that those fuels that are present are not in the ideal configuration for fuel spread within the exposing enclosure. A **very low** fuel load in the exposed enclosure inherently implies that fuels in the exposed enclosure are very sparse and are not conducive to fire spread. This combination of conditions implies that fire spread to the adjacent exposed enclosure is not credible and should not be postulated.

4.2.2.7 Group 1: Switchgear and Load Centers

Do not postulate fire spread between adjacent switchgear vertical sections.

Basis: According to NUREG-2178 [2], Group 1 includes the enclosures housing higher power electrical switching and interrupting devices, namely switchgear and load centers.

Both load centers and switchgears are completely enclosed on all sides and the top, resulting in a closed, vented enclosure configuration. Similar to MCCs, switchgears exist as banks of vertical sections made up of multiple switches. Low-voltage, load center vertical sections may house multiple switches [2]. Older medium-voltage switchgears, are typically limited to a single breaker, while newer vacuum switchgears normally contain two breakers [32]. Similar to MCCs, equipment in load centers is connected by metal enclosed vertical and horizontal bus bars. Medium-voltage switchgear compartments are separated from each other by metal barriers [32].

The characterization of the peak fire HRR distributions in NUREG-2178 concluded that when compared with other enclosures, switchgears and load centers have limited fuel loads [2]. Although the larger diameter power cables used in switchgears result in slightly greater fuel loads than what is described for an MCC, these larger cables are not expected to burn as easily as the smaller cables found in MCCs without a sufficient ignition source.

For switchgears and load centers, fire spread into an adjacent section would require that the fire breach, at a minimum, a solid steel partition into a space with a **low** to **very low** fuel load. Given these physical conditions, fire spread between adjacent vertical sections of a switchgear or load center bank is considered unlikely and does not need to be postulated.

Note that this applies only to thermal fires and does not apply to HEAF events. This guidance is not intended to modify the current treatment of HEAF fires.

4.2.2.8 Group 2: MCCs

Do not postulate fire spread between adjacent MCC vertical sections.

Basis: MCCs represent a very unique enclosure configuration. MCC stacks (that is, one vertical section of MCCs) typically consist of 3–6 motor control cubicles (commonly referred to as *cubes*) bolted one on top of another to form a vertical section (commonly referred to as a *stack*). Each MCC stack will be associated with a narrow vertical channel dedicated to, and along one side of, the cube stack. This channel allows for routing cables to/from the individual relay cubes in one stack. A horizontal bus is located in rear area of the MCC bank.

Penetrations in the walls of a given cubicle will lead into the vertical channel dedicated to that stack of cubicles. Several such stack-and-channel sections are typically lined up side by side to form a bank of MCCs. In such cases, the vertical channels are uniformly aligned on the same side of the cubes to which they are dedicated (for example, the typical configuration in the United States is for the vertical channel to be placed to the right of the corresponding cube stack when viewed from the front face of the bank). Therefore, the vertical channel dedicated to one stack of cubes will abut the cubicle walls of the adjacent cubicle stack. Further, there would be no penetrations from the vertical channel dedicated to one cubicle stack into an adjacent cubicle stack because the adjacent cubicle stack will have its own dedicated cable routing channel. The horizontal bus creates penetrations between the different banks; however, the fuel loading is not high enough to allow for propagation.

The characterization of peak fire HRR distributions for MCCs in NUREG-2178 Vol. 1 [2] concluded that the fuel load in each of the cubes was typically **very low** and that the most severe fires would be associated with fire spreading from a cube into its own vertical cable channel [2]. Fire spread into an adjacent cube stack would require that the fire breach, at a minimum, a solid steel partition (that is, the steel wall of the adjacent cube) with no penetrations into a space with a **low** to **very low** fuel load. Given these physical conditions, fire spread between adjacent vertical sections of an MCC bank is considered unlikely and does not need to be postulated.

This guidance does not apply to battery chargers because they have known differences in construction relative to MCCs.

4.2.3 Summary of Fire Spread Screening Guidance

The following summarizes the enclosure configurations for which fire spread between adjacent enclosures does not need to be postulated in the FPRA.

Double wall. Do not postulate fire spread between adjacent electrical enclosures if both the exposing and exposed enclosures have solid steel panels on their adjacent sides (that is, the double wall configuration).

Open top/vertically oriented cables. Do not postulate fire spread between adjacent electrical enclosures if: (1) the exposing or exposed enclosure (or both) has (have) an open top; and (2) there is an internal wall between the sections, even if that wall has some unsealed openings; and (3) there are no cables running in an upward direction (that is, either vertically or diagonally) leading from the exposing enclosure into the exposed enclosure through the partition wall between sections. (Note: all three conditions must be met for the exclusion to apply.)

An electrical enclosure with an open top configuration allows the heat generated by the fire to be transferred outside of the enclosure reducing the likelihood of propagation. An open top configuration consists of the top surface being substantially or effectively missing. That is, if half or more of the top surface is open or effectively missing.

Assessing the openings in a wall panel between sections will require judgment. In general, openings representing up to 5% of the total surface area would be acceptable.

Very low fuel load. Do not postulate fire spread to any adjacent electrical enclosure if the exposing enclosure has a **very low** fuel load according to NUREG-2178 Vol. 1 [2].

Group 4c: small enclosure. Do not postulate fire spread to any adjacent electrical enclosure if the exposing enclosure has been categorized as a *small electrical enclosure* according to NUREG-2178 Vol. 1 [2].

Low fuel/steel partition. Do not postulate fire spread between adjacent electrical enclosures if there is a full steel panel partition between the exposing and exposed enclosures possibly with some unsealed/open penetrations (up to 5% of the total area of the panel partition) in combination with any one of the following conditions:

- A **low** fuel load in the exposing enclosure
- A **low** fuel load in the exposed enclosure provided that the combustible fuels in the exposed enclosure do not come into contact with the separating steel partition
- A **very low** fuel load in the exposed enclosure

Low fuel exposing/very low exposed. Do not postulate fire spread to an adjacent electrical enclosure if the exposing enclosure has a **low** fuel load and the exposed enclosure has a **very low** fuel load regardless of the nature of the separation/partitions between enclosures. **Note**: For **default** fuel loading, you must assume propagation if there is no separating partition.

Group 2: MCC. Do not postulate fire spread between adjacent MCC vertical sections.

Group 1: Switchgear and load centers. Do not postulate fire spread between adjacent switchgear/load center vertical sections.

4.3 Assignment of a Conditional Probability to the Multi-Enclosure Fire Scenario

4.3.1 Background

Electrical enclosure peak fire intensity (that is, peak HRR) is characterized in probabilistic risk assessments (PRAs) using a probabilistic treatment to reflect the random nature of fire behavior and the implied variability in the evolution of an electrical enclosure fire given ignition. Given ignition in the exposing enclosure, there is some relatively low conditional probability that fire conditions would reach levels sufficient to potentially induce fire spread to an adjacent enclosure.

The recommended practice presented here is based on the premise that fire spread to an adjacent enclosure should only be postulated given an aggressively growing, high intensity fire in the exposing enclosure—a low-likelihood occurrence given the peak HRR distributions. Ideally, it would seem plausible to assume that some minimum HRR must be reached before fire spread to an adjacent enclosure would be considered plausible. Unfortunately, the data are not available to develop such a relationship.

As an alternative, this method recommends that, given ignition (that is, the electrical cabinet fire ignition frequency) and the guidance developed in the preceding sections has indicated that enclosure-to-enclosure fire spread should be postulated, a generic conditional probability of enclosure-to-enclosure fire spread can be applied that would reflect the anticipated low-likelihood of this event occurring. The details of this approach and the recommended generic numerical value to be applied are described in Section 4.3.2.

4.3.2 Discussion and Basis for the Likelihood Characterization Guidance

As noted previously, an obvious corollary to the current treatment of electrical enclosure fires is that some relatively low conditional probability should be assumed for the enclosure-to-enclosure fire spread scenario—that is, the only fires that could reasonably induce fire spread from one electrical enclosure to an adjacent electrical enclosure would be those fires that grow

aggressively and that will eventually reach an intense peak HRR. Therefore, a factor could reasonably be applied as a modifier on the base electrical enclosure fire frequency as either a severity factor on the multi-enclosure fire scenario or, more accurately, as a split fraction between single-enclosure and multi-enclosure fires arising from an ignition event.

The guidance consists of incorporating a 0.02 severity factor into the multi-electrical enclosure fire scenario; or equivalently, to apply a 0.98/0.02 split fraction between the single–versus multiple electrical enclosure fire scenarios given ignition of a fire in the exposing enclosure. These values are based on a conservative interpretation of both the actual in-plant experience and insights from testing (that is, these values overstate the likelihood of the multiple electrical enclosure fire scenario). This conclusion is based on the following points:

- The fire event experience for the U.S. nuclear power industry has been documented back to 1968 and represents on the order of 3726 years of combined plant operating experience.[2] This experience base *does not include a single case* where fire spread from one electrical enclosure to an adjacent enclosure except in the case of a HEAF-initiated event that is not relevant to this method.[3] Based on zero events in 3726 years of experience, a conservative Bayesian prior estimate of the frequency of such events would be as follows:

  $\lambda \approx 0.5$ events/3727 years = 1.3E-4 events/year

  The current estimate of electrical enclosure fire frequencies, plantwide, is 3.6E-2/yr.[4] Taking these two values together would imply a conservative point estimate of the conditional probability of fire spread to an adjacent enclosure given fire in the exposing enclosure of roughly 1.3E-4/3.6E-2 = 0.0037.

  This number (0.98/0.02) includes credit for plant intervention resulting in no fire spread (that is, detection and suppression), given that actual experience inevitably involves fire intervention. In practice, FPRA develops fire scenarios in the absence of fire intervention and then applies suppression credit independently. As noted in Section 1, NUREG/CR-6850 says to assume fire spread to an adjacent enclosure in 10–15 minutes after ignition of the exposing enclosure [1]. Given the current fire suppression statistics, the probability of non-suppression of an electrical enclosure fire within 15 minutes (the more conservative value in this context) is approximately 0.23.[5] Using this value to back out the suppression credit that would be applied under current FPRA practice for preventing fire spread (that is, suppression before fire spread occurs), the conditional probability of fire spread given fire ignition can be estimated as 0.0037/0.23 = 0.016.

- Another way to look at the U.S. experience base is to consider the total number of electrical enclosure fires rather than the estimated frequency. The experience base (through 2014) includes a total of 151 electrical enclosure fires as counted in the most recent fire frequency analysis.[6] A statistical analysis of zero occurrences of fire spread from cabinet to cabinet in 151 events would yield a conservative estimated likelihood of the multi-enclosure fire experience of 0.5/151 or about 0.0033. Although it is difficult to determine from the event reports which cabinets were arranged so that all of the rules described previously would

[2] Based on all modes of operation (which is applicable to electrical enclosure fires) as given in Table 3-8 of NUREG-2230, EPRI 3002006051 [33].

[3] The HEAF-initiated fire scenario has its own guidance that inherently covers damage to adjacent enclosure sections and is not intended to fall within the bounds of this methodology.

[4] The sum of Bins 4 and 15 mean values. Bin 4 is from Table 7-3 of this report and Bin 15 from Table 3-9 of NUREG-2230
(EPRI 3002016051 [33].

[5] Based on Table 5-3 of NUREG-2169 (EPRI 3002002936) and a suppression rate of 0.098 (electrical fires) [36].

[6] Based on Table 3-9 of NUREG-2230 (EPRI 3002016051) [33].

preclude cabinet-to-cabinet propagation, two of the rules may be applied to better characterize the number of electrical cabinet fire events that could have allowed for fire spread between cabinets—the switchgear and load center and motor control center rules. The consideration of these rules reduces the number of events to 107 and a resulting conservative estimated likelihood of 0.5/107 = 0.0047. As in the prior case, this number would include credit for plant intervention having prevented such spread (that is, detection and suppression), but that credit can be backed out as it was previously (that is, 0.0047/0.23 = 0.02) and, again, a conditional probability value of 0.02 on the multiple electrical enclosure scenario is shown to be a conservative interpretation of the event experience independent of detection and suppression credit.

- Although less fully documented, international nuclear industry fire experience does not include any events where fire spread from one electrical enclosure to an adjacent enclosure excluding HEAF-initiated events. This insight is not easily amenable to direct analysis but lends further credence to the conclusion that such events are very unlikely. Adding additional years of experience with no events to the analyses outlined previously would only add strength to the argument that a severity factor of 0.02 is a conservative interpretation of the existing event experience.
- The testing experience in the original NRC-RES/SNL enclosure fire tests showed that under most conditions, inducing fire spread in an electrical enclosure was difficult and that the various factors that enhance the fire spread potential (fuel types, cable bundling, ignition source energy, and so on) must converge before a fully involved electrical enclosure fire would be likely [30]. All of the NRC-RES/SNL tests used relatively large ignition sources (32 kW) as compared with actual fire events that tend to involve small ignition sources (for example, overheating components that eventually ignite). Of the 20 tests performed in that series (excluding the gas burner fires), only five can be argued to have reached full enclosure involvement despite the fact that the primary goal of the program was to assess the worst-case potential fire characteristics to be expected from an electrical enclosure fire. Even these early tests clearly show that most electrical enclosure fires will never see aggressive fire spread such as that needed to induce fire spread to an adjacent enclosure. In the other 15 tests, conditions in adjacent enclosures never approached those necessary to cause ignition of fuels in an exposed enclosure. Further, full involvement of the fuels in one electrical enclosure is no guarantee that fire will spread to an adjacent electrical enclosure. This is a necessary, but not sufficient, condition for such spread. The physical configuration of both the exposing and exposed enclosures, and their fuel loads, must also be conducive to such spread.
- Other more recent test programs, including the most recent NRC-RES/NIST tests [31], have confirmed, if not strengthened, the observations noted previously from the NRC-RES/SNL tests in that most of the fire tests show very limited fire growth within the exposing enclosure and only a small fraction reached full enclosure involvement (see the NUREG/CR-7197 report for details [31]). In fact, the NRC-RES/NIST tests support the severity factor recommended here in that out of the 112 tests only a handful approached, or actually resulted in, full fuel involvement and even for those there is no guarantee that fire would have spread to an adjacent enclosure had one been present. Indeed, in some tests, the fuels on one side of an enclosure became fully involved in the fire while fuels on the other side of the same enclosure remained un-touched. Again, without full involvement of the exposing enclosure, fire spread to an adjacent enclosure is not plausible and even with extensive fuel involvement, fire spread is not guaranteed.

4.3.3 Summary of the Likelihood Characterization Guidance

This section summarizes the quantification guidance for the multi-enclosure electrical fire scenario. The probability of fire spread from an exposing to exposed enclosure is 0.02, conditional on fire ignition in the exposing enclosure. This is clarified as follows:

- Assume that only those fires representing the top 2% of the HRR distribution in the exposing enclosure would be capable of creating the conditions necessary for enclosure-to-enclosure fire spread.
- The top 2% of the peak HRR distribution for cases where enclosure-to-enclosure fire spread is postulated will be uniquely represented by the multi-enclosure scenarios. That is, the analyst should take care not to double count the contribution of 98th plus percentile fires to fire risk.
- The 0.02 conditional probability of fire spread can be applied in the form of a modifier (severity factor) against the frequency of fires initiated in the exposing enclosure or, more correctly, in the form of a split fraction between single- and multi-enclosure fire scenarios.

  Clarification: In order to avoid double-counting, a complimentary severity factor of 0.98 may be applied to those scenarios that involve fires in the same exposing enclosure that do not propagate to an adjacent electrical enclosure (that is, single electrical enclosure fires that potentially impact targets outside of the electrical enclosure). This complimentary severity factor **does not apply** to cases where the guidance leads to a conclusion that propagation to adjacent enclosures is not plausible. That is, if propagation is not plausible, all scenarios in the exposing enclosure are single-enclosure scenarios and the normal treatment is applied.
- Fire spread should be postulated only between the exposing enclosure and one adjacent exposed enclosure. In instances where the guidance outlined previously suggests possible propagation in two directions (that is, to either of two adjacent exposed enclosures), a value of 0.01 (0.02/2) should be used and fire spread should be postulated to the enclosures on either side of the exposing enclosure (Note: when applying the probability in this manner, the fire is probabilistically being spread to a single cabinet in either direction with a modifier of 0.01. Therefore, the HRR profile for such a scenario will only be that of the exposing and a single exposed enclosure).

The 0.02 conditional probability of fire spread is independent of credit for fire suppression efforts, prior or subsequent to fire spread, and including both fixed and manual fire suppression.

4.4 Assignment of Fire Characteristics to the Multi-Enclosure Fire Scenario

4.4.1 Background

As written, NUREG/CR-6850 [1] provides no guidance for characterizing the multi electrical enclosure fire time/HRR profile beyond stating that fire spread should be assumed to occur 10–15 minutes after ignition in the exposing enclosure. In lieu of the guidance, conservative assumptions including 10-minute propagation, instantaneous peak fire intensity, and 98th percentile HRRs have typically been assumed. As a result, analysts are potentially creating a composite fire consisting of three or more enclosures all burning at their 98th percentile peak intensity. As noted in Section 4.3, there is no evidence that this type of fire propagation is realistic.

The test data from all of the electrical enclosure fire testing programs consistently show that the most intense electrical enclosure fires (that is, those that reach full fuel involvement) experience peak HRR conditions that average in duration for less than 1 minute before a rapid decay is observed. These high intensity fires tend to burn out the available fuel quickly so that the decay phase begins almost as soon as the peak HRR value is observed. In contrast, it is the lower intensity fires (those that involve only a fraction of the fuel present) that may persist for an extended time at much lower peak intensity values (for example, 10 or more minutes). As noted previously, it is assumed that only the higher intensity fires hold the potential for fire spread to an adjacent enclosure; therefore, it is appropriate to characterize the multi-enclosure scenario based on the behavior of the higher intensity fires from the testing.

One related insight here is the behavior noted for cable tray fires in the NUREG/CR-7010 testing, which included the development of the cable tray fire model called *FLASHCAT* [24]. The critical behavior that the testing demonstrated and that is now reflected in FLASHCAT is that, even given horizontal fire spread along a single cable tray, the overall fire intensity tends to reach a peak value that is roughly steady over time and involves the burning of only limited sections of each tray involved in the fire. This is because, as fuel is exhausted in the older sections of burning tray, fire spreads to new unburned sections of tray with an overall effect of maintaining steady fire intensity (as opposed to a continuously increasing fire intensity)—that is, new cable sections added to the fire do not continuously increase total fire intensity because older sections burn out and stop contributing to the overall fire. Similar behaviors might be anticipated for the multiple electrical enclosure fire scenario—that is, by the time fire spreads from an exposing enclosure to an exposed enclosure, the fire in the exposing enclosure will have already passed peak intensity and will be into its decay phase. Therefore, overall fire intensity likely would not significantly exceed the peak intensity of a single burning enclosure although the fire duration might be extended significantly barring intervention (suppression). However, there is no direct experience-based (not a single case where fire spread from one electrical enclosure to an adjacent enclosure except in the case of a HEAF-initiated event) or experimentally based data against which to baseline this hypothesis.

4.4.2 Recommended Fire Characterization

The growth, steady state, and decay stage times for fixed ignition sources are summarized in Table G-2 of NUREG/CR-6850 [1] and again in NUREG-2230 [33]. Given the available insights, the recommended fire characterization is based on the following:

- The exposing enclosure follows a HRR profile consistent with the growth profiles for growing or interruptible fires in NUREG-2230 [33].
- Assume that the peak fire intensity for the exposing enclosure corresponds to the 98th percentile of the HRR profile applicable to the exposing enclosure (that is, based on size, function, fuel/ventilation conditions, and so on).
- Fire spread to an adjacent electrical enclosure, where possible, is assumed to occur 10 minutes after the start of the growth period of the exposing enclosure for the HRR profiles in NUREG-2230 [33].
- Because only the top 2% of the exposing fire peak HRR distribution can result in spread, the exposed cabinet will see an ignition source that is larger than typical in-cabinet sources. As a result, the exposed enclosure will experience fires representing the 98th percentile peak HRR at 12 minutes after fire spread has occurred (that is, 22 minutes total fire time). Note that the exposing and exposed enclosures may be characterized by different peak HRR distributions depending on the characteristics of each.

- The exposed enclosure should be modeled following the growing HRR profile described in NUREG-2230, grow to peak in 12 minutes, maintain its peak intensity for 8 minutes, and a decay phase of 19 minutes (for a total fire duration in the exposed enclosure of 39 minutes).
- Fire spread should be limited to one adjacent enclosure. This assumes the following:
    - For fire to spread from the exposing enclosure to an adjacent exposed enclosure, the fire will need to be actively burning in the areas immediately adjacent to the partition between the two enclosures. Indeed, fire behavior as seen in those experiments where fuels became fully involved tends to be dominated by initial fire spread up one side of an exposing enclosure and subsequent, post-peak, fire spread down the opposite side of the exposing enclosure. Fire spread is most likely to occur during the initial growth period of fire spread, which corresponds to spread up the initial side of the enclosure and the peak of fire intensity.
    - Modern-day plant fire protection programs in the United States provide sufficient assurance that thermal electrical enclosure fires will be either fully suppressed or, at a minimum, brought under control before spread to multiple enclosures would occur. Plant response time may not be sufficiently rapid to prevent spread to the first exposed enclosure, but it is very likely to be fast enough to intervene prior to propagation beyond that point.
    - If it has been determined that fire spread should be considered from an exposing enclosure to each of two adjacent electrical enclosures (that is, the enclosures on both sides of the exposing enclosure), the fire analysis should still be limited to two enclosures (one exposing and one exposed). As noted previously, the fire would develop initially on one side of the exposing enclosure and fire spread to the enclosure on that side would be most likely. Because it is not possible to predict which side of the exposing enclosure the fire will initially develop on, the two possible scenarios (spread from the exposing to each of the two adjacent enclosures but one exposed enclosure at a time) should be analyzed as stated in Section 4.3.

4.5 Summary of Enclosure-to-Enclosure Fire Spread

The methodology for enclosure-to-enclosure fire spread explicitly considers the scenario likelihood and characteristics including guidance for characterizing the fire intensity (that is, HRR) associated with a multi-enclosure fire for Bin 4 (main control board) and Bin 15 (electrical cabinets).

The guidance presented in this section is summarized as follows:

- Electrical enclosures meeting the screening criteria in Section 4.2.2 do not need to postulate fire spread.
- When fire spread to an adjacent enclosure is postulated, a conditional probability of 0.02, can be applied against the frequency of fires initiated in the exposing enclosure or, more correctly, in the form of a split fraction between single- and multi-enclosure fire scenarios.
    - In instances where the guidance suggests propagation in two directions, a value of 0.01 (0.02/2) should be used and fire spread should be postulated to the enclosures on both sides of the exposing enclosure (Note: When applying the probability in this manner the fire is probabilistically being spread to a single cabinet in either direction with a modifier of 0.01. Therefore, the HRR profile for such a scenario will only be that of the exposing and a single exposed enclosure).

- Fire spread is limited to one adjacent enclosure. For an interior cabinet within a bank, HRR calculations should be postulated to a single cabinet on either side of the exposing cabinet but not to both adjacent cabinets.
- An example HRR profile for two adjacent enclosures is depicted in Figure 4-1 based on the following fire characteristics:
  - The exposing enclosure follows the HRR profiles in NUREG-2230 [33].
  - The exposing fire is at the 98th percentile of its peak HRR distribution (that is, based on size, function, and/or fuel loading conditions).
  - Fire spread to an adjacent electrical enclosure occurs 10 minutes after the start of the growth period of the exposing enclosure. Therefore, the exposed enclosure will begin its growth stage 10 minutes after start of the growth period in the exposing enclosure.
  - Both the exposing and exposed enclosures will reach the 98th percentile peak HRR of their respective enclosure classifications.
  - The exposed enclosure reaches the peak HRR at 12 minutes, maintains its peak intensity for 8 minutes, and decays for 19 minutes. The total fire duration in the exposed enclosure is 39 minutes (49 minutes from the start of the exposing enclosures growth period).

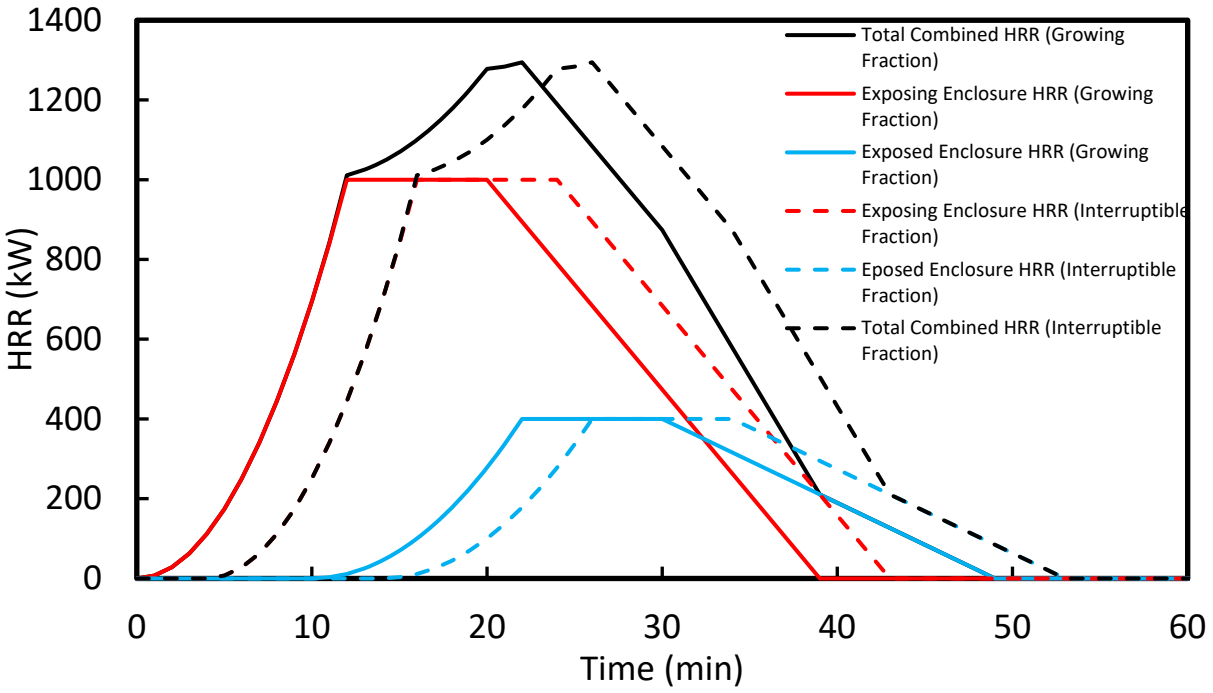

Figure 4-1
Total HRR for fire spread between the growing and interruptible (Option 2) fractions of an exposing Group 4a, open, thermoplastic, default fuel load enclosure and an adjacent Group 4a, closed thermoplastic, default fuel load enclosure

5
MOTOR AND TRANSFORMER FIRE CHARACTERISTICS

The heat release rates (HRRs) in Table G-1 of NUREG/CR-6850 (EPRI 1011989) [1] do not reference any experimental evidence to establish HRRs for pumps or motors but recommend values based on the available electrical cabinet data. Because the electrical cabinet data have been revised in NUREG-2178 Vol. 1 (EPRI 3002005578) [2], it is appropriate to revisit electrical fire HRRs for pumps and motors. Similarly, dry transformer fires are modeled using the HRR and probability density function of electric motor fires according to Table 8-1 of NUREG/CR-6850 and are included within the scope of this evaluation. The scope does not impact the treatment of oil fires associated with some pumps, motors, or transformers.

5.1 Electric Motors

5.1.1 Introduction

Fire probabilistic risk assessments (FPRAs) include scenarios where an electrical fire initiated in a pump or motor can propagate and cause damage to nearby equipment. The HRRs to develop these scenarios are published in Table G-1 of NUREG/CR-6850. This guidance has separate peak HRRs and distributions for motor-driven pumps versus other electric motors. However, the existing guidance makes no specific assessment of the contents or construction of pumps or motors that might influence the burning behavior of such equipment.

The approach described in the following sections explicitly considers the size, contents, and construction of motor-driven pumps and motors to develop guidance for characterizing the fire intensity (that is, HRR). The updated guidance defines electric motor scenarios based on the size (that is, horsepower) of the motor rather than motor application. This guidance provides updated HRR distributions for electric motors along with additional details for ignition source screening and other fire modeling inputs. Examples can be found in Section 5.3.

5.1.2 Overview of Methodology

The treatment for motor fires is described in three parts, each of which is covered in the sections that follow:

1. Ignition source counting guidance used to identify electric motors for which fire scenarios need not be postulated (see Section 5.1.4)
2. Background discussions relative to operating experience and the characteristics of common electric motors as used in the U.S. nuclear power industry along with a binning scheme that groups motor HRR based on motor size—that is, horsepower (hp) rating (see Section 5.1.5)
3. Recommendations for characterizing the fire intensity (that is, HRR) for the unscreened fire scenarios (see Section 5.1.6)

5.1.3 Assumptions and Limitations

The following assumptions and limitations are applicable:

- The guidance and analysis presented and described in this section apply only to the determination and analysis of electrical fires in electric motors (Bins 2, 9, 14, 21, 26, and 32). This guidance does not apply to lubricating oil spill fire scenarios.
- The hp rating of the motor is used to define the fire intensity. In the absence of a hp rating, the size of the motor can be used to estimate the category. If neither hp rating nor size is available, the highest HRR bin should be assumed.

5.1.4 FPRA Ignition Source Counting Criteria

The following are existing criteria used in the ignition source counting process for electrical fires in pumps and motors:

- Electric motors with hp ratings of 5 hp or less are assumed to have little or no significant contribution to risk and are excluded from ignition source counting (NUREG/CR-6850, Section 6.5.6 [1]).
- Motors that are totally enclosed, including motor-operated valve (MOV) drive motors, regardless of motor size, are excluded from ignition source counting (FAQ 07-0031 [34]) as defined:

  A totally enclosed motor is defined by the National Electrical Manufacturers Association (NEMA) as “a motor designed without air openings so there is no free exchange of air between the inside and outside of the enclosure but not necessarily air or water tight” (Reference: NEMA MG 2-201, Rev. 1, 2007).

  The guidance in FAQ 07-0031 is specific to Bin 14 motors but is expanded to the electrical split fraction portions of Bin 21 and Bin 26 if the definition of totally enclosed is satisfied.

5.1.5 Insights from Operating Experience

5.1.5.1 Fire Event Operating Experience

The Electric Power Research Institute (EPRI) fire events database (FEDB) [35], records fire events from U.S. nuclear power plant (NPP) experience. A review of the recorded events associated with Bins 2 (reactor coolant pumps), 9 (air compressors), 14 (electric motors), 21 (pumps), 26 (ventilation subsystems), and 32 (main feedwater pumps) provides insight into the types of fires that have occurred at NPPs for pump and motor ignition sources. There are approximately 46 pump and motor events that have been recorded and determined to be applicable for FPRA applications—events that have been determined to be challenging or potentially challenging and have been counted in the estimation of the fire ignition frequency and non-suppression probabilities as described in NUREG-2169 (EPRI 3002002936) [36]. Of these 46 events, a significant fraction—in excess of 80%—of the events describe a fire that was limited to the ignition source only. Only a small fraction—two events—describe fires that caused extensive damage to the ignition source. Even with extensive damage to the ignition source, the external extent of damage is not likely to be large.

5.1.5.2 Range of Typical NPP Motor Sizes

Typical motor sizes at NPPs range from less than 1 hp (for example, small crane hoist or localized ventilation fan motors) to greater than 3000 hp (for example, large condensate pumps). A review of the FPRA ignition sources as counted by four plants (three pressurized water reactors [PWRs] and one boiling water reactor [BWR]) provided a distribution of motor sizes for 303 motors greater than 5 hp for bins 14 and 21. The vast majority of motors were below 500 hp as seen in Figure 5-1 through Figure 5-3 with a median motor size of 30 hp.

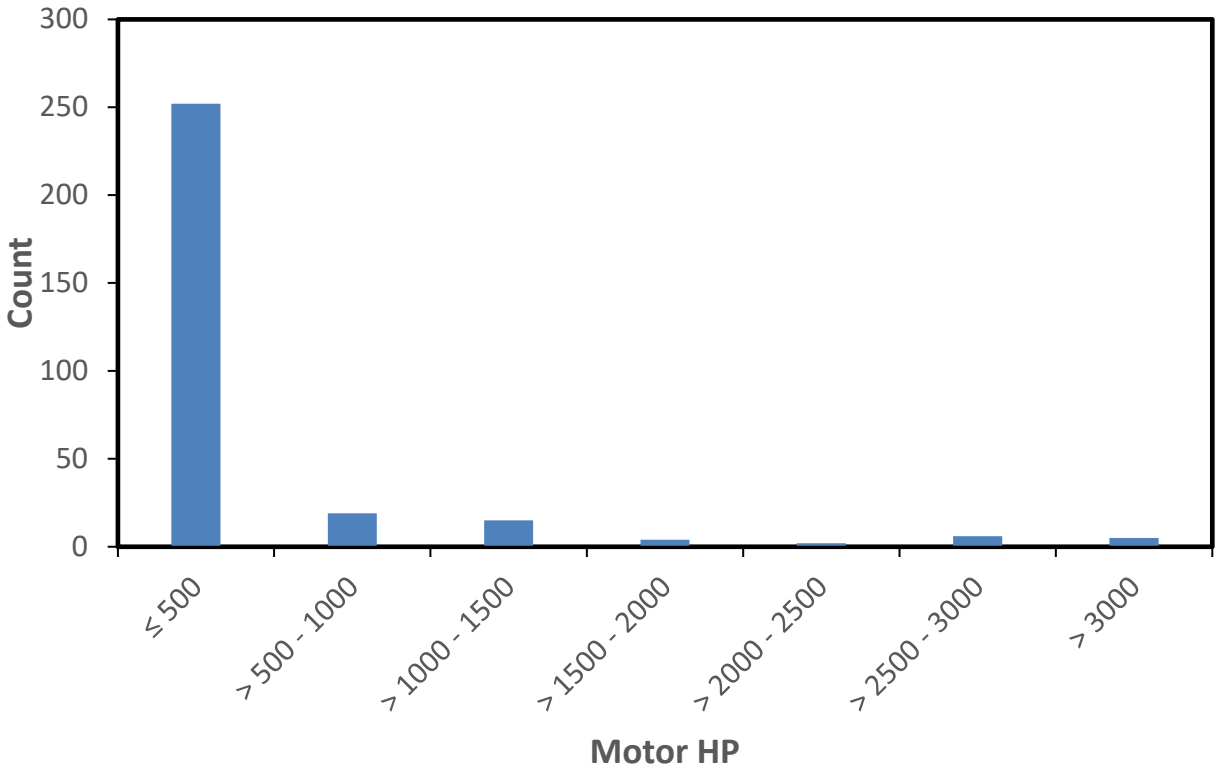

Figure 5-1
Count of motors by horsepower (Bins 14 and 21)

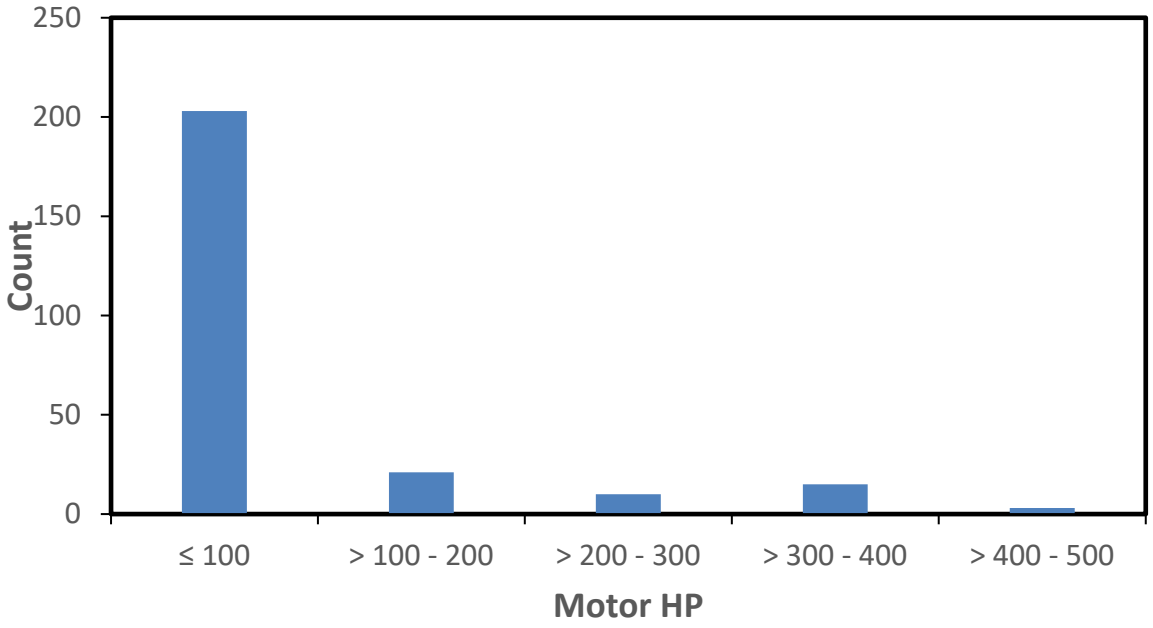

Figure 5-2
Count of motors by horsepower (under ≤500 hp) for Bins 14 and 21

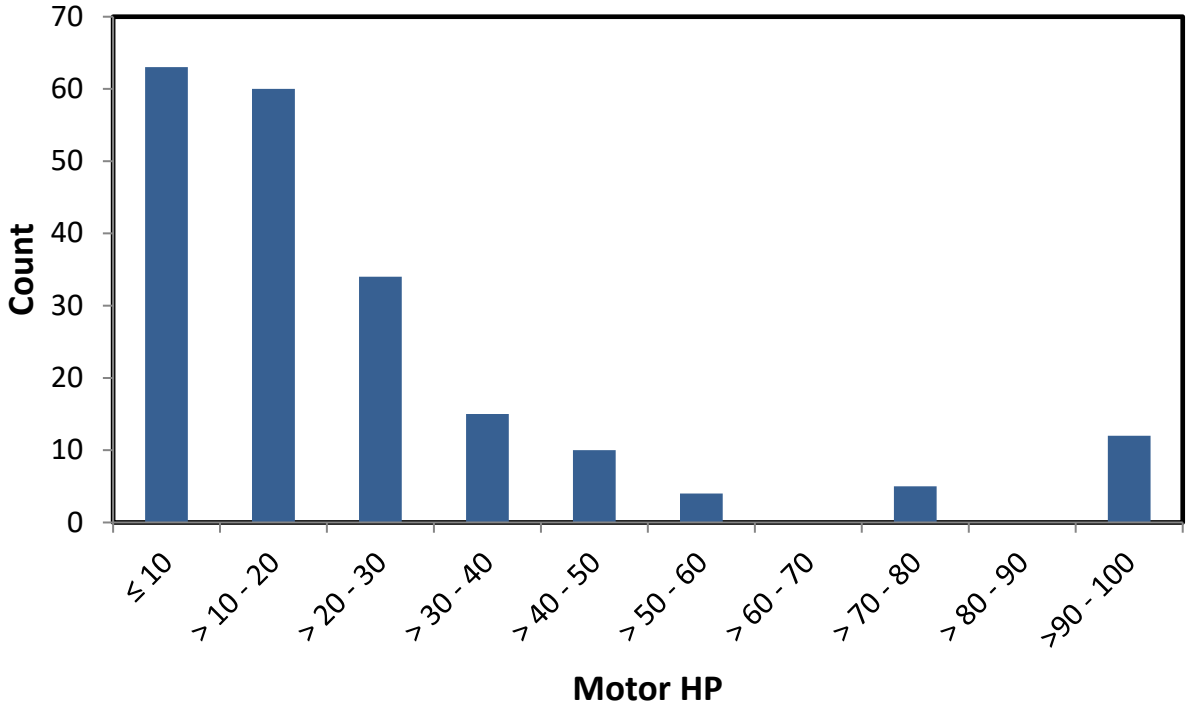

Figure 5-3
Count of motors by horsepower (under <100 hp) for Bins 14 and 21

In addition to the distributions of motor sizes observed in NPPs, pictures (see Figures 5-4 through 5-7) of motor ignition sources were reviewed for their size and configuration, casing robustness, approximation of internal combustibles, and venting characteristics. These observations led to classification of motors into three horsepower-based categories shown in Table 5-1: Group A motors (>5 hp to 30 hp), Group B motors (>30 hp to 100 hp), and Group C motors (>100 hp). The Group A motor category covers approximately half of all motors and contains similar motor sizes and characteristics. The Group B motor category is selected because it is geometrically larger than Group A and has the potential to produce a larger HRR than Group A. The Group C motor category constitutes approximately a third of all motors and will also produce a larger HRR than Group B.

Table 5-1
Motor classification groups by motor size (Bins 2, 9, 14, 21, 26, and 32)

Classification Group	Motor Size (hp)
A	>5–30
B	>30–100
C	>100

Figure 5-4
Examples of Group A motors (>5 hp, 15 hp)

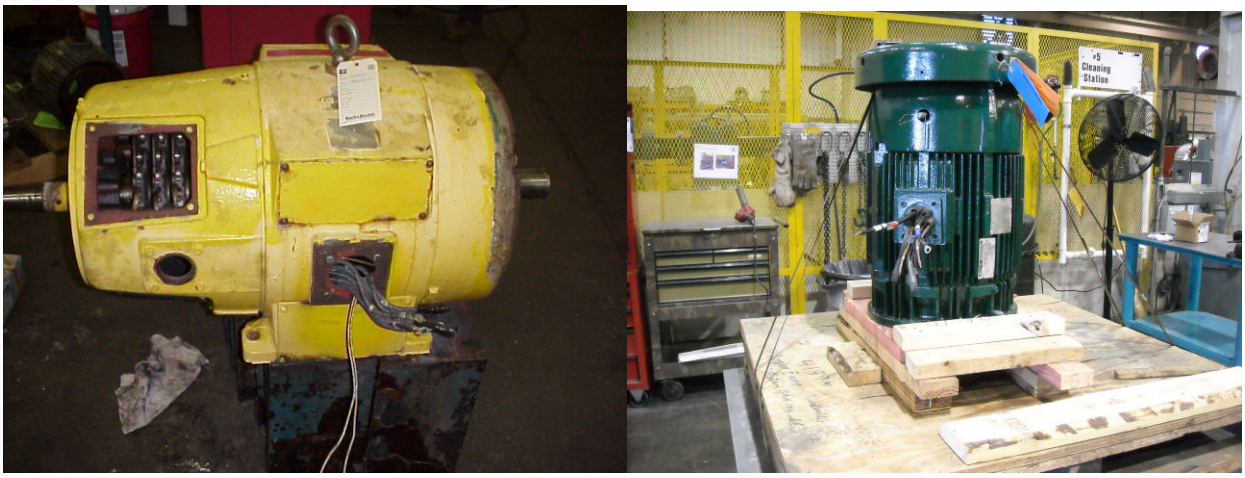

Figure 5-5
Examples of Group B motors (40 hp, 50 hp)

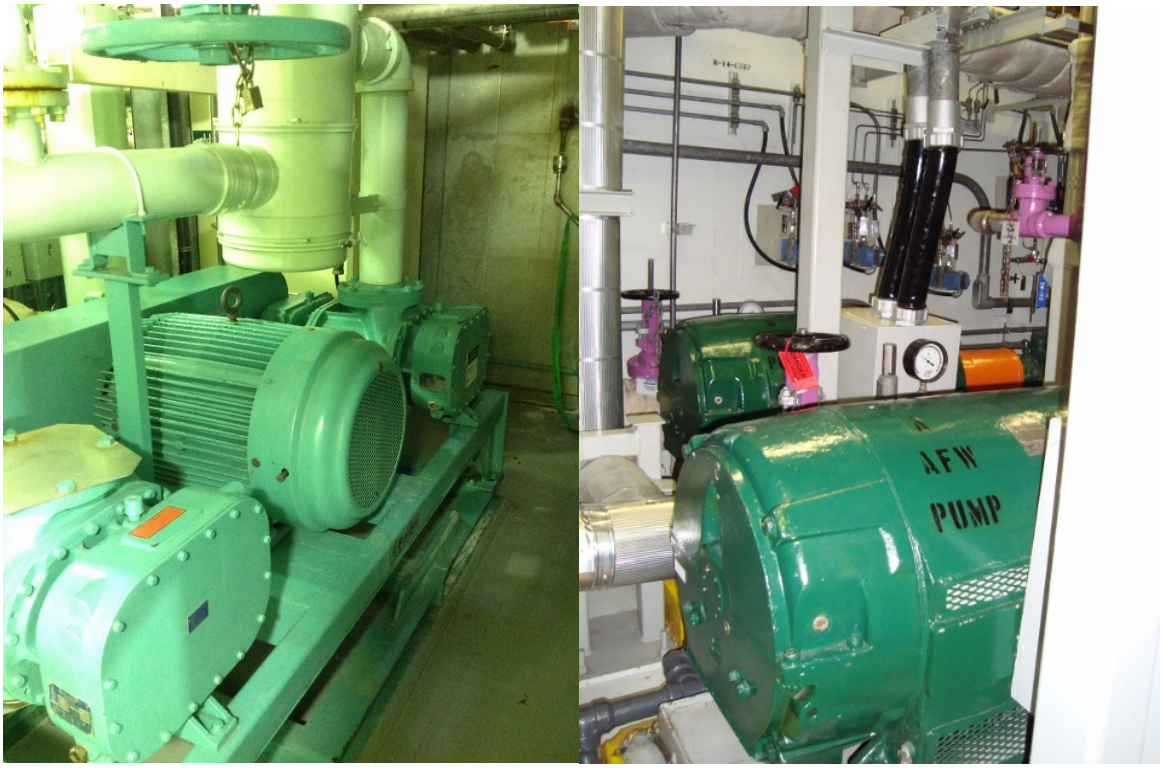

Figure 5-6
Examples of Group C motors (200 hp, 350 hp)

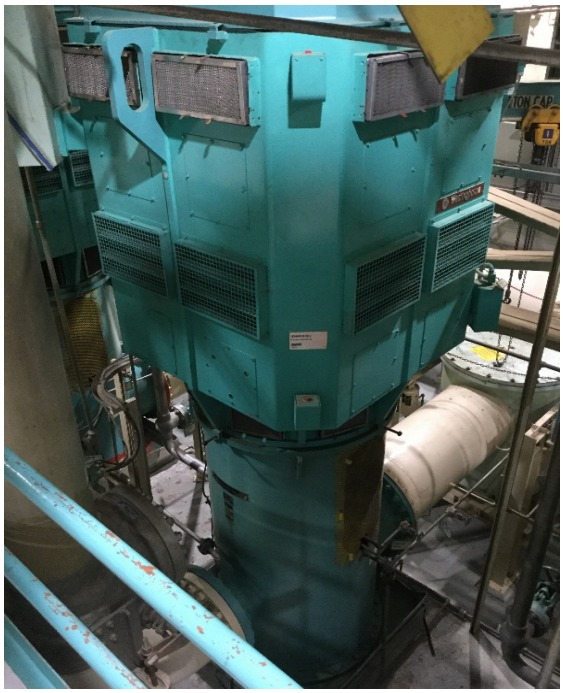

Figure 5-7
Example of Group C motor (3000 hp)

5.1.6 Assigning Fire Characteristics to Electric Motors

NUREG/CR-6850 recommended 211 kW as the 98th percentile HRR for pumps (electrical fires) and 69 kW as the 98th percentile for other motors. In general, there is little difference in design, if any, between motors that power pumps and other motors. The reason for the difference in recommended HRRs in NUREG/CR-6850 was not documented, but discussions indicate that it was based on a general understanding that the pump motors would be larger than other motors based on the function (pump driver). To some extent, this may be true; however, there is not a clear division, and the range in motor sizes varies greatly so that development of a new basis for HRR is warranted.

Task 6 of NUREG/CR-6850 groups electric motors into six ignition source types: Bin 2, reactor coolant pumps; Bin 9, air compressors; Bin 14, electric motors; Bin 21, pumps; Bin 26, ventilation subsystems; and Bin 32, main feedwater pumps. Ignition sources characterized in Bins 2, 9, 21, 26, or 32 can result in electric and oil fires. Split fractions for each fire type are provided based on operating experience categorized in the EPRI fire events database [35]. The split fractions can be found in NUREG-2169 [36] or the latest published generic fire frequency data.

A basic motor does not contain a significant amount of combustible materials. Generally, there is the incoming power cable, wiring to the motor stator/rotor and a limited amount of cables for monitoring or other control functions. In addition, the armature wiring is coated with a thin insulating material. Based on the limited amount of combustible material and characteristics of motor casing (or enclosure) designs, HRRs are expected to be low compared with electrical enclosures. The primary variable to consider is motor size and a potential corresponding range of HRRs.

Motors installed in NPPs were reviewed to determine significant characteristics. The review concluded that the motor casings are robust and provided with relatively limited ventilation. The substantial nature of the motor case is not expected to warp or lead to gaps during an internal fire.

Electric motors consist of the motor casing and the components within and directly attached, including the stator, rotor/armature, bearings, and conduit box. Motor casings can vary significantly, and this research does not attempt to evaluate how these differences can impact HRR.

5.1.6.1 Heat Release Rate

As assessed previously, the combustible material contained within an electric motor is limited to the incoming power cable, wiring to the motor rotor, stator, and any cables that provide monitoring or control functions (see Figure 5-8). The wiring used in the rotor and stator are insulated with a coating that is assumed to be flammable.

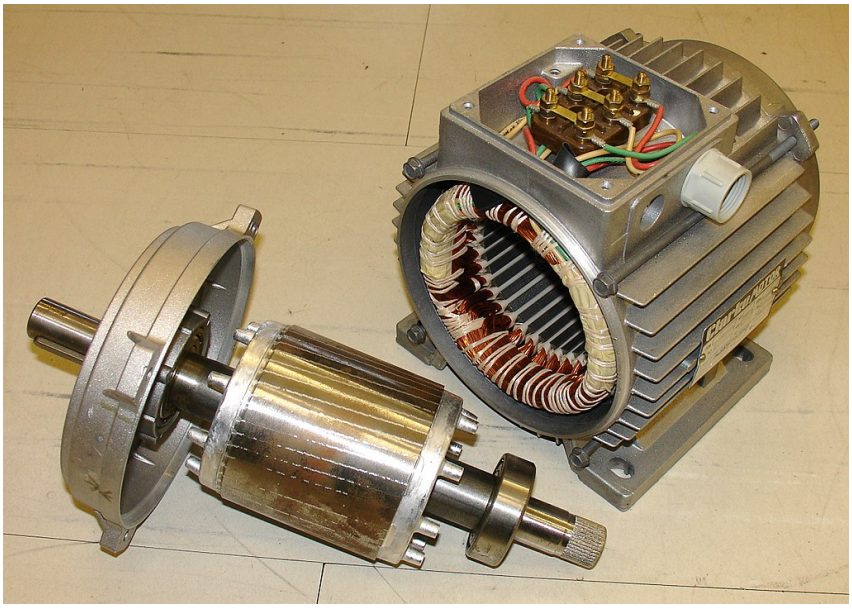

Figure 5-8
Electric motor cutout, rotor (left) and stator (right) [37]

Focusing on the cable contained within the motor (the primary combustible material within a motor), an approach was developed to estimate the amount of combustible coating/insulation material contained within a motor. To estimate the fuel load within a motor, cables are conservatively modeled as a cylinder within the motor casing—representing the cable wiring of the windings in the rotor and stator. The available combustible material is estimated using a range of parameters, including the following:

- Motor casing length
- Motor casing radius
- Wire coverage

Several characteristics of the wire and the rotor and stator windings were approximated based on expert judgement of images of exposed motor windings, motor specifications, and commercial product descriptions. Important characteristics were identified and assigned a randomized parameter appropriate to the observations.

Motor Casing Length

Based on a review of electric motor internals, the cables within do not appear to run the entire length of the motor casing (which is assumed to contain the cables and conductors). Therefore, cables are modeled as running along a fraction, α, of the length of a motor casing, defined as the total length of the motor minus the extension of the drive shaft. Based on the image reviews, the fraction α is postulated to range between 40% and 80% of the motor casing length.

Motor Casing Radius

Similarly, cables are not wrapped round the outermost edge of a motor casing, so an assumed fraction of the radius, β, of the external motor casing is included. Based on image reviews, the fraction β, ranging from 60% to 90% of the motor casing radius, is used to estimate the amount of cable material within a motor. To ensure a reasonable pairing of the motor length and radius estimates, the maximum and minimum ratio of motor radius to length for the different classification groups is used to bound each radius value. This allows for an estimation of surface area of cable material within a motor, as shown in Figure 5-9.

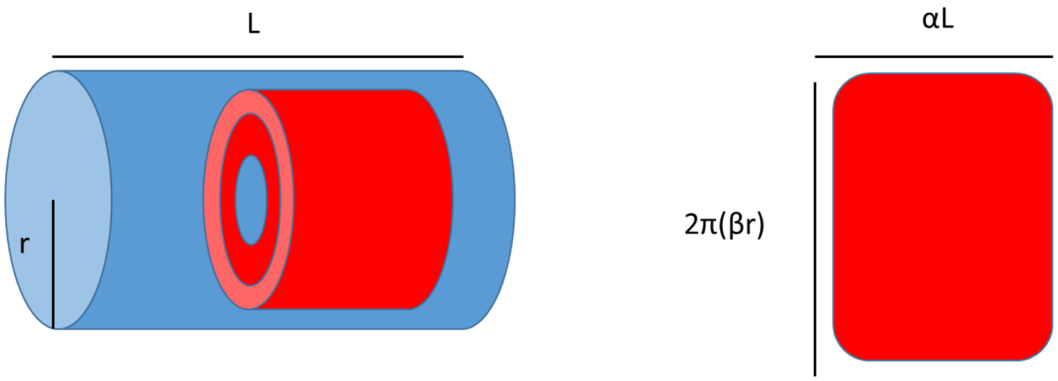

Figure 5-9
Simplified diagram of the combustible material arrangement considered for motors

Cable Enamel/Insulation Heat Release Rate per Unit Area

Electric motors have continuous temperature classifications of up to 220°C (428°F), which are designed to account for elevated ambient temperature and internal heating due to the electrical resistance or friction associated with the stator and drive shaft. The motor is capable of operating at these elevated temperatures without degradation of the components or reduction of the usable life expectancy. In some cases, these temperature ratings are greater than the steady-state failure criteria for thermoplastic electrical cables; therefore, it is appropriate to treat the insulation as having superior performance relative to a thermoplastic cable.

To determine the HRR associated with the estimated amount of cable material contained within an electric motor, the HRR per unit area (HRRPUA) for winding materials commonly found in NPPs is used.

Wire enamels are applied on copper and aluminum wires used in motors and transformers windings, which provide electrical insulation and keep the windings from short circuiting.

Chemically, the wire enamel range mainly consists of heat-resistant/thermally stable polymers such as polyurethane (PUR), modified polyesters, polyesterimide (PEI) and polyamide-imide (PAI). These products are commonly made of halogen-containing/flame-retarded (FR) plastics, which are difficult to ignite and have a low HRR. These enamel types include thermoset-type cable materials (no thermoplastic-type cable material was used).

The HRRPUA estimated range is between 50 and 100 kW/m^2. This is consistent with the HRRPUA for PAI and PEI (approximately 50 kW/m^2 and 100 kW/m^2, respectively) [38, 39].

It is likely that only a fraction of the motor winding will ignite during any given event. In some instances, a small fraction may ignite, and, in others, the full area of the cylinder could be involved. To capture a range of likelihoods, an ignited perimeter and length fraction is applied to account for the variability in the ignited surface area of the cylinder. Given the low certainty of what fraction of the surface area would reliably be expected to ignite, these fractions are postulated to range between 25 and 100%.

Wire Coverage

Finally, a significant fraction of the assumed cylinder of wiring is either open with gaps between the windings or encased in metal (see Figure 5-8). Therefore, a wire coverage fraction is applied to account for the available surface area for combustion. Given the significant fraction of wiring expected to be open and prone to igniting, this fraction is postulated to result in a range between 50 and 100% of the cable exposed.

Randomized Sampling

The sizes for electric motors over a range of horsepowers were reviewed to develop an estimation for the HRR of an electric motor fire. Applying the fractions covered previously, the resulting distributions of estimated HRR results per motor horsepower rating were developed. These values were determined through a uniform randomization of all variable parameters previously covered—exterior motor dimensions, length fraction, radius fraction, HRRPUA, ignited area fraction, and wire coverage fraction. These values are calculated using Monte Carlo sampling technique in order to approximate the distribution of fire sizes that may be possible given the possible range of determining factors (see Figure 5-10). Equation 5-1 is used to determine the HRR, where all parameters are variable within the ranges denoted:

$$\dot{Q} = \alpha L \times 2\pi\beta r \times \dot{q}'' \times F_L F_P F_C \qquad \textbf{(5-1)}$$

where, L (m) is the exterior length of the motor, α is the factor to determine the size of the interior rotor and stator length, r (m) is the exterior radius of the motor, β is the factor to determine the size of the interior rotor and stator radius, $\dot{q}''$ (kW/m²) is the HRR per unit area of the burning materials, F_L is the factor to determine the percentage of the length of cylinder ignited, F_P is the factor to determine the percentage of the perimeter of the cylinder ignited, and F_C is the factor crediting the percentage of non-combustible coverings.

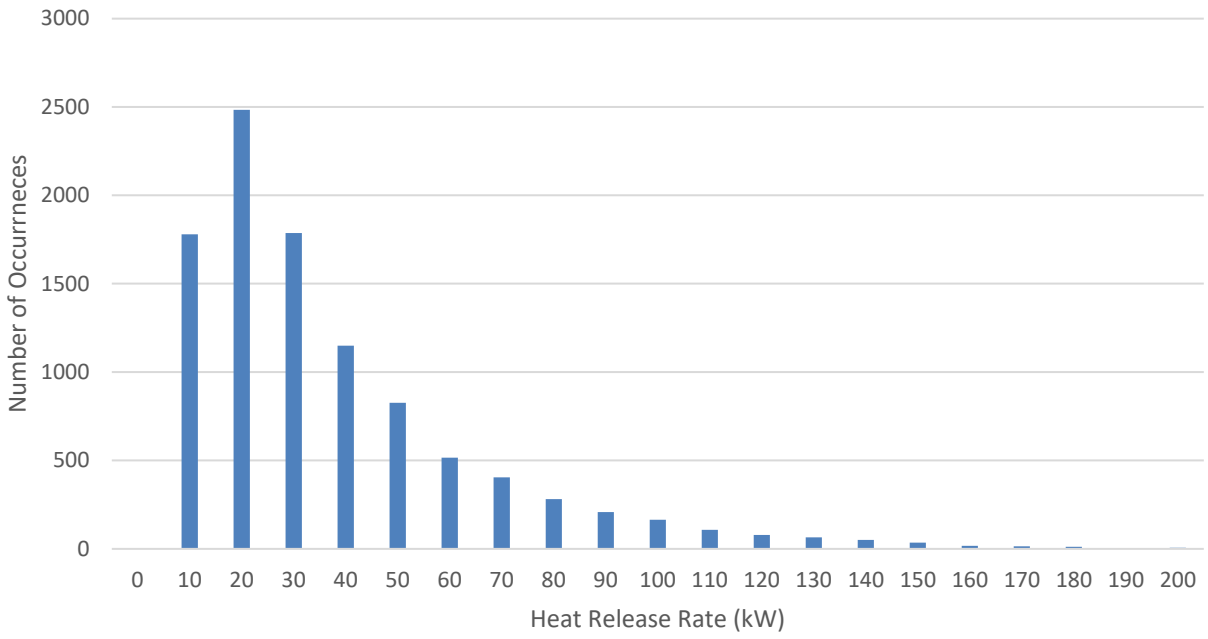

Figure 5-10
Motor Group C random samples

Using a detailed review of motor dimensions over various horsepower ratings, a randomized sample size of 10,000 occurrences was performed and the distribution of fire size was estimated. From this distribution a corresponding gamma distribution was fit to the resulting data. The results from this exercise are presented in Table 5-2. This sample size was observed to regularly result in approximately 98% of the simulated HRR values to be captured within the 98th percentile of the correspondingly estimated distribution. Similar to the HRRs presented in NUREG/CR-6850 [1] and NUREG-2178 [2], a gamma distribution is selected for two reasons: it distributes probabilities among positive, real numbers only, and it produces a fit representative of the data while maintaining a similar technical approach as previously used.

Table 5-2
Survey of motor dimensions and HRR analysis

Motor Horsepower (hp)	Motor Length Range (m [in.])	Motor Radius Range (m [in.])	HRR Range (kW)	Average (mean) HRR (kW)
5	0.23–0.52	0.25–0.37	0–21	3
	[9.02–20.35]	[9.97–14.51]		
10	0.31–0.55	0.22–0.37	0–27	3
	[12.26–21.74]	[8.8 –14.51]		
20	0.41–0.57	0.23–0.36	0–28	4
	[16.34–22.60]	[9.00–14.06]		
30	0.41–0.70	0.22–0.37	0–42	6
	[16.28–27.72]	[8.70–14.46]		
40	0.43–0.79	0.22–0.39	0–57	7
	[17.1 –31.19]	[8.66–15.27]		
50	0.45–0.94	0.21–0.36	0–72	9
	[17.5 –37.01]	[8.19–14.09]		
60	0.44–0.96	0.19–0.43	0–73	10
	[17.28–37.60]	[17.10–7.36]		
75	0.48–1.01	0.18–0.41	0–68	11
	[18.75–39.78]	[7.06–16.33]		
100	0.46–1.23	0.14–0.47	0–144	14
	[17.99–48.48]	[5.32–18.31]		

A similar set of HRR values may be developed for motors with power ratings greater than 100 hp, but the calculated HRR of the larger motors begins to increase substantially at this point due to their larger dimensions.

Based on the typical motor configuration for each size category defined in Table 5-1, a general treatment of motor combustible loading and data from the FEDB, the updated HRRs are presented in Table 5-3. These values are determined from a statistical best fit of the 10,000 randomized HRR estimates in each classification group. The gamma distribution parameters are approximated from the sample size where beta is determined from the variance of the sample set divided by the mean of the sample set, and then alpha is the mean of the sample set divided by beta. Because the randomized set of 10,000 occurrences can vary, the precise evaluation of these terms can also vary, but the resulting distributions are nearly indistinguishable.

Table 5-3
HRR distribution parameters for motor classification groups A, B, and C

Classification Group	Motor Size (horsepower)	α	β	75th Percentile (kW)	98th Percentile (kW)
A	>5–30	1.34	3.26	6	15
B	>30–100	1.17	8.69	14	37
C	>100	1.10	24.19	37	100

The results of the Monte Carlo analysis can also be used to estimate Froude numbers for the burning configurations where the fire diameter is calculated assuming a vertical or horizontal motor and the total projection of the burning surface. The statistical results are provided in Table 5-4 and can be used for detailed fire modeling.

Table 5-4
Froude Number distribution for motor classification groups A, B, and C

Classification Group	Motor Size (horsepower)	Mean	Median	16th Percentile	84th Percentile
A	>5–30	0.72	0.59	0.36	0.95
B	>30–100	0.62	0.49	0.29	0.81
C	>100	0.51	0.39	0.24	0.67
	Average	0.62	0.61	0.49	0.30

5.1.6.2 Fire Duration

The duration of the motor fire can also be approximated using the same approach as used to define the HRR distributions. Because the primary combustible component is associated with the rotor and stator winding wires, this analysis examines the wires in greater detail in order to estimate the duration of the motor fires. The wiring associated with the rotor and stator is sometimes referred to as *magnet wire* and consists of a copper wire with a thin resistive coating. The coatings provide resistance to internal shorts and are designed to operate at elevated temperatures. Because the copper wire will not contribute substantially to the fire HRR, the thickness and other characteristics of the coating were explored. Several of the characteristics of the wire and the rotor and stator windings were approximated based on expert judgement of images of exposed motor windings, motor specifications, and commercial product descriptions. Important characteristics were identified and assigned a randomized parameter appropriate to the observations.

The gauge of the stator wiring can range from nominally 6 to 20 American wire gauge (AWG) depending on the application. Furthermore, the thickness of resistive coating can range widely from 0.013 to 0.13 mm (0.0005 to 0.005 in.). Therefore, the quantity of combustible coating is considered a random variable in predicting the burn duration of the electrical motor. In order to estimate the burning duration, it is necessary to estimate the mass of the combustible material and the energy content of that material. Then, using the rate of energy released by the fire, one can estimate the burning duration. Here, the volume of the rotor and stator cylinder is required, along with the properties of the winding cables and the associated heat of combustion.

In the analysis, the internal radiuses of the rotor and stator windings were assumed to be a randomized parameter that ranged between 50 and 80% of the predicted outer radius. Additionally, it is considered that the fire may not fully penetrate the thickness of the rotor or the stator; therefore, an additional parameter evaluates a fire penetration depth of 50–100% of the thickness of the rotor and stator cylinder wall. These parameters provide the final geometric parameters for computing the volume of the hollow cylinder of combustible material impacted by the fire.

The properties of the rotor and stator winding wires were also approximated using a randomized parameter. Here, the product of the total density of the cable and the percentage of the mass that is combustible coating is used to determine the proportion of the mass of the hollow cylinder that is combustible coating (that is, as opposed to copper). This parameter was considered to fall between the values of 31 and 370 kg/m³. The variable parameters were then combined to estimate the combustible mass associated with the rotor and stator windings as shown in Equation 5-2:

$$\mathbf{m} = \left(\boldsymbol{\pi}(\boldsymbol{\beta r})^2 - \boldsymbol{\pi}(\boldsymbol{r_i})^2\right) \times \boldsymbol{\alpha L} \times \boldsymbol{\rho} \times \boldsymbol{F_L F_P F_C F_{Pn}} \quad \textbf{(5-2)}$$

where, *m* (kg) is the mass of the insulation, ρ (kg/m^3) is the density of cable, r_i (m) is the interior radius of the motor, F_{Pn} is the factor to determine the fire penetration depth, and all other terms have been identified.

The heat of combustion was also considered a random variable. Given the range of materials used in jacketing the rotor and stator windings, the observed heat of combustion range is between 15.3 and 21.0 MJ/kg [24, 38, 39] corresponding to the types of cable jackets identified.

Randomized Sampling

The sizes for electric motors over a range of horsepower ratings were reviewed to develop an estimation for the duration of an electric motor fire. Applying the fractions covered previously, the resulting distribution of duration per motor horsepower rating were developed. These values were determined through a uniform randomization of all variable parameters covered previously, namely HRR, mass of insulation, and heat of combustion. These values are calculated using Monte Carlo sampling technique in order to approximate the distribution of fire sizes that may be possible given the possible range of determining factors. Equation 5-3 is used to determine the duration where all parameters are variable within the ranges specified:

$$\mathbf{t} = \frac{\mathbf{m}\Delta\boldsymbol{H_c}}{\mathbf{60}\dot{\boldsymbol{Q}}}\ (\mathbf{minutes}) \quad \textbf{(5-3)}$$

where ΔH_c (kJ/kg) is the heat of combustion, and all other terms have been previously identified.

This method produces a very large range of potential outcomes, and, in some extreme cases, the predicted duration can be several hours if all randomized parameters are simultaneously optimized to a bounding value (that is, low HRR, high cylinder volume, high density, high heat of combustion); however, the median values were observed to be consistent and meaningful relative to data informed by the actual operating experience as documented in the EPRI FEDB. A summary of the randomized outcomes is provided in Table 5-5. The median of all randomized results is approximately 13 minutes. Note that the median value is skewed to the low side of the range of values due to the very high likelihood of short duration fires and the relatively low likelihood of higher duration fires.

Table 5-5
Survey of motor dimensions and burning duration analysis

Motor Horsepower (hp)	Motor Length Range (m [in.])	Motor Radius Range (m [in.])	Duration Range (min)	Median Duration (min)	Median Duration NUREG/CR-7010 [24] Method (min)
5	0.23–0.52	0.25–0.37	0–46	6	4
	[9.02–20.35]	[9.97–14.51]			
10	0.31–0.55	0.22–0.37	1–57	10	9
	[12.26–21.74]	[8.83–14.51]			
20	0.41–0.57	0.23–0.36	1–52	11	10
	[16.34–22.60]	[9.00–14.06]			
30	0.41–0.70	0.22–0.37	1–64	13	11
	[16.28–27.72]	[8.70–14.46]			
40	0.43–0.79	0.22–0.39	1–79	14	13
	[17.11–31.19]	[8.66–15.27]			
50	0.45–0.94	0.21–0.36	1–92	15	14
	[17.58–37.01]	[8.19–14.09]			
60	0.44–0.96	0.19–0.43	1–87	16	14
	[17.28–37.60]	[17.10–7.36]			
75	0.48–1.01	0.18–0.41	1 – 108	17	15
	[18.75–39.78]	[7.06–16.33]			
100	0.46–1.23	0.14–0.47	1 – 136	18	16
	[17.99–48.48]	[5.32–18.31]			

Because this is a complex analysis, a verification step was simultaneously performed to verify that reasonable burning durations are predicted. In this case, the verification method is Equation 9-2 of NUREG/CR-7010 [24], which calculates the local burning duration of a cable tray fire given the combustible loading, the burning rate, and the heat of combustion of the fuel. The average deviation between the analysis and the NUREG/CR-7010 [24] method in Table 5-5 is 15%, with the NUREG/CR-7010 method consistently predicting shorter durations. The burning duration analysis also provides a rationale for estimating the growth period of the fire as one sixth the steady burning duration as illustrated in Figure 9-1 of NUREG/CR-7010 [24].

The median duration of all of the results in Table 5-5 is 13 minutes, rounded up to the nearest minute. If a brief growth and decay period is added to the duration, the following profile is obtained (This profile can be used for electrical motor fires regardless of size—for example, horsepower—because the observed trend in duration is weakly dependent on motor size.):

- Growth duration: 2 minutes, t-squared growth
- Steady burning duration: 13 minutes
- Decay duration: 2 minutes, linear decay

5.1.6.3 Fire Base Height

No specific guidance for the fire base height of electrical motors has been recommended in previous guidance. However, motor fires have historically been treated as equivalent to electrical cabinets because of the electrical nature of the components. Therefore, the elevation of the fire base for electrical cabinets NUREG/CR-6850, Supplement 1, Chapter 12 [34] can be adapted for electric motors. In this case, all motors considered as ignition sources must be vented given the screening criteria for totally enclosed motors (FAQ 07-0031 [34]); therefore the guidance for unvented cabinets does not apply. The resulting guidance is summarized as follows:

- The assumed fire location for electrical motors sealed on the top (without top vents or openings that allow vertical air flow) should be the location of the highest vent. If the vent location is not known, assume the location to be 0.3 m (1 ft) below the top of the motor but not below the base of the motor housing.
- The assumed location for a fire within a motor that is not sealed at the top should be the top of the motor.

Note that these characterizations require field observations of the condition of the pump or motor as installed. Without field information, the fire base height should be located at the top of the motor.

5.1.7 Motor Fire Event Case Study

A 2016 fire event at a NPP resulted from electrical failure of a 40-hp motor resulting in overheating of the internal components. The fire involved an oil pump motor during a scheduled surveillance. The root cause evaluation determined that the fire was caused by a high armature current with a stalled rotor. The motor was secured and operators standing by in an adjacent room were dispatched to investigate. Upon opening the door, active flames were visible at the top and bottom of the motor along with light smoke in the room. Automatic detection in the area actuated after the fire had been visually detected by personnel and the fixed suppression did not actuate. The motor was de-energized, and a single carbon dioxide extinguisher was applied manually to the motor vents. The fire was extinguished within 3 minutes of discovery.

The fire was limited to flames coming out of the vent covers on the motor. A pump was located approximately 0.6 m (2 ft) from the location of the vent on the burning motor. Additionally, an electrical panel was located approximately 1.5 m (5 ft) above the motor. Both of these adjacent components were exposed to smoke but not damaged beyond smoke impingement and soot deposit. No secondary ignition occurred during the fire event. As shown in Figure 5-11, external flaming was limited to the vent location and the motor casing remained intact after the fire.

Figure 5-11
40 hp motor fire event-external impacts

Figure 5-12 provides an internal view of the damage indicating primarily damage to the stator, which did not fully consume the entire stator surface area. The feeder cable to the adjacent motor is routed directly behind and adjacent to the ignition source and was not damaged by the fire.

Figure 5-12
40 hp motor fire event-internal impacts

The maximum HRR can be estimated using the dimensions listed previously, the Solid Flame II radiation model, and Heskestad's fire plume model [3, 40]. The estimated HRR for a motor that does not damage a target located 0.6 m (2 ft), away horizontally, would be approximately 34.5 kW using the NUREG-1805, Supplement 1, calculation sheet Solid Flame II (elevated targets). Similarly, the HRR required to damage a target located 1.5 m (5 ft) above would be approximately 64 kW. A HRR of 64 kW is larger than the 98th percentile value presented in Table 5-3 for a 40-hp motor (that is, 37 kW). Because the cable behind the motor did not fail during the event, it is likely that the actual fire HRR was less than 34 kW. Given the observation that the adjacent equipment was not damaged, it can be deduced that the fire was less severe than the 98th percentile fire size estimated for a 40-hp motor. This is confirmed by investigation of Figure 5-12, which indicates that approximately half of the motor stator was involved in the fire, and the HRR was likely smaller than the 98th percentile fire size. The 75th percentile fire size for Group B electrical motors is 14 kW, and the average (mean) fire size listed for 40-hp electrical motors from Table 5-2 is 7 kW. Using the gamma distribution parameters from Table 5-3 suggests that only 3% of electrical motor fires from a 40-hp motor would exceed 34.5 kW, and the majority of fires from this size motor are less than 7 kW. This confirms that the outcome of the fire event was consistent with a probabilistic recreation of the event using the methods in Section 5.1, resulting in no damage to the nearest adjacent equipment approximately 97% of the time.

5.1.8 Summary of Electric Motor Fire Characteristics

Electric motors and motor-driven pumps have been consolidated into a single ignition source characterization scheme based upon the size (horsepower) of the motor. The characterization scheme consists of three bins based on horsepower following the screening criteria in Section 5.1.4. The scheme includes distributions of HRR, fire growth and decay parameters, and guidance on fire base height.

The recommended HRRs for electric motors counted in Bins 2, 9, 14, 21, 26, and 32 are summarized in Table 5-6.

Table 5-6
HRR distribution parameters for motors

Motor Classification Group	Motor Size (horsepower)	α	β	75th Percentile (kW)	98th Percentile (kW)
A	>5 -30	1.34	3.26	6	15
B	>30–100	1.17	8.69	14	37
C	>100	1.10	24.19	37	100

The following growth, steady burning, and decay durations should be used for electrical motor fires:

- Growth: 2 minutes, t-squared growth
- Steady burning: 13 minutes
- Decay: 2 minutes, linear decay

The following guidance for determining fire base height should be followed for electrical motor fires:

- The assumed fire location for electrical motors sealed on the top (without top vents or openings that allow vertical air flow) should the location of the highest vent. If the vent location is not known, assume the location to be 0.3 m (1 ft) below the top of the motor, but not below the base of the motor housing.
- The assumed location for a fire within a motor that is not sealed at the top should be the top of the motor.

5.2 Dry Transformers

5.2.1 Introduction

Similar to electric motors, FPRAs include scenarios where a fire in a dry transformer may propagate and damage nearby equipment. The guidance in NUREG/CR-6850 [1] for such fires does not reference any experimental evidence to establish HRRs for dry transformers but recommended values based on the available electrical cabinet experimental data (Table G-1, NUREG/CR-6850 [1]). The guidance makes no specific assessment of the contents or construction of dry transformers that might influence the burning behavior of such equipment. Because the electrical cabinet data has been revised in NUREG-2178 [2], it is appropriate to revisit electrical fire HRRs for transformers. The scope of this evaluation does not impact the treatment of fires in oil-filled transformers, which are expected to have substantially different burning characteristics due to the liquid fuel.

This section presents refined data for the analysis of dry transformer fire scenarios. The approach explicitly considers the size, contents, and construction of transformers to develop guidance for characterizing the fire intensity (that is, HRR).

5.2.2 Overview of Methodology

The revised method is presented in three parts, each of which is covered in the sections that follow:

- The ignition source counting criteria that identify credible ignition sources (see Section 5.2.4)
- Guidance to assign a transformer to a group category based on size (that is, kVA rating) (see Section 5.2.5)
- Recommendations for characterizing the fire intensity (that is, HRR) and duration for the resulting fire scenarios (see Section 5.2.6).

Examples are covered in Section 5.3.

5.2.3 Assumptions and Limitations

The following assumptions and limitations are applicable:

- The guidance and analysis presented and described in this section apply only to the determination and analysis of electrical fires in dry transformers. The guidance does not apply to oil-filled transformer fire scenarios.
- The size (that is, kVA rating) of the transformer is used to define the fire intensity. In the absence of a kVA rating, the size of the transformer may be used to estimate the category

with which to evaluate the scenario. If neither kVA rating nor size is available, the highest HRR bin should be assumed.

5.2.4 FPRA Ignition Source Counting Criteria

There is a single existing criterion for the counting of dry transformers from NUREG/CR-6850 and one additional criterion recommended based on the updated methods. They are as follows:

- Transformers with a power rating of 45 kVA or less are assumed to have little or no contribution to risk and are excluded from ignition source counting (Supplement 1 to NUREG/CR-6850 [34]).
- Transformers with solid cast coil construction can be screened from ignition source counting and further analysis. These transformers have been demonstrated to have a high level of fire resistance inherent to the design of the solid cast insulation surrounding the winding wires. The solid cast materials have been subjected to numerous small- and large-scale fire tests and electrical failure tests in which it was concluded that they produce little or no fire hazard [41]. This screening criterion is added to reflect the inherently reduced fire hazard associated with solid cast coil dry transformers. Note that determination that a transformer is solid cast coil may not be possible in the field and may require design specification review.

5.2.5 Insights from Operating Experience

5.2.5.1 Fire Event Operating Experience

A review of the events recorded in the FEDB associated with Bin 23 provides insight into the types of fires that have been experienced at NPPs for indoor transformer ignition sources. There are eight dry transformer events that have been recorded and determined to be applicable for FPRA applications—events that have been determined to be challenging or potentially challenging and have been counted in the estimation of the fire ignition frequency and non-suppression probabilities as described in NUREG-2169 [36]. The damage associated with each of these eight events is recorded as limited to the object of origin, with over half also listing the damage as localized or limited to a sub-component of the transformer. These events suggest that dry transformer fire events are not likely to be large, challenging fires that result in damage to targets outside the ignition source.

Some transformers have shown a propensity to fail due to an arc fault type or explosion. This failure appears to be far less severe than a typical HEAF, but it does share some similarities. The fault will produce a rapid release of energy, often described as a *pop*, *boom*, or *bang*, coupled with hot slag from the windings that are typically made of aluminum or copper. This arcing is sufficient to create hot slag resulting in openings in the sides of the transformer enclosure increasing the ventilation to the fire. This initial release of energy is very rapid and appears to decay rapidly, and it leaves a relatively steady burning fire in the insulation material associated with the windings.

5.2.5.2 Range of Typical NPP Transformer Sizes

Typical dry transformer sizes at NPPs range from less than 45 kVA (for example, small lighting transformers) to greater than 3000 kVA. The large yard transformers located in the switchyard or outside the turbine building are not included in Bin 23. A review of the FPRA ignition sources from two plants (one PWR, one BWR) provided a distribution of 38 dry transformers greater than 45 kVA evaluated as Bin 23. The size range of transformers is approximately equally distributed for ratings >45 kVA, as shown in Figure 5-13.

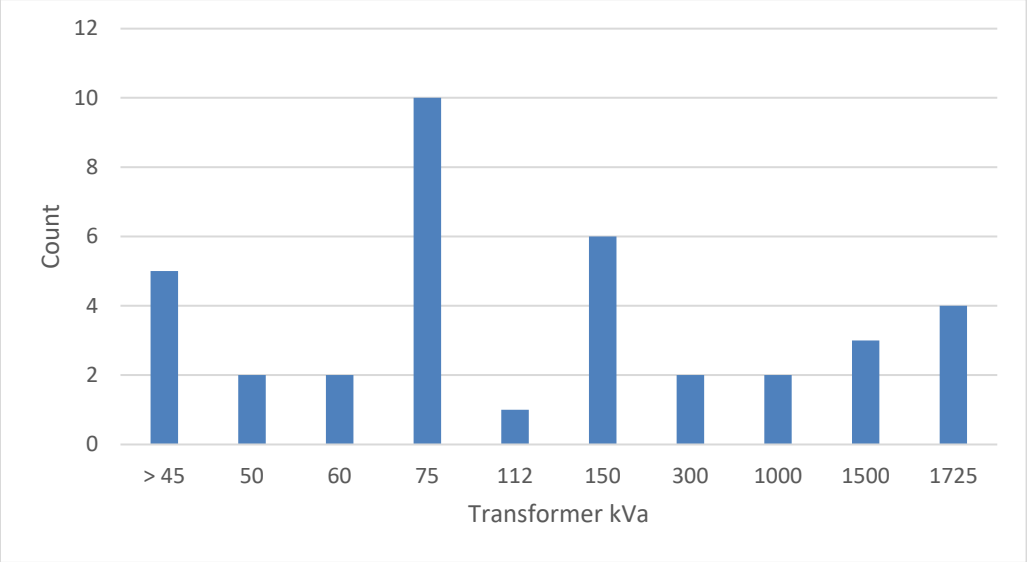

Figure 5-13
Sample dry transformer distribution by transformer rating (Bin 23)

Pictures (Figures 5-14 through 5-17) of dry transformers installed in NPPs were reviewed for overall size and configuration, casing/enclosure robustness, approximation of internal combustibles, and venting characteristics. These observations do not provide clear evidence to classify dry transformers into HRR categories. However, after more detailed analysis (see Section 5.2.6), it was determined that dry transformers could be split into three categories based on their power rating (see Table 5-7), each with a representative HRR.

Table 5-7
Dry transformer classification groups by rating (Bin 23)

Transformer Classification Group	Transformer Power Rating (kVA)
A	≥45–75
B	>75–750
C	>750

Figure 5-14
Examples of typical dry transformers, low end of range (50 kVA, 75 kVA)

Figure 5-15
Example of typical dry transformer, midrange (375 kVA)

Figure 5-16
Example of typical large dry transformers (2000 kVA)

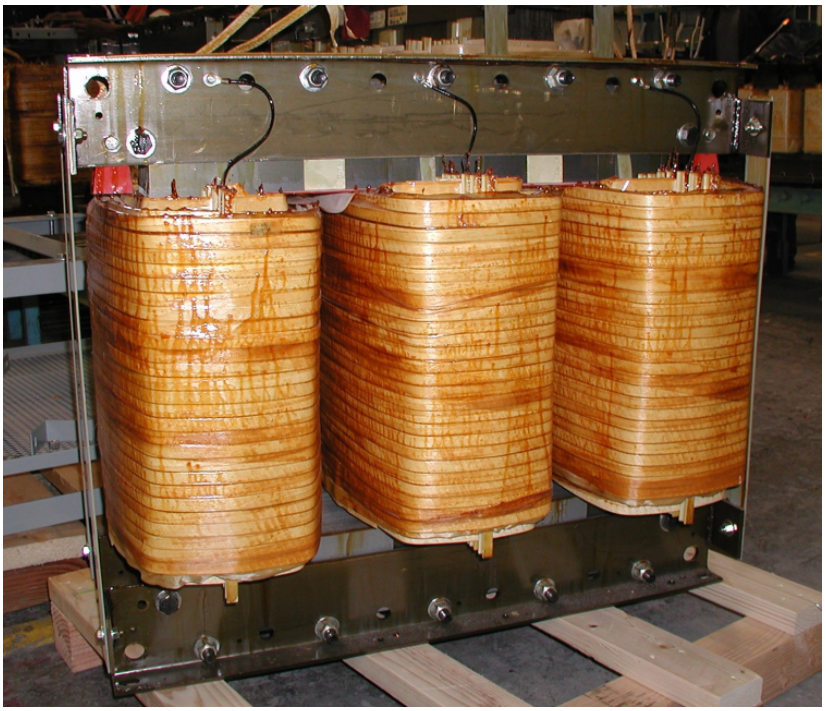

Figure 5-17
Example of typical dry transformer internal winding assembly

5.2.6 Assigning Fire Characteristics to Dry Transformers

NUREG/CR-6850 treats dry transformers as electric motors using 69 kW as the 98th percentile HRR. In general, the stator component of a motor is similar to a winding present inside a transformer. The decision to model transformers similarly to motors is driven by this similarity and the general lack of experimental data to support a unique fire size distribution for transformers. This decision is not documented in NUREG/CR-6850, and, given the update to the electrical motor ignition source, a similar update to the dry transformer ignition source is similarly justified.

According to Section 6.2.3 of Supplement 1 to NUREG/CR-6850 [34], Bin 23 groups plantwide transformers and nominally includes any indoor transformer that is not an integral part of a larger component. In particular, dry transformers with a rating greater than 45 kVA and all oil-filled transformers are included in this bin. This guidance is limited to the dry transformers with a rating greater than 45 kVA within the Bin 23 population, which is evaluated as an electrical fire. Guidance for oil-filled transformers is not revised as part of this effort.

A basic dry transformer does not contain a significant amount of combustible materials relative to the size of the transformer. The small amount of combustible material is mainly limited to the varnish/enamel and insulation used to coat the internal wire windings. Based on the limited amount of combustible material and the observation that most enclosure designs will have robust casing and limited ventilation (see further discussion immediately below), HRRs of transformers are expected to be similar to other generic electrical enclosures having a relationship with the size of the transformer enclosure. The larger transformers may contain a substantially larger quantity of fuel and have a correspondingly larger HRR. The primary variable to consider is transformer size and a corresponding range of HRRs.

5.2.6.1 Heat Release Rate

The dry transformers installed in NPPs are robust and provided with limited ventilation or are entirely encapsulated. The exterior housings (enclosures) are secured at numerous locations on each face and are not expected to warp or lead to gaps during an internal fire. However, some events may produce enough energy to either penetrate the steel barrier directly or create projectile hot slag resulting in a local penetration of the steel barrier. Some dry transformers have vented enclosures that are air cooled, while others are air tight and filled with insulating gas (typically nitrogen, sulfur hexafluoride, or halocarbon refrigerants that are mostly inert and non-combustible). The interior of a transformer typically consists of three insulated windings wrapped around a metallic core with steel framing in place to hold the assembly together.
A simple diagram of the interior of a transformer is provided in Figure 5-18.

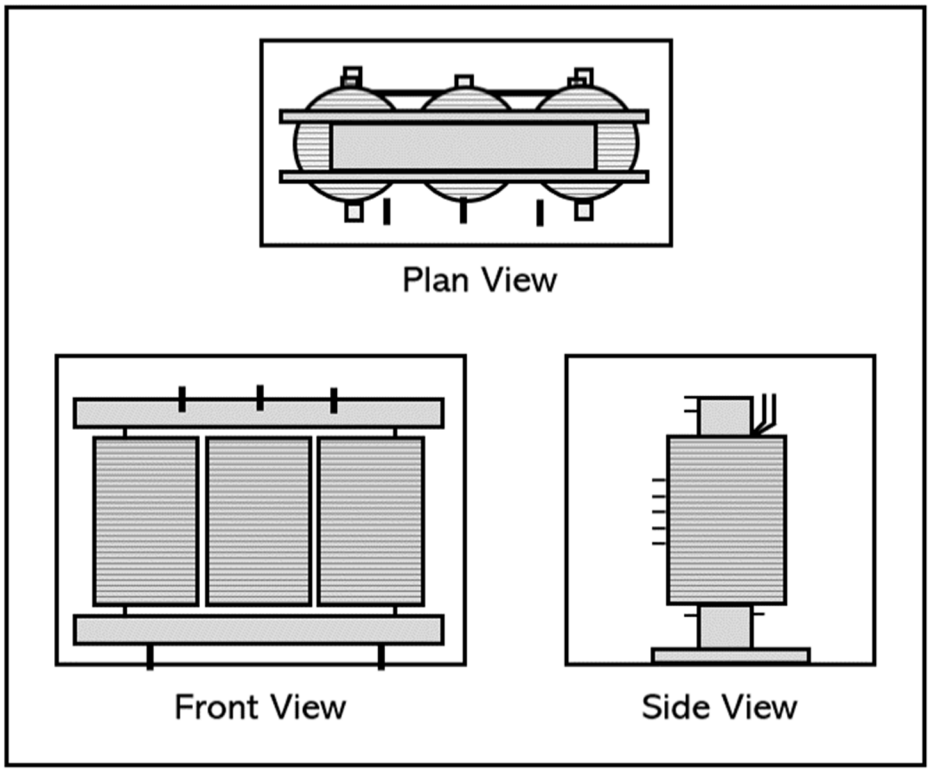

Figure 5-18
Dry transformer diagram of interior contents and arrangement

Note that existing guidance does not attribute any frequency of dry transformer fires to HEAF events; all fires are considered thermal-fires in nature, which may include lower energy forms of arcing faults.

The material contained within the transformer is the primary combustible contents associated with the ignition source. Based on a review of the internal components of dry transformers, the primary combustible material inside the enclosure is the insulating wrap used to isolate the high- and low-voltage windings. Most of the internal contents are metallic (for example, steel, iron, aluminum, and copper), which would not contribute to the combustion process but may be a source of hot slag in certain electrical failures. The metal enclosure walls, internal metal frame, and core metal surfaces are typically coated with epoxy paint or galvanized to limit corrosion. Although epoxy paint may be considered a combustible material, it generally does not contribute substantially to the fire HRR because the material is spread in a thin layer on surfaces with high thermal conductivity, limiting the amount that can volatilize and burn. Therefore, only the insulated windings are considered to contribute to the HRR. To estimate the fuel load within a transformer, the combustible material is conservatively modeled as three cylinders within the transformer enclosure—representing the windings and insulation of which there are typically three cylindrical assemblies in a transformer. The available combustible material will be estimated using a range of different parameters, including the following:

- Transformer enclosure height
- Transformer enclosure width or length
- Number of windings involved

Several of the internal characteristics of the transformer windings were approximated based on reviews of images of exposed transformer windings, specifications, and commercial product descriptions. Important characteristics were identified and assigned a randomized parameter appropriate to the observations.

Transformer Enclosure Height

The combustible material associated with the transformer is primarily considered as the insulation wrapping associated with the windings. Conservatively the combustible surface is modeled as a fraction, ε, of the height of a transformer enclosure because the large enclosure volume is necessary to accommodate the frame of the transformer and provide sufficient open air for cooling and electrical isolation from the exterior enclosure. The fraction, ε, is postulated to range between 40 and 70% of the transformer enclosure height.

Transformer Enclosure Width or Length

Similarly, the three cylindrical insulation sections require horizontal spacing both internally and from the exterior enclosure; so, the total width of the three cylinders is assumed to occupy a fraction of the transformer enclosure width. This fraction, η, is a range postulated between 50 and 80% of the widest dimension of the external transformer housing, ratioed with the smallest dimension. This method results in an estimation of the cylinder radius, *r,* that ensures that the three cylinders fit within the transformer enclosure. This allows for the estimation of the surface area of combustible material within a transformer, as shown in Figure 5-19.

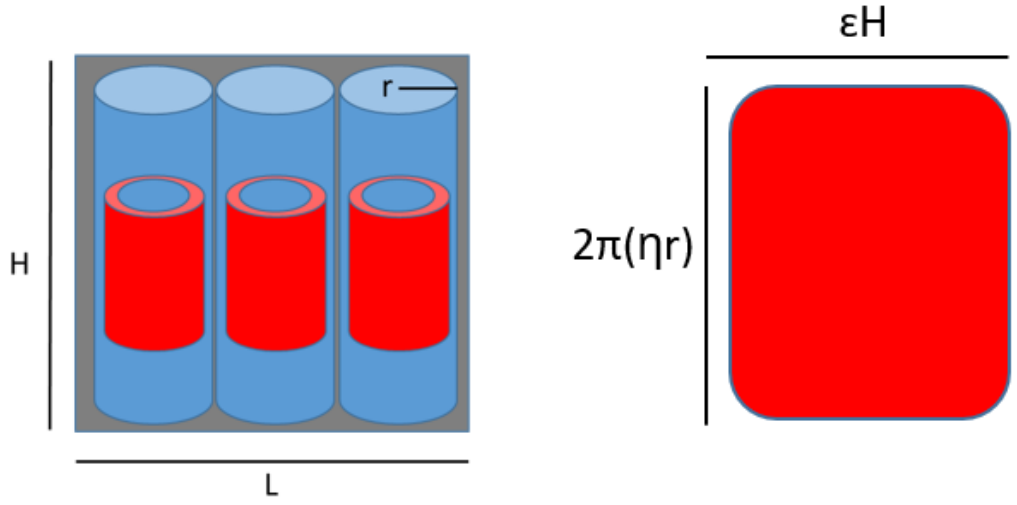

Figure 5-19
Simplified diagram of the combustible material arrangement considered for dry transformers (The illustration on the right represents a single cylinder.)

Cable Enamel/Insulation Heat Release Rate per Unit Area

Dry transformers have continuous temperature classifications of 150°C (65°F), 185°C (85°F), and 220°C (104°F) [42], which are designed to account for elevated ambient temperature, internal heating due to the winding, and insulation hot spots. The transformer is capable of operating at these elevated temperatures without degradation of the components or reduction of the usable life expectancy of the transformer. Some of these temperature ratings are greater than the steady-state failure criteria for thermoplastic (TP) electrical cables; therefore, the insulation material is treated as having superior performance relative to a TP cable. In many cases, the winding cables used inside dry transformers are identical to those used in electric motors for the stator and rotor. However, transformer windings often have fire-resistant insulations, wrappings, or varnishes interlayered with the windings that may impede burning. Therefore, the HRRPUA is assumed to be similar to those used in the estimation of the electric motor analysis presented in Section 5.1.6, with an estimated range of 50–100 kW/m^2.

It is likely that only a fraction of the windings will ignite during any given event. In some instances, a small fraction will ignite, and, in others, the full area of the cylinder(s) will be involved. Therefore, two parameters are used to define the ignited area to account for the variability in the ignited surface area of the cylinder(s). The two parameters are designed to randomly vary the fraction of the perimeter of the cylinder that is ignited and the fraction of the height of the cylinder that is ignited. These parameters are postulated to range between 10 and 100%. The perimeter fraction was evaluated using a beta distribution so that 50% of the cases would result in up to one full cylinder perimeter involved, 40% would result in up to two full cylinders involved, and the remaining 10% of cases could involve up to three full cylinders (alpha = 1.46, beta = 2.64). This characterization was based on observations from FEDB, in which, it was never observed that a dry transformer fire involved all three cylinders. An additional parameter is assumed to account for the non-combustible content of the coils or any additional internal divisions present to limit fire spread. This factor is assumed to limit the quantity of combustible materials involved by the fire and is postulated to range between 50 and 100%.

Number of Windings Involved

The sizes for dry transformer over a range of kVA were reviewed to develop an estimation for the HRR of a dry transformer fire. The review of dry transformer fires from the FEDB indicates that it is unlikely that the fire will consume a substantial portion of the entire transformer. The majority of the experiences indicate small fires, either self-extinguishing or smoldering without visible flaming. The remainder of the fire experience indicates that only a small fire occurred, and it was mostly limited to a single cylinder winding.

It is likely that the thermal failure will occur in one of the three windings and then spread to the adjacent windings only if the severity of the initial fire is sufficiently high and with sufficient duration to ignite the neighboring cylinder. Considering that the initial fire will originate at a weak point in the insulation, the fire will expose, at most, one adjacent cylinder early in the fire event. Over time, the fire may spread around the initial two cylinders to expose the third cylinder, but this behavior is considered unlikely given FEDB observations, suppression response by plant personnel, and the properties of the windings themselves. Therefore, the number of cylinders ignited is a random variable. In order to determine the probability of ignited cylinders during a random event, the location of the ignition is considered along with the potential spread outcomes. This analysis is provided in Figure 5-20, showing that there are 28 possible outcomes, 12 of which ignite one cylinder (42.9%), 10 ignite two cylinders (35.7%), and 6 ignite three cylinders (21.4%). The average (mean) outcome is approximately 1.79 cylinders ignited. This distribution is used to randomly select the number of cylinders involved in any given event. This approach

considers that the most likely occurrence is one cylinder ignited, while a smaller percentage of cases can result in all three cylinders involved. This is a conservative estimate given the observations from the FEDB; however, the ultimate impact on the predicted HRR distributions appears to be small.

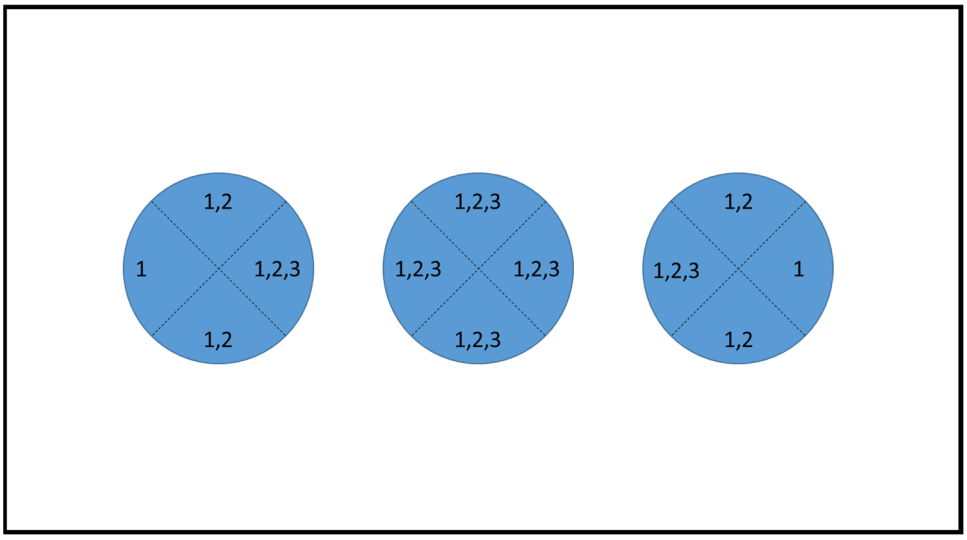

Figure 5-20
Simplified diagram of the potential outcomes of ignition of transformer contents (numbers correspond to the number of cylinders ignited)

Randomized Sampling

The sizes for dry transformers over a range of power ratings were reviewed to develop an estimate for the HRR of a dry transformer fire. Applying the fractions previously covered, the resulting distribution of estimated HRR results as a function of transformer power rating were developed. These values were determined through a randomization of all variable parameters—exterior enclosure dimensions, length fraction, radius fraction, HRRPUA, ignited area fraction, and number of windings ignited. These values are calculated using a sampling technique in order to approximate the distribution of fire sizes that may be possible given the possible range of determining factors (see Figure 5-20). Equation 5-4 is used to determine the HRR, where all parameters are variable within the ranges specified previously:

$$\dot{\boldsymbol{Q}} = \boldsymbol{\varepsilon H} \times \boldsymbol{2\pi\eta r} \times \dot{q}'' \times F_H F_P F_C \times n_c \qquad \textbf{(5-4)}$$

where, H (m) is the exterior height of the transformer, ε is the factor to determine the size of the interior winding height, r (m) is the maximum possible radius of the interior winding based on the maximum width of the transformer (that is, $W/6$), η is the factor to determine the size of the interior winding radius, $\dot{q}''$ (kW/m²) is the HRRPUA of the burning materials, F_H is the factor to determine the percentage of the height of winding ignited, F_P is the factor to determine the percentage of the perimeter of the winding ignited, F_C is the factor crediting the percentage of non-combustible coverings, and n_c is the number of windings ignited.

Using a randomized sample size of 10,000 occurrences (see Figure 5-21), the distribution of fires size is determined, and a gamma distribution is fit to the data. This sample size was observed to regularly result in approximately 98% of the simulated HRR values to be captured within the 98th percentile of the corresponding distribution. Similar to the HRRs presented in NUREG/CR-6850 [1] and NUREG-2178 [2], a gamma distribution is selected for the following three reasons:

- It distributes probabilities among positive, real numbers only.
- It produces a fit representative of the data while maintaining a similar technical approach as previously used.
- Uncertainty in the recommended HRRs values is, for the most part, distributed in the same order of magnitude.

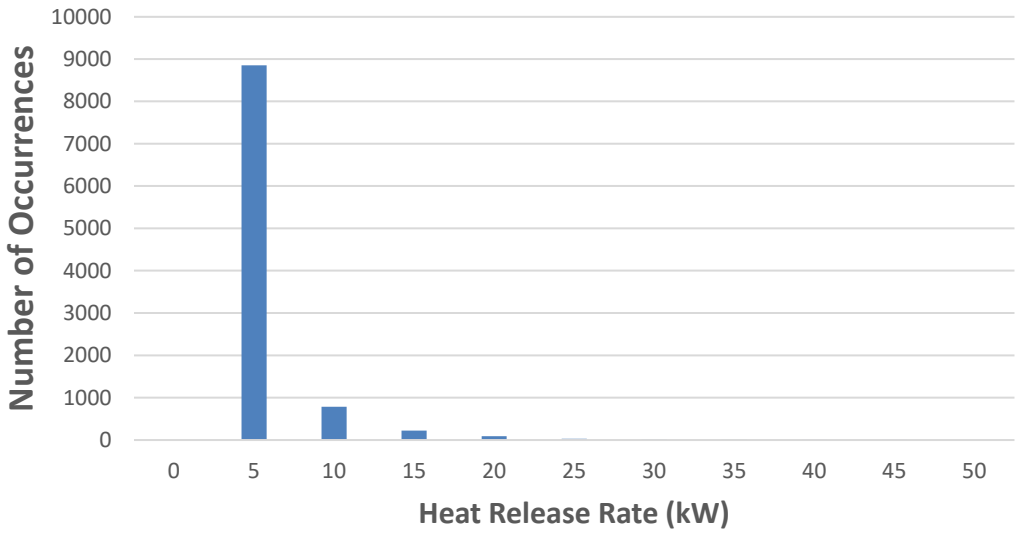

Figure 5-21
50 kVA dry transformer random samples

The resulting average (mean) estimated transformer HRRs per kVA ratings are presented in Table 5-8. The height and radius ranges for various power ratings were determined following a detailed review of transformer dimensions. These values are determined from a statistical best fit of the 10,000 randomized (that is, Monte Carlo simulation) HRR estimates for each power rating. Gamma distribution parameters are approximated from the sample size where beta is determined from the variance of the sample set divided by the mean of the sample set, and then alpha is the mean of the sample set divided by beta. Because the randomized set of 10,000 occurrences can vary, the precise evaluation of these terms can also vary, but the resulting distributions are nearly indistinguishable. Note that the average (mean) value is skewed to the low side of the range of values due to the very high likelihood of low HRR fires and the relatively low likelihood of higher HRR fires.

Table 5-8
Transformer dimensions and HRR analysis

Power Rating (kVA)	Transformer Coil Height Range (m [in.])	Transformer Coil Radius Range (m [in.])	HRR Range (kW)	Average (mean) HRR (kW)
50	0.10–1.07	0.10–0.13	0–39	2
	[3.83–42.03]	[3.78–5.03]		
75	0.10–1.60	0.09–0.12	0–102	4
	[4.04–62.91]	[3.54–4.88]		
100–12.5	0.12–1.60	0.09–0.11	0–82	4
	[4.70–62.91]	[3.54–4.44]		
150–67	0.12–1.60	0.09–0.11	0–79	4
	[4.70–62.91]	[3.54–4.44]		
225	0.12–1.52	0.09–0.11	0–68	4
	[4.70–60.00]	[3.67–4.16]		
300	0.13–1.58	0.08–0.13	0–81	4
	[5.24–62.18]	[3.32–4.92]		
500	0.19–2.32	0.10–0.19	0–350	12
	[7.37–91.50]	[3.87–7.38]		
750	0.19–2.32	0.10–0.17	0–256	12
	[7.37–91.50]	[3.87–6.87]		
1000	0.24–2.32	0.14–0.18	0–313	14
	[9.50–91.50]	[5.59–7.11]		
1250	0.27–2.32	0.14–0.18	0–343	15
	[10.50–91.50]	[5.59–7.13]		
1500	0.27–2.32	0.14–0.18	0–256	14
	[10.67–91.50]	[5.59–7.24]		

This analysis assumes that a transformer consists of the transformer enclosure and the components within and directly attached. This includes the core, windings, insulating materials, and associated components. Transformer enclosures designs can vary significantly, and this analysis does not attempt to evaluate how these differences can impact HRR.

Based on the typical transformer configuration for the various power ratings, a general review of transformer combustible loading, and data from the EPRI FEDB, the updated HRRs are presented in Table 5-9. These values are determined from a statistical best fit of the 10,000 randomized HRR estimates in each classification group. The gamma distribution parameters are approximated from the sample size, where beta is determined from the variance of the sample set divided by the mean of the sample set and alpha is the mean of the sample set divided by beta.

Table 5-9
HRR distributions for dry transformer classification Groups A, B, and C (Bin 23)

Transformer Classification Group	Transformer Power Rating (kVA)	α	β	75th Percentile HRR (kW)	98th Percentile HRR (kW)
A	>45–75	0.38	12.84	6	30
B	>75–750	0.41	28.57	15	70
C	>750	0.46	50.26	30	130

Recall that NUREG/CR-6850 [1] recommended a 98th percentile value of 69 kW to dry transformers. Following the HRR distributions presented inthose assigned to Groups A and B will see either no change (Group B) or a reduction (Group A) in the peak HRR and zone of influence (ZOI) when compared with the previous guidance. Transformers classified in Group C will likely be those associated with and located directly adjacent to switchgear and load centers (Group 1 electrical enclosures). Due to the increase in HRR, only a modest increase in the ZOI is expected and is likely to be bounded by the ZOI of the associated switchgear and load center thermal fire. The primary benefit for the smaller Group A transformers is the decrease in HRR. Group A transformers are anticipated to be the most common and will have reduced ZOIs and severity factors when compared with the previous method.

The results of the Monte Carlo analysis can also be used to estimate Froude numbers for the burning configurations where the fire diameter is calculated assuming a vertical transformer and the total projection of the burning surface. The results are provided in Table 5-10 and may be used to inform detailed fire modeling.

Table 5-10
Froude number distributions for dry transformer classification Groups A, B, and C (Bin 23)

Transformer Classification Group	Transformer Power Rating (kVA)	Mean	Median	16^{th} Percentile	84^{th} Percentile
A	>45–75	0.88	0.46	0.14	1.65
B	>75–750	0.67	0.35	0.12	1.11
C	>750	0.39	0.26	0.11	0.64
	Average	0.65	0.36	0.12	1.13

5.2.6.2 Fire Duration

The duration of the transformer fire can also be approximated using the same approach as used to define the HRR distributions and durations for the motor fires. Because the primary combustible component is associated with the winding wire insulation, this analysis examines the wires in greater detail in order to estimate the duration of the fires. The wiring associated with the windings is sometimes referred to as *magnet wire* and consists of a copper wire with a thin resistive coating. The coatings provide resistance to internal shorts and are designed to operate at elevated temperatures. Because the copper wire does not contribute substantially to the HRR, the thickness and other characteristics of the coating are explored.

The gauge of the winding wiring can range from 6 to 20 AWG depending on the application. Some winding wires may be square, rectangular, or other polygonal cross sections, but this analysis will focus on round cross-section wires. Furthermore, the thickness and type of resistive coating can range widely from 0.015 to 0.094 mm (0.0006 to 0.0037 in.). Therefore, the quantity of combustible coating can be considered a random variable in predicting the burn duration of the transformer. In order to estimate the burning duration, it is necessary to estimate the mass of the combustible material and the energy content of that material and, using the rate of energy released by the fire, estimate the burning duration. Here, the volume of the winding cylinders is required, along with the properties of the winding cables and their associated heat of combustion.

The internal radius of the windings was assumed to be a randomized parameter that ranged between 80 and 90% of the predicted outer radius. This provides the final geometric parameter for computing the volume of the hollow cylinder.

The properties of the winding wires were also approximated using a randomized parameter. The product of the total density of the cable and the percentage of the mass that is combustible (for example, jacket) is used to determine the proportion of the mass of the hollow cylinder, which is considered a combustible jacket. This parameter was observed to fall between 31 and 370 kg/m³.

The heat of combustion was also considered a random variable. Given the range of materials used in jacketing transformer windings, the observed range of heat of combustion is 15.3–21 MJ/kg.

This method produces a very large range of potential outcomes, and, in some extreme cases, the predicted duration can be several hours if all randomized parameters are simultaneously optimized to a bounding value (for example, low HRR, high cylinder volume, high density, high heat of combustion); however, the median values were observed to be very consistent and meaningful. A summary of the randomized outcomes is provided in Table 5-11. The median of all randomized results is approximately 10 minutes, and the mean value is 14 minutes.

Table 5-11
Transformer dimensions and burning duration analysis

Power Rating Range (kVA)	Transformer Coil Height Range (m [in.])	Transformer Coil Radius Range (m [in.])	Duration Range (min)	Median Duration (min)
50	0.10–1.07	0.10– 0.13	0 – 45	5
	[3.83–42.03]	[3.78–5.03]		
75	0.10–1.60	0.09–0.12	0 – 67	7
	[4.04–62.91]	[3.54–4.88]		
100-112.5	0.12–1.60	0.09–0.11	0 – 72	7
	[4.70–62.91]	[3.54–4.44]		
150-167	0.12–1.60	0.09–0.11	0 – 75	7
	[4.70–62.91]	[3.54–4.44]		
225	0.12–1.52	0.09 –0.11	0–50	6
	[4.70–60.00]	[3.67–4.16]		
300	0.13–1.58	0.08–0.13	0–66	7
	[5.24–62.18]	[3.32–4.92]		

Table 5-11
Transformer dimensions and burning duration analysis (continued)

Power Rating Range (kVA)	Transformer Coil Height Range (m [in.])	Transformer Coil Radius Range (m [in.])	Duration Range (min)	Median Duration (min)
500	0.19–2.32	0.10–0.19	0–167	14
	[7.37–91.50]	[3.87–7.38]		
750	0.19–2.32	0.10–0.17	0–131	13
	[7.37–91.50]	[3.87–6.87]		
1000	0.24–2.32	0.14–0.18	1–160	16
	[9.50– 91.50]	[5.59–7.11]		
1250	0.27–2.32	0.14–0.18	1–158	16
	[10.50–91.50]	[5.59–7.13]		
1500	0.27–2.32	0.14–0.18	0–228	16
	[10.67–91.50]	[5.59–7.24]		

As noted in Section 5.2.5.1, some dry transformer fires have been initiated by arcing faults, and, therefore, it is recommended that transformers be treated with a modified profile from the original guidance in NUREG/CR-6850, Appendix G, so that the fire is considered to have no growth period. The decay period is assumed to be equal to the steady duration. This is to conservatively account for the potential of the fire to spread around, to adjacent cylinders or through the cylinder to areas that were not initially ignited. This also echoes the behavior of electrical enclosure fires that have a decay period of similar or longer length than the steady duration.

The median duration of all of the results in Table 5-11 is 10 minutes, rounded up to the nearest minute. If a brief decay period is added to the duration, the following profile is obtained (This profile can be used for dry transformer fires regardless of size—for example, kVA—because the observed trend in duration is weakly dependent on transformer rating.):

- Growth: 0 minutes
- Steady burning: 10 minutes
- Decay: 10 minutes, linear decay

5.2.6.3 Fire Base Height

No specific guidance for the fire base height of dry transformers has been recommended in previous guidance. However, fire base heights have historically been treated as equivalent to electric motors. Dry transformers also share several characteristics with electrical cabinets. Therefore, it is valid to treat the elevation of the fire base for dry transformers as equivalent to the guidance provided for electrical cabinets in NUREG/CR-6850, Supplement 1, Chapter 12 [34]. The resulting guidance is summarized as follows:

- The assumed fire location for dry transformers sealed on the top (without top vents or openings that allow vertical air flow) is 0.3 m (1 ft) below the top of the transformer. This assumption is also valid (conservative) for fully sealed transformer enclosures.

- The assumed fire location for a fire within a dry transformer that is not sealed at the top (that is, openings located on the top surface of the transformer) should be the top of the transformer.
- Alternatively, for side-vented transformers where one or more vents are located on the side of the enclosure, the analyst can locate the fire at the uppermost vent. For example, if the enclosure includes two vertical vents on the side, the fire should be located at the elevation of the upper vertical vent.

5.2.7 Dry Transformer Fire Event Case Study

As stated in Section 5.2.5.1, of the events recorded in the FEDB and determined to be applicable for FPRA, none resulted in damage to anything other than the transformer of origin.

In 2013, a fire event at a NPP resulted from an electrical failure on a 2500- kVA dry transformer (see Figure 5-22). The root cause evaluation determined that the fire was caused by a turn-to-turn short of the primary winding of the transformer's A phase, likely due to degrading insulation. Both the main control board trouble and incipient fire detection alarms were received in the fire compartment containing the transformer. Responding operators were dispatched to the compartment and attempted to locate the source of smoke and troubleshoot the alarms. During this troubleshooting, a loud explosion was heard by an operator near the compartment containing the transformer. The fire brigade responded following reports of smoke (haze) in the compartment. Following an initial assessment, the fire brigade reported that the fire was out and the feeder breaker for the transformer was tripped, de-energizing the equipment. There was indication of visible damage from an explosion on the transformer.

Figure 5-22
Damaged dry transformer

Aside from the explosion and the report of smoke, there was no indication of a flaming fire. Just as with the events reviewed and covered in Section 5.2.5.1, damage was limited to the transformer.

Using the Solid Flame II radiation model and the Heskestad fire plume [3, 40], the ZOI for the transformer HRR is estimated. The peak HRR for the transformer is 130 kW (see Table 5-9) for a transformer with a rating greater than 750 kVA. Assuming TP damage criteria and using the NUREG-1805, Supplement 1 calculation sheet Solid Flame II (elevated targets), the horizontal ZOI is 1 m (3.3 ft). Similarly, the vertical ZOI expected is 2 m (6.6 ft). Because the event makes no mention of damage to surrounding equipment, it suggested that the 98th percentile fire size for a Class C Transformer (see Table 5-9) in the FPRA analysis bounds the damage observed in the event.

5.2.8 Summary of Dry Transformer Fire Characteristics

Dry transformers have been split into three groups of fire HRR profiles based on the size of the transformer following the screening guidance in Section 5.2.4. The recommended HRRs for dry transformers are summarized in Table 5-12.

Table 5-12
HRR distribution parameters for dry transformers

Transformer Classification Group	Transformer Power (kVA)	α	β	75th Percentile (kW)	98th Percentile (kW)
A	>45–75	0.38	12.84	6	30
B	>75–750	0.41	28.57	15	70
C	>750	0.46	50.26	30	130

The following growth, steady burning, and decay durations should be used for dry transformer fires:

- Growth: 0 minutes
- Steady burning: 10 minutes
- Decay: 10 minutes, linear decay

The following guidance for determining fire base height should be followed for electrical motor fires:

- The assumed fire location for dry transformers sealed on the top (without top vents or openings that allow vertical air flow) is 0.3 m (1 ft) below the top of the transformer. This assumption is also valid (conservative) for fully sealed transformer enclosures.
- The assumed fire location for a fire within a dry transformer that is not sealed at the top (that is, openings located on the top surface of the transformer) should be the top of the transformer.
- Alternatively, for side-vented transformers where one or more vents are located on the side of the enclosure, the analyst can locate the fire at the uppermost vent. For example, if the enclosure includes two vertical vents on the side, the fire should be located at the elevation of the upper vertical vent.

5.3 Examples

5.3.1 Electric Motors—Screening Analysis

A number of unscreened electrical motors have been identified during ignition source counting that require further analysis in the FPRA. The motors range in size from 10 hp to 1000 hp, and generic information about the exposed raceway targets has been provided from the walkdowns. The information provided includes the vertical separation from the motor to the nearest exposed raceway above the source. The analysis requires the definition of a ZOI to determine which raceways are within the damage region of the motor ignition sources. The vertical separation from the motor to the nearest exposed raceway can also be used to define a severity factor that identifies the smallest fire that will damage the target and calculates the percentage of fires that exceed the value based on the gamma distribution of the ignition source.

The following design inputs/limitations are provided:

- None of the target raceways is considered a secondary combustibles.
- The motors are located away from any wall surfaces.
- The motors are located in a compartment with a very high ceiling, and the development of a hot gas layer (HGL) has been screened based on fire modeling analysis.
- The ambient temperature in the compartment is 25°C (77°F).
- The compartments in which the motors are located do not have suppression or detection systems.
- The fire Froude is 0.49, which is the average median value for all motor classifications in Table 5-4. Note that all values presented in Table 5-4 are acceptable values.
- The fire plume temperature is calculated using NUREG-1805, Supplement 1, Chapter 9.
- The fire radiant heat flux is calculated using the revised Solid Flame II model as presented in Section 2. Reported ZOI values are from the edge of the fire source.
- Damage criteria are defined as 205°C (400°F) and 6 kW/m² for TP cable targets according to NUREG/CR-6850.
- The severity factor is calculated from the gamma distribution parameters using the equation in Excel: = 1 - GAMMADIST(HRR, ALPHA, BETA, TRUE).

The summary of the analysis inputs and results are provided in Table 5-13.

Table 5-13
Electric motor screening level analysis example

Motor horsepower (hp)	Motor Size Category	98th Percentile HRR (kW)	Target Vertical Separation (m [ft])	Vertical ZOI Dimension (m [ft])	Horizontal ZOI Dimension (m [ft])	Critical HRR (kW)*	Severity Factor
10	A	15	0.3 (1.0)	0.79 [2.59]	0.13 [0.42]	1.3	0.80
20	A	15	0.9 (3.0)	0.79 [2.59]	0.13 [0.42]	20.6	N/A
30	A	15	1.5 (5.0)	0.7 [2.3]	0.13 [0.42]	74.0	N/A
50	B	37	0.3 (1.0)	1.14 [3.74]	0.23 [0.76]	1.3	0.91
75	B	37	0.9 (3.0)	1.14 [3.74]	0.23 [0.76]	20.6	0.47
100	B	37	1.5 (5.0)	1.14 [3.74]	0.23 [0.76]	74.0	N/A
200	C	100	0.3 (1.0)	1.69 [5.54]	0.43 [1.41]	1.3	0.96
500	C	100	1.5 (5.0)	1.69 [5.54]	0.43 [1.41]	74.0	0.06
1000	C	100	3.0 (10.0)	1.69 [5.54]	0.43 [1.41]	418.5	N/A

* Although the horizontal ZOI is calculated and presented in this example, targets in the vertical direction are subject to damage by plume temperatures and are usually damaged at lower HRRs when compared with the equal distances in the horizontal direction. Therefore, the critical HRRs and severity factors shown are for damage to targets separated vertically from the motor.

N/A = The target is outside of the 98th percentile ZOI and can be screened from further analysis in the FPRA.

5.3.2 Electric Motors—Detailed Analysis

An electric motor is identified during walkdowns. The motor is approximately 0.9 m (3 ft) long, and the top of the motor is located 0.6 m (2 ft) from the floor. A plate on the motor states that the motor is 50 hp.

The same design inputs and limitations as defined in the previous example (see Section 5.3.1) are applicable to this example.

There are two electrical cabinets located near the motor. Electrical Cabinet A (EC A) is located approximately 1.2 m (4 ft) east of the motor. The second cabinet (EC B) is located 0.3 m (1 ft) north of the motor. There is a cable tray (Train A) located approximately 2.4 m (8 ft) above the floor that passes directly over the electric motor. The plan and elevation view of the area are provided in Figure 5-23.

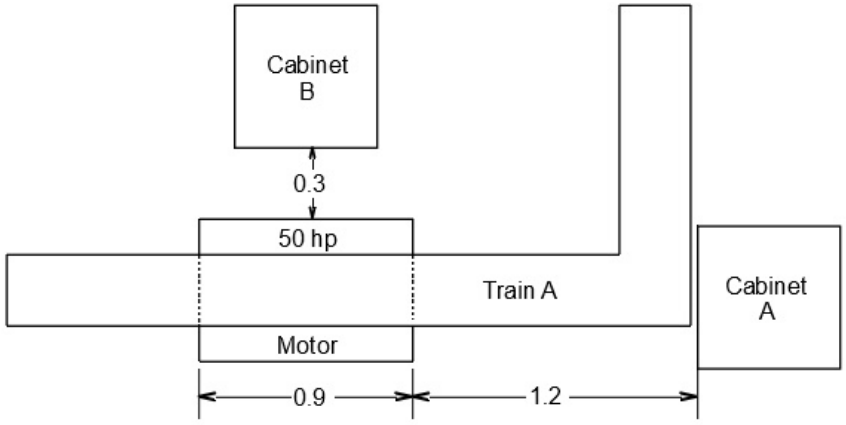

Plan View

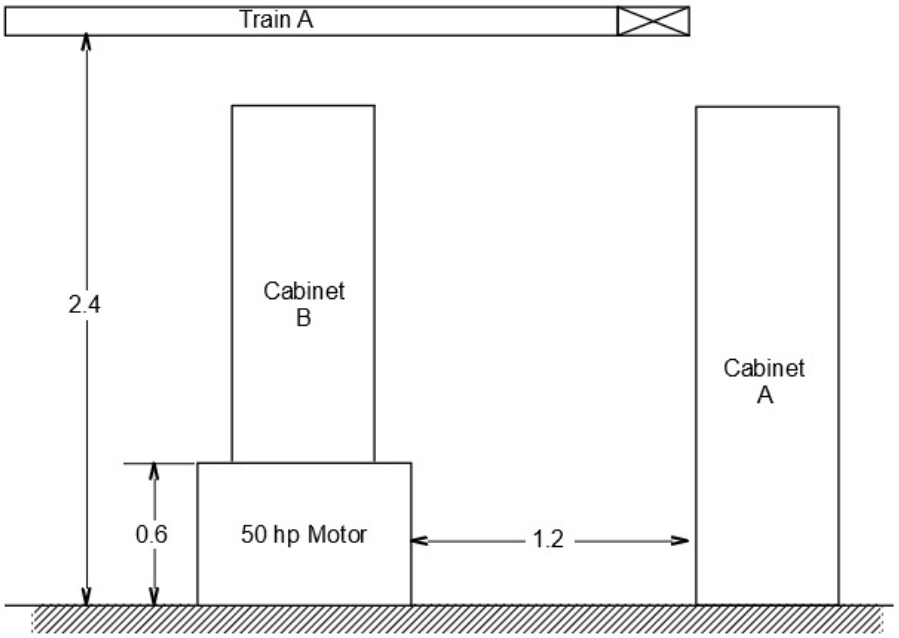

Elevation View

Figure 5-23
Plan and elevation view from walkdown (dimensions provided in meters)

The motor, 50 hp, falls within the Group B classification in Table 5-3. The resulting peak HRR is 37 kW. The NUREG-1805, Supplement 1, Chapter 5 (Solid Flame II) and Chapter 9 sheets are used to estimate the critical HRR required to expose the nearby targets.

The critical HRR, severity factor, and time to damage for each target is presented in Table 5-14. The time to damage is determined from the time to reach the critical HRR using a t-squared growth curve and using a growth time of 2 minutes from Section 5.1.6.2.

Table 5-14
Electric motor detailed fire modeling results

Target	Direction	Distances (m, [ft]) from Figure 5-23	Critical HRR (kW)	Severity Factor	Time to Damage (min)
EC A	Horizontal	1.2 [4]	600	N/A	N/A
EC B	Horizontal	0.3 [1]	56	N/A	N/A
Train A	Vertical	1.8 [6]	122	N/A	N/A

N/A = The target is outside of the 98th percentile ZOI and can be screened from the FPRA.

The results show that EC A, EC B, and Train A are outside the ZOI for the electric motor ignition source.

5.3.3 Dry Transformers—Screening Analysis

A number of unscreened transformers are identified during ignition source counting that require screening level analysis in the FPRA. The transformers range in size from 50 to 3000 kVA, and generic information about the exposed raceway targets has been provided from the walkdowns. The information includes the vertical separation from the transformer to the nearest exposed raceway above the source. Other targets have been identified with vertical and horizontal separation from the source. The analysis requires the definition of a ZOI in order to determine which raceways are within the damage region of the dry transformer ignition sources. The vertical separation from the transformer to the nearest exposed raceway may also be used to define a severity factor that identifies the smallest fire that will damage the target and calculate the percentage of fires that exceed the value based on the gamma distribution of the ignition source.

The following design inputs/limitations are provided:

- None of the target raceways are considered secondary combustibles.
- The transformers are located away from any wall surfaces.
- The transformers are located in a compartment with a very high ceiling, and the development of a HGL has been screened based on fire modeling analysis.
- The ambient temperature in the compartment is 25°C (77°F).
- The compartments in which the transformers are located do not have suppression or detection systems.
- The fire Froude number is 0.36, which is the average median value for all transformer classifications in Table 5-10. Note that all values presented in Table 5-10 are acceptable values.

- The fire plume temperature is calculated using NUREG-1805, Supplement 1, Chapter 9.
- The fire radiant heat flux is calculated using the revised Solid Flame II model in Section 2. Reported ZOI values are from the edge of the fire source.
- Damage criteria are defined as 205°C (400°F) and 6 kW/m² for TP cable targets, according to NUREG/CR-6850.
- The severity factor is calculated from the gamma distribution parameters using the equation in Excel: = 1 - GAMMADIST(HRR, ALPHA, BETA, TRUE).

The summary of the analysis inputs and results is provided in Table 5-15.

Table 5-15
Transformer screening level analysis examples

Transformer Rating (kVA)	Transformer Size Category	98th Percentile HRR (kW)	Vertical Separation (m [ft])	Vertical ZOI Dimension (m [ft])	Horizontal ZOI Dimension (m [ft])	Critical HRR (kW)*	Severity Factor
50	A	30	0.3 (1.0)	1.00 [3.28]	0.2 [0.66]	1.47	0.52
60	A	30	0.9 (3.0)	1.00 [3.28]	0.2 [0.66]	22.86	0.16
70	A	30	1.5 (5.0)	1.00 [3.28]	0.2 [0.66]	81.99	N/A
100	B	70	0.3 (1.0)	1.41 [4.63]	0.34 [1.13]	1.47	0.67
250	B	70	0.9 (3.0)	1.41 [4.63]	0.34 [1.13]	22.86	0.31
700	B	70	1.5 (5.0)	1.41 [4.63]	0.34 [1.13]	81.99	N/A
2000	C	130	0.9 (3.0)	1.80 [5.91]	0.5 [1.64]	22.86	0.31
2500	C	130	1.5 (5.0)	1.80 [5.91]	0.5 [1.64]	81.99	0.06
3000	C	130	3.0 (10.0)	1.80 [5.91]	0.5 [1.64]	463.82	N/A

* Although the horizontal ZOI is calculated and presented in this example, targets in the vertical direction are subject to damage by plume temperatures and are usually damaged at lower HRRs when compared with the equal distances in the horizontal direction. Therefore, the critical HRRs and severity factors shown are for damage to targets separated vertically from the motor.

N/A = The target is outside of the 98th percentile ZOI and can be screened from further analysis in the FPRA.

5.3.4 Dry Transformers—Detailed Analysis

A transformer is identified during walkdowns. The transformer is approximately 0.6 m (3 ft) long, and the top of the transformer is located 0.6 (2 ft.) from the floor. A plate on the transformer states that it is rated for 50 kVA, and it is air cooled (dry).

The same design inputs and limitations as defined in the previous example (see Section 5.3.3) are applied to this example.

There are two electrical cabinets located near the transformer. Electrical Cabinet A (EC A) is located approximately 1.2 m (4 ft) east of the transformer. The second cabinet (EC B) is located 0.3 m (1 ft) north of the transformer. There is a cable tray (Train A) located approximately 2.4 m (8 ft) above the floor that passes directly over the transformer. The plan and elevation view of the area are provided in Figure 5-24.

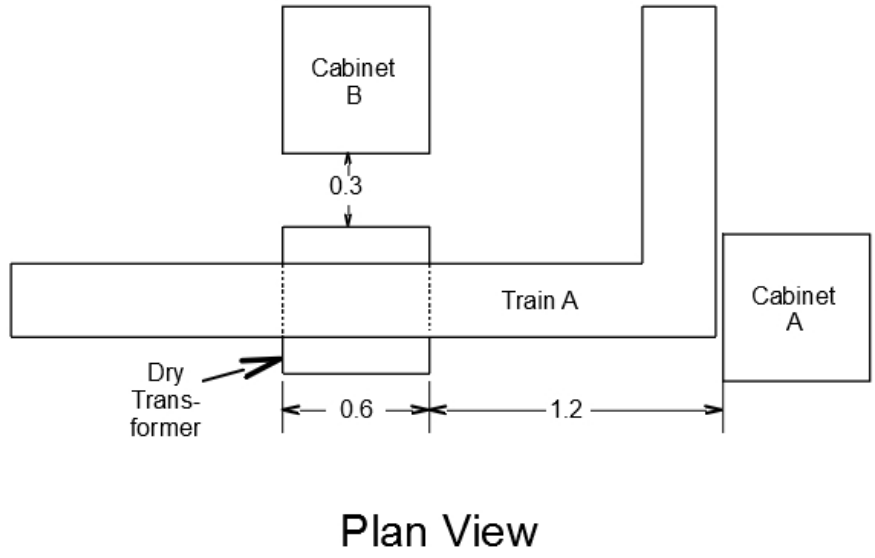

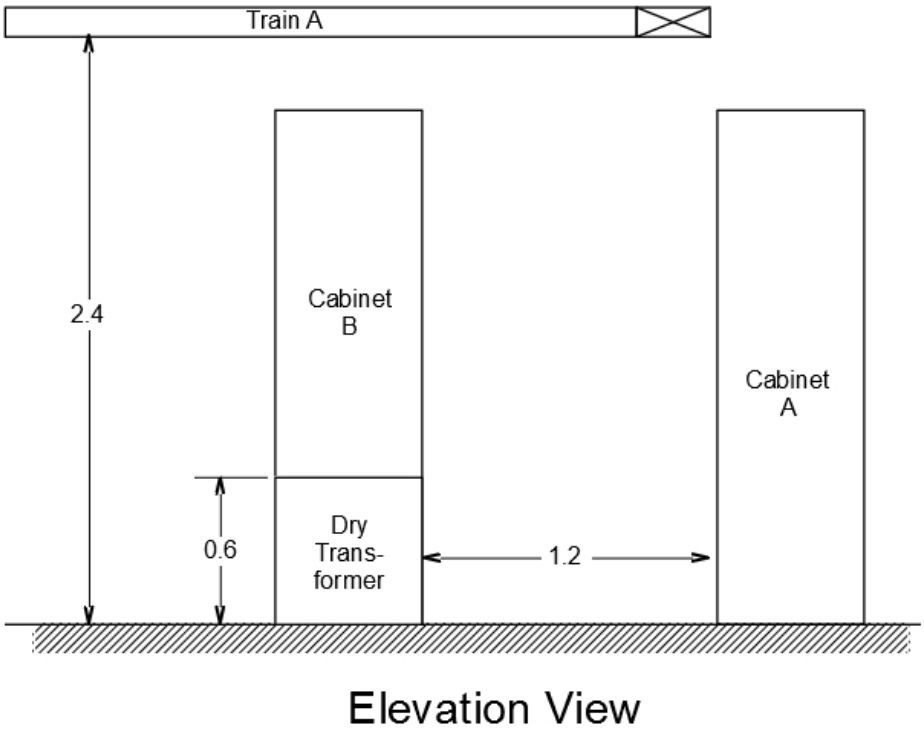

Figure 5-24
Plan and elevation view from walkdown (dimensions provided in meters)

With a rating of 50 kVA, the transformer falls within the Group A classification in Table 5-9. The peak HRR is 30 kW. The NUREG-1805, Supplement 1, Chapter 5 (Solid Flame II) and Chapter 9 sheets are used to estimate the critical HRR required to damage the nearby targets.

The critical HRR, severity factor, and time to damage for each target is presented in Table 5-16. Because transformer fires are considered to have no growth period, all targets are damaged at 1 minute based on the minimum time to damage reported in NUREG/CR-6850, Appendix H.

Table 5-16
Electric motor detailed fire modeling results

Target	Nearest Target Direction	Distances (m, [ft]) from Figure 5-24	Critical HRR (kW)	Severity Factor	Time to Damage (min)
EC A	Horizontal	1.2 [4]	606	N/A	N/A
EC B	Horizontal	0.3 [1]	56	N/A	N/A
Tray A	Vertical	1.8 [6]	135	N/A	N/A

N/A = global. The target is outside of the 98th percentile ZOI of the ignition source and it can be screened from the FPRA.

The results show that EC A, EC B, and Train A are outside the ZOI for the transformer ignition source.

6
WALL/CORNER NEW FIRE LOCATION FACTOR

6.1 Introduction

This section summarizes the latest guidance for determining fire plume temperatures when the fire is postulated near corners or along walls as described in the Electric Power Research Institute (EPRI) report, *Fire Modeling Enhancements for Fire Probabilistic Risk Assessment* [9]. When the fire is located near a wall or in a corner, less air can be entrained into the fire plume. Less air entrainment into the fire plume produces higher plume temperatures. The flames from fires in contact with wall and corner surfaces tend to be longer, also resulting in higher plume temperatures. For such fires, a location factor, traditionally 2 for fires near a wall or 4 for fires near a corner, is applied as a correction to the plume temperature calculation. One question that is often asked is "What does *near* mean in this context?" Detailed guidance on the appropriate use and selection of fire location factors suitable for fire plume temperature predictions in fire probabilistic risk assessment (FPRA) is provided and is intended for field application in a simplified manner for ease of use.

6.2 New Fire Location Factor Guidance

The guidance described in the EPRI report, *Fire Modeling Enhancements for Fire Probabilistic Risk Assessment* [9], outlines the appropriate selection of fire location factors for fire plume temperatures when the fire is postulated at various distances from a corner or wall surface. The fire location factor, k_F, is used in calculating plume temperatures for an ignition source fire that is located in a corner or along a wall. Its effect is to increase the plume temperature at a specified elevation compared with that for the same ignition source fire in the open. This is a mathematical evaluation of the image or mirror method as described in Section L.4 of NUREG/CR-6850 [1] and the NRC Fire Protection Significance Determination Process [43] using the Heskestad plume equation as the basis [40]. In order to explore the impacts for such fires, Version 6.0.1 of the Fire Dynamics Simulator (FDS) [4, 5, 21,44] software tool was used to simulate fire conditions in the open, near walls, and in corner configurations. FDS served as a tool for understanding how parameters such as heat release rate (HRR) and distance to wall or corner influence the fire behavior. Additionally, a modification to the Heskestad fire plume correlation [45, 46] is presented for use with the updated fire location factor guidance. The modified Heskestad fire plume correlation is shown in Equation 6-1:

$$\boldsymbol{T_{pl} = T_0 + 9.1\left[\frac{T_0}{(g c_p^2 \rho_0^2)}\right]^{1/3}\left(k_F \dot{Q}_c\right)^{2/3}(z - z_0)^{-5/3}} \qquad \textbf{(6-1)}$$

where: T_{pl} is the plume temperature (K), T_0 is the ambient temperature (K), g is the acceleration due to gravity (m/s^2), c_p is the specific heat of air (kJ/kg·K), ρ is the density of air (kg/m^3), k_F is the fire location factor identified in Table 6-1, $\dot{Q}_c$ is the convective HRR (kW), z is the height

above the top of the ignition source (m), z_0 is the height of the virtual source (m) as calculated from Equation 6-2:

$$z_0 = -1.02D_F + 0.083\left(k_F\dot{Q}\right)^{2/5} \quad \textbf{(6-2)}$$

D_F is the diameter of the fire source (m) as calculated from Equation 6-3:

$$D_F = D\sqrt{k_F} = \sqrt{\frac{k_F\dot{Q}}{\dot{q}''} \cdot \frac{4}{\pi}} \quad \textbf{(6-3)}$$

and $\dot{Q}$ is the HRR (kW) and $\dot{q}''$ is the heat release rate per unit area (HRRPUA) (kW/m^2).

This correlation is valid only above the mean flame height, F_h. The mean flame height (see Equation 6-4) can be calculated as:

$$F_h = -1.02D_F + 0.230\dot{Q}^{2/5} \quad \textbf{(6-4)}$$

Traditionally, the location factor, k_F, was set to 1 for fires in the open (away from walls), to 2 for fires near a wall, and to 4 for fires near a corner (the junction of two walls). Again, the question often asked, and being addressed here, is how far away from a wall or corner do you need to be for the fire to be considered *in the ope*n?

Fifty-one simulations using the FDS software were used to develop data to support the analysis. Four influencing factors were identified to define a test matrix: HRR, fire diameter, elevation above the fire where the plume temperature is measured, and the distance of the fuel package from the wall surfaces. The simulations used a compartment size measuring 6 m (19.7 ft) x 6 m (19.7 ft) x 6 m (19.7 ft). The revised values for k_F based on the FDS simulations (See *Fire Modeling Enhancements for Fire Probabilistic Risk Assessment* [9]) are presented in Table 6-1.

Table 6-1
New fire location factor

Configuration	Location Factor 0–0.3 m [0–1 ft]	Location Factor 0.3–0.6 m [1–2 ft]	Location Factor >0.6 m [2 ft]
Corner	4	2	1
Wall	1	1	1

For ignition sources located along walls or within corners, the following guidance is provided for the determination of plume temperatures with zone of influence (ZOI) analyses:

- Wall configuration—a value of 1 may be used at all distances for fires located near a single wall surface.
- Corner configuration—in a case where two wall surfaces are located within a distance of 0.3 m (1 ft), the corner configuration should be assumed, and a value of 4 should be used. If two wall surfaces are located within the range of 0.3–0.6 m (1–2 ft) of the ignition source, it should be considered a transitional corner configuration, and a value of 2 should be used for k_F. A value of 1 should be used in all other cases where the separation distance from wall surfaces is greater than 0.6 m (2 ft).

The new fire location factor may be used with all types of wall surfaces, including concrete, gypsum, and steel.

Additionally, there are a number of limitations that should be observed when using these new fire location factors. Many of these limitations are due to the limited scope of the evaluation [9] and are developed only to clarify that specific physical behaviors have not yet been studied in detail. These limitations are as follows:

- Values less than 1.0 should not be used for k_F. The value of 1.0 is equivalent to the unmodified Heskestad plume equation.
- The new fire location factor does not apply to configurations that include burning of secondary combustible materials. The modified Heskestad fire plume correlation, including the location factor, however, may be used to establish the likelihood that secondary combustibles may be ignited through the definition of the primary ignition source ZOI. The modified Heskestad fire plume correlation is limited to the ignition source only—that is, in the case of secondary combustible ignition (that is, cable trays), the subsequent analysis should follow existing information and modeling techniques.
- The new fire location factor does not apply to an analysis of hot gas layer (HGL) damage. The plume correlation may be used only for the duration of time in which thermal plume exposure is postulated but the HGL temperature has not yet reached the damage criteria. Existing information and modeling techniques should be used to evaluate the likelihood and timing of HGL damage. Modeling techniques can combine the effects of a thermal plume immersed in an HGL, although these techniques may be applied only to exposures within the thermal plume prior to the HGL damage state. In other words, while proximity to a corner can impact plume temperatures, it does not impact the HGL temperature.
- The new fire location factor does not apply to analyses that determine the visibility reduction due to smoke accumulation.
- The ceiling jet was not evaluated in the FDS simulations reviewed in this report. However, the findings of this report do not invalidate existing guidelines for the evaluation of the ceiling jet, and the new fire location factors presented may be used with ceiling jet evaluations pending further analysis.
- The new fire location factor does not apply to the evaluation of the horizontal thermal flame radiation ZOI. Existing information and modeling techniques should be used to evaluate the extent of the horizontal ZOI.
- The new location factor values are not to be applied to FDS predictions of fire plume temperatures. The new location factor does not apply to FDS results and is intended for use only with the Heskestad fire plume correlation. A qualified user of FDS should develop an appropriate set of inputs to address the effects of wall surfaces but not by adjusting the output data with a bias correction.

6.3 New Fire Location Factor Validation

The guidance detailed in *Fire Modeling Enhancements for Fire Probabilistic Risk Assessment* [9] was developed using fire model simulations. In August 2017, the National Institute of Standards and Technology (NIST) conducted a number of experiments involving fires near a corner or along a wall [18]. These experiments used a 0.6 m (2 ft) x 0.6 m (2 ft) burner with the surface located approximately 0.54 m (1.8 ft) above the floor. The experiments started with the burner in the corner or against the wall for the first 30 minutes. After 30 minutes, the burner was moved so that its edge(s) was 0.1 m (0.3 ft) away from the wall(s). After it was moved,

in 15-minute intervals, the burner was again moved to 0.2 m (0.7 ft), 0.3 m (1 ft), 0.5 m (1.6 ft), 1.0 m (3.3 ft), and 1.6 m (5.2 ft) from the starting position for a total experiment time of 2 hours.

Thermocouples were placed above the burner in a three-dimensional array. The thermocouples allowed for plume temperatures at heights of 2.1 m (6.9 ft), 2.7 m (8.9 ft), and 3.4 m (11.2 ft) above the floor.

The results of the experiments showed similar trends as expressed in the EPRI guidance. Temperature plots from two of the experiments, a fire located near a single wall surface and in a corner are shown in Figure 6-1 and Figure 6-2.

The plume temperatures for a single experiment are shown in Figure 6-1. The temperature profile presented in Figure 6-1 remains primarily steady at various separation distances from a single wall surface. This trend matches well with the reviewed guidance that a single wall surface has little effect on fire plume temperatures.

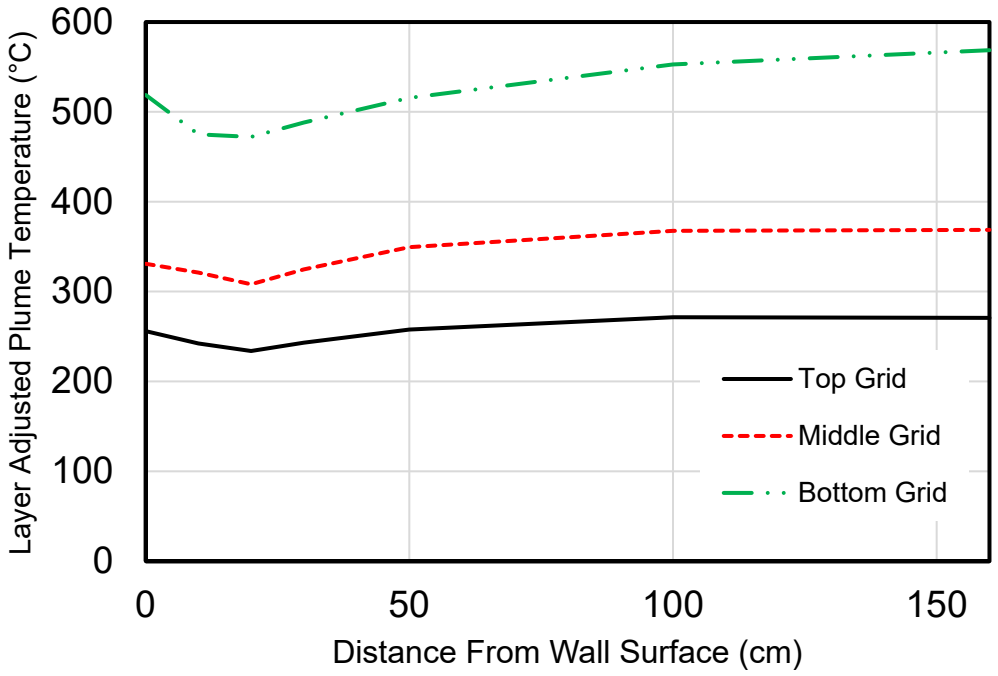

Figure 6-1
Plume temperature, single wall surface, 400 kW

The plume temperatures from one experiment of a fire in a corner are presented in Figure 6-2. The temperature profile again agrees with the reviewed guidance that the effect of a corner on plume temperature decreases rapidly as the fire is located at greater distances from the corner.

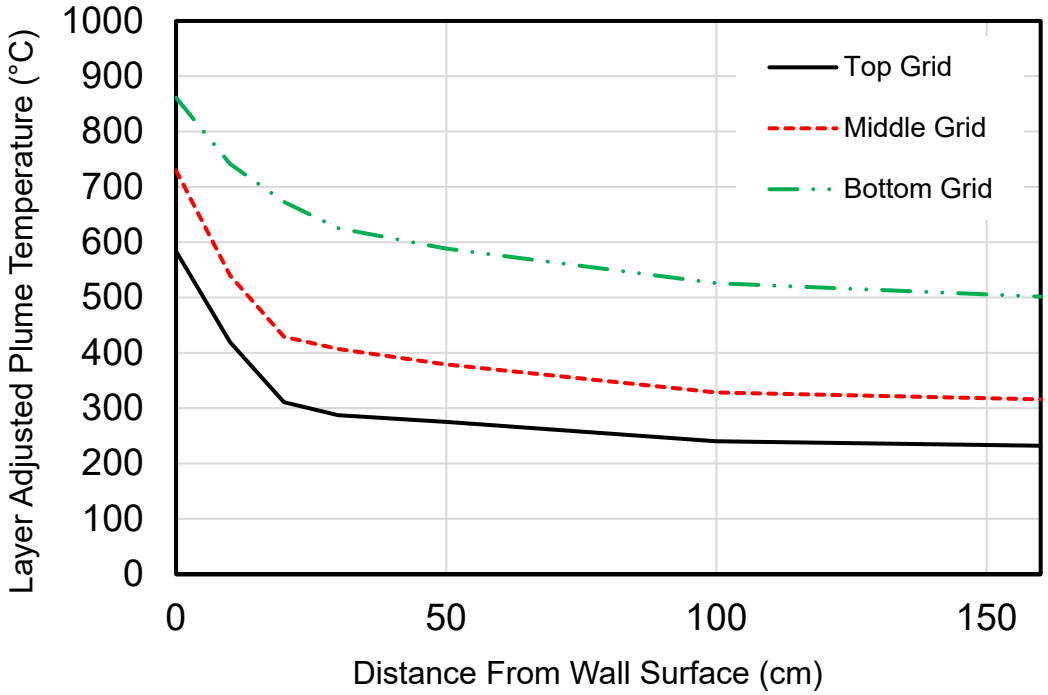

Figure 6-2
Plume temperatures, corner, 400 kW

The model bias and uncertainty statistics for the plume temperature rise are calculated using the Heskestad fire plume correlation and shown in Table 6-2. The results in Table 6-2 compare the different bias using both the traditional fire location factor and the modified fire location factor as developed in *Fire Modeling Enhancements for Fire Probabilistic Risk Assessment* [9]. The statistics provided were determined following the methods outlined in the *FDS Technical Reference Guide* [21].

Table 6-2
Bias and uncertainty of modified and unmodified Heskestad fire plume correlation for wall and corner configurations

Configuration, Location Factor Method	Bias	Model Uncertainty	Experimental Uncertainty [23]
Wall, traditional method (k_F = 2)	1.66	0.06	0.07
Wall, modified (k_F = 1)	1.10	0.13	0.07
Corner, traditional method (k_F = 4)	1.94	0.38	0.07
Corner, modified (k_F = 4,2,1)	1.27	0.15	0.07

In each case, a bias to constantly overpredict is made clear by comparing the plotted results to the perfect match line (see Figure 6-3 and Figure 6-4). This line signifies where the temperatures measured during the experiments and those predicted by the correlations were equal. Any values above this line represent an overprediction by the correlation and is conservative when applied to an analysis. A clear reduction in bias is shown when the modified Heskestad fire plume correlation is used.

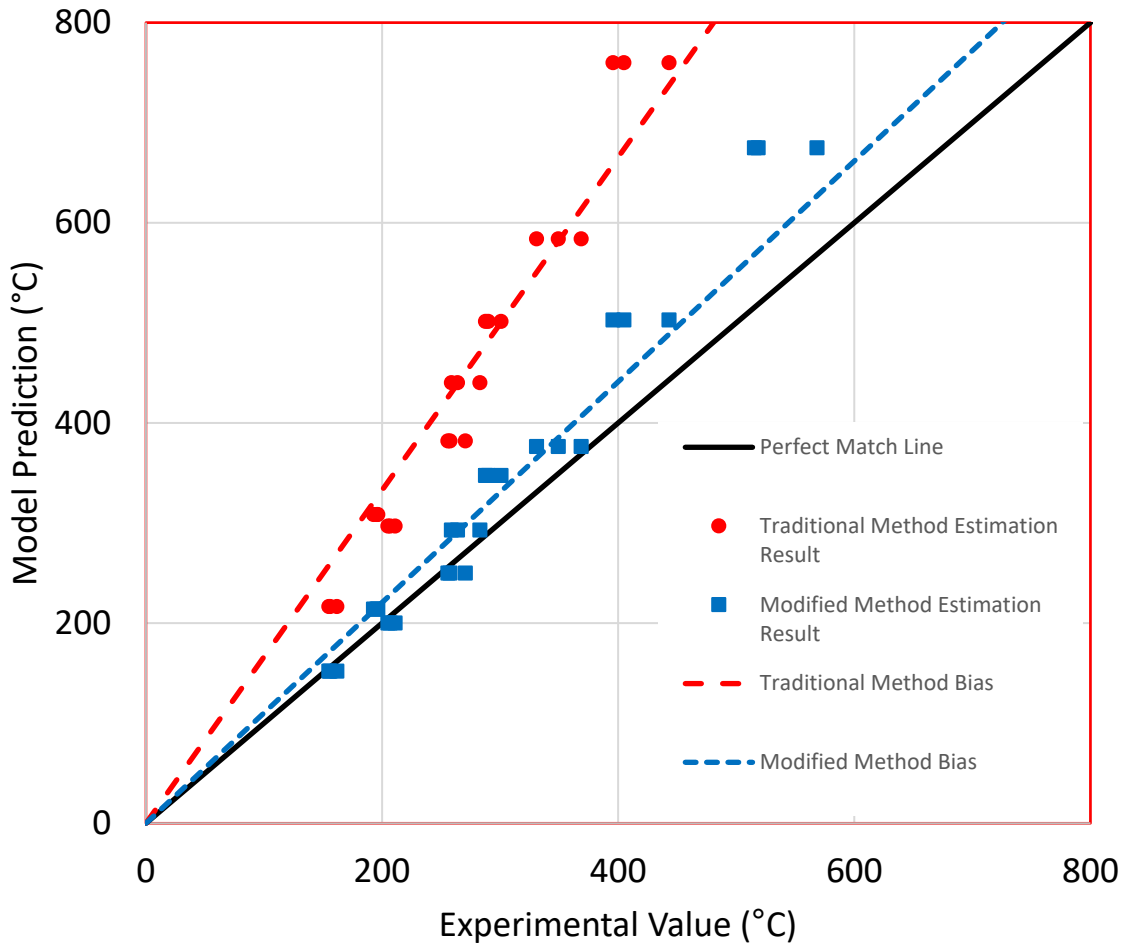

Figure 6-3
Comparison of Heskestad and modified Heskestad fire plume correlation predictions to experimental results for fires next to a single wall surface

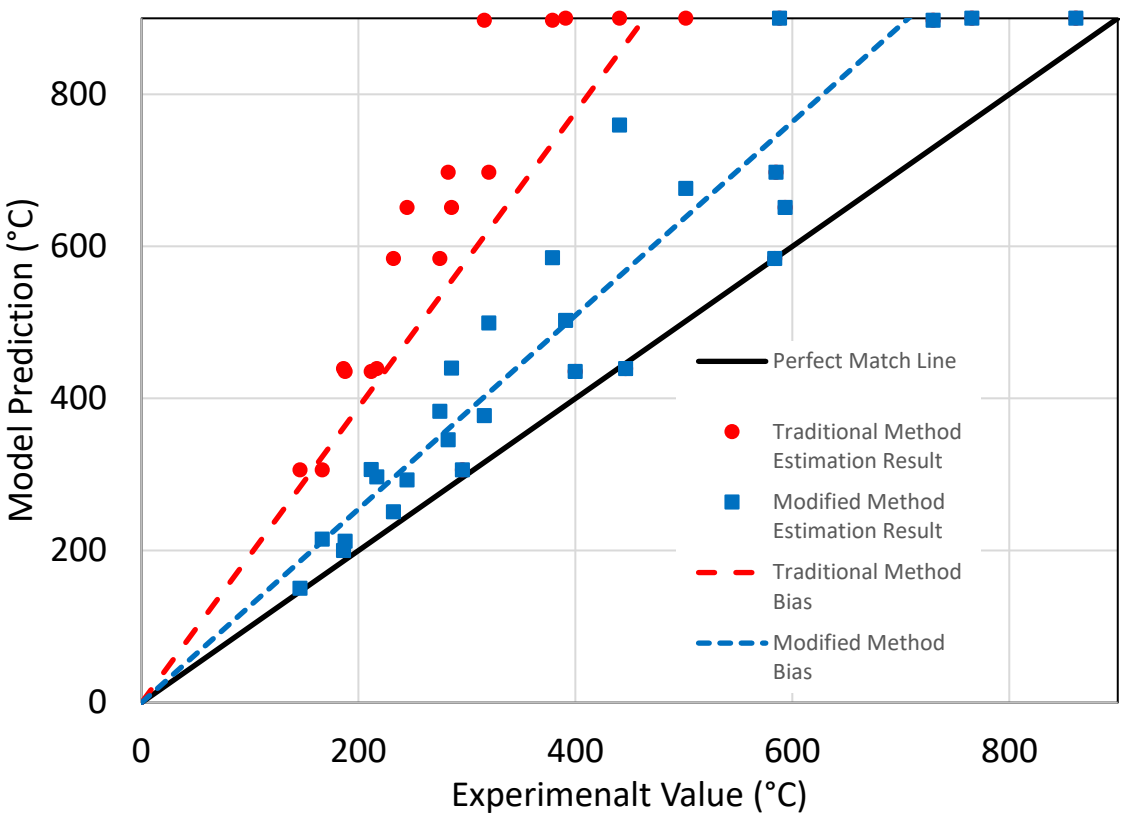

Figure 6-4
Comparison of Heskestad and modified Heskestad fire plume correlation predictions to experimental results for fires in a corner

6.4 Summary

The guidance presented in this section addresses two specific areas relative to the use of fire location factors with fire plume temperature analysis of ZOI applications in nuclear power plants (NPPs). These two areas are identified as when to use the fire location factor and what value of the location factor to use.

Results from FDS Version 6.0.1 simulations were used in a modified version of the Heskestad fire plume correlation to estimate values of the fire location factor, k_F, for fires located in wall and corner configurations. Several different parameters, including HRR, distance from the wall surfaces, fire source diameter, and the elevation above the fire source, were varied to determine their influence on the estimation of k_F. Using these estimated values of k_F, recommendations for the implementation of the fire location factor based on varying distances from wall surfaces were developed.

Although other researchers have reported that the mirror method is not always conservative, this investigation used simulations, supported by experimental results, to show that the implementation is, on average, conservative. For practical application in the commercial nuclear industry, the higher values of location factors observed are associated with low fire plume temperatures that are well below the damage threshold for cables. Therefore, the recommended guidance is appropriate for representing the hazards to cables due to fire plume temperatures.

Evidence suggests that for fires located adjacent to corners, the current guidance to use a k_F of 4 may be overestimated. At distances greater than 0.3 m (1 ft), the current guidance for a k_F of 4 is overly conservative and may be reduced for fires with greater than a 0.3 m (1 ft) separation from the corner. For fires located along a single wall surface, the current guidance to use a k_F of 2 has been shown to be more conservative than necessary, and a value of 1 is appropriate for all wall configurations, particularly when the plume temperature is greater than the cable damage threshold.

7
MAIN CONTROL BOARD FIRE SCENARIOS

This section documents guidance on evaluating the risk associated with main control board (MCB) fires. The guidance in this section provides an alternative to the method described in Appendix L of NUREG/CR-6850 [1] for evaluating the risk of fire events originating in the MCB. In this approach, MCB fire scenarios are modeled as a progression of damage states using an event tree model. In this formulation, each damage state requires the definition of a target set, which consists of one or more MCB functions that can be damaged by fire. The functions within the scope of this analysis are those that are represented with basic events in the plant response model and supported with cables routed within the MCB.

The model described in this section explicitly incorporates two characteristics of MCB fires observed in operating experience—relatively small fires in low-voltage panels and the ability for prompt detection and suppression by control room operators. Operating experience suggests that the majority of fires in the MCB are limited to a single subcomponent or group of subcomponents near the point of ignition. In addition, these fires are promptly detected and suppressed by control room operators. Therefore, the event tree model explicitly accounts for the operator's ability to quickly detect and suppress the fire before growth and/or propagation. In the context of this section, the term *subcomponent* refers to items such as switches, relays, resistors, and termination points that are part of the MCB. The remainder of the event tree covers the cases involving larger fires up to and including main control room (MCR) abandonment.

7.1 Introduction

The MCB consists of well-defined subdivisions typically referred to as *panels*. That is, each MCB has a set of panels lined up along the length of the board, each panel housing the controls of one or more plant systems. The type of separation between panels varies among plants. In some cases, panels are physically separated by metal barriers or partitions. In other cases, the panels may be open to each other.

As an ignition source modeled in a fire probabilistic risk assessment (FPRA), the MCB requires specific guidance for quantifying fire risk due to its unique characteristics, including the following:

- The MCB in the MCR is continuously occupied by personnel with a high degree of training and awareness.
- It is a relatively large set of cabinets with unique construction configurations and cable separation schemes relative to typical electrical cabinets located in other plant areas.
- It houses most of the plant control circuits within the scope of a FPRA.
- Fires in the MCB may generate the need for alternative or remote shutdown strategies (that is, shutdown outside of the MCR).

Given these characteristics, a fire postulated within the MCB may simultaneously impact multiple trains or multiple systems credited in the FPRA. In practice however, it is difficult to explicitly model fire growth inside the MCB. This generates the need for a comprehensive methodology for quantifying the scenario progression (that is, fire growth progression) of a fire starting in a subcomponent within the MCB that captures the operating experience as documented in fire event and the empirical evidence observed in fire testing of electrical cabinets.

Existing guidance for modeling MCB fires is available in Appendix L of NUREG/CR-6850. The guidance describes the process for estimating the conditional probability of damage to a set of internal targets in the MCB. This process relies on a model that calculates the probability of a fire starting at any point within the MCB and damaging a predefined set of targets. The resulting conditional probability is multiplied by the generic frequency for the MCB to obtain a fire scenario frequency. This model in Appendix L has the following three limitations:

- It is based on input values that, although conservative, have been superseded by guidance from NUREG-2169, NUREG-2178, or NUREG-2230. These inputs include the probability distribution for peak HRR and the manual suppression rate calculation.
- There is no comprehensive guidance on how to postulate scenarios in the MCB to capture the scenario progression as they have been observed in the operating experience. The guidance in NUREG/CR-6850 is focused on characterizing the likelihood of a damage profile and is not based on an event tree which can distinguish between the different progressions of expected fire scenarios. To overcome this limitation, analysts have postulated fire scenarios of different sizes and different target sets to ensure that the risk associated with MCB fires is reasonably accounted for in the FPRA.
- There is no guidance for determining how many individual scenarios should be postulated in order to ensure that the MCB risk is fully represented and to ensure that the MCB fire frequency is preserved without double-counting overlapping fire damage states.

7.2 Methodology Overview

The methodology is based on the following elements, which are described in detail in the following sections.

1. Review of the MCB operating experience to evaluate which fires produce damage to only the subcomponent of origin within a panel (see Section 7.4.1)
2. Characterization of an event tree that captures the scenario progression of fire growth in the MCB (see Figure 7-1). This characterization includes a description of the following:
    a. Apportioning the generic frequency of the MCB to the different MCB panels based on the size and construction of the MCB
    b. Characterization of fires with the potential of growing outside the ignited subcomponent and generating damage to nearby MCB subcomponents or cables
    c. Characterization of fires with the potential of spreading to one full MCB panel or multiple MCB panels

It is noted also that fires in the MCB have the potential of generating either loss of control or loss of habitability events. Either case may generate the need for shutdown outside of the MCR. These plant conditions are also included in the methodology as a potential outcome for a MCB fire.

7.2.1 Step 1: Calculate a Screening CDF for Individual MCB Panel Sections

The first step in the methodology consists of calculating the screening core damage frequency (CDF) of each panel within the MCB. The purpose of this step is to identify which panels will require detailed damage states—that is, those panels with relatively low risk contribution (that is, low CDF) may not need to be modeled with detailed damage states. The process for calculating a screening CDF for each panel includes the following:

1. Identification of each panel section within the MCB. This step may have already been completed as part of the ignition frequency task.
2. Identification of the FPRA cables associated with each panel (that is, cables starting, traveling through, or ending in each panel). This step may have already been completed as part of the cable selection, circuit analysis, and cable routing tasks.
3. Calculation of fire ignition frequencies for each panel within the MCB. The ignition frequency for this screening process is a multiplication of the following:
    a. The generic MCB frequency (Bin 4).
    b. The ignition source weighting factor to apportion the generic frequency to the individual panel (guidance for the calculation of weighting factors is provided in Section 7.3.2).
    c. The constant value of 1-0.78 = 0.22, which is the fraction of events derived from the review of operational experience in the Electric Power Research Institute (EPRI) fire events database (FEDB) representing fires that propagate outside the subcomponent (point of ignition). This value is described in detail later in Section 7.4.1.
4. Quantification of three conditional core damage probability (CCDP) values associated with each panel within the MCB, as follows:
    a. One CCDP assuming failure of all basic events mapped to the cables associated with each panel. This value will be associated with 22% of the panel fire frequency.
    b. One CCDP assuming failure of the single worst-case basic event associated with each panel. This value will be associated with 78% of the panel fire frequency.
    c. The screening analysis should also include the potential for a fire in a low risk panel to spread to an adjacent panel (which may have a higher CCDP) by quantifying a CCDP that includes the failure of the functions of the adjacent panel.

After the ignition frequencies and CCDPs per panel are calculated, the panels can be ranked by the screening CDF to determine those that are potentially risk-significant contributors and may require detailed fire modeling. This report does not propose specific screening values, and the analyst should follow existing guidance in selecting an appropriate screening value.

7.2.2 Step 2: Detailed Fire Scenario Analysis

Detailed modeling of the MCB requires a comprehensive characterization of the sequence of fire-induced events over time. The sequence of events is captured in an event tree model that starts with ignition, continues with localized fire damage within the MCB section (the term *MCB* section refers to a subdivision of the MCB and is described in Section 7.3.2) and propagation through MCB panels, and ends with the potential for MCR abandonment. The event tree structure is depicted in Figure 7-1. It captures the following chronology:

Event 1 (ignition event), MCB fire frequency. This is characterized as the generic MCB frequency apportioned to the specific panel.

Event 2, single subcomponent failure with no meaningful HRR. This event captures the fraction of small localized fires that damage the ignition source only. In this context, the ignition source refers to a subcomponent within a MCB panel such as a switch or a termination point. The top branch of this split represents the scenario where the fire is limited to the ignition source (that is, the subcomponent of fire origin). The bottom branch of the split represents the scenario where the fire propagates beyond the subcomponent of fire origin. The quantification of this split fraction is a constant and based upon the operating experience data.

Event 3, fire, is limited to a small group of subcomponents. This event captures the fraction of fires propagating beyond but near the ignition source (that is, in the immediate vicinity of the subcomponent where the fire starts). This event captures the progression of fire growth from damaged subcomponents that are located near the ignition source to the remainder of the panel. The top branch of this split represents the scenario where fire damage due to successful manual suppression is limited to a very localized set of subcomponents or cables near the ignition source. The bottom branch of the split represents the scenario where the fire continues to propagate from the small group of subcomponents to the rest of the panel due to unsuccessful manual suppression. The quantification of this split fraction is based upon the non-suppression probability (NSP) for the specific time in the scenario.

Event 4, fire effects limited to one panel? This branch point characterizes sequences that are associated with fires that do not propagate outside the panel of origin versus those propagating to an adjacent panel. The top branch represents the scenario where damage and ignition are limited to the panel of fire origin. The bottom branch of the split represents the scenario where the fire propagates to an adjacent panel within the MCB. The evaluation is solely a fire model evaluation and does not include the manual NSP in its quantification.

Event 5, does suppression occur before fire spread? This event captures the potential for fire suppression before a fire can spread from a single panel to an adjacent panel within the MCB. For the fires limited to the MCB panel of origin, it is assumed the content of that panel is failed by the fire. For the fires with the potential of spreading to an adjacent panel, the content of the second panel is also failed by the fire. This quantification is a probability of non-suppression.

Event 6, abandonment due to loss of habitability. This event characterizes those sequences in which the fire generates conditions that force abandonment due to habitability (that is, the heat or smoke generated by the fire prevents operators from staying inside the MCR). The top branch in the split represents scenarios where fire conditions will not force MCR abandonment due to loss of habitability. The bottom branch in the split represents scenarios where operators will abandon the MCR at some point during the fire event. This quantification is a probability of non-suppression.

Event 7, abandonment due to loss of control. This captures MCR abandonment due to loss of control for the fraction of the frequency where there is no forced abandonment due to loss of habitability. In cases where operators are able to stay in the MCR (that is, no loss of habitability), there is the potential for reliance on shutdown procedures outside the MCR depending on the plant controls affected by the fire (termed *loss of control*). The top branch in the split represents scenarios where fire conditions will not force MCR abandonment due to loss of control and operators can stay in the MCR. The bottom branch in the split represents scenarios where operators will abandon the MCR due to loss of control. This quantification is a probability of non-suppression.

The event tree headings described previously, as modeled in the event tree depicted in Figure 7-1, produce the following sequences:

- Branch A: fire in a single subcomponent
- Branch B: fire limited to a localized group of subcomponents (CCDP or conditional large early release probability [CLERP] of a group of subcomponents located on the same panel)
- Branch C: fire contained to a single MCB panel due to successful suppression—MCR remains habitable, no loss of control/loss of habitability (CCDP or CLERP of a single MCB panel)
- Branch D: fire in a single MCB panel that results in abandonment due to loss of control (CCDP or CLERP of a single MCB panel with loss of control abandonment actions)
- Branch E: fire contained to a single MCB panel that is not suppressed in time and results in loss of habitability (CCDP or CLERP of a single MCB panel with loss of habitability abandonment actions)
- Branch F: fire contained to a single MCB panel due to successful suppression (CCDP or CLERP of a single MCB panel, equivalent to Branch C)
- Branch G: fire in a single MCB panel with abandonment on loss of control (CCDP or CLERP of a single MCB panel with loss of control, equivalent to Branch D)
- Branch H: unsuppressed fire in single MCB panel resulting in loss of habitability (CCDP or CLERP of a single MCB panel with abandonment on loss of habitability, equivalent to Branch E)
- Branch I: fire in two adjacent MCB panels with fire suppressed (resulting in no loss of habitability or loss of control) (CCDP or CLERP of the two MCB panels)
- Branch J: fire in two adjacent MCB panels resulting in abandonment due to loss of control (CCDP or CLERP of the two MCB panels with loss of control)
- Branch K: fire in two adjacent MCB panels with fire not suppressed resulting in loss of habitability (CCDP or CLERP of the two MCB panels with abandonment on loss of habitability

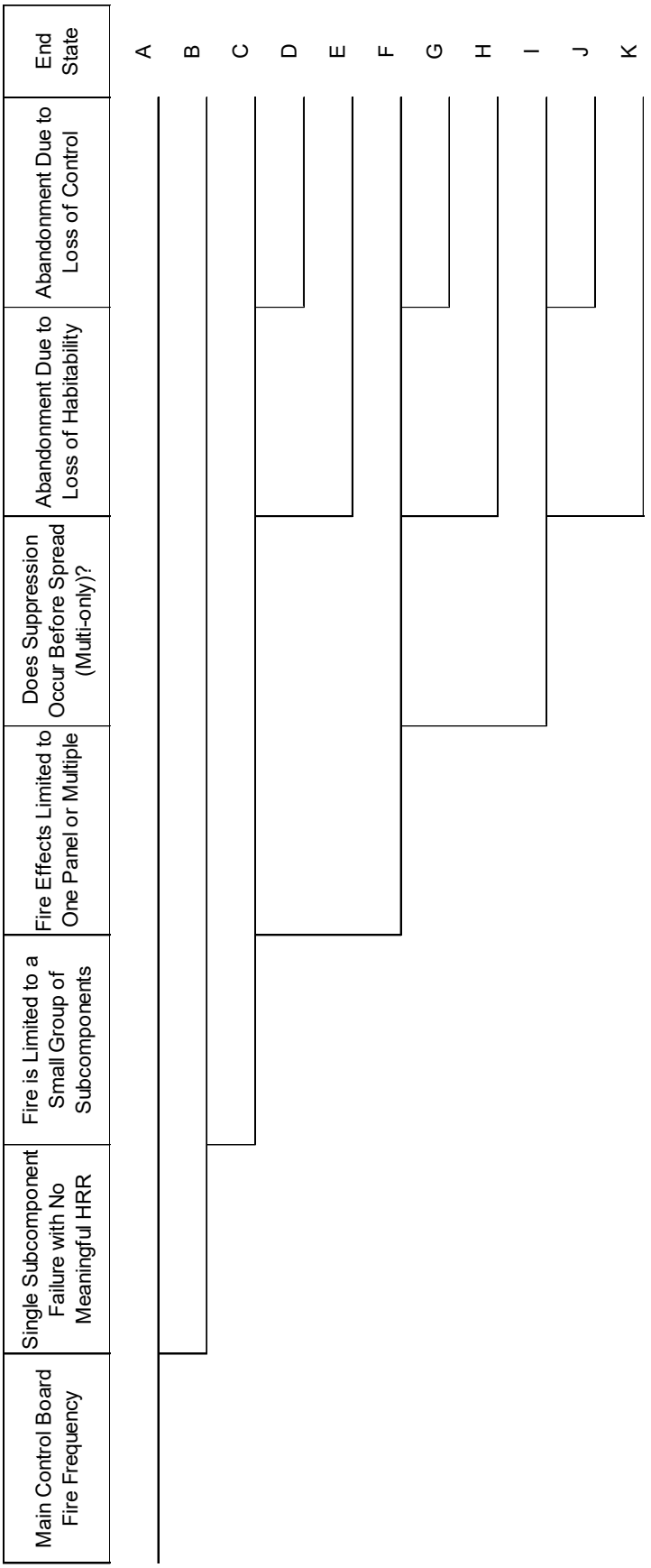

Figure 7-1
MCB fire event tree

7.3 Main Control Board Fire Frequency and Non-Suppression Probability

The MCB is treated as a unique ignition source and has its own generic ignition frequency (with applicable location weighting factor for dual-unit control rooms defined in NUREG/CR-6850). In contrast with the guidance provided in NUREG/CR-6850, this methodology requires that the generic frequency be apportioned to the different panels or sections within the MCB. These panels are often treated as endpoints (or terminations) for cable routing purposes and have been used for defining fire scenarios associated with the MCB as the cables within the scope of the FPRA that start or end in each panel provide a distinct list of failure modes (that is, basic events representing the functions that are mapped to the cables) affecting the systems associated with each panel. Care must also be taken to ensure that cables that pass through, but do not terminate in, a panel are also included.

NUREG/CR-6850 Appendix L, supplemented by FAQs 06-0018 [34] and 14-008 [47], defines the MCB (Bin 4) as follows:

- The *MCB* is defined as the collection of control panels inside the MCR of a nuclear power plant (NPP) from which operators control the plant on a day-to-day basis. This is typically referred to as the main *horseshoe* given the U shape of the MCB.
  - The MCB typically includes the front face of the horseshoe (a common configuration in most plants), other control or instrumentation display panels that are typically placed in full view of the areas where control room operators are expected to spend most of their time, and other panels in the control room proper that contain control switches or instrumentation displays that are used for plant control or emergency shutdown.
  - The MCB includes the back panel of the main board if the rear and front side are connected together as a single enclosure. This essentially creates an MCB with a continuous overhead or by an overhead with penetrations or vents along it longitudinally. That is, the presence of a MCB cabinet ceiling would connote a single cabinet. Also, cables may connect the front and back sides of the MCB. If the MCB meets this description, the rear side of the MCB is classified as an integral part of the MCB.
- The MCB also may include bench-board panels that were detached from, but directly in front of, the main horseshoe (at some plants such panels are referred to as *consoles*). These bench-board-type cabinets, usually one or two per control room, may be counted as part of the MCB. These panels serve as an integral part of the main plant monitoring and control functions, are located in the center of the operators' main work area, and are manned on a nearly continuous basis.

The MCB does not include other panels that would be counted as Bin 15 ignition sources, such as the following:

- Smaller detached panels housing such equipment as computers and the event recording equipment and printers. These panels typically are in full view of the operators (generally behind or to the side of their main work area).
- Back panels if the rear side of the MCB is separated from the front side by partitions or cabinet walls.
- Those electrical panels devoted primarily to housing control relays, printed cards (such as signal conditioning cards), or all other devices that the operators do not directly use to maintain plant control or safe shutdown if those electrical panels are separated from the main control switch and indicator panels.
- Other detached panels housing items such as balance-of-plant and off-site power controls and indicators.

This definition continues to be applicable to MCBs due to the correlation with the data used to determine the fire ignition frequency. However, NUREG/CR-6850 Appendix L proceeds directly from this level of MCB frequency characterization to individual scenarios involving groupings of controls on the panel faces. In order to develop scenarios that do not rely on the methodology described in Appendix L of NUREG/CR-6850, a process is needed to apportion the MCB frequency to the different sections or panels.

7.3.1 Generic Fire Ignition Frequency

The generic fire ignition frequency of the MCB (that is, Bin 4) is updated from NUREG-2169 [36] to correct a misclassified event, add additional operating experience, and split the frequencies based on power mode. The fire ignition frequency for Bin 4 in NUREG-2169 was presented for all modes (AA), meaning that it was applicable for full-power initiating events (FPIE) and low power shut down (LPSD) plant states. The updated frequencies in Table 7-3 are split between the time spent in FPIE and LPSD conditions. Maintenance activities during LPSD conditions may introduce a higher frequency of fires relative to FPIE (which may have procedural limits on the maintenance activities). This research makes use of the latest fire event data that were classified for fire severity (up through 2014) [48]. The fire event counts for Bin 4 are listed in Table 7-1.

Table 7-1
FPRA counts per time period

Bin	Location	Ignition Source	Power Modes	FPRA Counts			
				1968–1989	**1990–1999**	**2000–2009**	**2010–2014**
4	Control room	Main control board	FPIE	2	2	2	0
4	Control room	Main control board	LPSD	0.5	0	1	0.5

The time period 2000–2009 includes the 84 plants that completed the full data collection protocol and plant review for the EPRI FEDB update. This is consistent with fire frequency calculations in NUREG-2169. Fire event data for events occurring in 2010 or later are collected and managed through the Institute of Nuclear Power Operations. This process is industrywide and, as a result, all operating U.S. NPPs were included in the 2010–2014 time period. The reactor years for at-power and shutdown are presented in Table 7-2.

Table 7-2
Reactor years for fire ignition frequency update

	FPRA Time Period		
	1990–1999	**2000–2009**	**2010–2014**
At-power reactor years	848	771	467.7
Shutdown reactor years	233	78.5	45.7

The updated fire ignition frequency distribution for Bin 4 is presented in Table 7-3.

Table 7-3
Fire ignition frequency distributions for Bin 4

Bin	Location	Ignition Source	Power Modes	PRA Type	Time Period	Mean	Median	5th percent	95th percent
4	Control room	Main control board	AP	FPIE	1990-2014	2.05E-03	2.61E-04	4.27E-07	7.19E-03
4	Control room	Main control board	AL	LPSD	1990-2014	4.36E-03	9.61E-04	2.33E-06	1.36E-02

AP = all plants, at power
AL = all plants, low power shutdown

7.3.2 Apportionment of the Generic MCB Frequency

MCBs tend to be large benchboard-style cabinets with individual sections. In addition, MCBs can vary significantly from NPP to NPP. In some NPPs, the MCB may resemble electrical cabinets typically found throughout the plant, whereas in other cases the MCB may be a large walkthrough configuration. The bench section is mostly used for controls. The lower portion of the vertical section above the bench typically contains a combination of controls and indication whereas the upper vertical sections usually contain annunciators or other status displays.

Because most plants have existing defined sections for the MCB, these sections can be used as the starting point for panel counting. Furthermore, many plants have performed fire modeling based on these MCB sections to support risk quantification. This is because the cable routing databases also use the defined MCB sections for mapping termination cable endpoints. There is a general assumption that the defined sections are separated by some physical configuration (for example, partitions, structural elements, or even spatial separation) that will inhibit propagation or at a minimum provide the analyst with a practical basis (for example, existing cable routing by section) for modeling the panel sections.

Because there is a wide variety of MCB section geometries and configurations, the generic ignition frequency (that is, Bin 4) should be apportioned considering the section size and the total linear distance across the surfaces in which devices have been mounted (that is, section width) and, if applicable, the location weighting factor for dual-unit MCRs. For MCBs that include back panels, the linear distance measurement will include the front faces of the rear sections consistent with the guidance in FAQ 14-0008 [47]. Specifically, the following steps are recommended:

1. Identify and appropriately label each MCB section. Recall that in practice, it is useful to maintain the MCB sections identified as cable endpoints in the cable and raceway database to simplify the process of assigning targets to the scenarios.
2. Measure the length of each section along its longest horizontal distance. If the section has controls on both sides (that is, back panels), the horizontal distance of both sides should be included in the measurement. In the case of a walk-through MCB configuration where the back panels are included as a part of the MCB, it is recommended that the front and back panels be treated as separate sections with frequency assigned to each according to its width and provided that the cable routing information supports this distinction.
3. Measure the length of the full MCB. It is noted that the sum of the lengths of the individual sections should add to the full length of the MCB so that the full generic frequency is apportioned.
4. Calculate the ratio between each MCB section and the full length of the MCB. This ratio is the apportioning factor for the corresponding MCB section.

7.3.2.1 Frequency Apportionment Example 1

As an example, consider Figure 7-2 and Figure 7-3, which depict a MCB from a single-unit plant. The MCB was designed with the following sections/panels:

- Primary plant control: Panel A
- Reactor control: Panel B
- Secondary plant control Section I: Panel C
- Secondary plant control Section II: Panel D
- Turbine supervisory panel

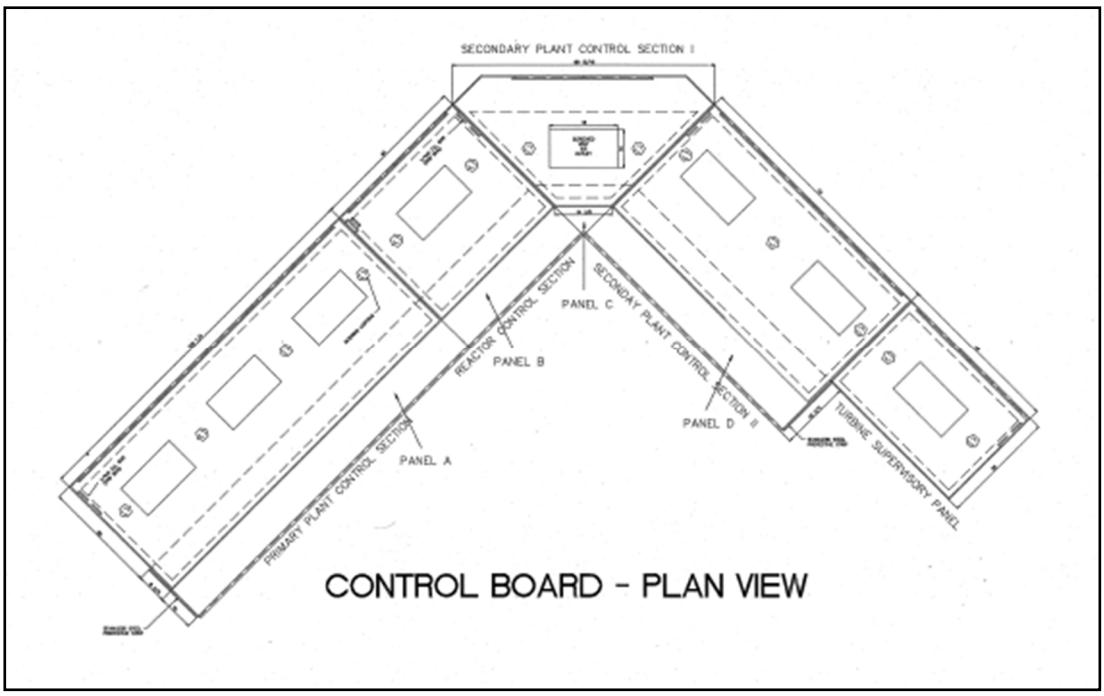

Figure 7-2
Example 1: MCB plan view

Figure 7-3
Example 1: MCB

The total linear distance across the front face of the MCB is depicted by the red line in Figure 7-4, equivalent to 7.3 m (24 ft). The generic Bin 4 frequency is 2.05E-03/year, which is apportioned per linear meter to the five MCB panels using 2.80E-4/year per m (8.54E-05/year per ft). The resulting total linear distance is illustrated in Table 7-4.

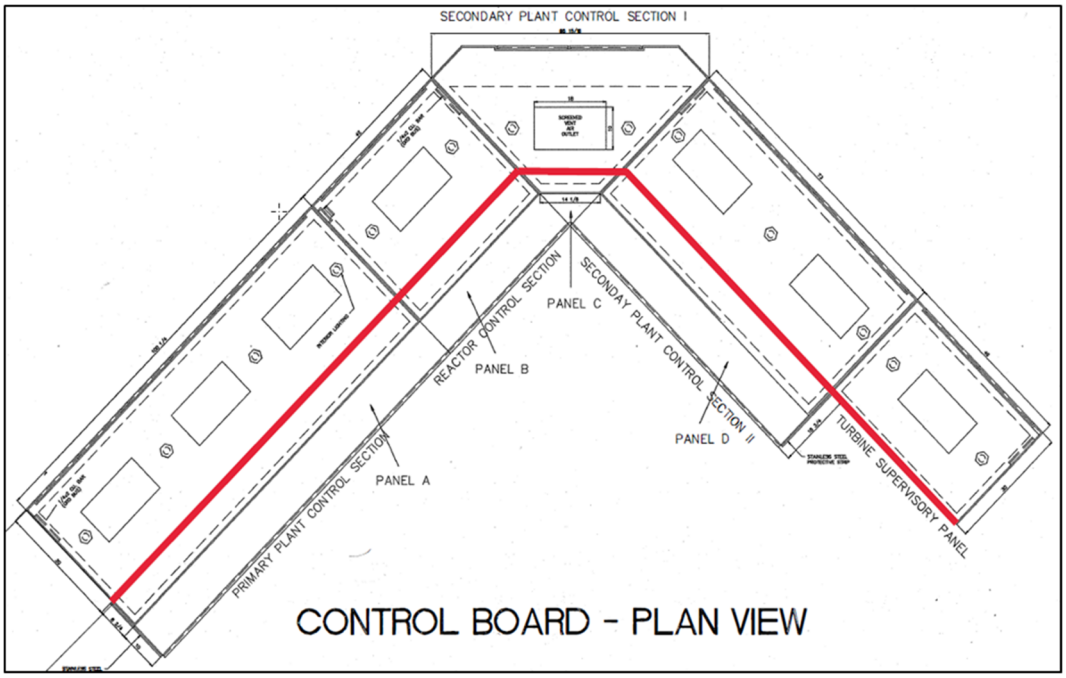

Figure 7-4
Example 1: MCB–apportioning counting approach

Based on the apportioning guidance, the per-panel frequencies are listed in Table 7-4.

Table 7-4
Example 1: frequencies per MCB panel

Section ID	Length (m)	Length (ft)	Frequency (1/year)
Primary plant control, Panel A	2.56	8.4	7.17E-04
Reactor control, Panel B	1.07	3.5	2.99E-04
Secondary plant control Section I	0.70	2.3	1.96E-04
Secondary plant control Section II	1.83	6.0	5.12E-04
Turbine supervisory panel	1.16	3.8	3.25E-04
Total	**7.32**	**24.0**	**2.05E-03**

7.3.2.2 Frequency Apportionment Example 2

Consider the walkthrough style MCB illustrated in Figure 7-5 through Figure 7-7. This configuration includes the back panels of the MCB because the rear and front sides are connected as a single enclosure. The configuration also includes an overhead section with penetrations and vents along its length. There are also cables connecting the front and back sides of the MCB enclosure.

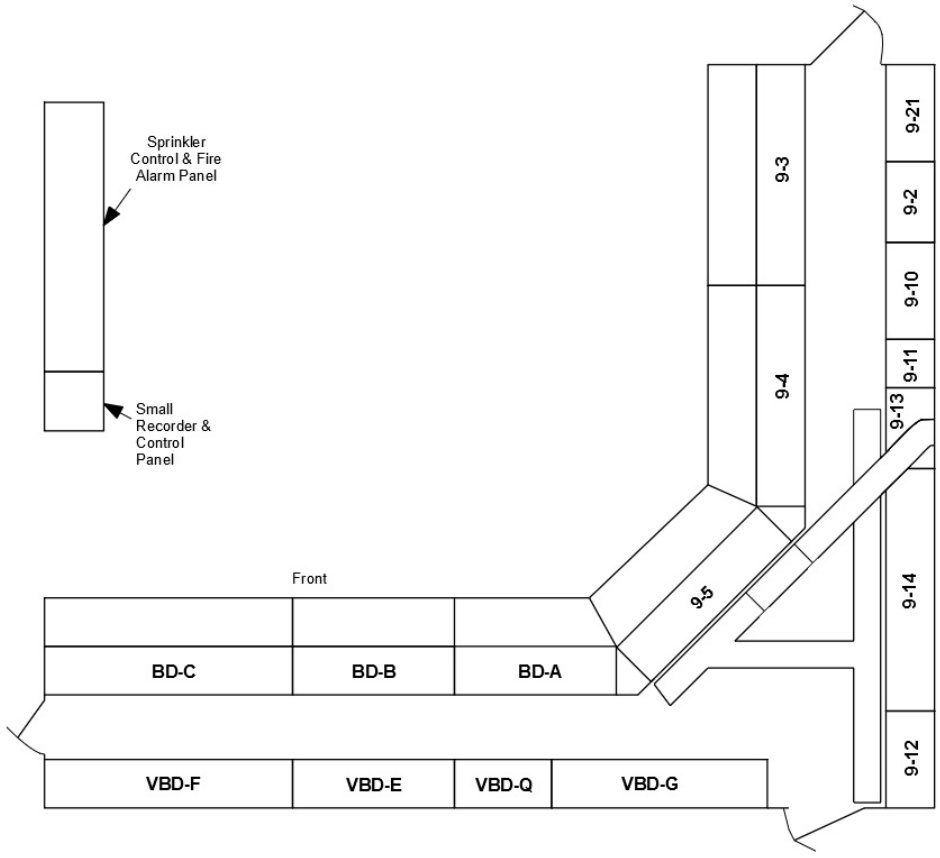

Figure 7-5
Example 2: MCB

Figure 7-6
Example 2: MCB Section 9-4, 9-5, and BD-A

Figure 7-7
Example 2: MCB Sections 9-3 and 9-4

The total linear distance across the front faces of the MCB is depicted by the red lines in Figure 7-8 and results in 74.4 m (244 ft). The generic Bin 4 frequency of 2.05E-3/year is then apportioned per linear meter to the 17 MCB panels using 2.76E-5/year per m (8.40E-6/year per ft). The frequencies per MCB panel are calculated in Table 7-5.

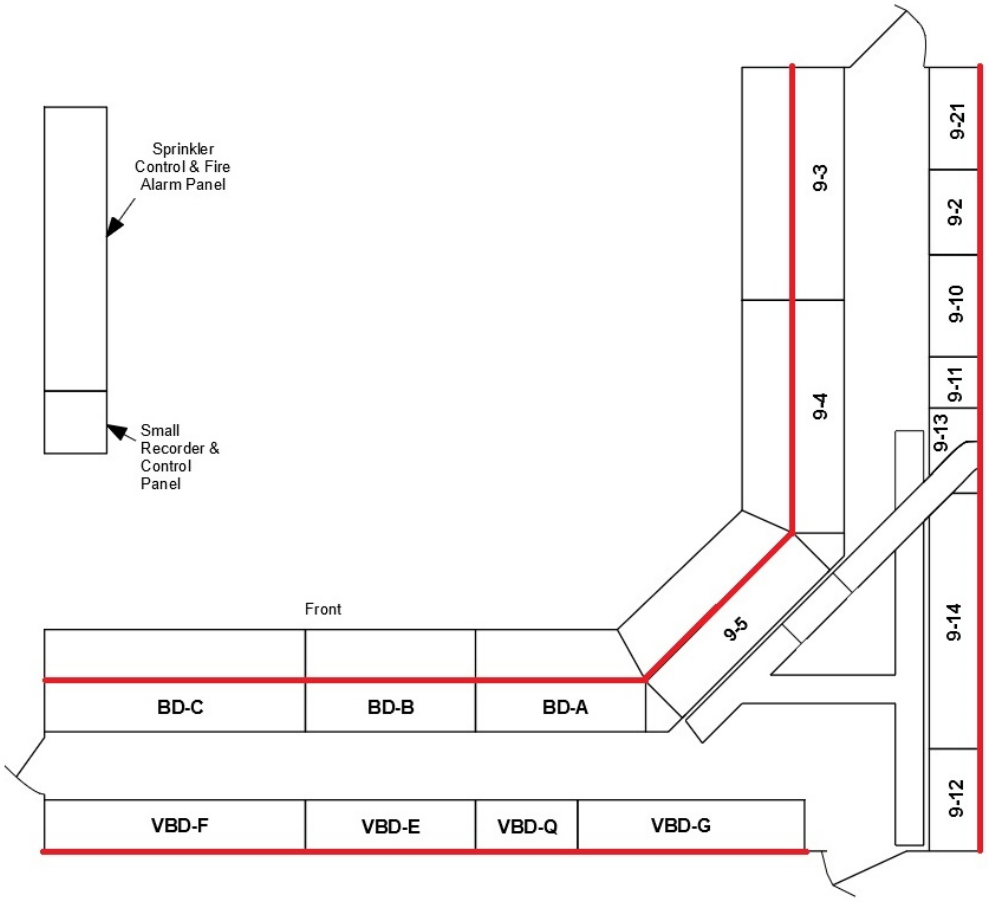

Figure 7-8
Example 2: MCB—apportioning counting approach

Table 7-5
Example 2: frequencies per MCB panel

Section ID	Length (m)	Length (ft)	Frequency (1/year)
BD-C	6	19.6	1.65E-04
BD-B	4.5	14.9	1.25E-04
BD-A	4.2	13.7	1.15E-04
9-5	6.3	20.8	1.75E-04
9-4	6.8	22.2	1.86E-04
9-3	6.2	20.2	1.70E-04
VBD-F	6.2	20.4	1.71E-04
VBD-E	4.2	13.9	1.17E-04
VBD-Q	2.6	8.4	7.06E-05
VBD-G	5.7	18.8	1.58E-04
19-12	3.7	12.1	1.02E-04
9-14	6.2	20.4	1.71E-04
9-13	2.1	6.8	5.71E-05
9-11	1.3	4.2	3.53E-05
9-10	3.2	10.4	8.74E-05
9-2	2.3	7.7	6.47E-05
9-21	2.9	9.5	7.98E-05
Total	**74.4**	**244**	**2.05E-03**

7.3.3 NSP Curve

The NSP curves are governed by a suppression rate constant developed using operational experience (that is, fire event data in EPRI's FEDB). In the case of MCB fires, the control room NSP curve is used for determining the probabilities of fire progression through damage states. Therefore, a review of the fire events was necessary to characterize suppression attempts within the framework of the event tree model.

Selected fire events were removed from the population of events used for determining the updated suppression rate constant because the fire was limited to the subcomponent of fire origin. *Fire limited to the subcomponent of origin* is an explicit sequence in the event tree model and is characterized by a probability generated using the fire event data. As a consequence, fire events where damage was limited to the subcomponent of fire origin for any reason (including active intervention by operators) are removed from the population of events used for determining the updated suppression rate constant. That is, consistent with the event tree model, the updated suppression rate constant is used for determining non-suppression probabilities for the fraction of fires that propagated outside the subcomponent of fire origin. It is noted that the updated suppression rate constant described in this section includes all fires that

occur within the MCR envelope (the current data set includes MCB, transients, and electrical cabinet fires in the control room) excluding only those fires within the MCB that were limited to the subcomponent of fire origin. Therefore, it can be used to model fire scenarios associated with fires outside the MCB because it applies to all ignition sources inside an MCR. At the same time, it should not be used for updating values generated using the MCB model documented in Appendix L of NUREG/CR-6850 due to the removal of the events where the fire damage was limited to the subcomponent of fire origin.

As a result of the preceding discussion, the suppression rate associated with the control room was updated. Just as in NUREG/CR-6850 Supplement 1 and NUREG-2169, the *suppression time* is defined as the time at which the fire was extinguished or the time at which the fire was reported to be under control by responding plant personnel, personnel discovering the fire, or the fire brigade at the scene. The event set from 1981 to 2014 was used to determine the rates for the development of the manual suppression rate. A summary of the counts, times and suppression rates is provided in Table 7-6 and shown graphically in Figure 7-9. The details of the suppression binning are provided in Table 7-8.

Table 7-6
Control room probability distribution for rate of fires suppressed per unit time

Suppression Curve	Number of Events	Total Duration (min)	Rate of Fire Suppressed (λ)			
			Mean	**5th Percent**	**50th Percent**	**95th Percent**
Control Room	10	26	0.385	0.209	0.372	0.604

Similar to NUREG-2169, the 5th, 50th, and 95th percentiles for the suppression rate, λ, presented in Figure 7-9 are calculated in using the Chi-square distribution as:

$$\boldsymbol{P(x,v)/t_D/2} \qquad \textbf{(7-1)}$$

where $P(x,v)$ is the lower cumulative distribution function of the Chi-square distribution, x is the desired percentile, v is the number of degrees of freedom (equal to the number of events used in the suppression curve), and t_D is the total suppression duration for the suppression curve.

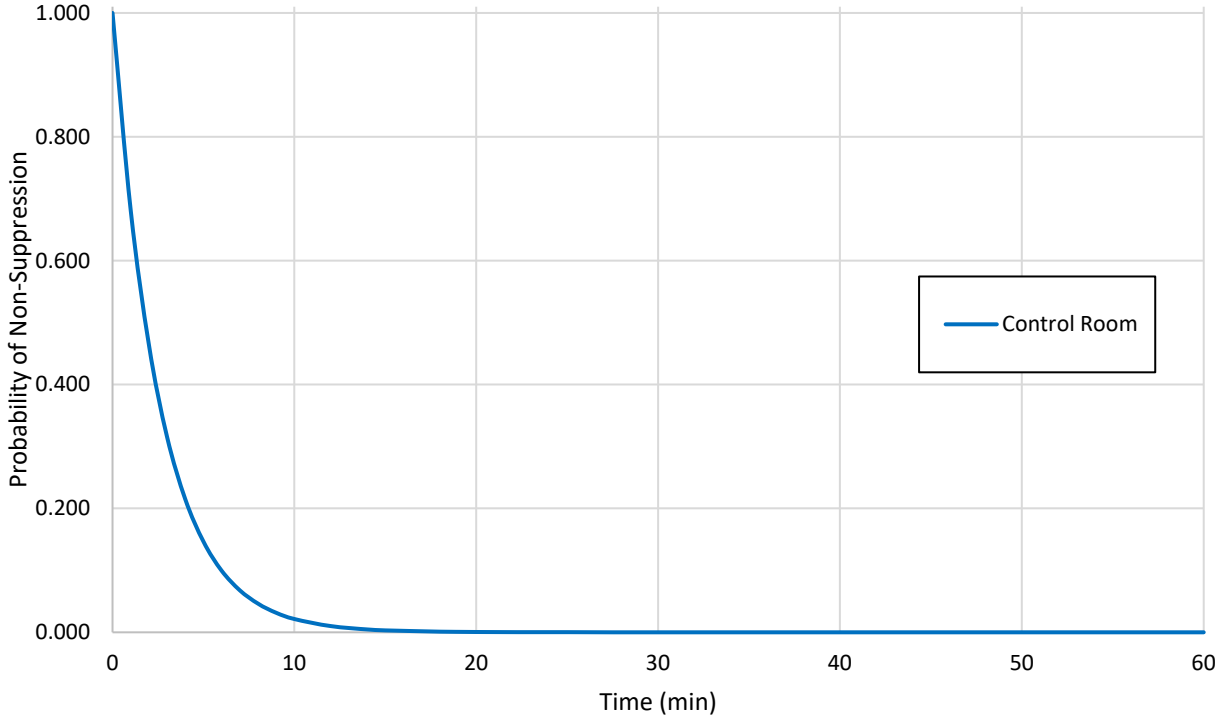

Figure 7-9
Control room non-suppression curve plot: probability versus time to suppression

Given the new NSP floor (see NUREG-2230 [33] for the basis), the numerical results for the control room suppression curve are presented in Table 7-7.

Table 7-7
Update numerical results for the control room suppression curve

Time (min)	Main Control Room
0	1.00E+00
5	1.46E-01
10	2.14E-02
15	3.12E-03
20	7.37E-04/8.15E-04
25	3.50E-04/4.94E-04
30	1.66E-04/2.99E-04
35	7.85E-05/1.81E-04
40	3.72E-05/1.10E-04
45	1.76E-05/6.64E-05
50	8.36E-06/4.02E-05
55	3.96E-06/2.44E-05
60	1.88E-06/1.48E-05
65	8.91E-07/8.94E-06
70	4.22E-07/5.42E-06
75	§/3.28E-06
80	§/1.99E-06
85	§/1.20E-06
90	§/7.29E-07
95	§/4.41E-07
100	§/§

§ A value 2.4E-07 should be used for single-unit control rooms and 4.8E-07 for dual-unit control rooms.

Table 7-8 lists the fire events used in the development of the MCR suppression rate constant.

Table 7-8
Fire event data for determination of control room suppression rate constant

ID	Event Date	Ignition Source	Power Condition	Fire Severity	Bin	Previous Supp. Time (min)	New Supp. Time (min)
537	9/4/1986	N//A	Pre-op testing	N/A	N/A	Occurred during pre-op testing (June 4, 1986, first elec. generation/NRC license Nov. 13, 1986)	
659	12/30/1987	Electrical cabinets	PO	U	15	2	2
756	10/14/1988	Electrical cabinets	LPSD	CH	15	1	1
928	3/1/1989	Main control board	PO	CH	4	Removed due to damage limited to the subcomponent of fire origin	
202	3/23/1990	Main control board	PO	PC	4	Removed due to damage limited to the subcomponent of fire origin	
236	1/6/1993	Transients	PO	U (NC-PC)	7	2	2
83.1	4/4/1996	Electrical cabinets (non HEAF)	RF	PC	15	9	9
84	4/19/1996	Main control board	PO	PC	4	Removed due to damage limited to the subcomponent of fire origin	
50553	5/2/2003	Main control board	RF	PC	4	2	2
10389	9/8/2003	Main control board	PO	PC	4	Removed due to damage limited to the subcomponent of fire origin	
30276	7/24/2006	Electrical cabinets (non-HEAF)	PO	PC	15	2	2
10407	6/3/2007	Main control board	PO	PC	4	2	2

Table 7-8
Fire event data for determination of control room suppression rate constant (continued)

ID	Event Date	Ignition Source	Power Condition	Fire Severity	Bin	Previous Supp. Time (min)	New Supp. Time (min)
30513	5/27/2008	Electrical cabinets	PO	PC	15	2	2
50914	6/8/2010	Electrical cabinets	HS	PC	15	N/A	3
50916	7/13/2010	Electrical cabinets	PO	PC	15	1	1
51002	11/10/2010	Main control board	RF	U	4	Removed due to damage limited to the subcomponent of fire origin; self-extinguished	

PO = power operation
NC = non-challenging
LPSD = low power shutdown
CH = challenging
U = undetermined
HS = hot shutdown
PC = potentially challenging
HEAF = high-energy arcing fault

7.4 Single Subcomponent Failure

All of the fire events associated with the MCB in the EPRI FEDB consist of small fires that are either limited to the subcomponent of fire origin or a limited number of subcomponents nearby. The consequences generated by these events typically include nothing more than replacing the subcomponent where the fire initiated. To capture this operational experience, the first damage state in the fire scenario progression is modeled as the failure of one subcomponent or function on the board (for example, a switch, a cable termination point, a relay, a circuit card, and so on). Given that fire damage is associated with the failure of one subcomponent, the risk contribution of such a fire should be bounded by the CCDP quantification of the internal events model as random failure probabilities including those associated with ignition of individual subcomponents credited in the model. For example, the plant risk calculated as the aggregate of all hazards includes the contribution of the risk associated with the internal events model. Therefore, the model quantification assuming a plant trip from the internal events model with no fire induced failures can provide a bounding CCDP value to use for calculating the CDF associated with this damage state (that is, failure of one subcomponent on an MCB). Note that the internal events model should consider the plant response, such as spurious operations of equipment caused by the failure of the initial subcomponent.

7.4.1 Review of Operational Experience

The EPRI FEDB [35, 48] maintains events from U.S. NPP fire experience. A review of the MCB fires provides insight on the characteristics of these fires. There are nine MCB events that have been recorded and determined to be applicable for FPRAs (See Table 7-9, notice that four events have been re-assigned after additional investigation to electrical cabinets, Bin 15).

These events have been determined to be challenging or potentially challenging and have been counted in the estimation of the fire ignition frequency and NSPs in NUREG-2169 [36]. Seventy eight percent (78%), or seven of the nine events describe a fire that was not a significant source of heat, and the damage was isolated to the initial subcomponent. These fires are more accurately described as a small electrical failure. The remaining 22% (two out of nine of the events) describe fires that caused damage beyond the initial subcomponent failure (none involved a full electrical enclosure). Table 7-9 lists the fire events in EPRI's FEDB that are classified using the following categories:

- **Single subcomponent**. Fire (flames) limited to subcomponent of origin. Flames from subcomponent may char nearby wires, cards, or equipment, but there must be no evidence of flames or ignition of any additional subcomponents
- **Group of subcomponent**s. Fire damage to subcomponents immediately adjacent to the subcomponent of fire origin
- **Partial panel**. Fire damage beyond the subcomponent of fire origin and the subcomponents immediately adjacent
- **Full pane**l. Fire involves damage to more than 50% of panel
- **Multi-panel**. Fire damage extends beyond panel of origin

Table 7-9
MCB fire event review

Incident Number	Event Date	Description of Event	Extent of Fire Damage
Old FEDB 2373	12/2/1976	Faulty coil on relay overheated, causing combustible material on relay to start burning. Fire put out immediately with fire extinguisher. Appears two relays were replaced, but event narrative describes only one relay involved in fire.	Single subcomponent
Old FEDB 163	7/12/1979	During maintenance, an electric module was pulled out and metal-to-metal contact was made between two printed circuit boards. This caused a short circuit in the module and put a large load on a resistor. A small fire occurred. The readout panel was located on the back panel in the control room. The fire was extinguished immediately by control room personnel using a CO_2 fire extinguisher. The readout panel's circuit boards sustained substantial damage and the entire readout panel was replaced. The radiation monitor was still in service and could be read locally. *The plant confirmed that this panel is not a main control board fire. The location of the fire is on a panel behind the horseshoe.	This is not a MCB fire (should be Bin 15 [1968-1989])
Old FEDB 480	7/14/1985	At 7:45, a control room operator noticed electro-hydraulic control) (EHC) transfer from auto to manual position. At 7:50, the plant experienced a reactor trip as a result of an electrical fault in the digital EHC panel. While investigating the cause of the incident, a computer technician observed smoke from the EHC panel. The fault was due to an overheated resistor on a solid-state circuit board. Fire brigade response was immediate, and the fire was quickly extinguished by the Halon fire extinguisher.	Single subcomponent
Old FEDB 928	3/1/1989	At 16:45, the operator placed the hand switch in the shut position. The shut light flickered, and a buzzing noise was heard. The operator attempted to trip the valve again with the same result. The operator and the control room supervisor removed the panel and found the hand switch on fire. The operator obtained a Halon fire extinguisher and used it once. At about this time the 10-amp circuit fuses blew. One more blast was used to extinguish the fire, which lasted 1–2 minutes. The only peripheral damage caused by the fire was the lead wires to the auxiliary feedwater steam inlet pressure indicators located near the hand switch. The leads were found slightly charred and were tagged out of service.	Single subcomponent

* New finding that was provided in follow-up

Table 7-9
MCB fire event review (continued)

Incident Number	Event Date	Description of Event	Extent of Fire Damage
202	3/23/1990	An operator was changing the light bulb in the auto side of the dilution pump #2 trip feature switch. When the operator screwed the new bulb in, he saw a flash. Going to the back of the panel, he saw flames from two wires on the back of the switch at which time he announced to the control room that there was a fire. A supervisor grabbed halon extinguisher, and the operator got a CO_2 extinguisher. Hit fire with one shot from halon extinguisher and then used the CO_2 extinguisher. The shift supervisor took dilution pump #2 feature switch to bypass and deenergized the circuit.	Single subcomponent
20351	6/21/1994	A small fire was observed in a control room panel for meteorological tower. Operations personnel noticed smoke coming from the panel. The door to the panel was opened, and flames from the bottom rear of the cabinet were visible. A Halon fire extinguisher was used to quickly extinguish the fire. The back panel was opened to observe the effects of the fire. Wires were burned off and some electrical terminations appear to be damaged (some damage to relay above and terminal block above relay. Cables burned themselves free of surge suppressor). *The plant confirmed that the meteorological tower panel is in a row of panels behind the horseshoe/main control board.	This is not a MCB fire (should be Bin 15 [1990–1999])
84	4/19/1996	At 10:19 fire alarms on control room panels C1, C2, and C3 occurred. Control room operator response included a report of smoke. The smoke, including a small flame, was due to failure of the coil of the turbine lockout relay 286-2. A carbon dioxide extinguisher was directed at the turbine lockout relay. The smoke condition did not affect control room operations, and damage was limited to turbine lockout relay coil.	Single subcomponent
50553	5/2/2003	At 6:32, there was a small fire in control room alarm panel. The fire was immediately extinguished with a handheld halon extinguisher. Two alarmed (tagged) cards were found to be damaged. Small fire occurred in an annunciator panel. Fire was immediately extinguished using small burst from halon extinguisher.	Group of subcomponents

* New finding that was provided in follow-up

Table 7-9
MCB fire event review (continued)

Incident Number	Event Date	Description of Event	Extent of Fire Damage
10389	9/8/2003	A burnt smell is coming from panel. After some investigation an amp switch was found to be sparking and smoking. Saw visible flame. Switch taken from 2 position to Off and sparking, smoking, and flames stopped.	Single subcomponent
10394	2/22/2005	Annunciator card for window 108 has burned out. Flames could be seen coming from the end of the annunciator card. The annunciator card for window 107 (which is next to the window 108 annunciator card) sustained burn damage and needs to be replaced also. The flame extinguished on its own, and no fire extinguisher had to be used. *The plant confirmed that this panel is not part of the MCR control panel horseshoe. This is a back panel.	This is not a MCB fire (should be Bin 15 [2000–2014])
10407	6/3/2007	Personnel in the MCR detected a burnt smell. Upon investigation the smell was determined to be coming from a power supply in the back of the panel. The power supply had visible flames coming out of the vent holes of power supply box along with smoke in the area. Personnel acquired portable fire extinguisher and extinguished the fire. Instrumentation and controls (I&C) personnel dispatched to investigate effects on instrumentation due to the fire. The fire was caused by failure of a capacitor on a circuit card in a five-unit instrument loop power supply assembly. Slight damage to the cards on either side. No damage to any component outside the five-slot power supply chassis.	Group of subcomponents
50916	7/13/2010	A new annunciator point card installed in a control room annunciator panel failed resulting in a small fire in the control room. I&C techs were installing new annunciator cards in a control room annunciator panel. Several minutes later one of the cards that had just been installed started smoking and caught fire. The fire was immediately extinguished by an operator with a mist fire extinguisher. The internal fuses for the panel and the adjacent panels were pulled to isolate power to all three panels. *The plant confirmed that this panel is not part of the main control board. This panel is in located in the back panel section of the main control room.	This is not a MCB fire (should be Bin 15 [2000–2014])

* New finding that was provided in follow-up

Table 7-9
MCB fire event review (continued)

Incident Number	Event Date	Description of Event	Extent of Fire Damage
51002	11/10/2010	During an outage, the reactor coolant pump hand switch was taken to the start position and damage occurred to the hand switch. A candle-sized flame on the hand switch was observed from the back of the MCB. The flame self-extinguished and damage was limited to the hand switch. It was determined that a wiring error at the 1A reactor coolant pump oil lift pump pressure switch was the cause of the fire and hand switch damage.	Single subcomponent

7.5 Fire Limited to a Small Group of Subcomponents

Given that a fire extends beyond a single subcomponent, the next damage state to consider is a small fire that remains confined to a small group of subcomponents. Determining the small group of subcomponents damage state is perhaps the most difficult for target selection because it involves a subset of impacts associated with the panel of origin in the MCB. Therefore, it is recommended only for those panels that require detailed modeling.

Recall that under Figure 7-1, this damage state is characterized by a relatively small fire with damage limited to a small portion of a panel near the ignition source. From a fire modeling perspective, the zone of influence (ZOI) generated by this relatively small fire is assumed to be an area of approximately 0.09 m^2 (1.0 ft^2). This corresponds to roughly 15 cm (6 in.) from the point of ignition in any direction if considering a circular ZOI. From an electrical design perspective, this size bounds the design guidelines established in IEEE 384 (including the supplements described in Regulatory Guide 1.75), *Standard Criteria for Independence of Class 1E Equipment and Circuits.* This standard provides criteria and requirements for establishing and maintaining the independence of safety-related equipment and circuits, and auxiliary supporting features by physical separation and electrical isolation. The standard indicates that internal control panel wiring (divisional Class 1E, or Class 1E and non-Class 1E) must be separated by a minimum distance of 1 in. (2.54 cm) of horizontal spacing and 6 in. (15.2 cm) of vertical spacing (for the control panel materials that are flame retardant). Consequently, selecting an area of 0.09 m^2 (1.0 ft^2) should bound the target sets associated with this damage state.

Based on this ZOI, the recommended process consists of identifying targets within circles of approximately 0.09 m^2 (1.0 ft^2) throughout the surface of the panel.[9] The intent is that the external surface of the panel be covered and targets within a 0.09-m^2 (1.0- ft^2) circle be identified as target sets. In addition, the circles along the edges of each panel should extend 7 in. into the adjacent panel if there are no internal partitions between panels (see Section 4.2 for configurations where no spread is postulated). Under this formulation, the following occur:

- The area of 0.09 m^2 (1.0 ft^2) can be used as an apportioning factor (that is, the area of the scenario over the total surface area of the panel) for each of the scenarios postulated in each panel in this damage state. The relatively small ZOI should simplify the process of defining plant impacts, because, in practice, target sets may be limited to one train of a

[9] This approach is preferred over a fixed grid approach because a fixed grid approach can miss important combinations of targets based on the arbitrary location of grid lines. The circles approach is intended to identify the worst combinations of targets in close proximity to each other on a given panel.

system or no more than one system. It is noted that “circles” can be combined if it is determined that a larger section of the panel contains targets of similar impact in the quantification process. If combined, the apportioning factor should reflect the surface area represented by the scenario. This apportioning should consider all sections of the MCB (including potential section(s) that do not have FPRA cables or components) when apportioning the ignition frequency.

- Panel configurations consisting of different systems close together (that is, within 0.09 m^2 [1.0 ft^2]) should be inspected and selected as target sets. This inspection should also consider the potential for multiple spurious operations (MSOs).

In summary, for this second damage state, the entire surface of the panel should be apportioned with a surface area ratio to ensure that the frequency is conserved. Each target set should be assigned a CCDP based on a representative (or bounding) damage set. For example, a panel may have one scenario consisting of damage to a 0.09 m^2 (1.0 ft^2) with a relatively high CCDP, while the remainder of the panel produces a low CCDP. In that situation, only two area apportionments are needed. The first would be the high CCDP portion of the panel with 0.09 m^2 (1.0 ft^2) area. The second would be the remaining area of the panel combined into another scenario that fails all of the functions outside the 0.09 m^2 (1.0 ft^2) area. The total CCDP for the panel is then the area weighted sum of the scenario involving the targets within the 0.09 m^2 (1.0 ft^2) circle and the scenario involving the remainder of the panel. This is achieved by defining the total surface area of the panel and then determining the surface area ratio of each scenario which is the area of the scenario divided by the total surface area. The CCDP is then determined as the sum of the product of the CCDP and area ratio for each scenario considered.

7.5.1 Monte Carlo Simulation for Characterizing Fires Limited to a Small Group of Subcomponents

The probabilities for Branch B (corresponding to the successful suppression split) are based on a Monte Carlo sampling technique to approximate the distribution of fire exposures that may be possible given the range of determining factors.

The Monte Carlo simulation consists of the following five parts:

1. Generate a fire HRR profile over time (random parameters: time to peak HRR, growth power factor (n), steady time, decay time, and peak HRR). See Section 7.5.2.
2. Calculate the time-dependent fire exposure at a radial distance of 0.15 m (6 in.) (random parameters: heat release rate per unit area (HRRPUA); required constant parameters: distance, fire Froude number parameters, radiant fraction). See Section 7.5.3.
3. Calculate the time response of an electrical target and determine time to damage, if appropriate (no additional random or constant parameters needed). See Section 7.5.4.
4. Calculate an NSP for the case given the time to damage calculation and credit for early detection if appropriate (additional random parameters: manual detection credit; additional constant parameters: in-cabinet detection system credit, system unavailability). See Section 7.5.5.
5. Average all NSP results over 20,000 occurrences. See Section 7.5.6.

The specifics of this process are described in further detail in the following sections with a summary of the input parameters in Table 7-10.

Table 7-10
Summary of Monte Carlo parameters for modeling non-severe MCB fires

Parameter	Distribution Type	α	β	Average Value	Notes
Distance from fire to target	Constant	N/A	N/A	0.1524 m	Target separation
MCR suppression rate	Constant	N/A	N/A	0.385 min^{-1}	NSP rate for MCR in Table 7-6 (see NUREG-2230 for additional detail including the interruptible/growing fire split)
Growing fire suppression rate	Constant	N/A	N/A	0.100 min^{-1}	NSP function (see NUREG-2230 for additional detail including interruptible/ growth split)
Interruptible fire suppression rate	Constant	N/A	N/A	0.149 min^{-1}	NSP function (see NUREG-2230 for additional detail including interruptible/ growth split)
NSP floor value	Constant	N/A	N/A	2.4E-07	Minimum value for NSP from NUREG-2230 (results are not sensitive to this parameter, and results apply to dual unit MCRs)
Ambient temperature	Constant	N/A	N/A	25°C	Typical ambient temperature in MCR
Ambient pressure	Constant	N/A	N/A	101325 Pa	Typical ambient pressure in MCR
HRR radiant fraction (thermoset)	Uniform	0.13 (min)	0.62 (max)	Varies	Fire radiant fraction selected randomly based on cable type from SFPE Handbook 5th Edition Table A.39 [49]
HRR radiant fraction (thermoplastic)	Uniform	0.48 (min)	0.63 (max)	Varies	Fire radiant fraction selected randomly based on cable type from SFPE Handbook 5th Edition Table A.39 [49]
Duration of the pre-growth and growth phases of the HRR profile	Gamma	2.33	5.59	13.1 min	Total of pre-growth and growth phase (see Section 7.5.2)
Growth power factor (n-1)	Gamma	0.345	5.80	2.98	Add 1.0 so that the distribution is never less than 1.0

Table 7-10
Summary of Monte Carlo parameters for modeling non-severe MCB fires (continued)

Parameter	Distribution Type	α	β	Average Value	Notes
Duration of the steady state HRR profile stage	Gamma	0.840	11.2	9.52 min	Steady burning duration (See Section 7.5.2)
Duration of the decay state HRR profile stage	Gamma	0.688	27.1	18.6 min	Decay burning duration (See Section 7.5.2)
HRRPUA (thermoset)	Uniform	100 kW/m^2 (min)	200 kW/m^2 (max)	150 kW/m^2	Recommended range from NUREG/CR-7010 for thermoset cables
HRRPUA (thermoplastic)	Uniform	200 kW/m^2 (min)	300 kW/m^2 (max)	250 kW/m^2	Recommended range from NUREG/CR-7010 for thermoplastic cables
Peak HRR	Gamma	Varies	Varies	Varies	See NUREG-2178, Table 4-2

7.5.2 Heat Release Rate Growth Profile

For the Monte Carlo simulation, the HRR profile selected for the cabinet is treated as a random variable based on the probability distributions described in NUREG-2178 (that is, the HRRs are defined using the existing distributions provided in Table 4-2 of NUREG-2178 [2]), where the fire is given a growth phase, steady, and decay phase, all of which are allowed to vary. In order to account for the pre-growth phases of the fire growth, a generic function has been developed of the form $\dot{Q} = \alpha t^n$ to allow for a fire to remain small for a period of time, then begin to grow to its peak HRR. In the case where n is 2, the fire is the commonly used t-squared profile. In some cases, the pre-growth time may be long, while the growth time may be short, in which case the parameter n would be large. Conversely, the pre-growth time could be short, and the growth time could be long, resulting in smaller values of n. However, the value of n is never allowed to be less than 1.0, which corresponds to a linear growth rate with time. The parameter α is always determined so that the fire growth curve achieves the desired peak HRR at the desired time. Table 7-11 lists the experiments that were selected for developing the range of fire growth profile and the peak HRR, pre-growth, and growth duration for each of the tests [30, 31, 39] evaluated in NUREG-2178 [2]. Tests were excluded if the test was a sub-set or continuation of a test (Ex. CBD-41_B) or if the ignition source was a liquid accelerant. The resulting durations of the growth profile are provided in Figure 7-10.

Table 7-11
Test results evaluated in NUREG-2178 [30, 31, 39]

Test ID	Validation Check	Peak HRR (kW)	Pre-Growth Time (min)	Growth (min)
SNL-ST1	Not valid	9	0	3
SNL-ST2	Not valid	12	0	3
SNL-ST3	Valid	45	0	6
SNL-ST4	Valid	55	0	4
SNL-ST5	Valid	107	0	6
SNL-ST6	Valid	57	0	7
SNL-ST7	Valid	71	6	9
SNL-ST8	Valid	61	0	7
SNL-ST9	Valid	42	0	6
SNL-ST10	Valid	248	0	11
SNL-ST11	Valid	474	0	11
SNL-PCT1	Valid	153	0	8
SNL-PCT2	Valid	963	0	11
SNL-PCT3	Valid	24	0	9
SNL-PCT5	Valid	791	20	9
SNL-PCT6	Valid	183	0	13
SNL-Test24	Valid	1300	20	7
SNL-Test25	Valid	840	17	5
VTT186-Exp1	Valid	388	0	41
VTT186-Exp2	Valid	50	9	4
VTT186-Exp3-1	Not valid	0	43	N/A
VTT186-Exp3-2	Valid	200	0	14
VTT269-Exp1	Valid	180	0	40
VTT269-Exp2A	Not valid	0	NA	N/A
VTT269-Exp2B	Not valid	0	NA	N/A
VTT269-Exp2C	Valid	120	0	33
VTT269-Exp3	Valid	100	0	13
VTT521-Exp7	Valid	35	0	3
VTT521-Exp8	Not valid	20	0	5

Table 7-11
Test results evaluated in NUREG-2178 [30, 31, 39] (continued)

Test ID	Validation Check	Peak HRR (kW)	Pre-Growth Time (min)	Growth (min)
VTT521-Exp9	Valid	40	0	9
VTT521-Exp10	Not valid	20	0	6
CBD-1	Not valid	2	45	N/A
CBD-2	Not valid	2	19	N/A
CBD-3	Not valid	2	19	N/A
CBD-4	Not valid	2	19	N/A
CBD-5	Not valid	1	18	N/A
CBD-6	Not valid	2	18	N/A
CBD-7	Not valid	9	0	8
CBD-8	Not valid	0	15	N/A
CBD-9	Not valid	1	15	N/A
CBD-10	Not valid	1	14	N/A
CBD-11	Not valid	1	20	N/A
CBD-12_A	Not valid	3	40	N/A
CBD-12_B	Not valid	39	0	24
CBD-12_C	Not valid	52	0	5
CBD-13	Not valid	2	38	N/A
CBD-14_A	Not valid	0	20	N/A
CBD-14_B	Not valid	4	12	N/A
CBD-15_A	Not valid	2.2	35	N/A
CBD-15_B	Not valid	4	19	N/A
CBD-16	Not valid	2	30	N/A
CBD-17	Not valid	0	15	N/A
CBD-18	Not valid	3	21	N/A
CBD-19	Not valid	3	55	N/A
CBD-20	Not valid	5	0	39
CBD-21	Not valid	4	29	N/A
CBD-22	Not valid	4	28	N/A
CBD-23	Not valid	18	8	4

Table 7-11
Test results evaluated in NUREG-2178 [30, 31, 39] (continued)

Test ID	Validation Check	Peak HRR (kW)	Pre-Growth Time (min)	Growth (min)
CBD-24	Not valid	4	37	N/A
CBD-25	Not valid	4	9	12
CBD-26	Not valid	1	18	N/A
CBD-27_A	Not valid	1.7	40	N/A
CBD-27_B	Not valid	7	0	7
CBD-28_A	Not valid	4.7	19	N/A
CBD-28_B	Not valid	11.3	0	11
CBD-28_C	Not valid	10	7	2
CBD-29	Valid	100	0	6
CBD-30	Valid	72	0	3
CBD-31	Valid	28	2	10
CBD-32_A	Not valid	5.6	16	N/A
CBD-32_B	Not valid	11	0	5
CBD-33	Valid	50	2	4
CBD-34	Valid	36	11	15
CBD-35	Valid	146	0	3
CBD-36_A	Not valid	2.5	12	N/A
CBD-36_B	Not valid	4	8	N/A
CBD-37	Valid	35	2	3
CBD-38	Valid	169	0	9
CBD-39	Valid	60	3	4
CBD-40	Not valid	2	40	N/A
CBD-41_A	Valid	122	0	7
CBD-41_B	Not valid	232	0	3
CBD-42	Valid	36	0	17
CBD-43	Not valid	13	2	4
CBD-44	Valid	31	0	18
CBD-45	Not valid	5	12	2
CBD-46	Valid	45	0	19

Table 7-11
Test results evaluated in NUREG-2178 [30, 31, 39] (continued)

Test ID	Validation Check	Peak HRR (kW)	Pre-Growth Time (min)	Growth (min)
CBD-47	Valid	40	0	17
CBD-48	Valid	87	0	18
CBD-49	Valid	50	0	12
CBD-50	Not valid	1	23	N/A
CBD-51	Valid	31	2	3
CBD-52	Valid	122	0	3
CBD-53_A	Valid	57	0	5
CBD-53_B	Not valid	85	4	4
CBD-54	Valid	98	5	10
CBD-55	Valid	21	8	8
CBD-56	Not valid	8	4	2
CBD-57	Not valid	5	28	N/A
CBD-58	Valid	26	0	5
CBD-59_A	Not valid	5.3	10	7
CBD-59_B	Not valid	22	0	6
CBD-60	Valid	88	18	5
CBD-61	Not valid	5	30	N/A
CBD-62	Not valid	11	21	6
CBD-63	Valid	113	10	12
CBD-64	Not valid	6	20	N/A
CBD-65	Not valid	7	20	N/A
CBD-66_A	Valid	26	0	17
CBD-66_B	Not valid	26	0	3
CBD-67_A	Valid	26	0	9
CBD-67_B	Not valid	29	0	1
CBD-68	Valid	216	1	6
CBD-69	Not valid	10	0	10
CBD-70	Not valid	2	7	N/A
CBD-71	Valid	138	2	11

Table 7-11
Test results evaluated in NUREG-2178 [30, 31, 39] (continued)

Test ID	Validation Check	Peak HRR (kW)	Pre-Growth Time (min)	Growth (min)
CBD-73	Not valid	4	27	N/A
CBD-74	Not valid	5	25	N/A
CBD-75	Not valid	15	0	8
CBD-76	Not valid	9	26	N/A
CBD-77_A	Not valid	10	0	10
CBD-77_B	Not valid	18	0	11
CBD-78_A	Valid	30	0	11
CBD-78_B	Not valid	54	0	1
CBD-79_A	Valid	41	3	4
CBD-79_B	Not valid	70	7	7
CBD-80_A	Valid	22	9	4
CBD-80_B	Not valid	102	0	11
CBD-81	Valid	24	0	6
CBD-82_A	Not valid	3.8	22	N/A
CBD-82_B	Not valid	65	0	3
CBD-83	Valid	577	9	4
CBD-84	Valid	57	6	13
CBD-85	Not valid	2	20	N/A
CBD-86_A	Not valid	0	27	N/A
CBD-86_B	Not valid	24	0	4
CBD-87	Valid	30	3	9
CBD-88	Valid	147	4	2
CBD-89	Valid	25	10	6
CBD-90	Not valid	12	0	20
CBD-91	Not valid	3	34	N/A
CBD-92	Not valid	15	0	6
CBD-93	Valid	59	0	9
CBD-94	Valid	37	0	11
CBD-95	Valid	30	0	13

Table 7-11
Test results evaluated in NUREG-2178 [30, 31, 39] (continued)

Test ID	Validation Check	Peak HRR (kW)	Pre-Growth Time (min)	Growth (min)
CBD-96	Valid	33	0	9
CBD-97_A	Not valid	9	7	3
CBD-97_B	Not valid	89	0	4
CBD-98	Valid	121	0	7
CBD-99	Not valid	3	29	N/A
CBD-100	Valid	34	0	26
CBD-101	Valid	66	3	3
CBD-102	Not valid	10	0	5
CBD-103	Valid	42	0	10
CBD-104	Valid	250	25	4
CBD-105	Valid	80	0	7
CBD-106_A	Not valid	17	0	8
CBD-106_B	Not valid	38	0	4
CBD-107	Valid	55	3	8
CBD-108	Valid	32	1	6
CBD-109	Valid	64	3	8
CBD-110_A	Not valid	7	14	N/A
CBD-110_B	Not valid	11	NA	N/A
CBD-111_A	Valid	49	5	5
CBD-111_B	Not valid	268	0	3
CBD-112	Valid	22	0	9

The distribution for the growth power factor, n, is determined by classifying the total time to peak HRR into a pre-growth and a growth phase. The pre-growth phase is defined as a negligibly small HRR above the ignition source. The growth phase is defined as the remaining time for the fire to grow from its small size to the peak HRR. Using these values, the parameter n can be calculated using a three-point curve fit solution, where the transition HRR from the pre-growth stage to the growth stage is assumed to be 5 kW. Equation 7-2 is used to determine the growth power factor:

$$\boldsymbol{n = \mathbf{MAX}\left(1.0, \frac{\ln\left(\frac{5}{Q_p}\right)}{\ln\left(\frac{t_i}{t_g}\right)}\right)} \qquad \textbf{(7-2)}$$

The max function is used to ensure that the value of n never falls below 1.0. The value Q_p is the peak HRR in kW, t_i is the time in the pre-growth phase, t_g is the total time to peak HRR which is

the total of the pre-growth time and the growth time. This parameter was calculated for each valid test and the gamma distribution determined for $n-1$. Because the gamma distribution is valid only for positive numbers, this assures that the parameter n is never less than 1.0 by evaluating the distribution for $n-1$ and later adding 1.0.

Figure 7-10 presents examples of growth profiles from nine different simulations. The growth profiles presented assume a peak HRR of 400 kW with *n* values varying between 1, 2, and 3 and growth times of 1, 12 and 25 minutes.

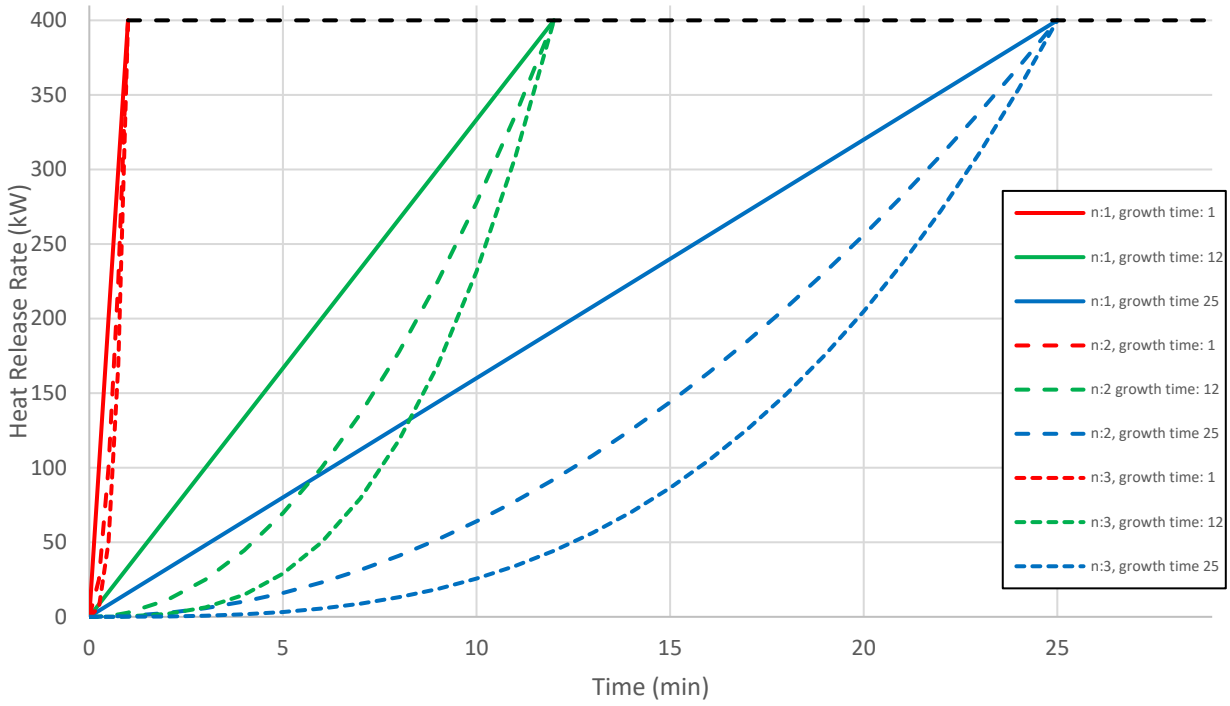

Figure 7-10
Example MCB growth profiles

The duration of the growth stage is used to classify the test as either a growing fire or interruptible fire, similar to NUREG-2230 [33]. If the total growth exceeds 16 minutes, the fire is considered interruptible. If the total growth is less than or equal to 16 minutes, it is considered a growing fire. This is necessary to accurately define NSPs for longer duration fires.

7.5.3 Evaluate Fire Exposure

The next step in the Monte Carlo analysis is to predict the fire-induced exposure to a target 0.15 m (6 in.) away from the point of ignition. In this case, there are two relevant exposure mechanisms for the fire to cause damage to a target at small separation distances. The first is through fire growth (for example, flaming) enveloping the target. The second is through radiative thermal exposure. The Monte Carlo analysis evaluates for each trial if these conditions occur.

In the first exposure (for example, flaming), as the fire HRR grows in time, it is also considered to grow in physical size. In this case, the diameter of the fire is determined through a randomized HRRPUA and the actual fire HRR at a given time. If the radius exceeds 0.15 m (6 in.), it is considered that a second subcomponent fails. All fires that exceed the critical dimension are considered potentially severe.

The fires that are smaller in physical dimension are then evaluated for potential radiant exposure to a target 0.15 m (6 in.) away. This is achieved by estimating the fire radiant exposure to the target, which varies with time as the fire grows and decays. The radiant exposure is evaluated using the updated guidance provided in Section 2.2.3.

7.5.4 Evaluate Target Response

The radiant exposure is then evaluated for potential damage using the heat soak method described in Appendix A. This is similar to Appendix H of NUREG/CR-6850 but considers preheating that may occur at lower exposures than those capable of producing damage (see Appendix A). This approach accounts for the exposure potential of the source fire and the delayed heating response of a target near the fire. The outcome of this analysis is to determine the time to damage, if appropriate. Some fires will remain physically small and never achieve a radiant exposure sufficient to fail a target at any duration. These fires are considered to never fail the target and assigned an NSP of zero. Slightly larger fires that produce a radiative exposure may not cause damage because the exposure duration is insufficient to heat the target to failure. In this case, the NSP is the floor value of 2.4E-07 from NUREG-2230 [33] is used. Note that the results were evaluated against the NSP floor value for dual unit control rooms (at 4.8E-07) and found not to be sensitive to this selection; therefore, the tabulated values are applicable to dual unit control rooms. The remaining fires produce damage, and the time to damage is either the time for the fire to physically grow to envelop the target or the time at which the target has been sufficiently exposed over time. In those cases, the NSP is determined using the time to damage and the manual suppression term. Note that detection credit may still be applied and the time to damage is not the only parameter needed to determine the final NSP.

7.5.5 Evaluate Probability of Non-Suppression

The results of the target response analysis can produce a time to damage for a target 0.15 m (6 in.) away from the initial fire. This time to damage is then used as an input to calculate the NSP using the updated manual suppression rate of 0.385 min^{-1} as determined for fires in the control room in Table 7-6 allowing for the growing or interruptible split described in NUREG-2230 [33].

Additionally, detection credit is applied in the determination of the NSP as a direct time credit. In-cabinet smoke detectors are given a fixed credit of 5 minutes based on guidance from NUREG/CR-6850, Appendix P. However, if automatic detection systems are credited, they should receive a system unavailability or random failure of 0.05 per NUREG/CR-6850. Because the MCR is continuously manned by highly trained and aware personnel, it is also considered that these personnel may act as manual smoke detectors in a similar manner as the in-cabinet detectors. In this case, a person is not considered to always detect a fire 5 minutes early as the smoke detector. Therefore, the manual detection is considered to be a random parameter with a uniform distribution between 0 and 5 minutes. This means that a person is at best equal to an in-cabinet detector, at worst ineffective, and on average provides 2.5 minutes of advance notification. In the Monte Carlo analysis, the system (automatic or manual) that provides the earliest response is credited by adding the applicable time to the damage time in the NSP calculation using Equations 7-3, 7-4, and 7-5:

$$\boldsymbol{P_{ns} = exp\left(-\lambda(t_{dam} + t_{det})\right)} \qquad \boldsymbol{(t_{dam} + t_{det}) \leq -\frac{\ln(0.001)}{0.385}} \tag{7-3}$$

Growing Fires:

$$\boldsymbol{P_{ns} = 0.001 \times exp\left(-\lambda_G\left(t_{dam} + t_{det} + \frac{\ln(0.001)}{0.385}\right)\right)} \quad \boldsymbol{(t_{dam} + t_{det}) > -\frac{\ln(0.001)}{0.385}} \tag{7-4}$$

Interruptible Fires:

$$\boldsymbol{P_{ns} = 0.001 \times exp\left(-\lambda_{IF}\left(t_{dam} + t_{det} + \frac{\ln(0.001)}{0.385}\right)\right)} \qquad \boldsymbol{(t_{dam} + t_{det}) > -\frac{\ln(0.001)}{0.385}} \tag{7-5}$$

where λ = 0.385 is the manual suppression rate (min^{-1}) from Table 7-6, $\lambda_G = 0.100$ is the growing fire manual suppression rate (min^{-1}), $\lambda_{IF} = 0.149$ is the interruptible fire manual suppression rate (min^{-1}), t_{dam} is the damage time determined from the target response analysis (min), and t_{det} is the time credited for early detection. Note that this manual detection credit approach is only applicable for the MCB analysis.

7.5.6 Perform Monte Carlo Analysis

Using a randomized sample size of 20,000 occurrences for each electrical enclosure classification and fuel type, the NSP was averaged. The parameters, the distribution of the parameters, and the other defining statistical properties used in the variation are provided in Table 7-10. The number produced is the probability that the fire is not suppressed before a second subcomponent can be damaged. The results of this analysis are provided for each electrical enclosure classification, fuel load, and cable type included in NUREG-2178, and the results are summarized in Table 7-12 for no in-cabinet detection and Table 7-13, which credits in-cabinet smoke detection (that is, adding 5 minutes to the available suppression time consistent with the guidance in Appendix P of NUREG/CR-6850). These values represent the quantification of $P_{ns}(t_1)$ for the second branch of the event tree (for example, fire is limited to a small group of components).

Table 7-12
Results of Monte Carlo modeling of non-severe MCB fires (no in-cabinet detection)

Enclosure Class/ Function Group	Enclosure Ventilation	Fuel Type	Probability of Non-Suppression, $P_{ns}(t_1)$		
			Default	**Low**	**Very Low**
4a: Large enclosures	Closed	TS/QTP/SIS	0.056	0.037	0.023
	Closed	TP	0.064	0.040	0.019
	Open	TS/QTP/SIS	0.080	0.056	0.022
	Open	TP	0.091	0.061	0.019
4b: Medium enclosures	Closed	TS/QTP/SIS	0.038	0.024	0.020
	Closed	TP	0.039	0.020	0.009
	Open	TS/QTP/SIS	0.049	0.026	0.019
	Open	TP	0.057	0.022	0.009

QTP = qualified thermoplastic
SIS = synthetic insulated switchboard wire or XLPE-insulated conductor

Table 7-13
Results of Monte Carlo modeling of non-severe MCB fires (with in-cabinet detection)

Enclosure Class/ Function Group	Enclosure Ventilation	Fuel Type	Probability of Non-Suppression, $P_{ns}(t_1)$		
			Default	**Low**	**Very Low**
4a:Large enclosures	Closed	TS/QTP/SIS	0.020	0.013	0.008
	Closed	TP	0.024	0.014	0.007
	Open	TS/QTP/SIS	0.028	0.020	0.008
	Open	TP	0.033	0.022	0.007
4b:Medium enclosures	Closed	TS/QTP/SIS	0.013	0.008	0.007
	Closed	TP	0.015	0.007	0.003
	Open	TS/QTP/SIS	0.017	0.010	0.007
	Open	TP	0.021	0.008	0.003

7.6 Fire Limited to One Panel with Potential to Spread to an Adjacent Panel if Suppression Fails

This event characterizes the potential for fire propagation from the panel of origin to an adjacent panel if suppression efforts fail. Based on the guidance described in Section 4 of this report, if propagation cannot be ruled out, only the top 2% of the HRR distribution for an electrical cabinet fire should be modeled as capable of propagating from an ignited panel to an exposed panel.

For MCB fires, the results of the Monte Carlo modeling are used to determine the fraction of fires that reach and exceed the 98th percentile HRR, were not initially suppressed in the non-severe Monte Carlo model, and are subsequently not suppressed prior to exposing a second panel.

These are the postulated fires that are capable of growing and igniting an adjacent panel. The NSP for the propagating fire to the exposed panel is conditional on the probability of the fire being suppressed prior to ignition in the exposed panel. The NSP for the scenario involving the exposing panel is shown in Table 7-12 and Table 7-13. The conditional NSP of damaging an exposed panel $(1 - \delta)$, is presented in Table 7-14 and Table 7-15.

Table 7-14
Results of Monte Carlo modeling MCB fires that spread to an adjacent panel (no in-cabinet detection)

Enclosure Class/ Function Group	Enclosure Ventilation	Fuel Type	Fraction of Fires that Spread to an Adjacent Panel $(1 - \delta)$		
			Default	**Low**	**Very Low**
4a: Large Enclosures	Closed	TS/QTP/SIS	0.082	0.126	0.000
	Closed	TP	0.074	0.094	0.000
	Open	TS/QTP/SIS	0.069	0.088	0.000
	Open	TP	0.058	0.067	0.000
4b: Medium Enclosures	Closed	TS/QTP/SIS	0.126	0.149	0.000
	Closed	TP	0.090	0.121	0.000
	Open	TS/QTP/SIS	0.094	0.138	0.000
	Open	TP	0.085	0.143	0.000

Table 7-15
Results of Monte Carlo modeling MCB fires that spread to an adjacent panel (with in-cabinet detection)

Enclosure Class/ Function Group	Enclosure Ventilation	Fuel Type	Fraction of Fires that Spread to an Adjacent Panel $(1-\delta)$		
			Default	**Low**	**Very Low**
4a: Large Enclosures	Closed	TS/QTP/SIS	0.093	0.125	0.000
	Closed	TP	0.068	0.094	0.000
	Open	TS/QTP/SIS	0.063	0.080	0.000
	Open	TP	0.063	0.073	0.000
4b: Medium Enclosures	Closed	TS/QTP/SIS	0.131	0.150	0.000
	Closed	TP	0.100	0.143	0.000
	Open	TS/QTP/SIS	0.085	0.166	0.000
	Open	TP	0.071	0.146	0.000

The values presented in Table 7-14 and Table 7-15 represent the fractions of fires that exceed the 98th percentile HRR and are not suppressed prior to spreading to an adjacent MCB panel at 10 minutes. It is clear that in each case these values $(1-\delta)$ suggest that more than 2% of fires are capable of spreading to an adjacent cabinet as outlined in Section 4. The difference results from that fact that these fires, those that exceed the 98th percentile HRR, grow at a faster rate than the lower percentile fires and result in higher probabilities of non-suppression given the damage criteria. Note that some values in Table 7-15 for cabinets with detection have higher probabilities than in Table 7-14 for cabinets without detection due to the previous suppression credit from Table 7-12 and Table 7-13. The more suppression credit that occurs in the prior branch, the less credit that can occur in the subsequent branch since the remaining fires will have a higher percentage of higher severity. The overall result, considering the product of the two values, is lower risk when cabinets are equipped with in-cabinet detection.

The values for **very low** fuel loading in Table 7-14 and Table 7-15 are set to a value of zero following the guidance in Section 4 that cabinets with a **very low** fuel have little potential for developing into large, aggressively growing fires. Finally, if panel-to-panel propagation is precluded by the rules presented in Section 4, a value of zero may be used.

7.7 Suppression Credit Before Fire Spread to an Adjacent Panel

This branch requires the determination of the probability of non-suppression that is dependent on a previous suppression credit. In the event tree, suppression is credited at multiple points along the scenario progression. Therefore, the resulting probabilities are dependent on any previously credited suppression. This is calculated using a conditional probability as shown in Equation 7-6:

$$\boldsymbol{P(B|A) = \frac{P(A \cap B)}{P(A)}} \qquad \textbf{(7-6)}$$

where Event A is the previous suppression credit and Event B is the current event suppression credit, $P(B|A)$ is the conditional probability of Event B occurring given that Event A has already

occurred, $P(A \cap B)$ is the intersection of Events A and B, which is the total probability that both events occur, and $P(A)$ is the probability that Event A has occurred. In this context, Events A and B are defined as the non-suppression events. The term $P(A \cap B) = P_{ns}(t_B)$ is the total probability of non-suppression at the time of the second event (that is, the current event time, t_B). The term $P(A) = P_{ns}(t_A)$ is the probability of non-suppression at the time of the previous event (that is, the time of Event A, t_A). Therefore, the dependent suppression function can be written:

$$\boldsymbol{P(B|A) = P_B^* = \frac{P_{ns}(t_B)}{P_{ns}(t_A)}} \quad \textbf{(7-7)}$$

And a subsequent Event C can be defined:

$$\boldsymbol{P(C|B) = P_C^{**} = \frac{P_{ns}(t_C)}{P_{ns}(t_B)}} \quad \textbf{(7-8)}$$

This allows for multiple suppression events to be credited along any single branch path of the event tree, and in all cases the total suppression credit is equivalent to the standard function in Equations 7-3 through 7-5, thereby ensuring that the total credit for suppression is equivalent to this function through the event tree.

7.8 Event Tree Summary

The section includes a description of the event tree, calculation of the branch probabilities, and a table summarizing the input parameters to the event tree. Specifically, Table 7-16 lists and describes the branch probabilities for the event tree in Figure 7-11.Table 7-17 summarizes the input parameters for the event tree.

Table 7-16
MCB event tree branch frequencies

Terminal Branch End State	Branch Frequency	Description
A	$\lambda_g \varepsilon$	A single subcomponent failure. The CCDP of the case can be approximated from internal events failures.
B	$\lambda_g(1-\varepsilon)\left(1-P_{ns}(t_1)\right)$	Fire limited to a small group of subcomponents. The CCDP of this case should be determined by failing components within a 0.3 m (1 ft) diameter circle as described in Section 7.5.
C	$\lambda_g(1-\varepsilon)P_{ns}(t_1)\delta\left(1-P^*_{ns}(t_2)\right)\eta_1$	The fire is confined to a single MCB panel and suppressed before abandonment due to loss of habitability or loss of habitability. The corresponding CCDP represents the loss of the MCB panel.
D	$\lambda_g(1-\varepsilon)P_{ns}(t_1)\delta\left(1-P^*_{ns}(t_2)\right)(1-\eta_1)$	The fire is confined to a single MCB panel and suppressed before abandonment due to loss of habitability, but results in loss of control. The corresponding CCDP represents the loss of the MCB panel with alternate shutdown.
E	$\lambda_g(1-\varepsilon)P_{ns}(t_1)\delta P^*_{ns}(t_2)$	The fire is confined to a single MCB panel and not suppressed resulting in abandonment due to loss of habitability. The corresponding CCDP represents the loss of the MCB panel with forced abandonment.
F	$\lambda_g(1-\varepsilon)P_{ns}(t_1)(1-\delta)\left(1-P^*_{ns}(10)\right)\mu\eta_1$	The fire is suppressed before the fire spreads to the adjacent panel at 10 minutes (which is also before loss of habitability and loss of control. The corresponding CCDP represents the loss of the MCB panel (equivalent to Branch C).
G	$\lambda_g(1-\varepsilon)P_{ns}(t_1)(1-\delta)(1-P^*_{ns}(10)\ \mu(1-\eta_1)$	The fire is suppressed before the fire spreads to the adjacent MCB panel at 10 minutes, which is before loss of habitability but loss of control occurs. The corresponding CCDP represents the loss of the MCB panel with alternate shutdown (equivalent to Branch D).
H	$\lambda_g(1-\varepsilon)P_{ns}(t_1)(1-\delta)\left(1-P^*_{ns}(10)\right)(1-\mu)$	The fire results in loss of habitability before it spreads to the adjacent panel at 10 minutes. The corresponding CCDP represents the loss of the MCB panel with forced abandonment (equivalent to Branch E).

Table 7-16
MCB event tree branch frequencies (continued)

Terminal Branch End State	Branch Frequency	Description
I	$\lambda_g(1-\varepsilon)P_{ns}(t_1)(1-\delta)P^{*}_{ns}(10)(1-P^{**}_{ns}(t_3))\eta_2$	The fire spreads to an adjacent MCB panel, but is suppressed before loss of habitability and loss of control. The CCDP represents the loss of two MCB panels.
J	$\lambda_g(1-\varepsilon)P_{ns}(t_1)(1-\delta)P^{*}_{ns}(10)\left(1-P^{**}_{ns}(t_3)\right)(1-\eta_2)$	The fire spreads to an adjacent MCB panel and is suppressed before loss of habitability, but loss of control occurs. The CCDP represents the loss of two MCB panels with alternate shutdown.
K	$\lambda_g(1-\varepsilon)P_{ns}(t_1)(1-\delta)P^{*}_{ns}(10)P^{**}_{ns}(t_3)$	The fire spreads to an adjacent MCB panel, then results in loss of habitability. The CCDP represents the loss of two MCB panels, with forced abandonment.

The resulting event tree is depicted in Figure 7-11.

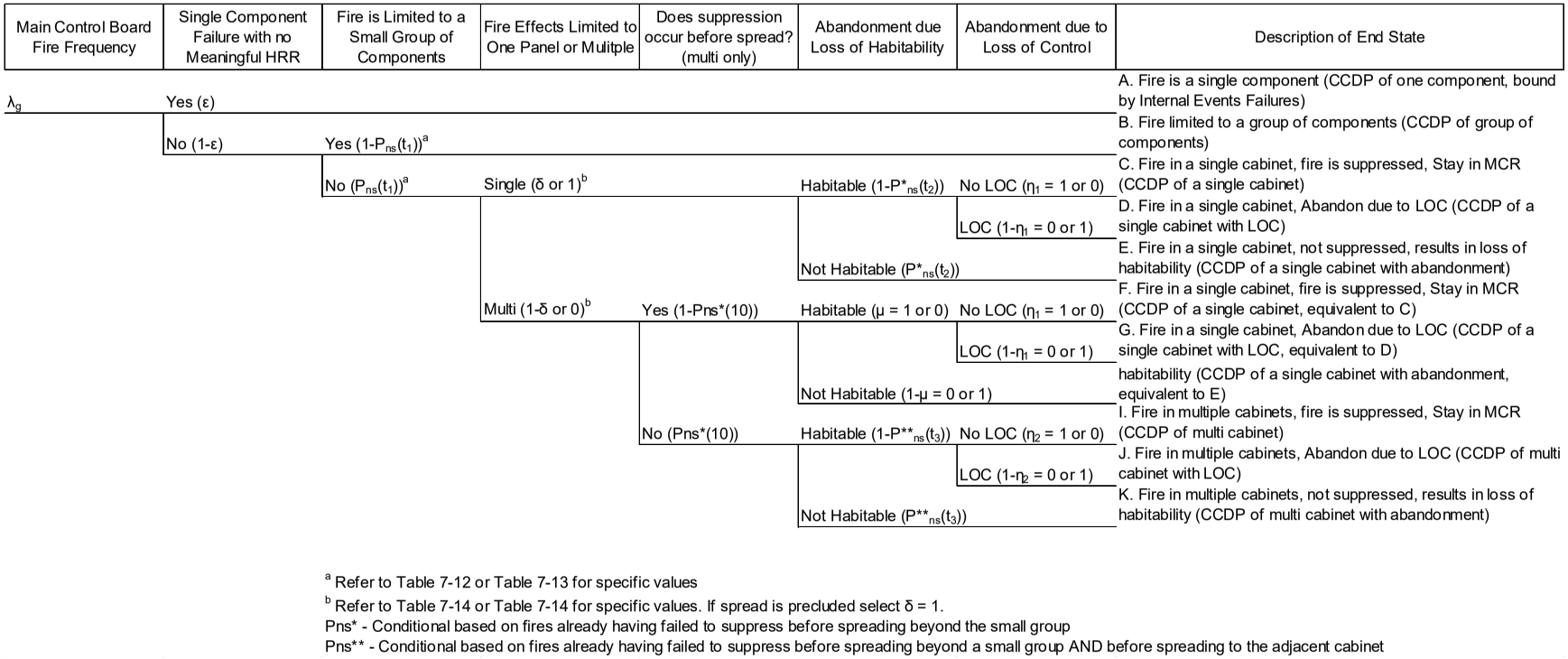

[a] Refer to Table 7-12 or Table 7-13 for specific values

[b] Refer to Table 7-14 or Table 7-14 for specific values. If spread is precluded select δ = 1.

Pns* - Conditional based on fires already having failed to suppress before spreading beyond the small group

Pns** - Conditional based on fires already having failed to suppress before spreading beyond a small group AND before spreading to the adjacent cabinet

Figure 7-11
Event tree for MCB application

Table 7-17
Input parameters selected for evaluation of MCB event tree

Parameter	Value	Description
λ	0.385 min^{-1}	Manual suppression rate constant for the control room from Table 7-6.
λ_G	0.100 min^{-1}	Manual suppression rate constant for *growing* fires from NUREG-2230.
λ_{IF}	0.149 min^{-1}	Manual suppression rate constant for *interruptible* fires from NUREG-2230.
λ_g	2.05E-03 yr^{-1}	Generic MCB frequency (FPIE) (see Table 7-3).
ε	0.78	Fraction of single subcomponent electrical failures counted as fires (see Section 7.4.1).
δ	Analysis specific	Fraction of fires effects limited to a single panel, Section 7.6 Table 7-14 or Table 7-15 for enclosures without and with in-cabinet detection, respectively. Note that spread may be precluded for some panels based on the screening rules in Section 4.
$P_{ns}(t_1)$	Analysis specific	Split fraction of small fires that are quickly suppressed before spreading to a second electrical subcomponent. Value is obtained from Table 7-12 or Table 7-13 for enclosures without and with in-cabinet detection, respectively.
t_2	Analysis specific	Time to loss of habitability in MCR (obtained through fire modeling analysis). This value represents time to abandonment for all fires below the 98th percentile fire size. This may be determined as a weighted average, or the tree may be solved for each fire size bin evaluated.
t_3	Analysis specific	Time to loss of habitability for fire spread to an adjacent enclosure (obtained through fire modeling analysis). This value represents the time to abandon given a 98th percentile fire that spreads to an adjacent MCB enclosure.
$P^*_{ns}(10)$	Analysis specific	This is the conditional probability that a fire is not suppressed at 10 minutes, given the failure to suppress at t_1. The value is calculated using equation: $$P^*_{ns}(10) = \text{MIN}\left(\frac{P_{ns}(10)}{P_{ns}(t_1)}, 1\right)$$
$P^*_{ns}(t_2)$	Analysis specific	This is the conditional probability that a fire is not suppressed at t_2 (before loss of habitability), given the failure to suppress at t_1. The value is calculated using equation: $$P^*_{ns}(t_2) = \text{MIN}\left(\frac{P_{ns}(t_2)}{P_{ns}(t_1)}, 1\right)$$

Table 7-17
Input parameters selected for evaluation of MCB event tree (continued)

Parameter	Value	Description
$P_{ns}^{**}(t_3)$	Analysis specific	This is the conditional probability that a fire is not suppressed at t_3 (before loss of habitability for the spreading fire), given the failure to suppress at 10 minutes. The value is calculated using equation: $P_{ns}^{**}(t_3) = \text{MIN}\left(\frac{P_{ns}(t_3)}{P_{ns}(10)}, 1\right)$
μ	Analysis specific	This is the evaluation of whether the MCR is still habitable at 10 minutes for cases in which the fire has been suppressed before spreading to an adjacent enclosure. A value of 1 represents a habitable condition.
η_1	Analysis specific	This is the evaluation of whether the failure of the first enclosure fire results in a loss of control event. A value of 1 represents that control has been maintained within the MCR.
η_2	Analysis specific	This is the evaluation of whether the failure of the spreading enclosure fire results in a loss of control event once the second enclosure becomes involved. A value of 0 represents that control has been lost and initiation of alternate shutdown is required.

7.9 MCB Example Application

This example is for a large, closed MCB with thermoplastic cables and no in-cabinet detection. In this example, the generic frequency reported in Table 7-3 of 2.05E-03/year is used, and in this case the full set of MCB enclosures are treated as a group. The manual suppression rate is defined as 0.385 min^{-1} from Table 7-6 with split formulas for growing and interruptible fires following the guidance in NUREG-2230 [33]. The remaining input parameters selected for this example application in the event tree have been defined in Table 7-18. The results of the apportioned frequencies are provided in Table 7-19. This approach results in several branches with zero apportioned frequency due to the binary parameters μ, η_1, and η_2. Also note that the lower branches have lower frequency apportionment to offset the potential higher CCDPs associated with those branches. In some cases, it may be possible or desirable to conservatively treat the spreading fire branches in a consolidated branch if the risk evaluation can show that the branch is negligible.

Table 7-18
Input parameters selected for an example evaluation of the MCB event tree

Parameter	Value	Description
$\boldsymbol{\lambda}$	0.385 min^{-1}	Manual suppression rate constant from Table 7-6
$\boldsymbol{\lambda_G}$	0.100 min^{-1}	Manual suppression rate constant for *growing* fires from NUREG-2230
$\boldsymbol{\lambda_{IF}}$	0.149 min^{-1}	Manual suppression rate constant for *interruptible* fires from NUREG-2230
$\boldsymbol{\lambda_g}$	2.05E-03 yr^{-1}	Generic Frequency for FPIE, see Section 7.3.1
$\boldsymbol{\varepsilon}$	0.78	Fraction of single subcomponent electrical failures counted as fires, See Section 7.4.1
$\boldsymbol{P_{ns}(t_1)}$	0.064	Split fraction of small fires that are quickly suppressed before spreading to a second electrical subcomponent. Value is obtained from Table 7-12 for large closed enclosures with **default** thermoplastic fuel loading and no in-cabinet detection.
$\boldsymbol{\delta}$	0.926	Fraction of fires effects limited to a single panel—see Section 7.6 (1 - 0.059 = 0.941)
$\boldsymbol{t_2}$	15 min	This value is obtained from fire modeling for the time to loss of habitability in the MCR. This value represents an average time to abandonment for simplicity which accounts for the severity factor of all fires below the 98th percentile fire size.
$\boldsymbol{t_3}$	12 min	This value is obtained from fire modeling for the time to loss of habitability in the MCR. This value represents the time to abandon given a 98th percentile fire which spreads to an adjacent MCB enclosure.
$\boldsymbol{P^*_{ns}(10)}$	0.331	This is the conditional probability that a fire is not suppressed at 10 minutes, given the failure to suppress at t_1. The value is calculated using equation: $$P^*_{ns}(10) = \text{MIN}\left(\frac{P_{ns}(10)}{P_{ns}(t_1)}, 1\right)$$

Table 7-18
Input parameters selected for an example evaluation of the MCB event tree (continued)

Parameter	Value	Description
$P_{ns}^{*}(t_2)$	0.0484	This is the conditional probability that a fire is not suppressed at t_2 (before loss of habitability), given the failure to suppress at t_1. The value is calculated using equation: $$P_{ns}^{*}(t_2) = \text{MIN}\left(\frac{P_{ns}(t_2)}{P_{ns}(t_1)}, 1\right)$$
$P_{ns}^{**}(t_3)$	0.463	This is the conditional probability that a fire is not suppressed at t_3 (before loss of habitability for the spreading fire), given the failure to suppress at 10 minutes. The value is calculated using equation: $$P_{ns}^{**}(t_3) = \text{MIN}\left(\frac{P_{ns}(t_3)}{P_{ns}(10)}, 1\right)$$
μ	1	This is the evaluation of whether the MCR is still habitable at 10 minutes for cases in which the fire has been suppressed before spreading to an adjacent enclosure. A value of 1 represents a habitable condition.
η_1	1	This is the evaluation of whether the failure of the first enclosure fire results in a loss of control event. A value of 1 represents that control has been maintained within the MCR.
η_2	0	This is the evaluation of whether the failure of the spreading enclosure fire results in a loss of control event once the second enclosure becomes involved. A value of 0 represents that control has been lost and initiation of alternate shutdown is required.

Table 7-19
Results of event tree evaluation with the example parameters from Table 7-18

Terminal Branch End State	Branch Frequency	Apportioned Frequency
A	$\lambda_g \varepsilon$	1.60E-03
B	$\lambda_g (1-\varepsilon)\big(1-P_{ns}(t_1)\big)$	4.22E-04
C	$\lambda_g (1-\varepsilon) P_{ns}(t_1)\delta\big(1-P^*_{ns}(t_2)\big)\eta_1$	2.55E-05
D	$\lambda_g (1-\varepsilon) P_{ns}(t_1)\delta\big(1-P^*_{ns}(t_2)\big)(1-\eta_1)$	0.00E+00
E	$\lambda_g (1-\varepsilon) P_{ns}(t_1)\delta P^*_{ns}(t_2)$	1.30E-06
F	$\lambda_g (1-\varepsilon) P_{ns}(t_1)(1-\delta)\big(1-P^*_{ns}(10)\big)\mu\eta_1$	1.43E-06
G	$\lambda_g (1-\varepsilon) P_{ns}(t_1)(1-\delta)(1-P^*_{ns}(10)\ \mu(1-\eta_1)$	0.00E+00
H	$\lambda_g (1-\varepsilon) P_{ns}(t_1)(1-\delta)\big(1-P^*_{ns}(10)\big)(1-\mu)$	0.00E+00
I	$\lambda_g (1-\varepsilon) P_{ns}(t_1)(1-\delta) P^*_{ns}(10)(1-P^{**}_{ns}(t_3))\eta_2$	0.00E+00
J	$\lambda_g (1-\varepsilon) P_{ns}(t_1)(1-\delta) P^*_{ns}(10)\big(1-P^{**}_{ns}(t_3)\big)(1-\eta_2)$	3.81E-07
K	$\lambda_g (1-\varepsilon) P_{ns}(t_1)(1-\delta) P^*_{ns}(10) P^{**}_{ns}(t_3)$	3.28E-07

8
SUMMARY AND CONCLUSIONS

This report provides several areas of refinement for fires within electrical cabinets (obstructed radiation, cabinet-to-cabinet propagation, and fire location factor), electric motors and indoor dry transformers (heat release rates [HRRs], duration, and fire base elevation), and the main control board.

8.1 Summary of Radiation

The horizontal zone of influence (ZOI) can be calculated through empirical models (that is, point source or solid flame), zone models (that is, CFAST or MAGIC) or through the use of field models (that is, Fire Dynamics Simulator (FDS)). This report documents two refinements to the empirical models; unobstructed radiation (applicable to all ignition source ZOIs), and obstructed radiation (applicable to ignition sources where the radiation source is shielded by a metal wall).

For unobstructed radiation, Section 2.2.3 discusses a correction to the emissive power in the solid flame model to ensure that the effective radiant fraction does not exceed the assumed radiant fraction.

For obstructed radiation, prior to this research, the horizontal ZOI is computed as if it were an unobstructed fire. Similar to the obstructed plume approach [2], a series of simulations were performed using FDS to gather data and insights on the horizontal ZOI. Table 3-5 and Table 3-6 provide a summary of the results for medium (open and closed respectively), and Table 3-7 and Table 3-8 for large electrical cabinets (open and closed respectively). Table 3-9 (unvented faces) and 3-10 (vented faces) present results for electrical cabinets binned as Groups 1, 2, and 3 in NUREG-2178 [2]. Small cabinet radiation guidance is in Table 3-11. The results of the FDS studies can be used to more realistically define the horizontal ZOI.

8.2 Summary of Cabinet-to-Cabinet Propagation

An update to the cabinet-to-cabinet fire propagation is provided in Section 4. Although the method in NUREG/CR-6850 was widely used, the guidance was silent on a limit of how many cabinets to involve in the fire scenario. The updated method provides additional screening guidance, a method for assigning a conditional probability of fire spread, and recommendations for characterizing the fire growth. Cabinet to cabinet fire propagation can be screened for the following configurations:

- Double wall
- Cabinets with open top and vertically oriented cables
- Cabinets containing **very low** fuel load
- Group 4c: small enclosures
- Cabinets containing **low** fuel load and steel partitions
- Cabinets with **low** fuel load (exposing) and **very low** load (exposed)

- Group 1: switchgear and load centers
- Group 2: motor control centers

For cabinets not meeting the screening criteria, a 0.02 conditional probability can be postulated to result in cabinet to cabinet fire spread for 98th percentile HRRs. Section 4.4 provides additional guidance for postulating the fire spread direction and fire behavior.

8.3 Summary of Electric Motor and Dry Transformer Fire Characteristics

Fire characteristics associated with motors and transformers are revisited explicitly considering the size, content, and construction. The guidance for each source is summarized in the following sections.

8.3.1 Electric Motors (Bins 2, 9, 14, 21, 26, and 32)

Electric motors can be screened in the fire probabilistic risk assessments (FPRA) if the following occur:

1. The motor has a horsepower rating of 5 hp or less. Motors of this size are assumed to have little to no contribution to risk and are excluded from ignition source counting (NUREG/CR-6850, Section 6.5.6 [1]).
2. The motor is totally enclosed, regardless of motor size. These motors are excluded from ignition source counting (FAQ 07-0031 [34]).

The HRRs for motors are summarized in Table 8-1.

Table 8-1
Motor peak heat release rate distribution

Motor Classification Group	Motor Size (horsepower)	α	β	75th Percentile (kW)	98th Percentile (kW)
A	>5–30	1.34	3.26	6	15
B	>30–100	1.17	8.69	14	37
C	>100	1.10	24.19	37	100

The following growth, steady burning, and decay durations should be used for motor fires.

- Growth: 2 minutes, t-squared growth
- Steady burning: 13 minutes
- Decay: 2 minutes, linear decay

The fire base height guidance is summarized as follows:

- For motors sealed on the top (without top vents or openings that allow vertical air flow), the fire base height should be 0.3 m (1 ft) below the top of the motor but not below the base of the motor housing. If the vent location is not known, assume the location to be 0.3 m (1 ft) below the top of the motor, but not below the base of the motor housing.
- For motors not sealed at the top, the fire base height should be at the top of the motor.

8.3.2 Dry Type Transformers (Bin 23)

Dry transformers can be screened in the FPRA if the following occur:

- Transformer power rating is 45 kVA or less. These transformers have little to no contribution to risk and are excluded from ignition source counting (Supplement 1 to NUREG/CR-6850 [34]).
- Transformer is of solid cast coil construction. These transformers have been demonstrated to have high levels of fire resistance inherent to the design of the solid cast insulation surrounding the winding wires. The solid cast materials have been subjected to numerous small and large scale fire tests and electrical failure tests in which it was concluded that they produce little or no fire hazard [41]. This screening criteria is added to reflect the inherently reduced risk associated with solid cast coil dry transformers. Note that determination that a transformer is solid cast coil may not be possible in the field and may require design specification review.

The HRRs for transformers are summarized in Table 8-2.

Table 8-2
Transformer peak heat release rate distribution

Transformer Classification Group	Transformer Power (kVA)	α	β	75th Percentile (kW)	98th Percentile (kW)
A	>45–75	0.38	12.84	6	30
B	>75–750	0.41	28.57	15	70
C	>750	0.46	50.26	30	130

The following growth, steady burning, and decay durations should be used for motor fires.

- Growth: 0 minutes
- Steady burning: 10 minutes
- Decay: 10 minutes, linear decay

The fire base height guidance is summarized as follows:

- For dry transformers sealed on the top (without top vents or openings that allow vertical air flow), the fire base height should be 0.3 m (1 ft) below the top of the transformer. This assumption is also valid (conservative) for fully sealed transformer enclosures.
- For dry transformers not sealed at the top, the fire base height should be at the top of the transformer.
- Alternatively, for side vented transformers where one or more vents are located on the side of the enclosure, the analysis can locate the fire at the uppermost vent. For example, if the enclosure includes two vertical vents on the side, the fire should be located at the elevation of the upper vertical vent.

8.4 Summary of New Fire Location Factor

Section 6 summarizes the latest guidance for determining plume temperatures for fires postulated in a corner or along a wall. The section provides validation of the new fire location factors based on the National Institute of Standards and Technology (NIST) experiments near walls and corners. Table 8-3 provides location factor values that should be used based on the configuration (wall or corner) and distance to the wall or corner. Definitions of wall and corner configurations are presented in Section 6.2. The new fire location factors provide a significant reduction in bias and model uncertainty over those recommended in NUREG/CR-6850 [1] and the NRC Significance Determination Process [43], as shown in Table 8-3.

Table 8-3
New fire location factor

Configuration	Location Factor 0–0.3 m (0–1 ft)	Location Factor 0.3–0.6 m (1–2 ft)	Location Factor >0.6 m (2 ft)
Corner	4	2	1
Wall	1	1	1

8.5 Summary of the Main Control Board Fire Modeling

Section 7 provides a new model for evaluating the fire risk of the main control board (MCB). The event tree presented in Figure 7-1 allows the MCB scenario development to unfold by the evaluation of increasingly severe fire damage states. This approach is also able to integrate the MCR abandonment scenarios into the event tree.

Section 7.3.1 provides an updated fire ignition frequency for Bin 4, guidance on how to partition the MCB (Section 7.3.2), and an updated MCR non-suppression rate (Section 7.3.3).

After partitioning, the analyst can use Section 7.2.1 to calculate a screening level core damage frequency (CDF) of the MCB panels to determine which panels require detailed evaluation using the event tree and Monte Carlo model.

Section 7.8 summarizes the event tree model development. Figure 7-11 presents the event tree and Table 7-17 summarizes the inputs required.

9
REFERENCES

1. EPRI 1011989 and NUREG/CR-6850, *EPRI/NRC-RES Fire PRA Methodology for Nuclear Power Facilities, Volume 2: Detailed Methodology*. Electric Power Research Institute, Palo Alto, CA and U.S. Nuclear Regulatory Commission, Washington, DC: September 2005.
2. NUREG-2178 Volume 1 and EPRI 3002005578, *Refining and Characterizing Heat Release Rates from Electrical Enclosures During Fire, Volume 1: Peak Heat Release Rates and Effect of Obstructed Plume,* U.S. Nuclear Regulatory Commission, Washington, DC, and Electric Power Research Institute, Palo Alto, CA: 2015.
3. NUREG-1805, Supplement 1, *Fire Dynamics Tools (FDT^S) Quantitative Fire Hazard Analysis Methods for the U. S. Nuclear Regulatory Commission Fire Protection Inspection Program*, U.S. Nuclear Regulatory Commission, Washington, DC: July 2013.
4. K. McGrattan, S. Hostikka, R. McDermott, J. Floyd, M. Vanella, C. Weinschenk, and K. Overholt, *Fire Dynamics Simulator Technical Reference Guide Volume 1: Mathematical Model*, NIST SP 1018-1, National Institute of Standards and Technology, Gaithersburg, MD: 2017.
5. K. McGrattan, S. Hostikka, R. McDermott, J. Floyd, M. Vanella, C. Weinschenk, and K. Overholt., *Fire Dynamics Simulator User's Guide*, NIST SP 1019-1, National Institute of Standards and Technology, Gaithersburg, MD: 2017.
6. C. Beyler, "Chapter 66: Fire Hazard Calculations for Large Open Hydrocarbon Fires," *SFPE Handbook of Fire Protection Engineering, 5th Edition*, Society of Fire Protection Engineers, Bethesda, MD: 2016.
7. J. Bevelacqua, *Contemporary Health Physics: Problems and Solutions, 2nd Edition*, Wiley-VCH Verlag GmBH & Co. KGaA, Weinheim, Germany: 2009.
8. NUREG-1824 Supplement 1 and EPRI 3002002182, *Verification and Validation of Fire Selected Fire Models for Nuclear Power Plant Applications: Supplement 1*, U.S. Nuclear Regulatory Commission, Washington, DC, and Electric Power Research Institute (EPRI), Palo Alto, CA: 2016.
9. EPRI 3002005303, *Fire Modeling Enhancements for Fire Probabilistic Risk Assessment: Fire Location Factor, Transient Fires, and Liquid Spill Heat Release Rate*, Electric Power Research Institute, Palo Alto, CA: 2015.
10. S. Shokri and C. Beyler, "Radiation from Large Pool Fires," *Journal of Fire Protection Engineering*, 1(4): pp 141–150 (1989.
11. Fleury, R., "Evaluation of Thermal Radiation Models for Fire Spread Between Objects," Master's thesis, University of Canterbury, Christchurch, New Zealand, 2010.
12. M. Bundy, A. Hamins, et al., *Measurements of Heat and Combustion Products in Reduced-Scale Ventilation-Limited Compartment Fires*, NIST Technical Note 1483, National Institute of Standards and Technology, Gaithersburg, MD: 2007.

13. A. Hamins, A. Maranghides, et al., *Federal Building and Fire Safety Investigation of the World Trade Center Disaster: Experiments and Modeling of Structural Steel Elements Exposed to Fire*, NIST NCSTAR 1-5B, National Institute of Standards and Technology, Gaithersburg, MD: 2005.
14. B. McCaffrey, *Purely Buoyant Diffusion Flames: Some Experimental Results,* NBSIR 79-1910, National Bureau of Standards, Washington, DC: 1979.
15. P. Veloo and J. Quintierre, "Convective heat transfer coefficient in compartment fires," *J. Fire Sci.,* 31:5, 2013, DOI: 10.1177/0734904113479001.
16. J. Holman, *Heat Transfer 7th Edition*, McGraw-Hill, Inc., New York, NY: 1990.
17. J. Howell, R. Siegel, and M. Menguc, *Thermal Radiation Heat Transfer, 6th Edition,* Taylor and Francis, New York, NY: 2010.
18. *The Influence of Walls, Corners and Enclosures on Fire Plumes.* National Institute of Standards and Technology. NIST Technical Note 1984. March 2018.
19. U. Wickström, "The plate thermometer—a simple instrument for reaching harmonized fire resistance tests," *Fire Technology*, 30:2, pp 195–208 (1994).
20. A. Putorti, N. Melly, S. Bareham, and J. Praydis, "Characterizing the Thermal Effects of High Energy Arc Faults," SMiRT 23, Manchester, UK: 2015.
21. K. McGrattan, S. Hostikka, R. McDermott, J. Floyd, M. Vanella, C. Weinschenk, and K. Overholt, *Fire Dynamics Simulator Technical Reference Guide Volume 3: Validation*, NIST SP 1018-3, National Institute of Standards and Technology, Gaithersburg, MD: 2017.
22. NUREG/CR-7102, *Kerite Analysis in Thermal Environment of FIRE (KATE-Fire): Test Results*, U.S. Nuclear Regulatory Commission, Washington, DC: June 2011.
23. NUREG-1934 and EPRI 1023259, *Nuclear Power Plant Fire Modeling Analysis Guidelines (NPP FIRE MAG)*, U.S. Nuclear Regulatory Commission, Washington, DC, and Electric Power Research Institute, Palo Alto, CA: 2012.
24. NUREG/CR-7010, *Cable Heat Release, Ignition, and Spread in Tray Installations During Fire (CHRISTIFIRE) Phase 1: Horizontal Trays*, U.S. Nuclear Regulatory Commission, Washington, DC: 2012.
25. R. Peacock, K. McGrattan, G. Forney, and P. Reneke, *CFAST—Consolidated Fire and Smoke Transport (Version 7), Volume 1: Technical Reference Guide*, NIST TN 1889v1, National Institute of Standards and Technology, Gaithersburg, MD: 2017.
26. R. Peacock, P. Reneke, and G. Forney, *CFAST—Consolidated Fire and Smoke Transport (Version 7), Volume 2: User's Guide*, NIST TN 1889v2, National Institute of Standards and Technology, Gaithersburg, MD: 2017.
27. D. Drysdale, *An Introduction to Fire Dynamics*, 3rd Edition," Wiley, 2011.
28. *Fire PRA Implementation Guide*. EPRI, Palo Alto, CA: 1995. TR-105928.
29. FAQ 13-0005: Cable Fire Special Cases: Self-Ignited and Caused by Welding and Cutting. Available through NRC ADAMS: https://www.nrc.gov/docs/ML1331/ML13319B181.pdf.
30. NUREG/CR-4527 and SAND86–0336, *An Experimental Investigation of Internally Ignited Fires in Nuclear Power Plant Control Cabinets Part I: Cabinet Effects Testing*, U.S. Nuclear Regulatory Commission, Washington DC, and Sandia National Laboratories, Albuquerque, NM: 1987.

31. NUREG/CR-7197, *Heat Release Rates of Electrical Enclosure Fires (HELEN-FIRE*), U.S. Nuclear Regulatory Commission, Washington, DC: 2015.

32. *Nuclear Maintenance Applications Center: Switchgear and Bus Maintenance Guide*. EPRI, Palo Alto, CA: 2006. 1013457.

33. NUREG-2230 and EPRI 3002016051, *Methodology for Modeling Fire Growth and Suppression Response of Electrical Cabinet Fires in Nuclear Power Plants*, Electric Power Research Institute, Palo Alto, CA, and U.S. Nuclear Regulatory Commission, Washington, DC: 2019.

34. NUREG/CR-6850, Supplement 1 and EPRI 1019259, *Fire Probabilistic Risk Assessment Methods Enhancements,* U.S. Nuclear Regulatory Commission, Washington, DC, and Electric Power Research Institute, Palo Alto, CA: 2010.

35. *The Updated Fire Events Database: Description of Content and Fire Event Classification Guidance*, EPRI, Palo Alto, CA: 2013. 1025284.

36. NUREG-2169 and EPRI 3002002936, *Nuclear Power Plant Fire Ignition Frequency and Non-Suppression Probability Estimation Using the Updated Fire Events Database*, Electric Power Research Institute, Palo Alto, CA, and U.S. Nuclear Regulatory Commission, Washington, DC: 2015.

37. Zureks, "Stator and rotor of a three-phase induction motor: 0.75 kW, 1420 rpm, 50 Hz, 230-400 V AC, 3.4-2.0 A," 2008, Own work. wikipedia.org (URL: https://commons.wikimedia.org/wiki/File:Stator_and_rotor_by_Zureks.JPG?uselang=en).

38. *Handbook of Building Materials for Fire Protection*, Ed. Charles A. Harper, McGraw-Hill, 2004.

39. VTT Working Papers 139—Design Fires for Fire Safety Engineering, Figure 35, p-61, Jukka Hietaniemi & Esko Mikkola, 2010 , ISBN 978-951-38-7479-7.

40. NUREG-1805, *Fire Dynamics Tools (FDT^S) Quantitative Fire Hazard Analysis Methods for the U. S. Nuclear Regulatory Commission Fire Protection Inspection Program*, U.S. Nuclear Regulatory Commission, Washington, DC: 2004.

41. S. A. McBride, *Cast Coil Transformer Fire Susceptibility and Reliability Study*, EG and G Idaho Inc., Idaho Falls, ID: 1991.

42. Institute of Electrical and Electronics Engineers Standard. C57.12.01-1998, IEEE Standard General Requirements for Dry-Type Distribution and Power Transformers Including Those with Solid Cast and/or Resin Encapsulated Windings.

43. *Technical Basis for Fire Protection Significance Determination Process (IMC 0609, Appendix F) at Power Operations*, U.S. Nuclear Regulatory Commission, Washington, DC: 2005.

44. K. B. McGrattan et al, *Fire Dynamics Simulator, Technical Reference Guide, Volume 2: Verification Guide*. National Institute of Standards and Technology, Gaithersburg, MD, and VTT Technical Research Centre of Finland, Espoo, Finland, 6th edition, 2013.

45. G. Heskestad, "Engineering Relations for Fire Plumes," *Fire Safety Journal*, Volume 7.1, pp. 25–32 (1984).

46. G. Heskestad, "Chapter 13: Fire Plumes, Flame Height, and Air Entrainment," *SFPE Handbook of Fire Protection Engineering, 5th Edition*, Society of Fire Protection Engineers, Bethesda, MD: 2016.

47. FAQ 14-0008: Main Control Board Treatment. Available through NRC ADAMS: https://www.nrc.gov/docs/ML1419/ML14190B307.pdf.

48. *Fire Events Database Update for the Period 2010-2014: Revision 1*. EPRI, Palo Alto, CA: 2016. 3002005302.

49. Table A.39, *SFPE Handbook of Fire Protection Engineering, 5th Edition*, Society of Fire Protection Engineers, Bethesda, MD: 2016.

50. NUREG/CR-6931, *Cable Response to Live Fire (CAROLFIRE) Volume 3: Thermally Induced Electrical Failure (THIEF) Model*, U.S. Nuclear Regulatory Commission, Washington, DC: 2008.

51. Prairie Island NFPA 805 LAR, PRA RAI 21.01, Available through NRC ADAMS: https://www.nrc.gov/docs/ML1703/ML17038A513.pdf.

52. Prairie Island Response to NFPA 805 LAR, PRA RAI 21.01, Available through NRC ADAMS: https://www.nrc.gov/docs/ML1706/ML17065A339.pdf.

53. Prairie Island Nuclear Generating Plant, Units 1 and 2—Issuance of Amendments Re: Transition to NFPA 805 "Performance-Based Standard for Fire Protection for Light Water Reactor Electric Generating Plants" CAC NOS. ME9374 and ME9735, Available through NRC ADAMS: https://www.nrc.gov/docs/ML1716/ML17163A027.pdf.

54. *Engineering Guide: Predicting 1st and 2nd Degree Skin Burns from Thermal Radiation*, Society of Fire Protection Engineers, Bethesda, MD: 2000.

55. C. A. Wade, J. T. Gerlich, and A. Abu, *The Relationship Between Fire Severity and Time-Equivalence*, BRANZ Study Report 314, Porirua, New Zealand: 2014.

56. J. F. Nyman, *Equivalent Fire Resistance Ratings of Construction Elements Exposed to Realistic Fires*, University of Canterbury, Department of Civil Engineering, Christchurch, New Zealand: 2002.

57. J. F. Nyman, J. T. Gerlich, C.A. Wade, and A. H. Buchanan, "Predicting Fire Resistance Performance of Drywall Construction Exposed to Parametric Design Fires—A Review," *Journal of Fire Protection Engineering*, 19, pp. 117–139 (2008).

58. F. Henriques, "Studies of Thermal Injury: The Predictability and the Significance of Thermally Induced Rate Processes Leading to Irreversible Epidermal Injury," *Archives of Pathology*, 43:489–502, 1947.

59. B. Y. Lattimer, "Chapter 25: Heat Transfer from Fires to Surfaces," *SFPE Handbook of Fire Protection Engineering, 5th Edition*, Society of Fire Protection Engineers, Bethesda, MD: 2016.

60. W. D. Walton, P. H. Thomas, and Y. Ohmiya, "Chapter 30: Estimating Temperatures in Compartment Fires," *SFPE Handbook of Fire Protection Engineering*, 5th Edition, Society of Fire Protection Engineers, Bethesda, MD: 2016.

APPENDIX A
HEAT SOAK METHOD

A.1 Overview

The following three methods for assessing damage to electrical cables are presented in NUREG/CR-6850 [1]:

1. **Use of an exposure threshold (Table H-1 in NUREG/CR-6850)**. This method consists of using the exposure gas temperature or heat flux for determining cable failure. This is the simplest of the approaches, but it can be fairly conservative because it does not account for the time it takes for cable heating to actually result in damage.
2. **Use of a lookup table for time-to-damage as a function of constant exposure (Tables H-5 through H-8 from NUREG/CR-6850)**. This approach allows one to credit the thermal inertia of cables in a generic manner. However, because the tables are based on constant exposures, they do not readily lend themselves to application in actual fire scenarios where temperatures will vary as a function of time.
3. **Use of the Thermally-Induced Electrical Failure (THIEF) Model (NUREG/CR-6931 [50] and Supplement 1 to NUREG-1805 [3]).** This model performs a one-dimensional (1-D), cylindrical heat transfer calculation for a cable exposed to a time-varying exposure to determine when the cable jacket will fail based on the jacket's inner temperature. Validation of the model shows that it does well at computing the temperature rise of the cable jacket; however, because it requires cable-specific data (dimensions and mass) it cannot be applied in a generic screening manner such as method 2.

The three methods have a gap—a generic approach for determining time to damage for a cable exposed to a time-dependent temperature or heat flux. Filling this gap provides a means to do rapid screening without the conservatisms of methods 1 and 2 and without the time-consuming data gathering and output data processing requirements of method 3. This appendix documents a new methodology for evaluating the time to damage for generic cables exposed to a time-dependent temperature of heat flux (accepted as part of the Prairie Island National Fire Protection Association (NFPA) 805 Licensee Amendment Request [51, 52, 53]).

A.2 Assumptions and Limitations

Assumptions have been made with the intent of producing conservative results. In the context of fire modeling, the intent is to overpredict fire-generated conditions so that the risk parameter reflects conservatism. The nature of the assumptions and justification for this approach is described throughout the appendix. Several generic assumptions are as follows:

- Cable damage times are adequately predicted by the data in Tables H-5 through H-8 in NUREG/CR-6850 [1].
- Cable failure can be determined through a damage integral approach [54] where the cable accrues damage at a rate determined by the exposure magnitude. When the accrued damage exceeds a threshold, the cable fails.

- Cable damage rates at exposures below those provided in Table H-5 through H-8 in NUREG/CR-6850 [1] can be derived using an integrated exposure approach [55, 56, 57].
- Cable failure requires the cable be exposed above the threshold exposures in Table H-1 in NUREG/CR-6850 [1].
- The method is derived from the Appendix H tables in NUREG/CR-6850 [1]. These tables used test data consisting primarily of cross-linked polyethylene cables for the thermoset data and polyethylene cables for the thermoplastic (TP) data. No specific limitations on cable type are presented in Appendix H. It is assumed that this lack of restriction on the cables transfers to the heat soak approach.
- Because the proposed approach is a method for interpolating the data in Tables H-5 through H-8 in NUREG/CR-6850 [1], the undefined but presumed conservatively biased uncertainties of those tables apply for temperatures within the ranges presented in the table. For lower temperatures there will be additional uncertainty and the effects are covered in Section A.3, which describes the methodology development.

The following limitations apply to this analysis based on the limited scope of the analysis and assessment of the assumptions made throughout the appendix. The following limitations are defined:

- The method does not account for any protective measures such as coatings, cable tray covers, or conduit. Taking credit for such measures would require a different or modified approach.
- The method is applicable for generic TP and thermoset (TS) cables. For very large diameter cables or cables with thick jackets, the generic approach may be overly conservative.
- The method is derived from the Appendix H tables in NUREG/CR-6850 [1], which show a reduction in time to failure as the exposure temperature increases. The tables stop at a time of 1 minute until failure. Because exposure temperatures increase beyond the last row in the Appendix H tables, it is expected there would be some continued decrease in survival time that is not accounted for the in the proposed method (or in the strict application of Appendix H). However, it is noted that in a time-dependent exposure there will be a finite time to increase to and beyond the final exposure values in Appendix H. In many cases that time is likely to mean rapid failure at the upper limits of the tables (for example, the preheating time before reaching and exceeding the final exposure values in Appendix H will result in accrued damage). Exposures that result in near instantaneous exposures above the values in the Appendix H tables may not be well predicted by this method.

A.3 Approach

This section provides a technical description of the generic model implemented to account for fire exposures as a function of time. Because the actual damage mechanism results from heating the cable jacket until it fails, it would be appropriate to credit periods of exposure at low temperature with having a lesser impact on the time to failure than periods of exposure at higher temperatures.

The cable damage problem is analogous to evaluating the potential for skin burns. In both cases one is evaluating an in-depth temperature (inside of the cable jacket or the epidermis-dermis boundary) and imposing a harm (cable failure or burn) based upon the temperature solution. As with the Appendix H tables in NUREG/CR-6850, there are a number of approaches for skin burns that have developed simple times to burn based on constant exposures [54]. Skin burn modeling has also used the concept of a damage integral:

$$\boldsymbol{\Omega = \int_0^t RR(t)dt} \qquad \textbf{(A-1)}$$

where Ω is the damage integral and $RR(t)$ is a time-dependent reaction rate. Damage occurs when Ω crosses a threshold value. In the case of skin burn modeling, the reaction rate is assumed to be an Arrhenius process [58]. The data in the Appendix H tables contain exposure durations as a function of temperature ranges. These can be modeled in a damage integral by assuming that the reaction rate is the inverse of the exposure duration. That is:

$$\boldsymbol{R(t) = \frac{1}{t'_{dam}(T(t))}} \qquad \textbf{(A-2)}$$

where $T(t)$ is the exposure temperature at time t and t'_{dam} is the time until damage for that temperature from the tables in Appendix H of NUREG/CR-6850. Cable failure would then occur with a damage integral of 1 or:

$$\boldsymbol{\Omega = \int_0^{t_{dam}} \frac{1}{t'_{dam}(T(t))} dt = 1} \qquad \textbf{(A-3)}$$

An example cable time history is shown in Table A-1 with the damage integral applied using trapezoidal integration. The cable fails at 4.75 minutes.

Table A-1
Example of applying the heat soak approach

Time **(min)**	Temperarture **(°C)**	Appendix H Time to Damage **(min)**	Damage Rate **(min^{-1})**	**Damage Integral**
0	210	30	0.033	0.00
1	320	5	0.20	0.12
2	350	3	0.33	0.38
3	320	5	0.20	0.65
4	320	5	0.20	0.85
5	320	5	0.20	1.05

One consideration in the damage integral approach is the treatment of the time when cables are below the minimum damage threshold. For example, consider a TP cable that spends a couple of hours at 200°C and then makes a transient to just over 205°C. It would be inappropriate to credit the cable with having 30 minutes of survival time because two hours of preheating should put the cable on the edge of failure. That is, if a cable spends time near but not over the minimum threshold and then rises over the minimum threshold, it would be reasonable to assume that the preheated cable would have a somewhat lower time to damage.

Figure A-1 shows the integrated exposure required to cause damage using the lower and upper temperature bound for each damage interval in Appendix H of NUREG/CR-6850. The integrated exposure, q'', in J/m^2 is computed as:

$$\boldsymbol{q''} = \boldsymbol{t'_d(T)}\left(\boldsymbol{\sigma(T^4 - T_a^4) + h(T - T_a)}\right) \quad \textbf{(A-4)}$$

where σ is the Stefan-Boltzmann constant (5.67 × 10^{-11} kW/(m^2·K^4)), T_a is the ambient temperature in K, T is the exposure temperature in K, and h is convective heat transfer coffecient is conservatively assumed at 50 W/(m^2·K) [59, 60].

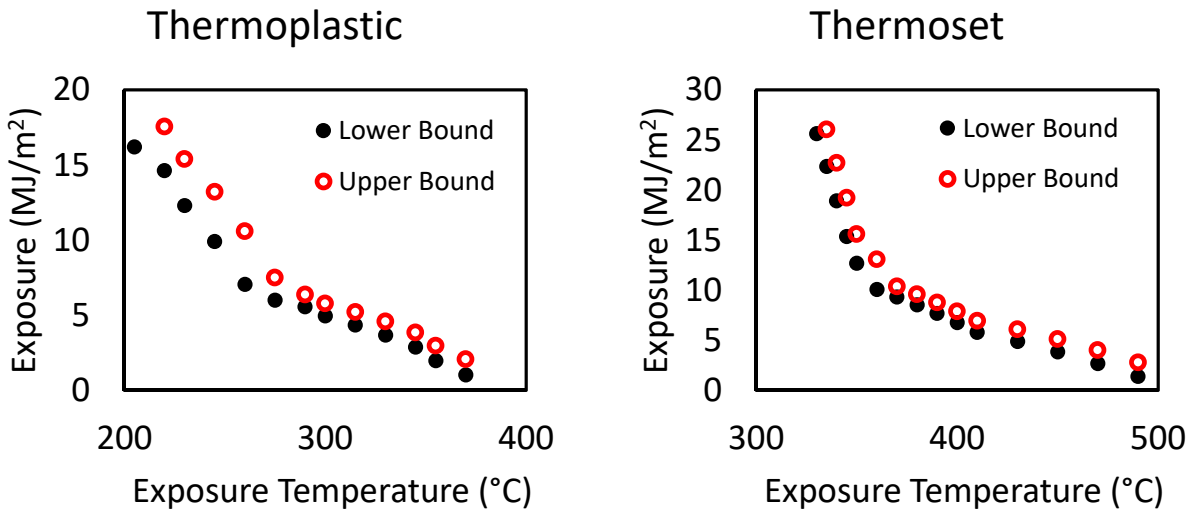

Figure A-1
Integrated exposure needed to cause cable damage for a given constant exposure temperature

As seen in Figure A-1, the net exposure required increases as the temperature decreases. A similar result is seen for the heat flux tables. One approach would be to fit a curve to the data in the figures and extrapolate to lower exposure temperatures. This approach has the significant issue that extrapolating an empirical dataset could result in non-conservative behavior. The only consideration that one can be confident in is that the total integrated exposure as a function of temperature should continue to increase as temperature decreases. Therefore, at exposure temperatures below the threshold exposure, a conservative assumption would be that the integrated exposure at the threshold is required for damage to occur. This will conservatively estimate the damage integral component for temperatures or heat fluxes below their respective thresholds.

As an example, if Equation A-4 is used to compute the incident fluxes for a temperature of 100°C and 205°C, the result is a ratio of 2.2:1. With the assumption of a constant integrated exposure, the $t'_{dam}(T)$ at 100°C would be 2.2 x 30 minutes or 66 minutes. This would apply similarly to thermoset cables using the threshold temperature of 330°C.

It is noted that this assumption means that a cable that sits long enough at low exposure, even at ambient conditions, would eventually reach a cable damage integral of 1. Because clearly a cable at ambient would not actually be damaged, in addition to a damage integral of 1, this heat soak method will also require that the cable exposure be over the threshold exposure when the integral of 1 is reached.

The assumption of constant integrated exposure below the Appendix H threshold temperature introduces some uncertainty of unknown magnitude to the calculation. However, the trend in Figure A-1 demonstrates that the assumption is conservatively biased and will not result in an undue lengthening of the predicted time to failure.

The implementation of this heat soak approach was done through two sets of Visual Basic for Application (VBA) subroutines—one for temperature exposure and one for heat flux exposure. Both routines are called with a table of values of time versus exposure and the cable type. The routines output the damage integral along with time to damage.

A.4 Verification

The following three sets of verification exercises were performed for the VBA subroutines:

1. Reproduce the Appendix H tables.
2. Demonstrate that the approach does not fail cables at low exposure.
3. Demonstrate that the approach yields the expected value for a time-dependent exposure.

A.4.1 Reproduce Appendix H

Tables A-2 through Table A-5 show the results of running the damage integral process with constant exposures. As seen, the Appendix H exposure durations are reproduced.

Table A-2
Verification of thermoplastic temperature exposures

Temperature (°C)	NUREG/CR-6850 Time to Damage (min)	Heat Soak Method Time to Damage (min)
205	30	30
220	25	25
230	20	20
245	15	15
260	10	10
275	8	8
290	7	7
300	6	6
315	5	5
330	4	4
345	3	3
355	2	2
370	1	1

Table A-3
Verification of thermoset temperature exposures

Temperature (°C)	NUREG/CR-6850 Time to Damage (min)	Heat Soak Method Time to Damage (min)
330	28	28
335	24	24
340	20	20
345	16	16
350	13	13
360	10	10
370	9	9
380	8	8
390	7	7
400	6	6
410	5	5
430	4	4
450	3	3
470	2	2
490	1	1

Table A-4
Verification of thermoplastic heat flux exposures

Heat Flux (kW/m^2)	NUREG/CR-6850 Time to Damage (min)	Heat Soak Method Time to Damage (min)
7	19	19
9	10	10
10.5	6	6
12	4	4
15	2	2
18	1	1

Table A-5
Verification of thermoset heat flux exposures

Heat Flux (kW/m^2)	NUREG/CR-6850 Time to Damage (min)	Heat Soak Method Time to Damage (min)
12	19	19
15	12	12
17	6	6
19	1	1
21	1	1

A.4.2 Low Exposure Failure

Three scenarios were run for both heat flux and temperature exposures to test low exposure failures.

The first scenario exposed a cable to a long-duration, subthreshold exposure that results in a damage integral over 1. In this case the expectation is for no damage, which is the result seen in Figure A-2.

Cable Type:	TP		Cable Type:	TP	
Damage Time (s):	No Damage		Damage Time (s):	No Damage	
Time (s)	Heat Flux (kW/m²)	Integral	Time (s)	Temperature (°C)	Integral
0	5	0.000	0	25	0.000
20	5	0.015	20	100	0.002
5000	5	3.655	5000	100	1.060

Figure A-2
Result of a long-duration subthreshold exposure

The second scenario is similar to the first but has a brief excursion over the threshold that ends prior to a damage integral of 1. In this case the expectation is also for no damage, which is the result seen in Figure A-3.

Cable Type:	TP		Cable Type:	TP	
Damage Time (s):	No Damage		Damage Time (s):	No Damage	
Time (s)	Heat Flux (kW/m²)	Integral	Time (s)	Temperature (°C)	Integral
0	5	0.000	0	25	0.000
20	5	0.015	20	100	0.002
1000	7	0.803	4500	100	0.953
1100	7	0.890	4600	206	0.992
1250	5	1.011	4700	200	1.046

Figure A-3
Result of a long-duration subthreshold exposure with a brief excursion over the threshold prior to a damage integral of 1

The third scenario moves the brief excursion to the end of the exposure after the damage integral as already reached 1. The expectation is that damage does not occur until the exposure exceeds the threshold. This is the result shown in Figure A-4.

Cable Type:	TP		Cable Type:	TP	
Damage Time (s):	4650		Damage Time (s):	4770	
Time (s)	Heat Flux (kW/m²)	Integral	Time (s)	Temperature (°C)	Integral
0	5	0.000	0	25	0.000
20	5	0.015	20	100	0.002
4500	5	3.289	4720	100	1.000
4600	5	3.363	4820	310	1.150
4700	7	3.443			

Figure A-4
Result of a long-duration subthreshold exposure with a brief excursion over the threshold after a damage integral of 1

A.4.3 Time-Dependent Exposure

Each type of cable was exposed to an exponentially increasing temperature or heat flux exposure. The damage integral was computed by hand as well as by the VBA subroutines. The results are shown below in Figure A-5.

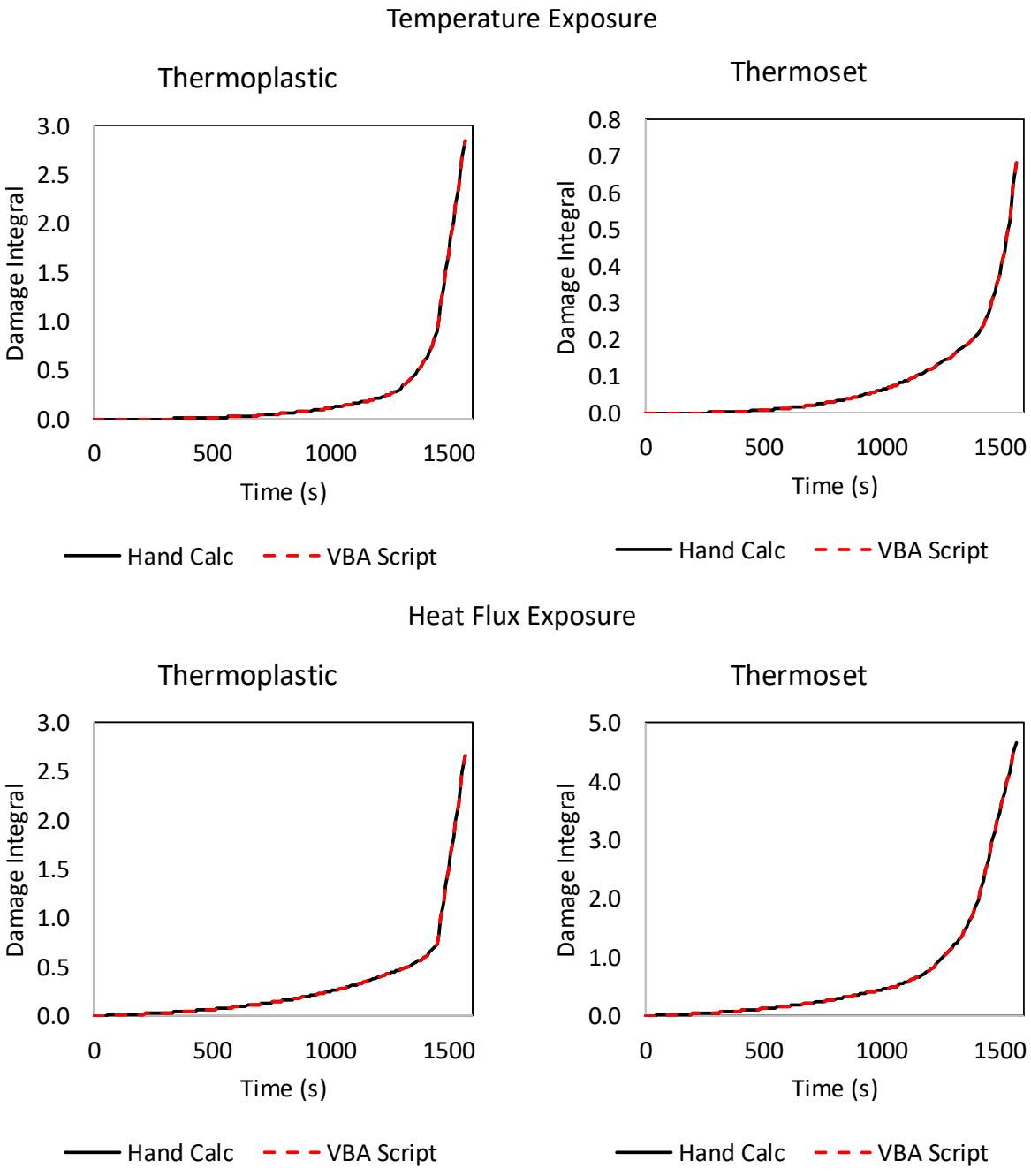

Figure A-5
Result of exposing each cable type to an exponentially increasing temperature or heat flux

A.5 Validation

Validation of the heat soak method was performed using intermediate scale test data from NUREG/CR-6931 [50]. This appendix contains data from a series of cable exposure tests that were used to develop and validate the THIEF model. Tests were performed using a range of cable types (sizes and jacket and insulator materials) that were exposed to a constant radiative flux. The end results of the THIEF validation were a bias of -15% (model predicts faster time to failure) and a standard deviation of 33%.

Using the THIEF model in NUREG-1805 [3], failure times for four single cables in a tray tests and five air-dropped cable tests were determined. These tests cover thermoplastic and thermoset cables at varying exposure levels. The same tests were also used with the strict application of the Appendix H tables and with the proposed heat soak method. Results are shown in Figure A-6. All of the Appendix H predictions are lower times than THIEF (on average 23% lower). Most heat soak predictions are lower times than THIEF, a few are slightly high (within 2%), and one is about 13% high. The average is a 5% under prediction. Because THIEF has a -15% bias, the fact that one result is 13% high is not considered significant as it is still within the THIEF bias. These validation results demonstrate that the heat soak method reduces the conservatism of the strict application of Appendix H while still maintaining a slight degree of conservatism when compared to the higher fidelity THIEF method.

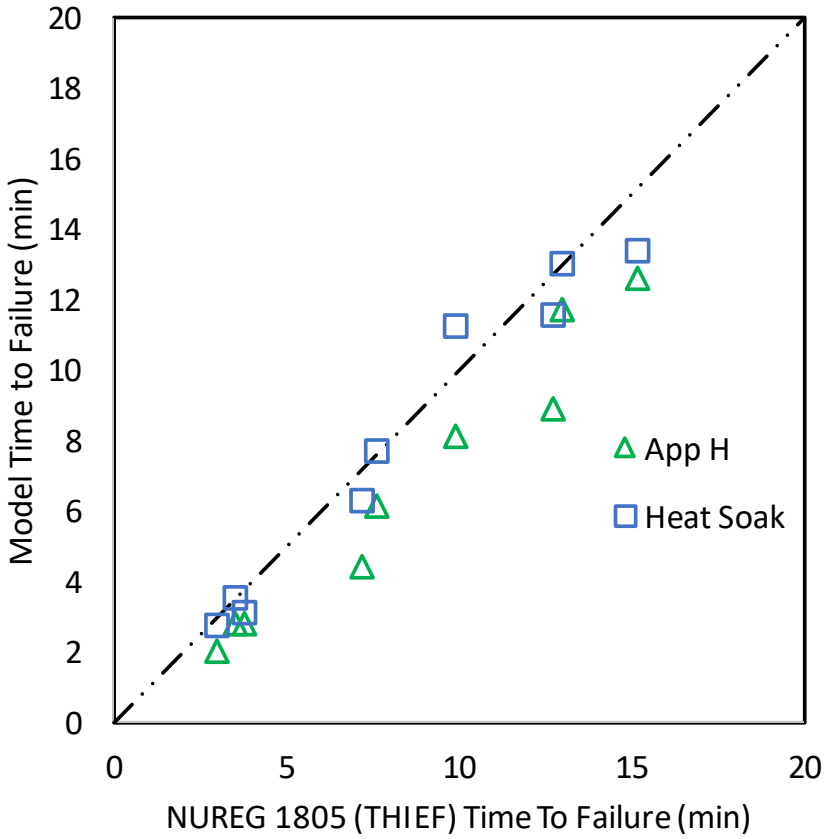

Figure A-6
Result comparing THIEF (NUREG-1805) with Appendix H tables and the heat soak approach

A.6 Conclusions

A new damage integral based method was developed to evaluate the time to failure for generic cables exposed to elevated temperatures or heat fluxes. The approach was motivated by engineering methods used to evaluate times to skin burn, an analogous problem. The reaction rate term in the damage integral was based upon the time to failure data provided in Appendix H of NUREG/CR-6850. The method was verified and validated and shown to be less conservative than Appendix H but still conservative when compared with THIEF which models 1-D, cylindrical heat transfer.

APPENDIX B
SECTION 3 TABLES RECOMPUTED USING ADJUSTED SOLID FLAME MODEL

The obstruction factor (Obs_fac) tables from Section 3 are reproduced in this appendix using the proposed adjusted Fire Dynamics Tools (FDT^s) for the reference zone of influence (ZOI) instead of the unadjusted FDT^s. Note that the maximum severity factor tables from Section 3 are computed solely from the Fire Dynamics Simulator results and there is no dependence on the FDT^s. Table B-1 and Table B-2 show the Obs_fac values for Group 4a and Group 4b for unvented cabinet faces and vented cabinet faces respectively. Table B-3 shows the results for Groups 1, 2, and 3. Note that significant differences are seen compared with the tables in Section 3.1 and Section 3.4. As seen in Figure 2-4, the unadjusted FDT^s results in effective radiant fractions that are a factor of 2 or more larger than typically assumed in probabilistic risk assessments. Additionally, the cabinet acts like a small compartment that causes the fire to lean toward the vented face (that is, effectively closer to the target), which, when combined with the long-term heating of the cabinet interior, can result in cases where the cabinet exposure based on the FDS predictions becomes more severe than a fire exposure using the FDT^s alone.

Table B-1
Obstructed radiation (horizontal) ZOI factor (Obs_fac) for Group 4a (large) and Group 4b (medium) unvented[1] cabinet faces using the adjusted solid flame FDT^s

Cabinet Size	Cabinet Ventilation[2]	Cable Type	Threshold Approach ZOI Factor[3] (Very Low/Low/Default)	Damage Integral Approach ZOI Factor[3] (Very Low/Low/Default)
Large	Open	TP	SCRN/0.88/0.88	SCRN/0.66/0.71
		TS	SCRN/0.98/0.75	SCRN/0.65/0.75
	Closed	TP	SCRN/0.91/1.21	SCRN/0.68/1.06
		TS	SCRN/0.94/1.16	SCRN/0.94/1.16
Medium	Open	TP	SCRN/0.71/0.93	SCRN/0.71/0.81
		TS	SCRN/0.70/0.76	SCRN/0.70/0.76
	Closed	TP	SCRN/0.95/1.25	SCRN/0.95/1.09
		TS	SCRN/1.12/1.43	SCRN/1.12/1.43

1 Unvented indicates a face that does not support significant ventilation (for example, a louver, meshed opening, missing panel, or the face with a door for a non-robustly secured cabinet).
2 *Open/Closed* refers to open/closed definitions in NUREG-2178.
3 SCRN indicates the scenario screens at the 98th percentile.
TS = thermoset
TP = thermoplastic

Table B-2
Obstructed radiation (horizontal) ZOI factor (Obs_fac) for Group 4a (large) and Group 4b (medium) vented cabinet faces using the adjusted solid flame FDT^s

Cabinet Size	Cabinet Ventilation[2]	Cable Type	Threshold Approach ZOI Factor[3] (Very Low/Low/Default)	Damage Integral Approach ZOI Factor[3] (Very Low/Low/Default)
Large	Open	TP	0.72/1.43/1.41	SCRN/1.21/1.32
		TS	SCRN/1.31/1.51	SCRN/1.31/1.51
	Closed	TP	0.59/0.91/1.36	0.59/0.68/1.21
		TS	SCRN/0.96/1.74	SCRN/0.96/1.74
Medium	Open	TP	0.27/1.41/1.51	0.27/1.24/1.39
		TS	SCRN/1.40/1.71	SCRN/1.40/1.71
	Closed	TP	0.93/0.95/1.56	0.93/0.95/1.25
		TS	1.50/1.16/1.72	1.50/1.16/1.72

[1] Vented indicates a face that supports significant ventilation (for example, a louver, meshed opening, missing panel, or the face with the door for a non-robustly secured cabinet).
[2] *Open/Closed* refers to open/closed definitions in NUREG-2178.
[3] SCRN indicates the scenario screens at the 98th percentile.
TS = thermoset
TP = thermoplastic

Table B-3
Obstructed radiation (horizontal) ZOI factor (Obs_fac) for Groups 1, 2, and 3 using the adjusted solid flame FDT^s

Cabinet Type	Size	98th Fire Size (kW)	Obs_fac[1]			
			Vented[2]		Unvented[3]	
			TP	TS	TP	TS
Switchgear and load centers	Medium (0.3 m^3 [12 ft^3) to 1.4 m^3 [50 ft^3])	170	1.46 1.11	1.70 1.70	1.20 1.03	1.54 1.54
	Large (>1.4 m^3 [50 ft^3])	170	0.76 0.80	0.99 0.99	0.42 0.34	0.34 0.34
Motor control centers and battery chargers	Medium (0.3 m^3 [12 ft^3] to 1.4 m^3 (50 ft^3])	130	1.24 0.96	1.52 1.52	1.10 0.96	1.51 1.51
	Large (>1.4 m^3 [50 ft^3])	130	0.67 0.67	0.62 0.62	0.03 0.03	SCRN SCRN
Power inverters	Medium (0.3 m^3 [12 ft^3] to 1.4 m^3 (50 ft^3])	200	1.57 1.25	1.74 0.72	1.25 1.09	1.46 0.61
	Large (>1.4 m^3 [50 ft^3])	200	0.91 0.69	0.97 0.97	0.89 0.67	0.90 0.90

1 Threshold ZOI presented in top portion, damage integral ZOI in bottom portion.
2 Vented indicates a face that supports significant ventilation (for example, a louver, meshed opening, missing panel, or the face with the door for a non-robustly secured cabinet).
3 Unvented indicates a face that does not support significant ventilation (for example, a louver, meshed opening, missing panel, or the face with a door for a non-robustly secured cabinet).

APPENDIX C
FDS INPUT FILES FOR OBSTRUCTED RADIATION

Fire Dynamics Simulator (FDS) input example files are shown in this section. These are the 98th percentile open and closed input files for the 0.3 m^3 (12 ft^3) medium cabinet and 1.4 m^3 (50 ft^3) large cabinet with a time-dependent fire. Fire size for other similar simulations is controlled by varying the HRRPUA parameter on the Fire &SURF input line. To reduce space, only one triplet of &DEVC for measuring heat flux is shown for each cabinet type along with a notation discussing total set of &DEVC inputs. Additionally, the &RAMP input for defining the fire is only shown for the first input.

C.1 FDS Input File: 0.3 m^3 (12 ft^3) Medium Open Cabinet, 98th Percentile

```
&HEAD CHID='m12-98th-open-cyl-cor-sq', TITLE='Medium (12 ft^3) cabinet, 98th
percentile, open, cylindrical source in corner, square aspect ratio'/
&TIME T_END=2340.0/
&MISC HVAC_PRES_RELAX=0.3/
&PRES
VELOCITY_TOLERANCE=0.001,MAX_PRESSURE_ITERATIONS=50,PRESSURE_TOLERANCE=20000,SUSPEND_P
RESSURE_ITERATIONS=.TRUE./
&DUMP DT_DEVC=1, DT_RESTART=30.0/

&SURF ID             = 'WALL'
     COLOR          = 'TAN'
     MATL_ID        = 'CONCRETE'
     THICKNESS      = 0.6
     DEFAULT = .TRUE.     /

&MATL ID            = 'CONCRETE'
     FYI           = 'TABLE 3-1 NUREG 1934'
     CONDUCTIVITY = 1.6
     SPECIFIC_HEAT = 0.1
     DENSITY       = 2400./

&SURF ID             = 'CAB'
     COLOR          = 'GRAY'
     MATL_ID        = 'STEEL'
     THICKNESS      = 0.0015
     BACKING        = 'EXPOSED'/

&MATL ID            = 'STEEL'
     FYI           = 'TABLE 3-1 NUREG 1934'
     CONDUCTIVITY = 54
     SPECIFIC_HEAT = 0.1
     DENSITY       = 7850./
```

```
&VENT MB='XMIN', SURF_ID='OPEN'/
&VENT MB='YMIN', SURF_ID='OPEN'/
&VENT MB='XMAX', SURF_ID='OPEN'/
&VENT MB='YMAX', SURF_ID='OPEN'/
&VENT MB='ZMAX', SURF_ID='OPEN'/

&REAC FUEL='ETHYLENE', SOOT_YIELD=0.12,RADIATIVE_FRACTION=0.3  /
&RADI NUMBER_RADIATION_ANGLES=200/

&MESH XB=-2.54000,2.54000,-2.54000,2.54000,0.00000,2.84480,IJK=100,100,56/
&OBST XB=0.30480,0.35560,-0.35560,0.35560,0.00000,0.96520,SURF_ID='CAB'/
&OBST XB=-0.35560,0.35560,-0.35560,-0.30480,0.00000,0.96520,SURF_ID='CAB'/
&OBST XB=-0.35560,0.35560,0.30480,0.35560,0.00000,0.96520,SURF_ID='CAB'/
&OBST XB=-0.35560,0.35560,-0.35560,0.35560,0.91440,0.96520,SURF_ID='CAB'/

&SURF ID='FIRE',COLOR='RED',HRRPUA=874.5677,RAMP_Q='FIRE RAMP'/
&OBST XB=0.1016,0.2032,0.1016,0.2032,0.00000,0.91440,SURF_ID='FIRE'/

&SLCF PBX = 0.0,QUANTITY='TEMPERATURE',VECTOR=.TRUE./
&SLCF PBY = 0.0,QUANTITY='TEMPERATURE',VECTOR=.TRUE./

&SLCF PBX = 0.0, QUANTITY='INTEGRATED INTENSITY'/
&SLCF PBY = 0.0, QUANTITY='INTEGRATED INTENSITY'/

&BNDF QUANTITY='WALL TEMPERATURE'/

&DEVC QUANTITY='RADIATIVE HEAT FLUX GAS',XYZ=-0.5080,0.0000,0.2286,ID='N1-
1H',ORIENTATION=1,0,0/
&DEVC QUANTITY='RADIATIVE HEAT FLUX GAS',XYZ=-0.5080,0.0000,0.2286,ID='N1-
1U',ORIENTATION=0,0,1/
&DEVC QUANTITY='RADIATIVE HEAT FLUX GAS',XYZ=-0.5080,0.0000,0.2286,ID='N1-
1D',ORIENTATION=0,0,-1/
```

The DEVC ID is WX-YZ. W is N for the North or Vented Face of the cabinet, S for the South Face, and W for the West Face. The East Face was not instrumented as it will be less than or equal to the W Face (the fire source was a cylinder in the SW corner). X is the vertical position starting at 0.2286 m (approximately 25% of the cabinet height) and going to 2.7432 m in 0.2286 m increments. Y is the horizontal position starting at 0.6096 m (0.1524 m from the face) and going to 2.3368 m in 0.1016 m increments. Z is H for a device pointed at the cabinet, U for a device pointed vertically upward, and D for a device pointed vertically downward. The same array spacing was used for each of the N, S, and W arrays of devices.

```
&RAMP ID='FIRE RAMP', T=0, F=0.0000/
&RAMP ID='FIRE RAMP', T=10, F=0.0002/
&RAMP ID='FIRE RAMP', T=20, F=0.0008/
&RAMP ID='FIRE RAMP', T=30, F=0.0017/
&RAMP ID='FIRE RAMP', T=40, F=0.0031/
&RAMP ID='FIRE RAMP', T=50, F=0.0048/
&RAMP ID='FIRE RAMP', T=60, F=0.0069/
&RAMP ID='FIRE RAMP', T=70, F=0.0095/
&RAMP ID='FIRE RAMP', T=80, F=0.0123/
&RAMP ID='FIRE RAMP', T=90, F=0.0156/
&RAMP ID='FIRE RAMP', T=100, F=0.0193/
&RAMP ID='FIRE RAMP', T=110, F=0.0233/
&RAMP ID='FIRE RAMP', T=120, F=0.0278/
&RAMP ID='FIRE RAMP', T=130, F=0.0326/
&RAMP ID='FIRE RAMP', T=140, F=0.0378/
&RAMP ID='FIRE RAMP', T=150, F=0.0434/
&RAMP ID='FIRE RAMP', T=160, F=0.0494/
&RAMP ID='FIRE RAMP', T=170, F=0.0557/
&RAMP ID='FIRE RAMP', T=180, F=0.0625/
```

```
&RAMP ID='FIRE RAMP', T=190, F=0.0696/
&RAMP ID='FIRE RAMP', T=200, F=0.0772/
&RAMP ID='FIRE RAMP', T=210, F=0.0851/
&RAMP ID='FIRE RAMP', T=220, F=0.0934/
&RAMP ID='FIRE RAMP', T=230, F=0.1020/
&RAMP ID='FIRE RAMP', T=240, F=0.1111/
&RAMP ID='FIRE RAMP', T=250, F=0.1206/
&RAMP ID='FIRE RAMP', T=260, F=0.1304/
&RAMP ID='FIRE RAMP', T=270, F=0.1406/
&RAMP ID='FIRE RAMP', T=280, F=0.1512/
&RAMP ID='FIRE RAMP', T=290, F=0.1622/
&RAMP ID='FIRE RAMP', T=300, F=0.1736/
&RAMP ID='FIRE RAMP', T=310, F=0.1854/
&RAMP ID='FIRE RAMP', T=320, F=0.1975/
&RAMP ID='FIRE RAMP', T=330, F=0.2101/
&RAMP ID='FIRE RAMP', T=340, F=0.2230/
&RAMP ID='FIRE RAMP', T=350, F=0.2363/
&RAMP ID='FIRE RAMP', T=360, F=0.2500/
&RAMP ID='FIRE RAMP', T=370, F=0.2641/
&RAMP ID='FIRE RAMP', T=380, F=0.2785/
&RAMP ID='FIRE RAMP', T=390, F=0.2934/
&RAMP ID='FIRE RAMP', T=400, F=0.3086/
&RAMP ID='FIRE RAMP', T=410, F=0.3243/
&RAMP ID='FIRE RAMP', T=420, F=0.3403/
&RAMP ID='FIRE RAMP', T=430, F=0.3567/
&RAMP ID='FIRE RAMP', T=440, F=0.3735/
&RAMP ID='FIRE RAMP', T=450, F=0.3906/
&RAMP ID='FIRE RAMP', T=460, F=0.4082/
&RAMP ID='FIRE RAMP', T=470, F=0.4261/
&RAMP ID='FIRE RAMP', T=480, F=0.4444/
&RAMP ID='FIRE RAMP', T=490, F=0.4632/
&RAMP ID='FIRE RAMP', T=500, F=0.4823/
&RAMP ID='FIRE RAMP', T=510, F=0.5017/
&RAMP ID='FIRE RAMP', T=520, F=0.5216/
&RAMP ID='FIRE RAMP', T=530, F=0.5419/
&RAMP ID='FIRE RAMP', T=540, F=0.5625/
&RAMP ID='FIRE RAMP', T=550, F=0.5835/
&RAMP ID='FIRE RAMP', T=560, F=0.6049/
&RAMP ID='FIRE RAMP', T=570, F=0.6267/
&RAMP ID='FIRE RAMP', T=580, F=0.6489/
&RAMP ID='FIRE RAMP', T=590, F=0.6715/
&RAMP ID='FIRE RAMP', T=600, F=0.6944/
&RAMP ID='FIRE RAMP', T=610, F=0.7178/
&RAMP ID='FIRE RAMP', T=620, F=0.7415/
&RAMP ID='FIRE RAMP', T=630, F=0.7656/
&RAMP ID='FIRE RAMP', T=640, F=0.7901/
&RAMP ID='FIRE RAMP', T=650, F=0.8150/
&RAMP ID='FIRE RAMP', T=660, F=0.8403/
&RAMP ID='FIRE RAMP', T=670, F=0.8659/
&RAMP ID='FIRE RAMP', T=680, F=0.8920/
&RAMP ID='FIRE RAMP', T=690, F=0.9184/
&RAMP ID='FIRE RAMP', T=700, F=0.9452/
&RAMP ID='FIRE RAMP', T=710, F=0.9724/
&RAMP ID='FIRE RAMP', T=720, F=1.0000/
&RAMP ID='FIRE RAMP', T=730, F=1.0000/
&RAMP ID='FIRE RAMP', T=740, F=1.0000/
&RAMP ID='FIRE RAMP', T=750, F=1.0000/
&RAMP ID='FIRE RAMP', T=760, F=1.0000/
&RAMP ID='FIRE RAMP', T=770, F=1.0000/
&RAMP ID='FIRE RAMP', T=780, F=1.0000/
&RAMP ID='FIRE RAMP', T=790, F=1.0000/
&RAMP ID='FIRE RAMP', T=800, F=1.0000/
&RAMP ID='FIRE RAMP', T=810, F=1.0000/
```

```
&RAMP ID='FIRE RAMP', T=820, F=1.0000/
&RAMP ID='FIRE RAMP', T=830, F=1.0000/
&RAMP ID='FIRE RAMP', T=840, F=1.0000/
&RAMP ID='FIRE RAMP', T=850, F=1.0000/
&RAMP ID='FIRE RAMP', T=860, F=1.0000/
&RAMP ID='FIRE RAMP', T=870, F=1.0000/
&RAMP ID='FIRE RAMP', T=880, F=1.0000/
&RAMP ID='FIRE RAMP', T=890, F=1.0000/
&RAMP ID='FIRE RAMP', T=900, F=1.0000/
&RAMP ID='FIRE RAMP', T=910, F=1.0000/
&RAMP ID='FIRE RAMP', T=920, F=1.0000/
&RAMP ID='FIRE RAMP', T=930, F=1.0000/
&RAMP ID='FIRE RAMP', T=940, F=1.0000/
&RAMP ID='FIRE RAMP', T=950, F=1.0000/
&RAMP ID='FIRE RAMP', T=960, F=1.0000/
&RAMP ID='FIRE RAMP', T=970, F=1.0000/
&RAMP ID='FIRE RAMP', T=980, F=1.0000/
&RAMP ID='FIRE RAMP', T=990, F=1.0000/
&RAMP ID='FIRE RAMP', T=1000, F=1.0000/
&RAMP ID='FIRE RAMP', T=1010, F=1.0000/
&RAMP ID='FIRE RAMP', T=1020, F=1.0000/
&RAMP ID='FIRE RAMP', T=1030, F=1.0000/
&RAMP ID='FIRE RAMP', T=1040, F=1.0000/
&RAMP ID='FIRE RAMP', T=1050, F=1.0000/
&RAMP ID='FIRE RAMP', T=1060, F=1.0000/
&RAMP ID='FIRE RAMP', T=1070, F=1.0000/
&RAMP ID='FIRE RAMP', T=1080, F=1.0000/
&RAMP ID='FIRE RAMP', T=1090, F=1.0000/
&RAMP ID='FIRE RAMP', T=1100, F=1.0000/
&RAMP ID='FIRE RAMP', T=1110, F=1.0000/
&RAMP ID='FIRE RAMP', T=1120, F=1.0000/
&RAMP ID='FIRE RAMP', T=1130, F=1.0000/
&RAMP ID='FIRE RAMP', T=1140, F=1.0000/
&RAMP ID='FIRE RAMP', T=1150, F=1.0000/
&RAMP ID='FIRE RAMP', T=1160, F=1.0000/
&RAMP ID='FIRE RAMP', T=1170, F=1.0000/
&RAMP ID='FIRE RAMP', T=1180, F=1.0000/
&RAMP ID='FIRE RAMP', T=1190, F=1.0000/
&RAMP ID='FIRE RAMP', T=1200, F=1.0000/
&RAMP ID='FIRE RAMP', T=1210, F=0.9999/
&RAMP ID='FIRE RAMP', T=1220, F=0.9997/
&RAMP ID='FIRE RAMP', T=1230, F=0.9993/
&RAMP ID='FIRE RAMP', T=1240, F=0.9988/
&RAMP ID='FIRE RAMP', T=1250, F=0.9981/
&RAMP ID='FIRE RAMP', T=1260, F=0.9972/
&RAMP ID='FIRE RAMP', T=1270, F=0.9962/
&RAMP ID='FIRE RAMP', T=1280, F=0.9951/
&RAMP ID='FIRE RAMP', T=1290, F=0.9938/
&RAMP ID='FIRE RAMP', T=1300, F=0.9923/
&RAMP ID='FIRE RAMP', T=1310, F=0.9907/
&RAMP ID='FIRE RAMP', T=1320, F=0.9889/
&RAMP ID='FIRE RAMP', T=1330, F=0.9870/
&RAMP ID='FIRE RAMP', T=1340, F=0.9849/
&RAMP ID='FIRE RAMP', T=1350, F=0.9827/
&RAMP ID='FIRE RAMP', T=1360, F=0.9803/
&RAMP ID='FIRE RAMP', T=1370, F=0.9778/
&RAMP ID='FIRE RAMP', T=1380, F=0.9751/
&RAMP ID='FIRE RAMP', T=1390, F=0.9722/
&RAMP ID='FIRE RAMP', T=1400, F=0.9692/
&RAMP ID='FIRE RAMP', T=1410, F=0.9661/
&RAMP ID='FIRE RAMP', T=1420, F=0.9628/
&RAMP ID='FIRE RAMP', T=1430, F=0.9593/
&RAMP ID='FIRE RAMP', T=1440, F=0.9557/
```

```
&RAMP ID='FIRE RAMP', T=1450, F=0.9519/
&RAMP ID='FIRE RAMP', T=1460, F=0.9480/
&RAMP ID='FIRE RAMP', T=1470, F=0.9439/
&RAMP ID='FIRE RAMP', T=1480, F=0.9397/
&RAMP ID='FIRE RAMP', T=1490, F=0.9353/
&RAMP ID='FIRE RAMP', T=1500, F=0.9307/
&RAMP ID='FIRE RAMP', T=1510, F=0.9261/
&RAMP ID='FIRE RAMP', T=1520, F=0.9212/
&RAMP ID='FIRE RAMP', T=1530, F=0.9162/
&RAMP ID='FIRE RAMP', T=1540, F=0.9110/
&RAMP ID='FIRE RAMP', T=1550, F=0.9057/
&RAMP ID='FIRE RAMP', T=1560, F=0.9003/
&RAMP ID='FIRE RAMP', T=1570, F=0.8947/
&RAMP ID='FIRE RAMP', T=1580, F=0.8889/
&RAMP ID='FIRE RAMP', T=1590, F=0.8830/
&RAMP ID='FIRE RAMP', T=1600, F=0.8769/
&RAMP ID='FIRE RAMP', T=1610, F=0.8707/
&RAMP ID='FIRE RAMP', T=1620, F=0.8643/
&RAMP ID='FIRE RAMP', T=1630, F=0.8577/
&RAMP ID='FIRE RAMP', T=1640, F=0.8510/
&RAMP ID='FIRE RAMP', T=1650, F=0.8442/
&RAMP ID='FIRE RAMP', T=1660, F=0.8372/
&RAMP ID='FIRE RAMP', T=1670, F=0.8300/
&RAMP ID='FIRE RAMP', T=1680, F=0.8227/
&RAMP ID='FIRE RAMP', T=1690, F=0.8153/
&RAMP ID='FIRE RAMP', T=1700, F=0.8076/
&RAMP ID='FIRE RAMP', T=1710, F=0.7999/
&RAMP ID='FIRE RAMP', T=1720, F=0.7919/
&RAMP ID='FIRE RAMP', T=1730, F=0.7839/
&RAMP ID='FIRE RAMP', T=1740, F=0.7756/
&RAMP ID='FIRE RAMP', T=1750, F=0.7672/
&RAMP ID='FIRE RAMP', T=1760, F=0.7587/
&RAMP ID='FIRE RAMP', T=1770, F=0.7500/
&RAMP ID='FIRE RAMP', T=1780, F=0.7412/
&RAMP ID='FIRE RAMP', T=1790, F=0.7321/
&RAMP ID='FIRE RAMP', T=1800, F=0.7230/
&RAMP ID='FIRE RAMP', T=1810, F=0.7137/
&RAMP ID='FIRE RAMP', T=1820, F=0.7042/
&RAMP ID='FIRE RAMP', T=1830, F=0.6946/
&RAMP ID='FIRE RAMP', T=1840, F=0.6848/
&RAMP ID='FIRE RAMP', T=1850, F=0.6749/
&RAMP ID='FIRE RAMP', T=1860, F=0.6648/
&RAMP ID='FIRE RAMP', T=1870, F=0.6546/
&RAMP ID='FIRE RAMP', T=1880, F=0.6442/
&RAMP ID='FIRE RAMP', T=1890, F=0.6337/
&RAMP ID='FIRE RAMP', T=1900, F=0.6230/
&RAMP ID='FIRE RAMP', T=1910, F=0.6121/
&RAMP ID='FIRE RAMP', T=1920, F=0.6011/
&RAMP ID='FIRE RAMP', T=1930, F=0.5900/
&RAMP ID='FIRE RAMP', T=1940, F=0.5786/
&RAMP ID='FIRE RAMP', T=1950, F=0.5672/
&RAMP ID='FIRE RAMP', T=1960, F=0.5556/
&RAMP ID='FIRE RAMP', T=1970, F=0.5438/
&RAMP ID='FIRE RAMP', T=1980, F=0.5319/
&RAMP ID='FIRE RAMP', T=1990, F=0.5198/
&RAMP ID='FIRE RAMP', T=2000, F=0.5075/
&RAMP ID='FIRE RAMP', T=2010, F=0.4952/
&RAMP ID='FIRE RAMP', T=2020, F=0.4826/
&RAMP ID='FIRE RAMP', T=2030, F=0.4699/
&RAMP ID='FIRE RAMP', T=2040, F=0.4571/
&RAMP ID='FIRE RAMP', T=2050, F=0.4441/
&RAMP ID='FIRE RAMP', T=2060, F=0.4309/
&RAMP ID='FIRE RAMP', T=2070, F=0.4176/
```

```
&RAMP ID='FIRE RAMP', T=2080, F=0.4041/
&RAMP ID='FIRE RAMP', T=2090, F=0.3905/
&RAMP ID='FIRE RAMP', T=2100, F=0.3767/
&RAMP ID='FIRE RAMP', T=2110, F=0.3628/
&RAMP ID='FIRE RAMP', T=2120, F=0.3487/
&RAMP ID='FIRE RAMP', T=2130, F=0.3345/
&RAMP ID='FIRE RAMP', T=2140, F=0.3201/
&RAMP ID='FIRE RAMP', T=2150, F=0.3056/
&RAMP ID='FIRE RAMP', T=2160, F=0.2909/
&RAMP ID='FIRE RAMP', T=2170, F=0.2760/
&RAMP ID='FIRE RAMP', T=2180, F=0.2610/
&RAMP ID='FIRE RAMP', T=2190, F=0.2458/
&RAMP ID='FIRE RAMP', T=2200, F=0.2305/
&RAMP ID='FIRE RAMP', T=2210, F=0.2151/
&RAMP ID='FIRE RAMP', T=2220, F=0.1994/
&RAMP ID='FIRE RAMP', T=2230, F=0.1837/
&RAMP ID='FIRE RAMP', T=2240, F=0.1677/
&RAMP ID='FIRE RAMP', T=2250, F=0.1517/
&RAMP ID='FIRE RAMP', T=2260, F=0.1354/
&RAMP ID='FIRE RAMP', T=2270, F=0.1190/
&RAMP ID='FIRE RAMP', T=2280, F=0.1025/
&RAMP ID='FIRE RAMP', T=2290, F=0.0858/
&RAMP ID='FIRE RAMP', T=2300, F=0.0689/
&RAMP ID='FIRE RAMP', T=2310, F=0.0519/
&RAMP ID='FIRE RAMP', T=2320, F=0.0348/
&RAMP ID='FIRE RAMP', T=2330, F=0.0175/
&RAMP ID='FIRE RAMP', T=2340, F=0.0000/

&TAIL/
```

C.2 FDS Input File: 0.3 m^3 (12 ft^3) Medium Closed Cabinet, 98th Percentile

```
&HEAD CHID='m12-98th-tbl-cyl-cor-sq', TITLE='Medium (12 ft^3) cabinet, 98th
percentile, top-bottom louvers, cylindrical source in corner, square aspect ratio'/
&TIME T_END=2340.0/
&MISC HVAC_PRES_RELAX=0.3/
&PRES
VELOCITY_TOLERANCE=0.001,MAX_PRESSURE_ITERATIONS=50,PRESSURE_TOLERANCE=20000,SUSPEND_P
RESSURE_ITERATIONS=.TRUE./
&DUMP DT_DEVC=1, DT_RESTART=30.0/

&SURF ID             = 'WALL'
     COLOR          = 'TAN'
     MATL_ID        = 'CONCRETE'
     THICKNESS      = 0.6
     DEFAULT = .TRUE.     /

&MATL ID            = 'CONCRETE'
     FYI           = 'TABLE 3-1 NUREG 1934'
     CONDUCTIVITY = 1.6
     SPECIFIC_HEAT = 0.1
     DENSITY       = 2400./

&SURF ID             = 'CAB'
     COLOR          = 'GRAY'
     MATL_ID        = 'STEEL'
     THICKNESS      = 0.0015
     BACKING        = 'EXPOSED'/

&MATL ID            = 'STEEL'
     FYI           = 'TABLE 3-1 NUREG 1934'
     CONDUCTIVITY = 54
     SPECIFIC_HEAT = 0.1
```

```
     DENSITY       = 7850./

&VENT MB='XMIN', SURF_ID='OPEN'/
&VENT MB='YMIN', SURF_ID='OPEN'/
&VENT MB='XMAX', SURF_ID='OPEN'/
&VENT MB='YMAX', SURF_ID='OPEN'/
&VENT MB='ZMAX', SURF_ID='OPEN'/

&REAC FUEL='ETHYLENE', SOOT_YIELD=0.12,RADIATIVE_FRACTION=0.3  /
&RADI NUMBER_RADIATION_ANGLES=200/

&MESH XB=-2.54000,2.54000,-2.54000,2.54000,0.00000,2.84480,IJK=100,100,56/
&ZONE XB=-0.30480,0.30480,-0.30480,0.30480,0.00000,0.91440/
&OBST XB=-0.35560,-0.30480,-0.35560,0.35560,0.00000,0.96520,SURF_ID='CAB'/
&OBST XB=0.30480,0.35560,-0.35560,0.35560,0.00000,0.96520,SURF_ID='CAB'/
&OBST XB=-0.35560,0.35560,-0.35560,-0.30480,0.00000,0.96520,SURF_ID='CAB'/
&OBST XB=-0.35560,0.35560,0.30480,0.35560,0.00000,0.96520,SURF_ID='CAB'/
&OBST XB=-0.35560,0.35560,-0.35560,0.35560,0.91440,0.96520,SURF_ID='CAB'/

&SURF ID='FIRE',COLOR='RED',HRRPUA=538.1955,RAMP_Q='FIRE RAMP'/
&OBST XB=0.1016,0.2032,0.1016,0.2032,0.00000,0.91440,SURF_ID='FIRE'/

&VENT XB=-0.35560,-0.35560,-
0.25400,0.25400,0.05080,0.10160,SURF_ID='CAB',ID='VENTo1',COLOR='GREEN'/
&VENT XB=-0.35560,-0.35560,-
0.25400,0.25400,0.10160,0.15240,SURF_ID='CAB',ID='VENTo2',COLOR='BLUE'/
&VENT XB=-0.35560,-0.35560,-
0.25400,0.25400,0.15240,0.20320,SURF_ID='CAB',ID='VENTo3',COLOR='GREEN'/
&VENT XB=-0.35560,-0.35560,-
0.25400,0.25400,0.20320,0.25400,SURF_ID='CAB',ID='VENTo4',COLOR='BLUE'/

&VENT XB=-0.35560,-0.35560,-
0.25400,0.25400,0.66040,0.71120,SURF_ID='CAB',ID='VENTo13',COLOR='GREEN'/
&VENT XB=-0.35560,-0.35560,-
0.25400,0.25400,0.71120,0.76200,SURF_ID='CAB',ID='VENTo14',COLOR='BLUE'/
&VENT XB=-0.35560,-0.35560,-
0.25400,0.25400,0.76200,0.81280,SURF_ID='CAB',ID='VENTo15',COLOR='GREEN'/
&VENT XB=-0.35560,-0.35560,-
0.25400,0.25400,0.81280,0.86360,SURF_ID='CAB',ID='VENTo16',COLOR='BLUE'/

&VENT XB=-0.30480,-0.30480,-
0.25400,0.25400,0.05080,0.10160,SURF_ID='CAB',ID='VENTi1',COLOR='GREEN'/
&VENT XB=-0.30480,-0.30480,-
0.25400,0.25400,0.10160,0.15240,SURF_ID='CAB',ID='VENTi2',COLOR='BLUE'/
&VENT XB=-0.30480,-0.30480,-
0.25400,0.25400,0.15240,0.20320,SURF_ID='CAB',ID='VENTi3',COLOR='GREEN'/
&VENT XB=-0.30480,-0.30480,-
0.25400,0.25400,0.20320,0.25400,SURF_ID='CAB',ID='VENTi4',COLOR='BLUE'/

&VENT XB=-0.30480,-0.30480,-
0.25400,0.25400,0.66040,0.71120,SURF_ID='CAB',ID='VENTi13',COLOR='GREEN'/
&VENT XB=-0.30480,-0.30480,-
0.25400,0.25400,0.71120,0.76200,SURF_ID='CAB',ID='VENTi14',COLOR='BLUE'/
&VENT XB=-0.30480,-0.30480,-
0.25400,0.25400,0.76200,0.81280,SURF_ID='CAB',ID='VENTi15',COLOR='GREEN'/
&VENT XB=-0.30480,-0.30480,-
0.25400,0.25400,0.81280,0.86360,SURF_ID='CAB',ID='VENTi16',COLOR='BLUE'/

&HVAC TYPE_ID='LEAK',VENT_ID='VENTo1',VENT2_ID='VENTi1',ID='VENT1',AREA=0.013/
&HVAC TYPE_ID='LEAK',VENT_ID='VENTo2',VENT2_ID='VENTi2',ID='VENT2',AREA=0.013/
&HVAC TYPE_ID='LEAK',VENT_ID='VENTo3',VENT2_ID='VENTi3',ID='VENT3',AREA=0.013/
&HVAC TYPE_ID='LEAK',VENT_ID='VENTo4',VENT2_ID='VENTi4',ID='VENT4',AREA=0.013/
```

```
&HVAC TYPE_ID='LEAK',VENT_ID='VENTo13',VENT2_ID='VENTi13',ID='VENT13',AREA=0.013/
&HVAC TYPE_ID='LEAK',VENT_ID='VENTo14',VENT2_ID='VENTi14',ID='VENT14',AREA=0.013/
&HVAC TYPE_ID='LEAK',VENT_ID='VENTo15',VENT2_ID='VENTi15',ID='VENT15',AREA=0.013/
&HVAC TYPE_ID='LEAK',VENT_ID='VENTo16',VENT2_ID='VENTi16',ID='VENT16',AREA=0.013/

&SLCF PBX = 0.0,QUANTITY='TEMPERATURE',VECTOR=.TRUE./
&SLCF PBY = 0.0,QUANTITY='TEMPERATURE',VECTOR=.TRUE./

&SLCF PBX = 0.0, QUANTITY='INTEGRATED INTENSITY'/
&SLCF PBY = 0.0, QUANTITY='INTEGRATED INTENSITY'/

&BNDF QUANTITY='WALL TEMPERATURE'/
```

This input uses the same array of devices and the same fire ramp as the 0.3 m^3 (12 ft^3) medium open cabinet.

```
&TAIL/
```

C.3 FDS Input File: 1.4 m^3 (50 ft^3) Large Open Cabinet, 98th Percentile

```
&HEAD CHID='l50-98th-op-cyl-cor-sq', TITLE='large (50 ft^3) cabinet, 98th percentile,
open, cylindrical source in corner, square aspect ratio'/
&TIME T_END=2340.0/
&MISC HVAC_PRES_RELAX=0.3/
&PRES
VELOCITY_TOLERANCE=0.001,MAX_PRESSURE_ITERATIONS=50,PRESSURE_TOLERANCE=20000,SUSPEND_P
RESSURE_ITERATIONS=.TRUE./
&DUMP DT_DEVC=1, DT_RESTART=30.0/

&SURF ID             = 'WALL'
     COLOR          = 'TAN'
     MATL_ID        = 'CONCRETE'
     THICKNESS      = 0.6
     DEFAULT = .TRUE.     /

&MATL ID            = 'CONCRETE'
     FYI           = 'TABLE 3-1 NUREG 1934'
     CONDUCTIVITY = 1.6
     SPECIFIC_HEAT = 0.1
     DENSITY       = 2400./

&SURF ID             = 'CAB'
     COLOR          = 'GRAY'
     MATL_ID        = 'STEEL'
     THICKNESS      = 0.0015
     BACKING        = 'EXPOSED'/

&MATL ID            = 'STEEL'
     FYI           = 'TABLE 3-1 NUREG 1934'
     CONDUCTIVITY = 54
     SPECIFIC_HEAT = 0.1
     DENSITY       = 7850./

&VENT MB='XMIN', SURF_ID='OPEN'/
&VENT MB='YMIN', SURF_ID='OPEN'/
&VENT MB='XMAX', SURF_ID='OPEN'/
&VENT MB='YMAX', SURF_ID='OPEN'/
&VENT MB='ZMAX', SURF_ID='OPEN'/

&REAC FUEL='ETHYLENE', SOOT_YIELD=0.12,RADIATIVE_FRACTION=0.3  /
&RADI NUMBER_RADIATION_ANGLES=200/
```

```
&MESH XB=-3.44620,3.44620,-3.44620,3.44620,0.00000,4.22031,IJK=94,94,60/
&OBST XB=0.43994,0.51326,-0.51326,0.51326,0.00000,1.89914,SURF_ID='CAB'/
&OBST XB=-0.51326,0.51326,-0.51326,-0.43994,0.00000,1.89914,SURF_ID='CAB'/
&OBST XB=-0.51326,0.51326,0.43994,0.51326,0.00000,1.89914,SURF_ID='CAB'/
&OBST XB=-0.51326,0.51326,-0.51326,0.51326,1.82880,1.89914,SURF_ID='CAB'/

&SURF ID='FIRE',COLOR='RED',HRRPUA=1864.376,RAMP_Q='FIRE RAMP'/

&OBST XB=0.21997,0.293293,0.21997,0.293293,0.00000,1.82880,SURF_ID='FIRE'/

&SLCF PBX = 0.0,QUANTITY='TEMPERATURE',VECTOR=.TRUE./
&SLCF PBY = 0.0,QUANTITY='TEMPERATURE',VECTOR=.TRUE./

&SLCF PBX = 0.0, QUANTITY='INTEGRATED INTENSITY'/
&SLCF PBY = 0.0, QUANTITY='INTEGRATED INTENSITY'/

&BNDF QUANTITY='WALL TEMPERATURE'/

&DEVC QUANTITY='RADIATIVE HEAT FLUX GAS',XYZ=-0.7332,0.0000,0.4572,ID='N1-
1H',ORIENTATION=1,0,0/
&DEVC QUANTITY='RADIATIVE HEAT FLUX GAS',XYZ=-0.7332,0.0000,0.4572,ID='N1-
1U',ORIENTATION=0,0,1/
&DEVC QUANTITY='RADIATIVE HEAT FLUX GAS',XYZ=-0.7332,0.0000,0.4572,ID='N1-
1D',ORIENTATION=0,0,-1/
```

The DEVC ID is WX-YZ. W is N for the North or Vented Face of the cabinet, S for the South Face, and W for the West Face. The East Face was not instrumented as it will be less than or equal to the W Face (the fire source was a cylinder in the SW corner). X is the vertical position starting at 0.4572 m (approximately 25% of the cabinet height) and going to 4.1148 m in 0.4572 m increments. Y is the horizontal position starting at 0.6096 m (0.2933 m from the face) and going to 3.5195 m in 0.1467 m increments. Z is H for a device pointed at the cabinet, U for a device pointed vertically upward, and D for a device pointed vertically downward. The same array spacing was used for each of the N, S, and W arrays of devices.

This input uses the same fire ramp as the 12 ft^3 medium open cabinet.

```
&TAIL/
```

C.4 FDS Input File: 1.4 m^3 (50 ft^3) Large Closed Cabinet, 98th Percentile

```
&HEAD CHID='l50-98th-tbl-cyl-cor-sq', TITLE='large (50 ft^3) cabinet, 98th percentile,
top-bottom louvers, cylindrical source in corner, square aspect ratio'/
&TIME T_END=2340.0/
&MISC HVAC_PRES_RELAX=0.3/
&PRES
VELOCITY_TOLERANCE=0.001,MAX_PRESSURE_ITERATIONS=50,PRESSURE_TOLERANCE=20000,SUSPEND_P
RESSURE_ITERATIONS=.TRUE./
&DUMP DT_DEVC=1, DT_RESTART=30.0/

&SURF ID             = 'WALL'
     COLOR          = 'TAN'
     MATL_ID        = 'CONCRETE'
     THICKNESS      = 0.6
     DEFAULT = .TRUE.     /

&MATL ID            = 'CONCRETE'
     FYI           = 'TABLE 3-1 NUREG 1934'
     CONDUCTIVITY = 1.6
     SPECIFIC_HEAT = 0.1
     DENSITY       = 2400./
```

```
&SURF ID             = 'CAB'
     COLOR          = 'GRAY'
     MATL_ID        = 'STEEL'
     THICKNESS      = 0.0015
     BACKING        = 'EXPOSED'/

&MATL ID            = 'STEEL'
     FYI           = 'TABLE 3-1 NUREG 1934'
     CONDUCTIVITY = 54
     SPECIFIC_HEAT = 0.1
     DENSITY       = 7850./

&VENT MB='XMIN', SURF_ID='OPEN'/
&VENT MB='YMIN', SURF_ID='OPEN'/
&VENT MB='XMAX', SURF_ID='OPEN'/
&VENT MB='YMAX', SURF_ID='OPEN'/
&VENT MB='ZMAX', SURF_ID='OPEN'/

&REAC FUEL='ETHYLENE', SOOT_YIELD=0.12,RADIATIVE_FRACTION=0.3  /
&RADI NUMBER_RADIATION_ANGLES=200/

&MESH XB=-3.44620,3.44620,-3.44620,3.44620,0.00000,4.22031,IJK=94,94,60/
&ZONE XB=-0.43994,0.43994,-0.43994,0.43994,0.00000,1.82880/
&OBST XB=-0.51326,-0.43994,-0.51326,0.51326,0.00000,1.89914,SURF_ID='CAB'/
&OBST XB=0.43994,0.51326,-0.51326,0.51326,0.00000,1.89914,SURF_ID='CAB'/
&OBST XB=-0.51326,0.51326,-0.51326,-0.43994,0.00000,1.89914,SURF_ID='CAB'/
&OBST XB=-0.51326,0.51326,0.43994,0.51326,0.00000,1.89914,SURF_ID='CAB'/
&OBST XB=-0.51326,0.51326,-0.51326,0.51326,1.82880,1.89914,SURF_ID='CAB'/

&SURF ID='FIRE',COLOR='RED',HRRPUA=745.7505,RAMP_Q='FIRE RAMP'/

&OBST XB=0.21997,0.293293,0.21997,0.293293,0.00000,1.82880,SURF_ID='FIRE'/

&VENT XB=-0.51326,-0.51326,-
0.36662,0.36662,0.07034,0.14068,SURF_ID='CAB',ID='VENTo1',COLOR='GREEN'/
&VENT XB=-0.51326,-0.51326,-
0.36662,0.36662,0.14068,0.21102,SURF_ID='CAB',ID='VENTo2',COLOR='BLUE'/
&VENT XB=-0.51326,-0.51326,-
0.36662,0.36662,0.21102,0.28135,SURF_ID='CAB',ID='VENTo3',COLOR='GREEN'/
&VENT XB=-0.51326,-0.51326,-
0.36662,0.36662,0.28135,0.35169,SURF_ID='CAB',ID='VENTo4',COLOR='BLUE'/
&VENT XB=-0.51326,-0.51326,-
0.36662,0.36662,0.35169,0.42203,SURF_ID='CAB',ID='VENTo5',COLOR='GREEN'/
&VENT XB=-0.51326,-0.51326,-
0.36662,0.36662,0.42203,0.49237,SURF_ID='CAB',ID='VENTo6',COLOR='BLUE'/

&VENT XB=-0.51326,-0.51326,-
0.36662,0.36662,1.33643,1.40677,SURF_ID='CAB',ID='VENTo19',COLOR='GREEN'/
&VENT XB=-0.51326,-0.51326,-
0.36662,0.36662,1.40677,1.47711,SURF_ID='CAB',ID='VENTo20',COLOR='BLUE'/
&VENT XB=-0.51326,-0.51326,-
0.36662,0.36662,1.47711,1.54745,SURF_ID='CAB',ID='VENTo21',COLOR='GREEN'/
&VENT XB=-0.51326,-0.51326,-
0.36662,0.36662,1.54745,1.61778,SURF_ID='CAB',ID='VENTo22',COLOR='BLUE'/
&VENT XB=-0.51326,-0.51326,-
0.36662,0.36662,1.61778,1.68812,SURF_ID='CAB',ID='VENTo23',COLOR='GREEN'/
&VENT XB=-0.51326,-0.51326,-
0.36662,0.36662,1.68812,1.75846,SURF_ID='CAB',ID='VENTo24',COLOR='BLUE'/

&VENT XB=-0.43994,-0.43994,-
0.36662,0.36662,0.07034,0.14068,SURF_ID='CAB',ID='VENTi1',COLOR='GREEN'/
```

```
&VENT XB=-0.43994,-0.43994,-
0.36662,0.36662,0.14068,0.21102,SURF_ID='CAB',ID='VENTi2',COLOR='BLUE'/
&VENT XB=-0.43994,-0.43994,-
0.36662,0.36662,0.21102,0.28135,SURF_ID='CAB',ID='VENTi3',COLOR='GREEN'/
&VENT XB=-0.43994,-0.43994,-
0.36662,0.36662,0.28135,0.35169,SURF_ID='CAB',ID='VENTi4',COLOR='BLUE'/
&VENT XB=-0.43994,-0.43994,-
0.36662,0.36662,0.35169,0.42203,SURF_ID='CAB',ID='VENTi5',COLOR='GREEN'/
&VENT XB=-0.43994,-0.43994,-
0.36662,0.36662,0.42203,0.49237,SURF_ID='CAB',ID='VENTi6',COLOR='BLUE'/

&VENT XB=-0.43994,-0.43994,-
0.36662,0.36662,1.33643,1.40677,SURF_ID='CAB',ID='VENTi19',COLOR='GREEN'/
&VENT XB=-0.43994,-0.43994,-
0.36662,0.36662,1.40677,1.47711,SURF_ID='CAB',ID='VENTi20',COLOR='BLUE'/
&VENT XB=-0.43994,-0.43994,-
0.36662,0.36662,1.47711,1.54745,SURF_ID='CAB',ID='VENTi21',COLOR='GREEN'/
&VENT XB=-0.43994,-0.43994,-
0.36662,0.36662,1.54745,1.61778,SURF_ID='CAB',ID='VENTi22',COLOR='BLUE'/
&VENT XB=-0.43994,-0.43994,-
0.36662,0.36662,1.61778,1.68812,SURF_ID='CAB',ID='VENTi23',COLOR='GREEN'/
&VENT XB=-0.43994,-0.43994,-
0.36662,0.36662,1.68812,1.75846,SURF_ID='CAB',ID='VENTi24',COLOR='BLUE'/

&HVAC TYPE_ID='LEAK',VENT_ID='VENTo1',VENT2_ID='VENTi1',ID='VENT1',AREA=0.026/
&HVAC TYPE_ID='LEAK',VENT_ID='VENTo2',VENT2_ID='VENTi2',ID='VENT2',AREA=0.026/
&HVAC TYPE_ID='LEAK',VENT_ID='VENTo3',VENT2_ID='VENTi3',ID='VENT3',AREA=0.026/
&HVAC TYPE_ID='LEAK',VENT_ID='VENTo4',VENT2_ID='VENTi4',ID='VENT4',AREA=0.026/
&HVAC TYPE_ID='LEAK',VENT_ID='VENTo5',VENT2_ID='VENTi5',ID='VENT5',AREA=0.026/
&HVAC TYPE_ID='LEAK',VENT_ID='VENTo6',VENT2_ID='VENTi6',ID='VENT6',AREA=0.026/

&HVAC TYPE_ID='LEAK',VENT_ID='VENTo19',VENT2_ID='VENTi19',ID='VENT19',AREA=0.026/
&HVAC TYPE_ID='LEAK',VENT_ID='VENTo20',VENT2_ID='VENTi20',ID='VENT20',AREA=0.026/
&HVAC TYPE_ID='LEAK',VENT_ID='VENTo21',VENT2_ID='VENTi21',ID='VENT21',AREA=0.026/
&HVAC TYPE_ID='LEAK',VENT_ID='VENTo22',VENT2_ID='VENTi22',ID='VENT22',AREA=0.026/
&HVAC TYPE_ID='LEAK',VENT_ID='VENTo23',VENT2_ID='VENTi23',ID='VENT23',AREA=0.026/
&HVAC TYPE_ID='LEAK',VENT_ID='VENTo24',VENT2_ID='VENTi24',ID='VENT24',AREA=0.026/

&SLCF PBX = 0.0,QUANTITY='TEMPERATURE',VECTOR=.TRUE./
&SLCF PBY = 0.0,QUANTITY='TEMPERATURE',VECTOR=.TRUE./

&SLCF PBX = 0.0, QUANTITY='INTEGRATED INTENSITY'/
&SLCF PBY = 0.0, QUANTITY='INTEGRATED INTENSITY'/

&BNDF QUANTITY='WALL TEMPERATURE'/
```

This input uses the same array of devices as the 1.4 m^3 (50 ft^3) large open cabinet and the same fire ramp as the 0.3 m^3 (12 ft^3) medium open cabinet.

```
&TAIL/
```

APPENDIX D
EXAMPLE APPLICATION OF ENCLOSURE-TO-ENCLOSURE PROPAGATION

D.1 Example 1: Determining Enclosure-to-Enclosure Fire Propagation

D.1.1 Equipment Configuration, Fire Modeling Parameters, and Assumptions

Determine the potential for enclosure-to-enclosure propagation for the bank of enclosures in Figure D-1.

A bank of 10, non-switchgear, non-MCC, electrical enclosures are analyzed using detailed fire modeling. The enclosures (Enclosure 1 through Enclosure 10 for this example) run east to west. Each of the enclosures falls within the Group 4b enclosure class with a 200 kW peak HRR according to Table 4-2 of NUREG-2178 [2]. These enclosures have solid back panels and are vented on the front approximately 0.3 m (1 ft) below the top of the enclosure. Each enclosure has a height of 2.3 m (7.5 ft), a depth of 0.61 m (2 ft), and a width of 0.61 m (2 ft). Enclosure 9 is unique with a height of 2.3 m (7.5 ft), a depth of 0.3 m (1 ft), and a width of 0.3 m (1 ft). according to Table 4-2 of NUREG-2178, this cabinet falls within the Group 4c enclosure class with a 45 kW peak HRR.

The bank of enclosures is presented in Figure D-1.

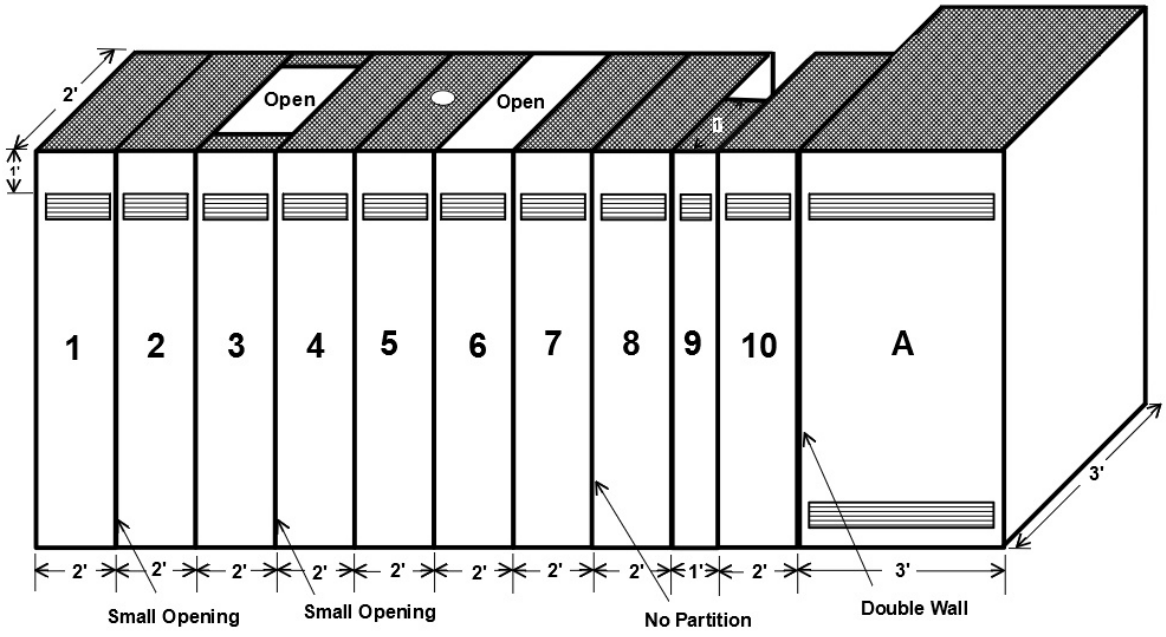

Figure D-1
Bank of enclosures

At the end of the bank, adjacent to Enclosure 10, is an Enclosure A. Enclosure A has a height of 2.3 m (7.5 ft), a depth of 0.91 m (3 ft), and a width of 0.91 m (3 ft). Enclosure A has vents located on the front and back of the enclosure approximately 0.3 m (1 ft) below the top of and approximately 0.3 m (1 ft) above the bottom of the enclosure. According to Table 4-2 of NUREG-2178, this cabinet falls within the Group 4a enclosure class with a 400 kW peak HRR.

There are no cable trays located above or nearby to these electrical enclosures.

The enclosures are located in a compartment with a very high ceiling, and the development of a hot gas layer (HGL) has been screened based on detailed fire modeling of the worst configuration in the compartment. The ambient temperature in the compartment is 20°C (68°F).

The compartment does not have suppression or detection systems.

During walkdowns Enclosures 1 through Enclosure 8 and Enclosure A were opened, and the internals of the cabinets are summarized in Table D-1.

Table D-1
Walkdown summary

Enclosure	Notes
1	Solid top Some cables on east side (**low** fuel load) Solid steel partition separating Enclosure 1 and Enclosure 2 Small opening on bottom (<5%) into Enclosure 2 for grounding strip
2	Solid top Some cables oriented horizontally in the middle of the cabinet (**low** fuel load) Solid steel partition separating Enclosure 2 and Enclosure 1 Solid steel partition separating Enclosure 2 and Enclosure 3 Small opening on bottom (<5%) into Enclosure 1 for grounding strip
3	Large opening on top, ~80% of total area Multiple cable bundles running from top to bottom (These cables come into contact with all faces of the enclosure.) Solid steel partition separating Enclosure 3 and Enclosure 2 Solid steel partition separating Enclosure 3 and Enclosure 4 Small opening (<5%) on bottom into Enclosure 4 for grounding strip
4	Solid top Multiple cable bundles running from top to bottom (These cables come into contact with all faces of the enclosure.) Solid steel partition separating Enclosure 4 and Enclosure 3 Solid steel partition separating Enclosure 4 and Enclosure 5 Small opening (<5%) on bottom into Enclosure 3 for grounding strip
5	Small circular opening on top, ~1 inch in diameter. Multiple cable bundles at all elevations of the enclosure (A bundle of cables on west face of the enclosure runs from bottom of the enclosure to the top and has communication with cables in Enclosure 6 - through the partition between Enclosure 5 and 6.) Solid steel partition separating Enclosure 5 and Enclosure 4 Solid steel partition separating Enclosure 5 and Enclosure 6
6	Totally open top Multiple cables located in the enclosure (A horizontal bundle of cables on east face of the enclosure has communication with cables in Enclosure 5 - through the partition between Enclosure 5 and 6.) Solid steel partition separating Enclosure 6 and Enclosure 5 Solid steel partition separating Enclosure 6 and Enclosure 7
7	Solid top Some cables on west side (**low** fuel load) Solid steel partition separating Enclosure 7 and Enclosure 6 No partition to the east separating Enclosure 7 from Enclosure 8

Table D-1
Walkdown summary (continued)

Enclosure	Notes
8	Solid top Almost no cables—maybe two—individual, not bundled (**very low** fuel loading)—on rear of cabinet No partition to the west separating Enclosure 8 from Enclosure 7 Solid steel partition separating Enclosure 8 and Enclosure 9
9	Not opened
10	Not opened
A	Solid top Multiple cable bundles running from top to bottom (These cables come into contact with all faces of the enclosure.) Solid steel partition observed on east face of Enclosure A

D.1.2 Assessment of Enclosure-to-Enclosure Propagation

Using the guidance provided in Section 4.3, determine the potential for enclosure-to-enclosure propagation.

Enclosure 1

East: N/A—There is no enclosure to the east of Enclosure 1.

West: Enclosure 2 is separated from Enclosure 1 by a solid partition with limited unsealed penetrations. The fuel loading in both Enclosure 1 and Enclosure 2 is determined to be **low**. No propagation from Enclosure 1 to Enclosure 2 based on low fuel/steel partition rule.

Enclosure 2

East: Enclosure 1 is separated from Enclosure 2 by a solid partition with limited unsealed penetrations. The fuel loading in both Enclosure 2 and Enclosure 1 is determined to be **low**. No propagation from Enclosure 2 to Enclosure 1 based on low fuel/steel partition rule.

West: Enclosure 2 is separated from Enclosure 3 by a solid partition. Enclosure 3 has a substantial, >50%, opening on the top of the enclosure. Enclosure 3 has cables running in a vertically oriented direction; however, none communicates through the partition into Enclosure 2. No propagation from Enclosure 2 to 3 based on the open top/vertically oriented rule.

Additionally, with the **low** fuel load in Enclosure 2 and considering the solid partition between Enclosure 2 and Enclosure 3, propagation to Enclosure 3 is not postulated based on the low fuel/steel partition rule even if the cables in Enclosure 3 are in contact with the solid partition separating the two enclosures.

Enclosure 3

East/West: Enclosure 3 has a substantial, >50%, opening on the top of the enclosure. There are solid partitions with limited unsealed penetrations separating Enclosure 3 from Enclosure 2 and Enclosure 4. Finally, there are no vertically oriented cables leading into either adjacent exposed enclosure through the partitions. No propagation from Enclosure 3 to either Enclosure 2 or 4 based on the open top/vertically oriented cables rule.

Additionally, with the **low** fuel load in Enclosure 2, with no cables in contact with the west wall, and considering the solid partition between Enclosure 3 and Enclosure 2, propagation to Enclosure 3 is not postulated based on the low fuel/steel partition rule, even though the fuel load in Enclosure 3 would be considered **default** according to the guidance in NUREG-2178.

Enclosure 4

East: Enclosure 4 is separated from Enclosure 3 by a solid partition. Enclosure 3 has a substantial, >50%, opening on the top of the enclosure. Enclosure 3 has cables running in a vertically oriented direction; however, none communicates through the partition into Enclosure 4. No propagation from Enclosure 4 to Enclosure 3 based on the open top/vertically oriented rule.

West: Enclosure 4 is separated from Enclosure 5 by a solid partition. Both enclosures have a **default** fuel loading. Both enclosures have tops with greater than 50% of their surface area solid. No guidance is provided restraining the propagation of fire from Enclosure 4 to Enclosure 5.

Enclosure 5

East: Enclosure 5 is separated from Enclosure 4 by a single solid partition. Both enclosures have a **default** fuel loading. Both enclosures have tops with greater than 50% of their top surface area solid. No guidance is provided restraining the propagation from Enclosure 5 to Enclosure 4.

West: Enclosure 5 is separated from Enclosure 6 by a solid partition. Enclosure 6 has no top. There are cables running vertically in Enclosure 5 that lead through the partition separating Enclosure 5 from Enclosure 6. Despite the open top, with vertically oriented cables communicating with cables in Enclosure 6, the open top/vertically oriented cables rule does not apply and propagation should be postulated.

Enclosure 6

East/West: Enclosure 6 is separated from Enclosure 5 by a solid partition. Enclosure 6 has no top. There are cables running horizontally in Enclosure 6 that lead through the partition separating Enclosure 6 from Enclosure 5. Because the cables communicating with Enclosure 5 do not run in a vertical manner, the open top/vertically oriented cables rule does not require propagation to be postulated to Enclosure 6.

Enclosure 7

East: Enclosure 7 is separated from Enclosure 6 by a solid partition. Enclosure 6 has no top. None of the cables in Enclosure 7 communicate through the partition into Enclosure 6. No propagation from Enclosure 7 to Enclosure 6, based on the open top/vertically oriented rule.

Additionally, with the **low** fuel load in Enclosure 7, with no cables in contact with the east wall, and the solid partition between Enclosure 7 and Enclosure 6, propagation to Enclosure 6 is not postulated based on the low fuel/steel partition rule even though the fuel load in Enclosure 6 would be considered **default** according to the guidance in NUREG-2178.

West: No partition separates Enclosure 7 from Enclosure 8. The fuel loading in Enclosure 7 is **low**. The fuel loading in Enclosure 8 is determined to be **very low**. Based on the low fuel exposing/very low exposed rule, no propagation is postulated from Enclosure 7 to Enclosure 8.

Enclosure 8

East/West: Enclosure 8 has a **very low** fuel loading. No propagation from Enclosure 8 to adjacent enclosures based on the very low fuel load rule.

Enclosure 9

East/west: Enclosure 9 falls within the small enclosure functional class in NUREG-2178. No propagation is considered based upon the Group 4c: small enclosure rule.

Enclosure 10

East: No information is available with respect to the conditions inside Enclosure 10 and the connection to Enclosure 9. Fire propagation is postulated from Enclosure 10 to Enclosure 9.

West: Enclosure 10 and Enclosure A are separate enclosures with their own solid partitions. No propagation from Enclosure 10 to Enclosure A is modeled based on the double wall rule.

Enclosure A

East: Enclosure A and Enclosure 10 are separate enclosures with their own solid partitions. No propagation from Enclosure A to Enclosure 10 is modeled based on the double wall rule.

West: N/A—There is no enclosure to the west of Enclosure A.

D.2 Example 2: Fire Modeling of Enclosure-to-Enclosure Fire Spread

D.2.1 Enclosures to Postulate Fire Spread

In the previous example (see Section D.1), enclosure-to-enclosure fire spread was determined to be possible from the following:

- Enclosure 4 to Enclosure 5
- Enclosure 5 to Enclosure 4
- Enclosure 5 to Enclosure 6
- Enclosure 10 to Enclosure 9

Determine the heat release rate (HRR) profiles versus time for each configuration vulnerable to fire spread.

D.2.2 Fire Modeling for Enclosure-to-Enclosure Fire Spread

Enclosures 4, 5, and 6 all fall within the NUREG-2178 4b enclosure class and the resulting HRR considering enclosure-to-enclosure fire spread may be represented by a HRR profile combining both enclosures. Ignition in the exposing enclosure (Enclosure 5) take places at time = 0. The peak HRR of 200 kW will be reached in 12 minutes following a t^2 growth profile for the growing fraction of fires and within 16 minutes for the interruptible fraction of fires per NUREG-2230. Ten minutes after the start of the growth period, the exposed enclosure will ignite.

As stated in Section 4.4, the spread of fire must be postulated to occur in one adjacent cabinet. Therefore, the HRR profile of a fire spreading from Enclosure 5 will only include the contribution of a single adjacent enclosure.

The exposing cabinet will hold at the peak HRR of 200 kW for 8 minutes before starting to decay—total time from ignition 20 minutes for the growing fraction and 24 minutes for the interruptible fraction of fires. The exposed enclosure will follow the same timing, with an end to the steady HRR period starting 30 minutes (10+12+8 minutes) for the growing fraction of fires and 34 minutes (4+10+12+8 minutes) for the interruptible fraction of fires after the exposing enclosure ignition.

For both enclosures the decay period will last approximately 19 minutes. The exposing enclosure will fully decay at a total time of 39 minutes. The exposed enclosure will burn out at 49 minutes from the start of the growth period.

The resulting total HRR profile for the two cabinets is presented in Figure D-2.

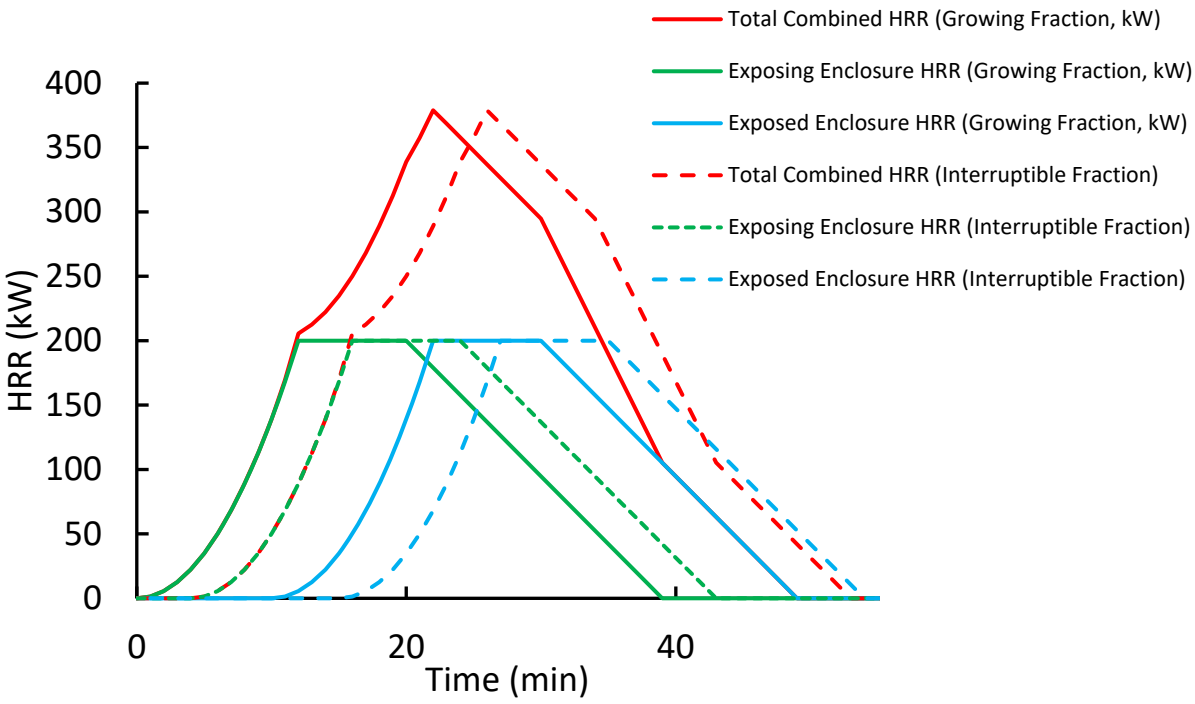

Figure D-2
Enclosures 4 to 5, 5 to 4, and 5 to 6: enclosure-to-enclosure fire spread HRR profile

Enclosure 9 is a small enclosure according to NUREG-2178 (for example, a peak HRR of 45 kW). The HRR profile from Enclosure 10 (a 200 kW peak HRR) to Enclosure 9 is presented in Figure D-3.

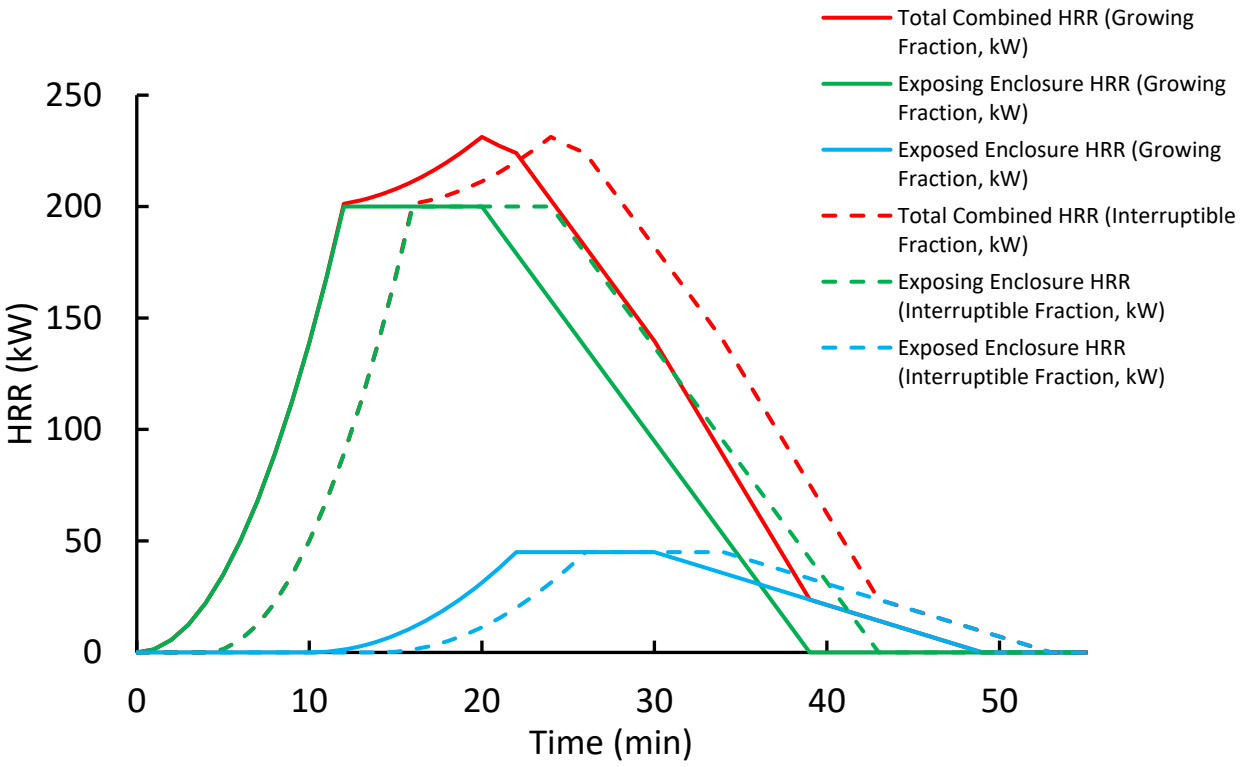

Figure D-3
Enclosure 10 to 9: enclosure-to-enclosure fire spread HRR profile

For the scenarios that do not propagate, the existing HRR profiles (for example, NUREG-2178) and growth profiles (for example, NUREG-2230) would be used. The HRR profiles presented in Figure D-2 plus the single cabinet timing profiles would be used in detailed fire modeling to determine the ZOI, time to damage, HGL analysis, and so on for this bank of enclosures.

D.3 Example 3: Conditional Probability of Fire Spread for Enclosure-to-Enclosure Fire Scenarios

D.3.1 Configuration of Electrical Enclosures

The scenarios in Table D-2 are evaluated for enclosure-to-enclosure fire spread.

Table D-2
Fire scenario description

Scenario	Description
ENC_1	Fire in Enclosure 1
ENC_2	Fire in Enclosure 2
ENC_3	Fire in Enclosure 3
ENC_4	Fire in Enclosure 4
ENC_4_S5	Fire in Enclosure 4 that propagates to Enclosure 5
ENC_5	Fire in Enclosure 5
ENC_5_S4	Fire in Enclosure 5 that propagates to Enclosure 4
ENC_5_S6	Fire in Enclosure 5 that propagates to Enclosure 6
ENC_6	Fire in Enclosure 6
ENC_7	Fire in Enclosure 7
ENC_8	Fire in Enclosure 8
ENC_9	Fire in Enclosure 9
ENC_10	Fire in Enclosure 10
ENC_10_S9	Fire in Enclosure 10 that propagates to Enclosure 9
ENC_A	Fire in Enclosure A

D.3.2 Calculation of Fire Propagation Likelihood

The first step is to calculate the scenario frequency as described in Section 11.3 of NUREG/CR-6850 [1]. After the scenario frequency is calculated, the split fraction in Section 4.3 is applied to scenarios for where propagation was postulated. Table D-3 presents the split fractions for each scenario where the possibility of propagation to an adjacent cabinet was postulated.

Table D-3
Split fraction for likelihood of fire spread to adjacent enclosures

Scenario	Enclosure Propagation Split Fraction
ENC_4	0.98
ENC_ 4_S5	0.02
ENC_5	0.98
ENC_5_S4	0.01
ENC_5_S6	0.01
ENC_10	0.98
ENC_10_S9	0.02

For the scenarios involving spread from Enclosure 5, the split fraction is set to 0.01 for spread in each direction. This apportions the split fraction equally between the two enclosures because the actual direction is uncertain.

D.4 Example 4: Postulation of Enclosure-to-Enclosure Fire Spread

D.4.1 Un-Opened Bank of Enclosures

Walkdown notes of a bank of four, non-switchgear, non-MCC enclosures are shown in Figure D-4. No enclosures were opened. The analyst needs to determine the possibility of fire spread within the bank of enclosures.

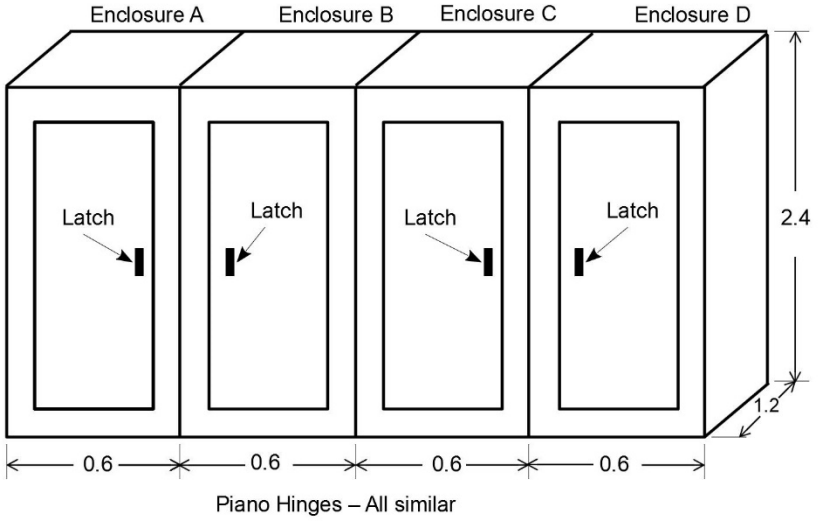

Figure D-4
Walkdown of bank of enclosures

From the notes recorded during the walkdowns, the following information is available:

- There are four apparent vertical sections (treated as separate enclosures).
- All enclosures measure 1.2 m (4 ft) in depth, 0.6 m (2 ft) in width, and 2.4 m (8 ft) in height.
- Each enclosure has at least one door. The doors have a robust latch and piano hinge opposite the latch.
- There are no vents on the enclosures.
- The enclosures have solid tops with no openings.
- Enclosure separation is not determined.

This information is used to determine if fire spread should be modeled between the enclosures. In Table D-4, the guidance for fire spread to adjacent enclosures presented previously are reviewed for application in these scenarios.

Table D-4
Screening guidance for un-opened cabinet-to-cabinet fire spread

Guidance	Disposition
Double wall	No clear separation between the enclosures
Open top/vertically oriented cables	N/A—solid top observed during walkdowns/enclosures not opened during walkdowns
Very low fuel load	N/A—enclosures not opened during walkdowns
Small enclosure	N/A—not NUREG-2178 Enclosure Class 4c
Low fuel/steel partition	N/A—enclosures not opened during walkdowns
Low fuel exposing/very low exposed	N/A—enclosures not opened during walkdowns
MCC	N/A—not an MCC
Switchgear	N/A—not a switchgear or load center

There are no screening rules applicable to this configuration, and fire propagation should be postulated for each enclosure.

D.4.2 Opened Bank of Enclosures

At a later date, walkdowns were performed. An updated summary of the notes is presented in Table D-5.

Table D-5
Walkdown summary

Enclosure	Notes
A	Solid steel partition walls—no openings into Enclosure B **Low** fuel load.
B	Solid steel partition walls—no openings in either direction. **Very low** fuel load.
C	Solid steel partition—no openings separating Enclosure C from Enclosure B **Low** fuel load—All cables on wall separating Enclosure C from Enclosure B Open partition (~25% openings) separating Enclosure C from Enclosure D
D	Open partition (~25% openings) separating Enclosure D from Enclosure C **Low** fuel load—all cables on outside wall of Enclosure D

Using the new information gathered, the screening rules are re-reviewed to determine whether propagation may be screened in certain scenarios. The results are presented in Table D-6.

Table D-6
Opened cabinet application

Guidance	Disposition
Double wall	N/A—no double walls separating enclosures.
Open top/vertically oriented cables	N/A—solid top observed during walkdowns.
Very low fuel load	Enclosure B has a **very low** fuel load. No fire spread from Enclosure B to Enclosures A or C according to Very Low Fuel.
Small enclosure	N/A—Not NUREG-2178 Enclosure Class 4c.
Low fuel/steel partition	Enclosure A and C have **lo**w fuel loads and are separated from Adjacent enclosures by a steel partition with < 5% openings. No fire spread from Enclosure A to Enclosure B according to Low Fuel/Steel Partition. No fire spread from Enclosure C to Enclosure B according to Low Fuel/Steel Partition.
Low fuel exposing/very low exposed	Enclosure A and Enclosure C have **low** fuel loads, and Enclosure B has a **very low** fuel load. No fire spread from Enclosure A to Enclosure B according to Low Fuel Exposing/Very Low Exposed. No fire spread from Enclosure A to Enclosure B according to Low Fuel Exposing/Very Low Exposed.
MCC	N/A—not an MCC
Switchgear	N/A—not a switchgear or load center

From the results in Table D-6, the only possible enclosure-to-enclosure fire spread is from Enclosure C to Enclosure D and Enclosure D to Enclosure C.

D.5 Example 5: Assessing Fire Suppression in Multi-Enclosure Fire Scenarios

In this example, the non-suppression probability (NSP) will be estimated for a scenario that includes enclosure-to-enclosure fire spread.

A bank of two non-switchgear, non-MCC electrical enclosures were analyzed. Enclosure 1 is separated from Enclosure 2 by a solid steel partition. Each enclosure had a solid top with no openings. Each enclosure contained multiple bundles of cables, oriented in both vertical and horizontal directions, located across all elevations of the enclosures. According to the guidance provided previously, fire spread between these enclosures should be modeled.

Additionally, the following characteristics are applicable to the example:

- The split between interruptible and growing fire profiles is 0.723/0.277, respectively (NUREG-2230).
- Room is equipped with a smoke detection system. The time to automatic smoke detection is 1 minute for the growing fraction of the fire.

- Room is not equipped with an automatic fixed suppression system.
- Room is equipped with a manually activated fixed gaseous suppression system with a probability of failure to activate the system on time of 0.15 (probability of human error activating the system: 0.1 and unreliability of the system: 0.05).
- The cabinets are Group 4b medium, closed enclosures with thermoset cable insulation and **default** fuel loadings according to Table 4-2 in NUREG-2178 Vol. 1 [2].
- The cabinets are not monitored in the MCR, and there would be no special indication of a fault in the exposing or exposed cabinet prior to or concurrent with the automatic fire detection.
- The ineffectiveness of the automatic smoke detection system is 0.72 according to Table 5-2 in NUREG-2230.
- The smoke detection system has an unavailability of 0.01.
- A pre-growth period of 4 minutes is included in the interruptible fraction of fires (interruptible fire option 2, NUREG-2230).
- The cabinets are located in a room that has been determined to have medium occupancy and medium maintenance rating levels. No credit is taken for the rating in an adjacent space. This results in a probability that personnel are not present to detect the fire of 0.475 according to Table 5-6 in NUREG-2230.
- The interruptible and growing fire suppression rates are 0.149 and 0.100, respectively, per NUREG-2230.

A cable tray is located above the enclosures and fire modeling shows that, if the HRR exceeds 300 kW, the cable tray will be damaged. From Figure D-2, the time to failure would be 19 minutes.

Using the detection-suppression event tree in NUREG-2230 [33], the resulting detection failure probabilities are as follows:

- First interruptible: 3.5E-01
- Second interruptible: 1.0
- First growing: 4.75E-01
- Second growing: 7.38E-01

The NSP for the fire brigade branch (D-IF) following the first detection path is calculated and shown in Equation D-1.

$$e^{-\lambda t} \rightarrow e^{-0.149\cdot(19+4-0)} = \mathbf{0.03} \quad \textbf{(D-1)}$$

There is no second detection path to calculate for the interruptible fraction of fires in this example. For the delayed detection path fire, The NSP for the fire brigade branch (L-IF) is calculated and shown in Equation D-2.

$$e^{-\lambda t} \rightarrow e^{-0.149\cdot(23-15)} = \mathbf{0.3} \quad \textbf{(D-2)}$$

For the growing fraction of fires, the NSP for the fire brigade branch (D-GF) following the first detection path is calculated and shown in Equation D-3.

$$e^{-\lambda t} \rightarrow e^{-0.100 \cdot (19-0)} = 0.15 \quad \textbf{(D-3)}$$

The NSP for the second detection branch (H-GF) is calculated and shown in Equation D-4.

$$e^{-\lambda t} \rightarrow e^{-0.100 \cdot (19-1)} = 0.17 \quad \textbf{(D-4)}$$

For the delayed detection path fire of the growing fire, the NSP for the fire brigade branch (L-GF) is calculated and shown in Equation D-5.

$$e^{-\lambda t} \rightarrow e^{-0.100 \cdot (19-15)} = 0.67 \quad \textbf{(D-5)}$$

This is outlined in Figure D-5 and Figure D-6.

Example Application of Enclosure-to-Enclosure Propagation

Fire	First Detection (MCR, Personnel, Smoke)	Second Detection (Heat)	Automatic Suppression	Manual Fixed	Fire Brigade	Sequence	End State	Pr (Non-Suppression)
FI	DET		AS	MF	FB			
1.000	0.6496		0.00			A-IF	OK	0.00E+00
			1.00	0.00		B-IF	OK	0.00E+00
				1.00	0.97	C-IF	OK	6.28E-01
					0.03	D-IF	NS	2.11E-02
	3.50E-01	0.00	0.00			E-IF	OK	0.00E+00
			1.00	0.00		F-IF	OK	0.00E+00
				1.00	0.96	G-IF	OK	0.00E+00
					0.04	H-IF	NS	0.00E+00
		1.00	0.00			I-IF	OK	0.00E+00
			1.00	0.85		J-IF	OK	2.98E-01
				0.15	0.70	K-IF	OK	3.66E-02
					0.30	L-IF	NS	1.60E-02
							Total	3.71E-02

Figure D-5
Solution for the NSP event tree for enclosure fire spread, interruptible fraction

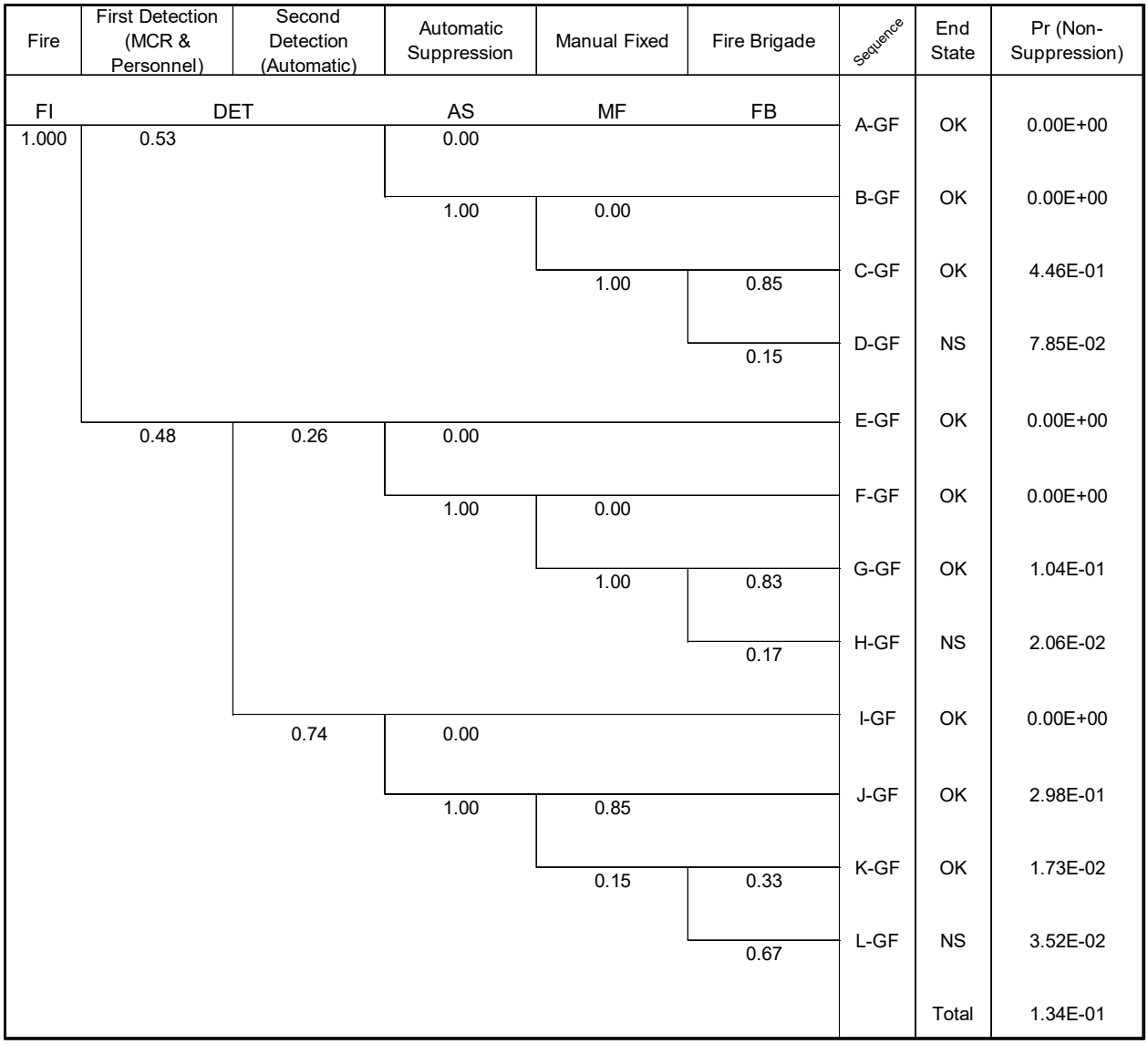

Figure D-6
Solution for the NSP event tree for enclosure fire spread, growing fraction

The overall NSP for the enclosure-to-enclosure fire propagation scenario is calculated as follows:

- For the interruptible fraction of fires:

  $(0.723 \times 3.72 \times 10^{-2}) = 2.68 \times 10^{-2}$

- For the growing fraction of fires:

  $(0.277 \times 1.34 \times 10^{-1}) = 3.72 \times 10^{-2}$

The resulting total NSP for enclosure propagation is 6.4E-02.

NRC FORM 335
(12-2010)
NRCMD 3.7

U.S. NUCLEAR REGULATORY COMMISSION

BIBLIOGRAPHIC DATA SHEET

(See instructions on the reverse)

1. REPORT NUMBER
(Assigned by NRC, Add Vol., Supp., Rev., and Addendum Numbers, if any.)

NUREG-2178
Volume 2

2. TITLE AND SUBTITLE

Refining and Characterizing Heat Release Rates from Electrical Enclosures During Fire (RACHELLE-FIRE) Volume 2: Fire Modeling Guidance for Electrical Cabinets, Electric Motors, Indoor Dry Transformers, and the Main Control Board

3. DATE REPORT PUBLISHED

MONTH	YEAR
June	2020

4. FIN OR GRANT NUMBER

5. AUTHOR(S)

N. Melly, B. Metzger, D. Stroup (NRC)
S. Nowlen (Consultant)
D. Miskiewicz (EPM)
J. DeJoseph, J. Floyd, F. Joglar, V. Ontiveros (Jensen-Hughes)
A. Lindeman (EPRI)
T. Groch (Duke Energy)

6. TYPE OF REPORT
Technical

7. PERIOD COVERED (Inclusive Dates)

8. PERFORMING ORGANIZATION - NAME AND ADDRESS (If NRC, provide Division, Office or Region, U. S. Nuclear Regulatory Commission, and mailing address; if contractor, provide name and mailing address.)

9. SPONSORING ORGANIZATION - NAME AND ADDRESS (If NRC, type "Same as above", if contractor, provide NRC Division, Office or Region, U. S. Nuclear Regulatory Commission, and mailing address.)

Division of Risk Analysis
Office of Nuclear Regulatory Research
U.S. Nuclear Regulatory Commission
Washington, DC 20555-0001

Electric Power Research Institute
3420 Hillview Avenue
Palo Alto CA 94304

10. SUPPLEMENTARY NOTES
M.H. Salley, NRC Project Manager

11. ABSTRACT (200 words or less)

NUREG-2178 Volume 1 refined the heat release rates (HRRs) associated with electrical cabinets and introduced an obstructed fire plume model for refining the vertical zone of influence (ZOI). As a result, Volume 1 has been implemented in a number of nuclear power plant (NPP) fire probabilistic risk assessments (PRAs) to obtain a more realistic estimate of risk associated with electrical cabinet fires. While the methodology in Volume 1 is focused on data analysis and the ZOI, it was realized that modeling refinements associated with other aspects of cabinet fires and the location of fires should be investigated. These targeted areas are further investigated in this report.

This report describes improved methods that may increase the realism in the modeling of selected ignition sources. The areas further investigated include the treatment of flame radiation and obstructed radiation, fire propagation between adjacent electrical cabinets, HRRs for electric motors and dry transformers, fire location factor, non-suppression probability floor values, and the modeling of the main control board.

12. KEY WORDS/DESCRIPTORS (List words or phrases that will assist researchers in locating the report.)

Fire probabilistic risk assessment (Fire PRA), Fire modeling, Fire Dynamics Simulator (FDS), Heat release rate (HRR), Obstructed fire plume, Nuclear power plant (NPP), Zone of influence (ZOI)

13. AVAILABILITY STATEMENT
unlimited

14. SECURITY CLASSIFICATION
(This Page)
unclassified
(This Report)
unclassified

15. NUMBER OF PAGES

16. PRICE

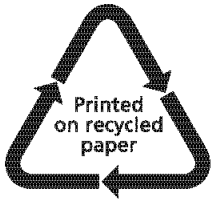

Federal Recycling Program

UNITED STATES
NUCLEAR REGULATORY COMMISSION
WASHINGTON, DC 20555-0001

OFFICIAL BUSINESS

NUREG-2178
Volume 2

Refining and Characterizing Heat Release Rates from Electrical Enclosures during Fire (RACHELLE-FIRE), Vol. 2: Fire Modeling Guidance for Electrical Cabinets, Electric motors, Indoor Dry Transformers, and the Main Control Board

June 2020